UNIVERSITY OF CALIFORNIA SAN DIEGO

Establishment and Validation of the Freshwater Planarian, *Dugesia japonica*, as an Alternative Animal Model for Developmental Neurotoxicology using Organophosphorus Pesticides

A dissertation submitted in partial satisfaction of the requirements for the degree Doctor of Philosophy

in

Biology

by

Danielle Hagstrom

Committee in charge:

Professor Eva-Maria Schoetz Collins, Chair
Professor James Posakony, Co-Chair
Professor Palmer Taylor
Professor Robert Tukey
Professor Jing Wang
Professor Deborah Yelon

2018

The Dissertation of Danielle Hagstrom is approved, and it is acceptable in quality and form for publication on microfilm and electronically:

_____

_____

_____

_____

_____

Co-Chair

_____

Chair

University of California San Diego
2018

TABLE OF CONTENTS

LIST OF FIGURES

LIST OF TABLES

ACKNOWLEDGEMENTS

I would like to acknowledge Professor Eva-Maria S. Collins for her amazing support as the chair of my committee and as a fantastic mentor. I would also like to thank my committee members for all of their support and guidance through my graduate work.

I would like to acknowledge Siqi Zhang for being my partner through most of my research. Our well-oiled teamwork was instrumental for our success. Her creation of the planarian medium-throughput screening platform was essential to my work.

Chapter 1, in full, is a reprint of the material as it appears in Hagstrom, Danielle; Cochet-Escartin, Olivier; and Collins, Eva-Maria S. "Planarian brain regeneration as a model system for developmental neurotoxicology", Regeneration, vol. 3, 2016. The final version is available online at: https://onlinelibrary.wiley.com/doi/full/10.1002/reg2.52. The authors retain copyright of this manuscript, which is an open access article permitting the use herein. Danielle Hagstrom, Olivier Cochet-Escartin, and Eva-Maria S. Collins co-wrote and edited the manuscript. Danielle Hagstrom was the primary investigator and author of this paper.

Chapter 2, in full, is a reformatted reprint of the material as it appears in Hagstrom, Danielle; Cochet-Escartin, Olivier; Zhang, Siqi; Khuu, Cindy; and Collins, Eva-Maria S. "Freshwater planarians as an alternative animal model for neurotoxicology", Toxicological Sciences, vol. 147, 2015. The version of record is available online at: https://academic.oup.com/toxsci/article/147/1/270/1642148. Use of this manuscript in the dissertation herein is covered by the rights permitted to the authors by Oxford Journals. Danielle Hagstrom, Olivier Cochet-Escartin, and Eva-Maria S. Collins designed the experiments and co-wrote the manuscript. Danielle Hagstrom, Olivier Cochet-Escartin, and Siqi Zhang designed and performed the experiments, analyzed, and interpreted the data. Cindy Khuu helped with

experiments and data analysis. Danielle Hagstrom and Olivier Cochet-Escartin were the primary investigators and authors of this material.

Chapter 3, in full, is a reformatted reprint of the material as it appears in Zhang, Siqi; Hagstrom, Danielle; Hayes, Patrick; Graham, Aaron; and Collins, Eva-Maria S. "Multi-behavioral endpoint testing of an 87-chemical compound library in freshwater planarians," Toxicological Sciences, kfy145, 2018 (in press). The version of record is available online at: https://academic.oup.com/toxsci/advance-article/doi/10.1093/toxsci/kfy145/5034903?guestAccessKey=3ddabc3c-f78a-4814-914b-0469e0d3f7d4. Use of this manuscript in the dissertation herein is covered by the rights permitted to the authors by Oxford Journals. Danielle Hagstrom, Siqi Zhang, and Eva-Maria S. Collins designed the experiments and coauthored the manuscript. Danielle Hagstrom set up the chemicals and experiments, and analyzed and interpreted the data. Siqi Zhang built the automatic screening platform, performed the screening experiments and analyzed and interpreted the data. Patrick Hayes and Aaron Graham developed the neural network platform to analyze eye regeneration. Danielle Hagstrom and Siqi Zhang were the primary investigators and authors of this material.

Chapter 4, in full, is a reformatted reprint of the material as it appears in Hagstrom, Danielle; Truong, Lisa; Zhang, Siqi; Tanguay, Robert L; and Collins, Eva-Maria S. "Comparative analysis of zebrafish and planarian model systems for developmental neurotoxicity screens using an 87-compound library", which has been submitted for publication at Toxicological Sciences. Use of this manuscript in the dissertation herein is covered by the rights permitted to the authors by Oxford Journals. The original planarian screening data was obtained by Danielle Hagstrom, Siqi Zhang, and Eva-Maria S. Collins as described in Chapter 3.

Lisa Truong and Robert Tanguay designed, executed, and analyzed the experiments associated with the zebrafish screening data. Danielle Hagstrom performed the direct system comparisons while Lisa Truong performed the comparisons with available mammalian data and physico-chemical properties. Danielle Hagstrom, Eva-Maria S. Collins, and Lisa Truong co-wrote the manuscript with Robert Tanguay and Siqi Zhang contributing to the editing of the manuscript. Danielle Hagstrom and Lisa Truong were the primary investigators and authors of this material.

Chapter 5, in full, is a reformatted reprint of the material as it appears in Hagstrom, Danielle; Hirokawa, Hideto; Zhang, Limin; Radić, Zoran; Taylor, Palmer; and Collins, Eva-Maria S. "Planarian cholinesterase: in vitro characterization of an evolutionarily ancient enzyme to study organophosphorus pesticide toxicity and reactivation", Archives of Toxicology, vol. 91, 2017. The final publication is available at: https://link.springer.com/article/10.1007%2Fs00204-016-1908-3#enumeration. Permission to use this manuscript was granted to Danielle Hagstrom by Springer Nature. Danielle Hagstrom, Zoran Radić, Palmer Taylor, and Eva-Maria Collins designed the experiments, interpreted the data and co-authored the manuscript. Danielle Hagstrom, Hideto Hirokawa, and Limin Zhang performed the experiments. Danielle Hagstrom and Hideto Hirokawa were the primary investigators and authors of this material.

Chapter 6, in full, is a reformatted reprint of the material as it appears in Hagstrom, Danielle; Zhang, Siqi; Ho, Alicia; Tsai, Eileen S.; Radić, Zoran; Jahromi, Aryo; Kaj, Kelson J.; He, Yingtian; Taylor, Palmer; and Collins, Eva-Maria S. "Planarian cholinesterase: molecular and functional characterization of an evolutionarily ancient enzyme to study organophosphorus pesticide toxicity", Archives of Toxicology, vol. 92, 2018. The final publication is available at: https://link.springer.com/article/10.1007%2Fs00204-017-2130-7. Permission to use this manuscript was granted to Danielle Hagstrom by Springer Nature. Danielle Hagstrom and Eva-

Maria S. Collins designed the experiments and co-wrote the manuscript. Danielle Hagstrom, Siqi Zhang, Alicia Ho, Eileen S. Tsai, Aryo Jahromi, and Yingtian He performed the experiments and analyzed the associated data. Kelson Kaj assembled the *Dugesia japonica* transcriptome. Zoran Radić and Palmer Taylor performed analysis of the sequence and protein structure characteristics and contributed to writing and editing of the manuscript. Danielle Hagstrom was the primary investigator and author of this material.

A modified version of Chapter 7 will be submitted for publication as a Research Article (Hagstrom, Danielle; Zhang, Siqi; and Collins, Eva-Maria S. Comparative analysis of the mechanisms of organophosphorus pesticide developmental neurotoxicity in a freshwater planarian). Danielle Hagstrom, Siqi Zhang, and Eva-Maria S. Collins designed the experiments, interpreted the data and co-wrote the manuscript. Danielle Hagstrom set up all chemicals and experiments and analyzed the data. Siqi Zhang updated the screening platform, performed the screening of the chemicals, and analyzed the data. Danielle Hagstrom and Siqi Zhang were the primary investigators and authors of this material.

The appendix, in full, is a reformatted reprint of the material as it appears in Vista SSEP Mission 11 Team; Hagstrom, Danielle; Bartee, Christine; and Collins, Eva-Maria S. "Studying planarian regeneration aboard the International Space Station within the Student Space Flight Experiment Program", Frontiers in Astronomy and Space Sciences, vol. 5, 2018. The authors retain copyright of this manuscript, which is an open access article permitting the use herein. Vista SSEP Mission 11 Team, a team of 5 middle school students, designed the original space experiment. Vista SSEP Mission 11 Team, Danielle Hagstrom, and Eva-Maria S. Collins conducted experiments. All authors co-wrote the paper.

VITA

2012 Bachelor of Science, University of California San Diego

2018 Doctor of Philosophy, University of California San Diego

PUBLICATIONS

Hagstrom, Danielle; Cochet-Escartin, Olivier; Zhang, Siqi; Khuu, Cindy; and Collins, Eva-Maria S. "Freshwater planarians as an alternative animal model for neurotoxicology", Toxicological Sciences, vol. 147, 2015.

Hagstrom, Danielle; Cochet-Escartin, Oliver; and Collins, Eva-Maria S. "Planarian brain regeneration as a model system for developmental neurotoxicology", Regeneration, vol. 3, 2016.

Hagstrom, Danielle; Hirokawa, Hideto; Zhang, Limin; Radić, Zoran; Taylor, Palmer; and Collins, Eva-Maria S. "Planarian cholinesterase: in vitro characterization of an evolutionarily ancient enzyme to study organophosphorus pesticide toxicity and reactivation", Archives of Toxicology, vol. 91, 2017.

Hagstrom, Danielle; Zhang, Siqi; Ho, Alicia; Tsai, Eileen S.; Radić, Zoran; Jahromi, Aryo; Kaj, Kelson J.; He, Yingtian; Taylor, Palmer; and Collins, Eva-Maria S. "Planarian cholinesterase: molecular and functional characterization of an evolutionarily ancient enzyme to study organophosphorus pesticide toxicity", Archives of Toxicology, vol. 92, 2018.

Vista SSEP Mission 11 Team; Hagstrom, Danielle; Bartee, Christine; and Collins, Eva-Maria S. "Studying planarian regeneration aboard the International Space Station within the Student Space Flight Experiment Program", Frontiers in Astronomy and Space Sciences, vol. 5, 2018.

Zhang, Siqi; Hagstrom, Danielle; Hayes, Patrick; Graham, Aaron; and Collins, Eva-Maria S. "Multi-behavioral endpoint testing of an 87-chemical compound library in freshwater planarians", Toxicological Sciences, kfy145, 2018 (in press).

ABSTRACT OF THE DISSERTATION

Establishment and Validation of the Freshwater Planarian, *Dugesia japonica,* as an Alternative Animal Model for Developmental Neurotoxicology using Organophosphorus Pesticides

by

Danielle Hagstrom

Doctor of Philosophy in Biology

University of California San Diego, 2018

Professor Eva-Maria Schoetz Collins, Chair
Professor James William Posakony, Co-Chair

A paradigm shift has recently occurred in the field of toxicology, transitioning away from traditional mammalian models in favor of time- and cost-efficient alternatives, such as *in vitro* systems and non-mammalian animal models, which are amenable to high-throughput screening. We have pioneered the asexual freshwater planarian, *Dugesia japonica,* as an alternative model for developmental neurotoxicology. Planarians have strong regenerative capabilities, wherein

after decapitation, the resulting tail piece will regenerate a new head, including a brain, within 2 weeks. Moreover, planarians possess several quantifiable behaviors coordinated by distinct neuronal subpopulations, enabling testing of both adult and developing/regenerating animals with the same assays to directly compare effects on neuronal function. We have established and begun validating the planarian toxicology platform through screens testing 10-87 compounds. We demonstrate that planarians have similar sensitivity to existing alternative animal models, such as developing zebrafish. Planarians are particularly sensitive to pesticides and are good predictors of known developmentally neurotoxic pesticides, such as organophosphorus pesticides (OPs), one of the most used class of pesticides in the world. OPs are acutely toxic due to inhibition of acetylcholinesterase (AChE), leading to accumulation of acetylcholine and subsequent cholinergic overstimulation. However, growing evidence suggests that chronic, low dose exposure to OPs, particularly during development, may cause toxicity independent of effects on AChE. Alternative mechanisms of OP developmental neurotoxicity have been proposed, but direct connections between molecular/cellular defects with their functional significance have been limited using traditional models. Our planarian screening platform, on the other hand, is uniquely suited to provide the necessary link between mechanism and functional effects. First, we characterized the *in vitro* and *in vivo* properties of planarian cholinesterase and its structural and functional interactions with OPs to contextualize known OP mechanisms. Second, through a comparative screen of 6 OPs and chemicals targeting suggested alternative OP targets, including the endocannabinoid system, cytoskeleton and oxidative stress, we correlate the distinct toxicological profiles of different OPs with specific toxic pathways. Together, these studies demonstrate the utility of the planarian system to the modern toxicology pipeline, through its ability to directly connect mechanisms with their functional significance.

Chapter 1: Planarian brain regeneration as a model system for developmental neurotoxicology

Reprinted from: Hagstrom, Danielle; Cochet-Escartin, Oliver; and Collins, Eva-Maria S. "Planarian brain regeneration as a model system for developmental neurotoxicology", Regeneration, vol. 3, 2016.

ABSTRACT

Freshwater planarians, famous for their regenerative prowess, have long been recognized as a valuable *in vivo* animal model to study the effects of chemical exposure. In this review, we summarize the current techniques and tools used in the literature to assess toxicity in the planarian system. We focus on the planarian's particular amenability for neurotoxicology and neuroregeneration studies, owing to the planarian's unique ability to regenerate a centralized nervous system. Zooming in from the organismal to the molecular level, we show that planarians offer a repertoire of morphological and behavioral readouts while also being amenable to mechanistic studies of compound toxicity. Finally, we discuss the open challenges and opportunities for planarian brain regeneration to become an important model system for modern toxicology.

INTRODUCTION

Toxicological studies, particularly those focused on neurotoxicology, have predominantly relied on the use of in vivo animal models to assess potential adverse effects on human health. Traditionally, toxicological screens have been performed in rodents and higher mammalian models because of their evolutionary proximity to humans. However, because toxicity testing in these animals is ethically questionable, time-consuming and expensive, it is impossible to use this approach to achieve the necessary coverage of the increasingly vast number of environmental toxicants. The non-confidential portion of the Environmental Protection Agency (EPA)'s Toxic Substances Control Act (TSCA) Chemical Substance Inventory (http://www2.epa.gov/tsca-inventory/) currently lists more than 67,000 chemicals that are manufactured or processed in the U.S. Since it is projected that global chemical production will double within the next 24 years (Wilson and Schwarzman, 2009) and new compounds will be continually added to the market, traditional toxicology testing is inadequate and new methodologies and systems are necessary to meet the demand.

To this end, in 2008, the "Tox21" initiative (http://epa.gov/ncct/Tox21/) was launched. This multi-government agency collaboration has two aims. First, it strives to more quickly and effectively characterize the molecular and cellular pathways involved in the toxicity of known compounds. Second, it fosters the development of reliable high-throughput screening (HTS) assays to evaluate chemicals for which little or no testing has been carried out in the past. To achieve the desired coverage and mechanistic insight, both HTS in vitro assays as well as medium-throughput screening (MTS) in alternative animal models are necessary. Alternative animal models, including invertebrates and lower vertebrates, are ideal for MTS as they are free of ethical dilemma, inexpensive to maintain and amenable to automation, leading to increased

screening throughput at reduced cost. Importantly, since many genes and core pathways are conserved between these simpler organisms and humans, their amenability for molecular studies allows for mechanistic insight into compound toxicity (Lein et al., 2005).

Freshwater planarians have arisen as one such possible alternative animal model (Hagstrom et al., 2015). Planarians have fascinated researchers for centuries for their regenerative prowess and ability to reproduce asexually via binary fission (Newmark and Sánchez Alvarado, 2002). Studies in the early 1900s used physical and chemical manipulations to gain insight into the animals' physiological and regenerative properties (Child, 1909; Child, 1911). These efforts led to the discovery of many of the different morphological and behavioral readouts used in planarian toxicology today.

Because planarians were found to be highly susceptible to substances added to their aquatic environment, this feature is frequently employed to monitor water quality in environmental studies (Kapu and Schaeffer, 1991; Rivera and Perich, 1994). After exposure to water samples, different markers at the molecular (Prá et al., 2005) or organismal levels (Knakievicz, 2014) can be used to assess the water pollution level and identify specific pollutants.

In addition, it has been recognized for over 30 years (Best and Morita, 1982) that planarians are well-suited to study the effect of chemicals on brain development and function. Planarians are one of the simplest organisms that display cephalization and are unique in their ability to regenerate their entire central nervous system (CNS) following tissue loss, damage or asexual reproduction (Cebrià, 2007). For asexual planarians, regeneration is the sole mechanism of neurodevelopment. This complex process of de novo neuroregeneration involves many of the same processes that occur during vertebrate neurodevelopment: stem cell migration, proliferation

and differentiation and axonal guidance (Cebrià, 2007; Cebrià and Newmark, 2005; Umesono et al., 2011). Thus, neurodevelopment can be "induced at will" by amputation allowing toxicological studies to be performed directly on free-living developing animals, without the complications of maternal effects.

Importantly, planarians provide a variety of quantifiable morphological, behavioral and molecular endpoints to analyze toxic effects on different aspects of development. Furthermore, the planarian CNS shares many of the same neurotransmitters and neuronal populations with the mammalian brain (Cebrià, 2007; Cebrià et al., 2002; Mineta et al., 2003). For example, it has been demonstrated that neuro-muscular communication is under the control of acetylcholine in planarians like in humans (Nishimura et al., 2010). Thus, mechanistic studies in planarians can provide insight into relevant mechanisms in humans.

Together, these characteristics render planarians specifically valuable as a model for neurodevelopmental toxicology. Importantly, because amputated and intact worms are of similar size, behavioral assays can be performed in parallel on both adult and regenerating/developing animals to determine whether chemicals, or particular concentrations, are specifically toxic or show greater potency to the developing brain. Because of this unique feature and its intermediate neuronal complexity, the planarian system is an ideal complement to existing alternative animal models in toxicology, such as zebrafish and nematodes, for which more extensive molecular toolkits are available (Hagstrom et al., 2015).

Complementary toxicology studies across multiple animal species are necessary to assay compound toxicity for humans, because species-specific differences in sensitivity to toxicants exist (Hagstrom et al., 2015). High-throughput, low-cost alternative animal systems such as zebrafish, nematodes and planarians offer the opportunity to rapidly screen hundreds to

thousands of potential toxicants to identify and prioritize candidates and mechanisms for further in-depth studies in mammalian systems to assay their relevancy to humans (Lein et al., 2005). This approach would greatly enhance screening efficacy and thus save time and resources.

The goal of this review is to summarize the literature on toxicological studies in planarians, focusing on neurotoxicology. Zooming in from the organismal to the molecular level, we highlight behavioral, morphological, cellular and molecular readouts that have been used for the assessment of (neuro-)toxicity. We end with a critical outlook on the limitations, challenges and opportunities of the planarian system for modern high-throughput toxicology screens.

ORGANISMAL READOUTS TO STUDY NEUROTOXICITY IN PLANARIANS

Signs of toxic effects are most readily observed at the whole organism level. Since planarians can be studied with the naked eye, organismal observations are accessible to manual scoring and have been used as early as the seminal studies by Child (Child, 1909; Child, 1911). Lethality is the most dramatic effect, but it is also the least informative readout about a compound's toxicity, because dead planarians generally disintegrate, hindering further examination. More interesting readouts include morphological aberrations, body distortions or changes in behavior, which may be specific to certain chemical classes (Passarelli et al., 1999; Raffa and Valdez, 2001).

It is worth noting that body shape and behavioral readouts in planarians have also been used in pharmacology for decades (Raffa and Rawls, 2008). In particular, locomotor activities have been extensively used by the Raffa lab to study the effect of numerous neuroactive drugs (caffeine, cocaine, etc…) on the planarian brain (Pagán et al., 2012; Raffa et al., 2001) as well as planarian withdrawal behaviors (Raffa and Desai, 2005; Raffa and Valdez, 2001; Raffa et al., 2003). For the purpose of this review, we will focus solely on the field of toxicology and we refer the interested reader to the following reviews (Buttarelli et al., 2008; Raffa and Rawls, 2008) for details on pharmacological studies in planarians.

In 1991, Grebe and Schaeffer introduced the first qualitative scoring system to assess organismal toxicity of phenol in planarians (Grebe and Schaeffer, 1991). This landmark paper provided a matrix for analyzing compound toxicity using well-defined criteria, which has since been used by a large number of researchers (Kapu and Schaeffer, 1991; Pagán et al., 2006; Villar et al., 1993) The Grebe-Schaeffer (GS) scoring system comprises five main categories: Locomotive, Morphological, Neurological, Morbidity and Protective (Figure 1.1). Each of these

categories contains between two and five criteria to be assessed visually, providing 18 different readouts to describe compound toxicity. Combinations of some of these readouts had been used previously in planarian toxicology by numerous groups; however, the GS-system was the sole scoring system incorporating all of them.

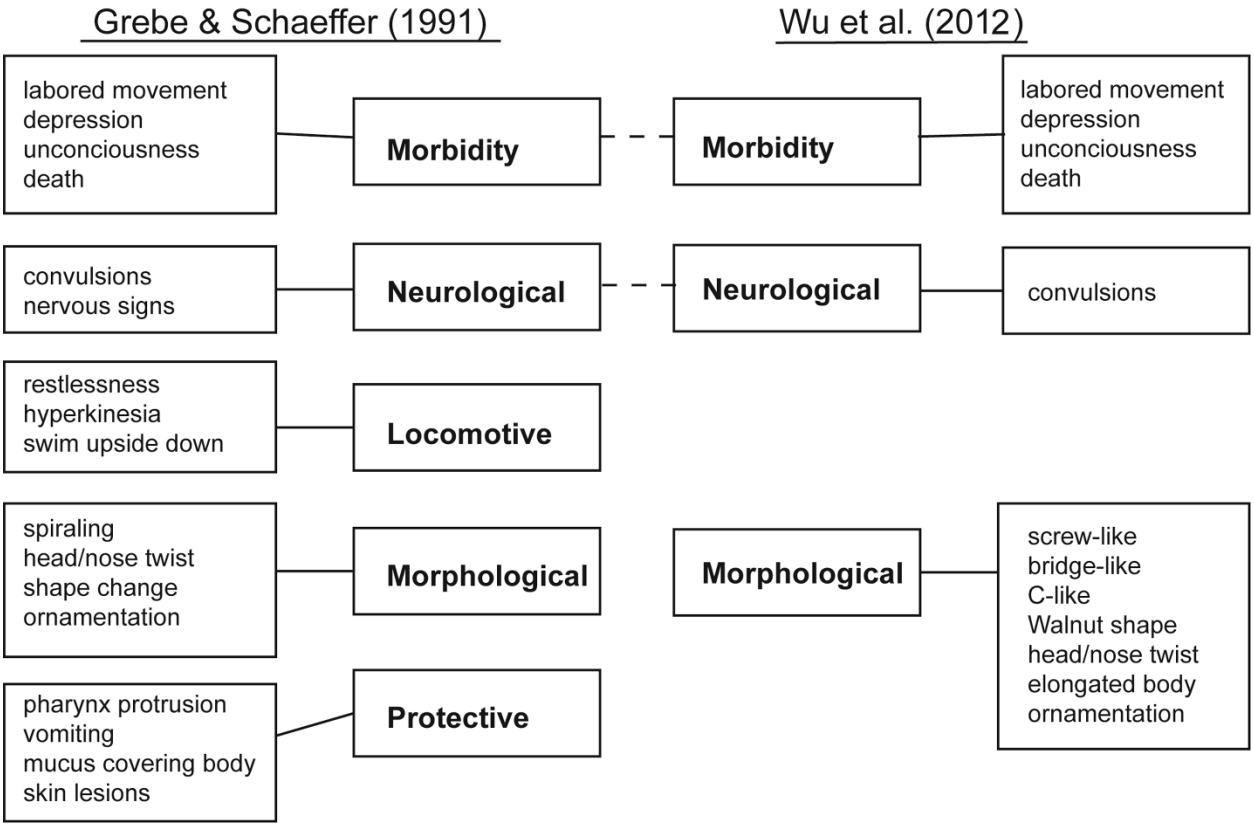

Figure 1.1. Comparison of the two scoring systems by Grebe and Schaeffer (GS-system) (Grebe and Schaeffer, 1991) and Wu et al (Wu et al., 2012b). While substantial overlap exists between the two systems, the GS-system provides more readouts (18 vs. 13). The Wu-system has the advantage of clear categories of shape changes.

Most recently, Wu et al (Wu et al., 2012b), studying cadmium toxicity in planarians, modified the GS-scoring system by condensing most of the same readouts into three main categories (Morphological, Neurological and Morbidity). According to Wu's system, morphological readouts contain both body shapes and behavior, whereas neurological readouts only contain convulsions (Wu et al., 2012b). One of the advantages of the Wu system is the clear

definition of possible shape changes (C-like, screw-like, etc; see Figure 1.2). However, the readouts of the "protective" category of the GS-system were dropped. This is unfortunate, because more readouts improve robustness of toxicant categorization.

Therefore, we prefer a classification system containing all GS-system readouts, keeping the same level of detail, but using the three category labels of the Wu system (morbidity, morphological and neurological function). We incorporate "vomiting", also known as defecation in the planarian community, into the original GS-Morbidity category, and the other readouts of the GS-Protective category into the GS-Morphological category. The latter thus contains all phenotypes manifested in changes in worm shapes. Finally, our Neurological Function category refers to all worm behaviors whereby translational motion is observed, thus comprising the GS-Locomotive and GS-Neurological categories. Below, we discuss each of these three categories in detail.

Morbidity

The first step in toxicity screening is to determine which concentrations are lethal. This is frequently achieved through range-finding tests to determine which concentrations are non-lethal or to determine the concentration at which 50% of the animals die (LC50). The GS-system not only includes death as a readout, but also potential death indicators such as unconsciousness or pharynx protrusion to refine the observations and capture the dynamics of lethality for certain chemicals (Fig. 1). Of note, pharynx protrusion does not always imply that death with follow.

Death is easily scored in planarians since the worms disintegrate after dying (Buchanan, 1935), allowing for high throughput lethality assays. Various methods have been employed in the literature, ranging from manual scoring (Alonso and Camargo, 2011; Grebe and Schaeffer, 1991) to bulk studies (Pagán et al., 2006; Pagán et al., 2009) and automated screening (Hagstrom

et al., 2015). For example, in (Pagán et al., 2009), planarians were distributed in four separated quadrants in a Petri dish with each quadrant containing 6-7 worms in a different chemical and/or a different concentration. The fraction of worms alive at time t was determined by counting the number of worms in the quadrant. The data can be fitted to a classic Hill equation (Hagstrom et al., 2015) to obtain the desired LC50. This method allows lethality to be assessed quickly, using several time points, concentrations and a large number of worms in a single lethality assay.

Because some chemicals may preserve the worm tissue, preventing complete disintegration, the approach above has limited sensitivity compared to a scoring system that also includes death indicators, such as the GS-system. The latter, however, are difficult to score in an automated fashion and largely depend on manual visual inspection of individual worms, limiting its throughput capacity.

Morphological readouts

The combination of morphological and behavioral readouts into a single category, as first proposed by Wu (Wu et al., 2012b), makes sense insofar as the morphological readouts reported in the literature can largely be defined as behavioral. For instance, criteria such as “body elongation” or “nose twist” (Grebe and Schaeffer, 1991; Wu et al., 2012b) are not morphological in the sense of developmental malformations, but, instead, are a consequence of improper muscle control (Passarelli et al., 1999). In contrast, body shape changes such as lesions, pharynx extrusions or wrinkles/ornamentation (Figure 1.2A, B) (Grebe and Schaeffer, 1991; Wu et al., 2012b) are not necessarily indicative of changes on the neuronal level. Thus, morphological readouts are a mixed category in the sense that some morphological changes are the result of improper neuronal functions while others are not. However, because all reflect in body shape changes, we prefer to keep them in one category.

Morphological readouts have been used in a variety of contexts in the literature. The first naming convention for specific shapes was introduced in 1989 by the Palladini group. Working on the dopaminergic system in planarians, they standardized terms for common morphological observations, including C-like shapes (Figure 1.2C, (Venturini et al., 1989)), screw-like hyperkinesia (Figure 1.2D, (Venturini et al., 1989)) and snake-like motion (Figure 1.2E, (Passarelli et al., 1999; Wu et al., 2012b)). These specific shape changes are a consequence of impaired neuro-muscular control as has been shown in (Buttarelli et al., 2000; Venturini et al., 1989).

Although most morphological analysis has been done by eye, shape changes can be quantified using automated shape analysis. Because the body shapes are not always as distinct as in the examples shown in Figure 1.2, machine learning algorithms (Jeanray et al., 2015) may be necessary to achieve a reliable automated categorization of body shapes, as for example used for *C. elegans* phenomics (Wählby et al., 2012).

Overall, changes in worm shape are common tools in assessing the toxicity of chemicals on planarians. However, their observation has been qualitative and relied on visual inspection of the worms, which is slow, prone to observer bias and leads to small numbers of samples. In addition, because research groups use different scoring systems, it is difficult to compare results between studies.

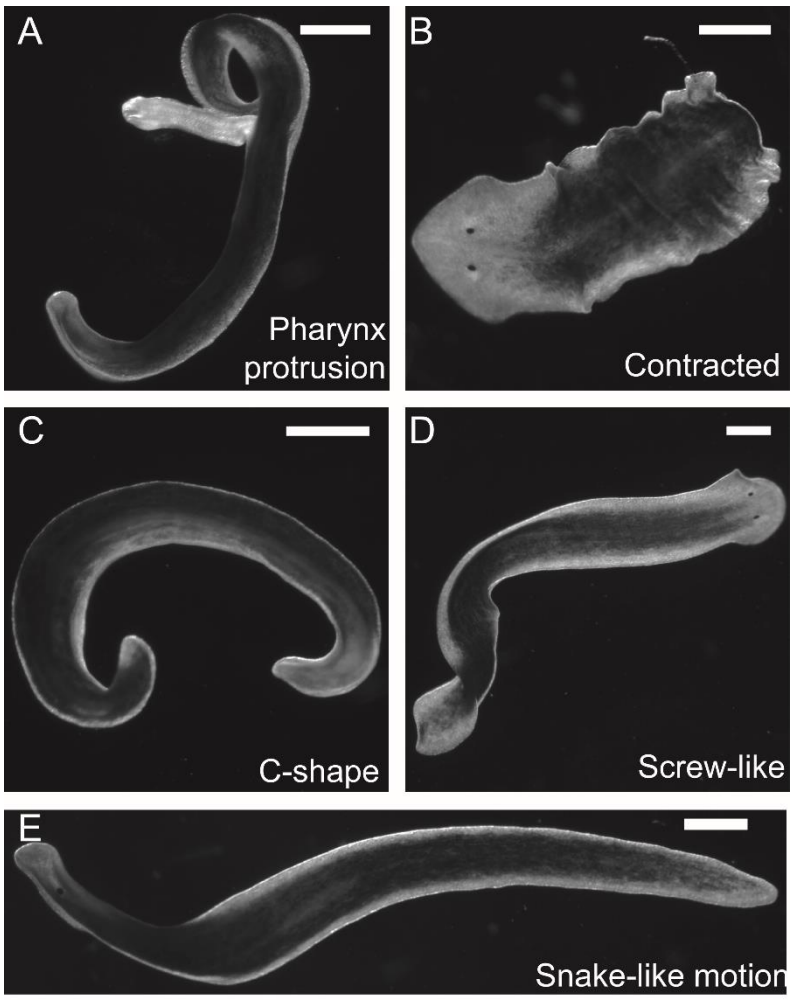

Figure 1.2. Examples of planarian morphological readouts and body shapes. (A) Pharynx is extended outside of the body. Animal treated with 0.4% chloretone. (B) Body is contracted. Often associated with wrinkles/ornamentation in the periphery of the animal. Animal treated with 20µM chlorpyrifos oxon. (C) Body is curled in a C-shape. Also referred to as a banana curl or coil. Animal treated with 0.4% chloretone. (D) Body is twisted around itself in a screw-like fashion. Also referred to as spiraling. Animal treated with 100mM serotonin. (E) Animal is extended and moves along its side in a snake-like motion. Animal treated with 100mM serotonin. Scale bar: 0.5mm

Neurological (behavioral) readouts

Unstimulated locomotion is probably the most accessible type of behavior in planarians. Without stimulation, planarians can either rest, swim or glide (Hagstrom et al., 2015). These three behaviors can be distinguished by eye (Figure 1.3) and are informative about a chemical's effect on worm activity in general. Individual planarians, however, show intrinsically different

preferences for resting, swimming and gliding under the same conditions (Hagstrom et al., 2015). Thus, unless a dramatic change in the relative frequency of these behaviors occurred or a significantly large sample size is studied, it is difficult to draw reliable conclusions regarding these behaviors. Similarly, a comparison of worm speed by naked eye, as done in earlier studies (Child, 1911; Grebe and Schaeffer, 1991), is intrinsically subjective and unreliable when it comes to subtle changes in locomotion.

These limitations and the increased interest in planarians as a model for toxicology and pharmacology prompted the community to develop objective and quantitative measurements. The most extensively used technique to date is the planarian locomotor velocity (pLMV) method, first introduced by Raffa (Raffa et al., 2001) and since used by a large number of research labs (Alonso and Camargo, 2011; Lowe et al., 2015; Ramakrishnan et al., 2014; Stevens et al., 2015; Zhang et al., 2013). The pLMV method is similar to methods used for quantifying rodent behaviors, see e.g. (Yamin et al., 2013). A single worm is placed in a standard 10cm diameter Petri dish on top of a squared grid (primarily 0.5cm or 1cm wide mesh, Figure 1.3A). The worm is allowed to move freely and the number of lines crossed in a given amount of time is recorded.

The same measurement can be performed on worms exposed to specific toxicants and directly compared to their wild type counterparts, providing a quantitative assessment of planarian activity. pLMV has been used to assess the toxicity of various chemicals, including ammonia (Alonso and Camargo, 2011), dimethyl sulfoxide (DMSO) (Pagán et al., 2006; Stevens et al., 2015), cadmium (Wu et al., 2012b) and the dopamine D2-receptor antagonist sulpiride (Raffa et al., 2001), as well as in the pharmacological study of the dopaminergic (Passarelli et al.,

1999; Raffa et al., 2001), serotoninergic (Farrell et al., 2008) and opioid systems (Buttarelli et al., 2002) in planarians.

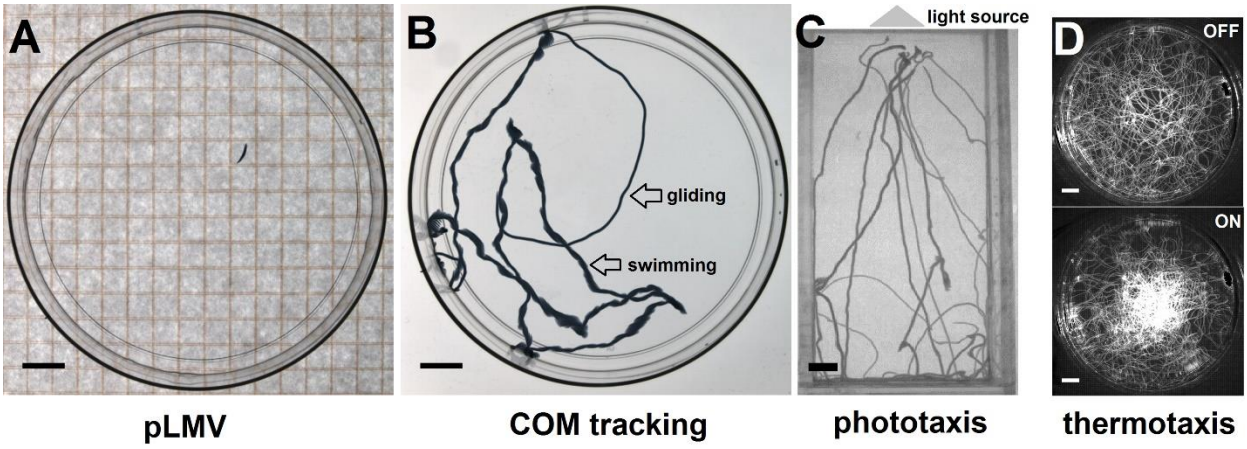

Figure 1.3. Overview of behavioral assays employed in the literature to quantify neuronal function after toxicant exposure. (A) The planarian locomotor velocity (pLMV) method measures worm speed by counting the number of gridlines crossed in a given time. (B) Center of mass (COM) tracking to determine type of locomotion, worm velocity and exploratory behavior. (C) Phototaxis is generally tested using a linear light gradient. (D) Thermotaxis can be tested using a Peltier element to generate a cooler center, which worms prefer. Scale bar: 1cm.

pLMV allowed researchers to discover effects that would have eluded qualitative characterizations. However, it suffers from a few drawbacks. Counting line crossings that are 0.5cm apart is imprecise for determining planarian speed. Also, across its many uses, the details of the pLMV technique have varied among groups through the use of different grid sizes and different time frames, making direct comparison of the results challenging. Moreover, pLMV only estimates absolute speeds but does not take into account the worm's trajectory, which could also yield important information, for example on the frequency of turning or exploratory behavior (Talbot and Schötz, 2011). Finally, the scoring of line crossings is performed manually, leading to slow throughput.

In recent years, we (Hagstrom et al., 2015; Talbot and Schötz, 2011) and others (Li, 2012) have replaced pLMV with real-time center of mass (COM) tracking, which allows the

reconstruction of full worm trajectories to measure instantaneous velocities (Figure 1.3B, (Hagstrom et al., 2015; Talbot and Schötz, 2011)). This approach gives access to new properties of the worm's behavior such as the type of locomotion – e.g. swimming versus gliding (Figure 1.3B and (Hagstrom et al., 2015)) –, the frequency of sharp turns and head wiggles or the time spent at the center versus the periphery of the testing arena (Talbot and Schötz, 2011). It can thus reveal more subtle changes in behaviors and underlying defects in neuronal functions. Using COM tracking, we were able to show that two different compounds, sulpiride and chloretone, gave distinctively different phenotypes (Talbot and Schötz, 2011). It is also worth noting that these last examples are quantitative measurements of readouts already present in the GS-system (see nervous signs in Figure 1.1).

Clearly, to assay the function of specific neuronal populations, studying gliding alone is insufficient. We have recently introduced a new planarian gait, scrunching (Cochet-Escartin et al., 2015), which can be induced in a well-controlled fashion using external noxious stimuli. Scrunching relies on coordinated muscular contractions and has a characteristic signature of asymmetric body contractions that can be quantified using simple image analysis tools. As such, it could become an important readout for both proper sensory apparatus and neuromuscular communication.

Furthermore, the Agata group has made significant advances in quantifying more complex behaviors in *D. japonica*, including thermo-, chemo-, photo- and thigmo-taxis (Inoue et al., 2004; Inoue et al., 2015) and showed that these behaviors depend on neuronal activity (Inoue et al., 2015). Using binary combinations of the respective stimuli, they further showed that a hierarchy exists with chemotaxis as the predominant behavior (Inoue et al., 2015). We have applied similar semi-automated assays to quantify phototaxis (Figure 1.3C and (Lambrus et al.,

2015)) and thermotaxis (Figure 1.3D and (Hagstrom et al., 2015)) in *S. mediterranea* and *D. japonica*, respectively, and found that they are reliable readouts of neuronal function. Thus, even without any knowledge of the underlying toxicity mechanisms, behavioral assays allow assessment of whether proper neuronal functions are maintained after toxicant exposure.

Importantly, how these different behaviors are regulated at the neuronal level is beginning to be unraveled. For example, gliding was shown to depend on serotonin signaling (Currie and Pearson, 2013), thermotaxis on TRPMa sensory neurons and serotonergic neurons (Inoue et al., 2014) and phototaxis on visual neurons and GABAergic neurons (Inoue et al., 2004). Because we have some insight into the neuronal control of these behaviors, it is imperative to incorporate as many behavioral endpoints as possible in the next generation of toxicology screenings to reveal dysfunctions of specific neuronal subpopulations.

Another future avenue is the use of conditioning in planarians. This field bloomed in the 1950s and 1960s with the seminal work of McConnell and coworkers (Thompson and McConnell, 1955), who showed that planarians could learn simple tasks using classical conditioning (Block and McConnell, 1967; Thompson and McConnell, 1955). In addition, their experiments indicated that memories could be retained through brain regeneration (McConnell et al., 1959) and even be transferred across specimen through cannibalism (McConnell, 1962). For a more detailed review, see (Shomrat and Levin, 2013). McConnell's studies, however, were executed manually and difficult to replicate and thus have remained controversial (Kartry et al., 1964; Walker and Milton, 2013). However, a recent study by the Levin group, using automated tracking of a large number of worms, showed that planarians are capable of environmental familiarity. Furthermore, their results suggest that environmental familiarity may be sustained through brain regeneration (Shomrat and Levin, 2013). Given the intrinsic variability in

behaviors among even clonal planarians, more studies of this sort will be necessary to further explore learning and memory in planarians. The ability to test toxicological effects on such cognitive tasks would greatly broaden the scope of planarian toxicology.

NEUROREGENERATION AND NEUROTOXICOLOGY

Because of their unique neuroregenerative capabilities, and the large array of organismal readouts, planarians have prompted a growing number of toxicologists to study developmental neurotoxicity of natural and synthetic toxicants in this system over more than three decades (Best and Morita, 1982; Schaeffer, 1993). This has included studies of known or suggested developmental toxicants or teratogens, such as ethanol (Hagstrom et al., 2015; Lowe et al., 2015), methylmercury (Best et al., 1981a), N,N-dimethlyformamide (DMF) (Zhang et al., 2013) and organophosphate pesticides (Hagstrom et al., 2015; Villar et al., 1993), known neurotoxicants, such as DMSO (Hagstrom et al., 2015; Stevens et al., 2015), and substances with unclear toxicity, such as the natural alkaloid berberine (Balestrini et al., 2014) or silver nanoparticles (Kustov et al., 2014). Although at first, planarian toxicology relied primarily on qualitative characterization of gross morphological developmental defects (Best and Morita, 1982; Best et al., 1981b; Villar et al., 1993), more recent work has begun to address developmental toxicity through quantitative and mechanistic approaches.

The oldest and simplest morphological characterization of regeneration has been used for decades in planarian toxicology studies (Villar et al., 1993). It was originally introduced by (Child, 1911) and consists of scoring the reappearance of head structures such as the eye spots or auricles, which typically reappear within 4-5 and 9 days of regeneration, respectively, in untreated animals (Inoue et al., 2004; Zhang et al., 2013) (Figure 1.4A). Comparison of different morphological endpoints provides increased sensitivity as certain chemicals may affect the

regeneration of one structure but not the other, as evidenced by the effect of DMF on auricle but not eye regeneration (Zhang et al., 2013). Auricles, however, are not equally striking in all planarian species, with *D. dorotocephala* and *D. tigrina* being the most apparent and *S. mediterranea* the least (Carter et al., 2015), limiting the applicability of this particular readout.

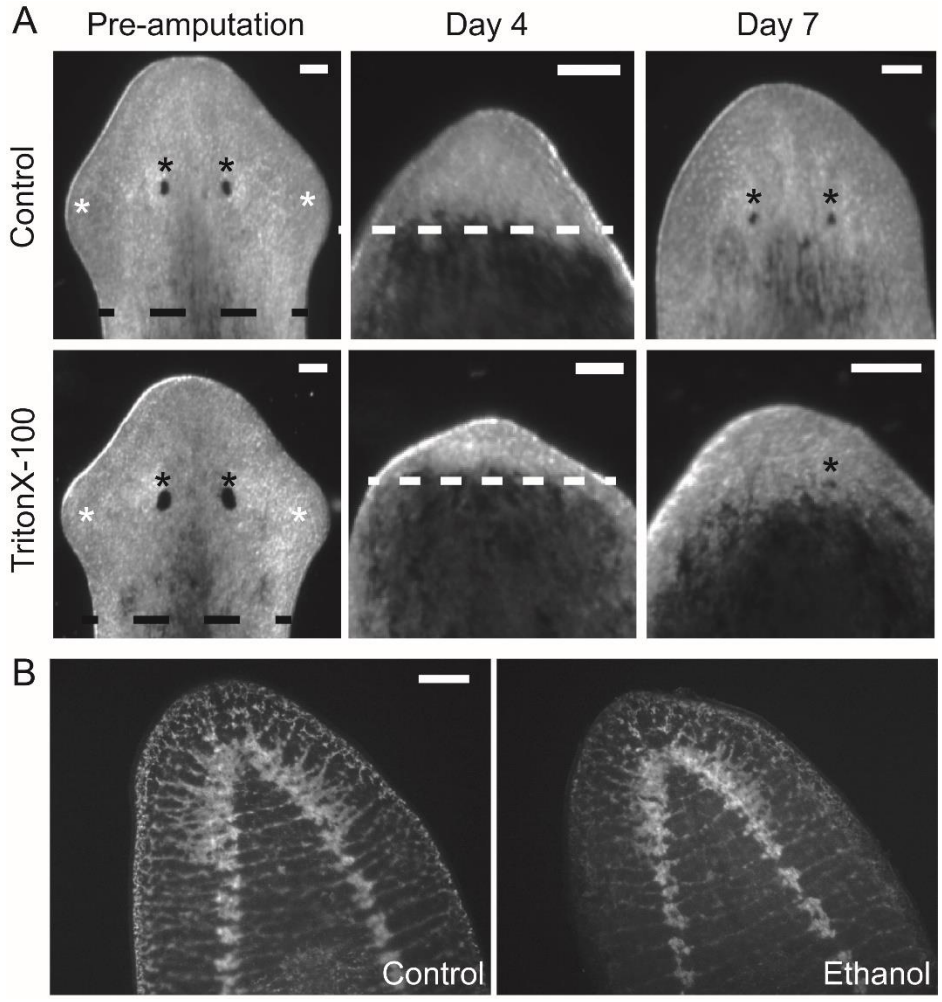

Figure 1.4. Morphological and anatomical readouts of developmental neurotoxicity in planarians. (A) Time-course of regeneration of control (top) and 15mg/ml TritonX-100 treated (bottom) worms. On day 1, animals are amputated along the black dotted line. On day 4, the unpigmented blastema (indicated by white dotted line) is clearly distinguishable. On later days, the reappearance of eyes (black asterisk) and auricles (white asterisk) can be scored. (B). Brain structure is visualized by immunohistochemistry with anti-synapsin antibody (anti- SYNORF1, Developmental Studies Hybridoma Bank) in control and 0.1% ethanol treated regenerating animals 2 weeks post-amputation. Scale bar: 0.1mm.

With the availability of higher resolution imaging techniques, quantitative morphological analysis has become possible. We and others have used high-resolution light microscopy to quantify the rate of blastema growth during regeneration (Balestrini et al., 2014; Hagstrom et al., 2015; Kustov et al., 2014). Because the blastema is unpigmented, it can easily be distinguished from the rest of the pigmented worm body, allowing for automated image analysis (Balestrini et al., 2014; Hagstrom et al., 2015; Kustov et al., 2014). However, since different sized worms may have different regeneration rates, the size of the blastema must be normalized by worm size. While other groups have normalized by the area of the worm (Balestrini et al., 2014; Kustov et al., 2014), we found that normalizing by the square of the worm's width was the most accurate way to account for size variation (Hagstrom et al., 2015). Blastema growth rate is best used as an indicator of general developmental toxicology (Hagstrom et al., 2015) since it is not specific to neurodevelopmental defects per se. For example, we found that while a neurotoxic pesticide, permethrin, did not affect blastema growth rate, it did delay eye reappearance (Hagstrom et al., 2015).

In addition, developmental neurotoxicity can be characterized based on the return of different behaviors. As neuronal subpopulations are regenerated, specific behavioral functions are restored, allowing researchers to differentiate between the effects of different chemicals on neuronal subpopulations. This unique opportunity provided by the planarian system was recognized as early as 1982 by Best and Morita (Best and Morita, 1982) and has since been utilized to study the effects of several neurotoxicants, including ethanol and DMSO (Hagstrom et al., 2015; Lowe et al., 2015; Stevens et al., 2015). However, as with studies on adult worms, these behavioral tests have been limited in their throughput and range of behaviors tested, primarily relying on pLMV and phototaxis (Balestrini et al., 2014; Lowe et al., 2015; Stevens et

al., 2015). In a recent paper, we have used automated COM tracking to measure gliding speed, locomotion type and thermotaxis (Hagstrom et al., 2015), as a first step to overcome this limitation.

Importantly, behavioral tests can be conducted in parallel on both regenerating and intact animals allowing determination of development-specific toxicity. For example, this type of comparison has led us and others to demonstrate the increased sensitivity of regenerating planarians to DMSO and ethanol (Hagstrom et al., 2015; Lowe et al., 2015; Stevens et al., 2015). These studies also demonstrate the importance of using multiple time points as developmental toxicity could be manifested as either the complete loss of a behavior or just delayed reacquisition.

In summary, automated behavioral testing allows for time and cost efficient screening of potential impairment of neuronal function before investigating the underlying mechanisms. Because the specific neurotransmitters and pathways involved in some of these behaviors have been determined (Inoue et al., 2004; Inoue et al., 2015; Umesono et al., 2011), characterizing behavioral neurodevelopmental defects upon neurotoxicant exposure can serve as a starting point for in-depth analysis of the responsible molecular mechanisms.

These mechanisms can begin to be delineated using molecular localization techniques, such as in situ hybridization and immunohistochemistry, to characterize effects on specific developing anatomical and cellular structures. Pan-neuronal markers such as synaptogamin and synapsin have been used to visualize gross toxic effects to the regenerating planarian brain (Balestrini et al., 2014; Hagstrom et al., 2015). Because of its structural simplicity, quantification of brain size can be used to quantify toxic effects on neuroregeneration (Balestrini et al., 2014; Hagstrom et al., 2015). However, this technique only provides information on gross anatomical

defects, as we found with DMSO, permethrin, chlorpyrifos, ethanol, methanol, TritonX-100 and acrylamide, but may not be sensitive enough to detect less obvious defects (Hagstrom et al., 2015). To address this issue, markers to specific neuronal sub-populations, such as the optic chiasm marker, arrestin/VC-1 (Agata et al., 1998), or the dopaminergic marker, tyrosine hydroxylase, have been used to identify toxic effects specific to certain structures or neuronal subpopulations (Balestrini et al., 2014; Nishimura et al., 2011). The recent availability of a large array of planarian markers to specific neuronal populations (Cebrià et al., 2002; Robb and Sánchez Alvarado, 2002; Ross et al., 2015) provides an exciting opportunity to perform more targeted mechanistic studies to analyze effects on specific neuronal subpopulations.

MECHANISMS AND METABOLISM

One of the strengths of the planarian system is the ability to connect morphological and behavioral effects on the organismal level with effects on the molecular and cellular levels. Arguably, these mechanistic findings may be the most relevant aspect of planarian toxicology studies to human toxicology, particularly as core mechanisms are conserved.

Researchers have begun to investigate how various neurotoxicants affect important conserved molecular targets in planarians (Table 1.1). For example, several studies have analyzed how the activity of different biomarkers changes during the course of toxicant exposure (Wu et al., 2012b; Yuan et al., 2012; Zhang et al., 2014; Zhang et al., 2015) using colorimetric assays on homogenates of exposed animals. This technically simple approach has been used to assay important neurological enzymes (acetylcholinesterase and monoamine oxidase (Wu and Li, 2015)) and antioxidants involved in controlling oxidative stress (catalase, superoxide dismutase, glutathione peroxidase (Yuan et al., 2012; Zhang et al., 2014; Zhang et al., 2015)). Furthermore, Yuan and colleagues found that while short exposures to moderate concentrations

of DMSO increased antioxidant activity, longer exposures and higher concentrations significantly decreased activity (Yuan et al., 2012). These results emphasize the importance of testing several concentrations at different time points during exposure for a mechanistic understanding of toxicity.

However, easily quantifiable biomarkers are not available for all toxicant-affected pathways. Thus, expression-based approaches, including in situ hybridization, quantitative RT-PCR and immunohistochemistry, have been used to characterize effects on a broader array of molecular pathways, such as cancer, neurodevelopment and stem cell maintenance (Stevens et al., 2015). These approaches allow for analysis of effects on a variety of cell and tissue types to narrow down precisely which populations are most affected and how. For example, using a combination of these approaches, Balestrini and colleagues reported that berberine toxicity may be a result of inhibition of metalloproteinases controlling extra-cellular matrix remodeling (Balestrini et al., 2014).

Expression-based techniques in the literature consist of PCR-based assays and structural localization studies. PCR-based techniques, such as quantitative RT-PCR allow for rapid analysis of many different pathways in a short time, which is necessary for studies wherein the mechanisms of toxicity are completely unknown (Balestrini et al., 2014). However, since toxicity may manifest through anatomical malformations due to the functional inhibition of molecular targets which may be independent of changes to mRNA levels, localization studies are useful to identify structural and anatomical toxic effects. Together, these techniques provide rapid insight into the mechanisms underlying the observed toxicity. By comparing morphological and behavioral readouts with biochemical and molecular readouts, we can begin to unravel how toxicants manifest their toxic effects.

Table 1.1. Mechanistic pathways tested in planarian toxicology.

Pathways	Markers	Technique	Toxicants tested	References
Oxidative stress	Catalase (CAT), superoxide dismutase (SOD), glutathione peroxidase (GPX), glutathione (GSH), reactive oxygen species (ROS)	Colorimetric assays	Surfactants	(Li 2008)
			DMSO	(Yuan et al. 2012)
			Cadmium	(Wu, Chen, et al. 2012)
			Copper	(Zhang et al. 2014)
			1-octyl-3-methylimidazolium bromide	(Zhang et al. 2015)
Lipid peroxidation	Malondialdehyde (MDA)	Colorimetric assays	Surfactants	(Li 2008)
			Cadmium	(Wu, Chen, et al. 2012)
			1-octyl-3-methylimidazolium bromide	(Zhang et al. 2015)
Apoptosis	Caspase-3	Colorimetric activity assays	Berberine	(Balestrini et al. 2014)
			Pain relievers	(Wu & Li 2015)
Nervous system	*Prohormone convertase 2 (pc2), synaptogamin (syt), glutamic acid decarboxylase (gad), retinal homeobox (rax), Orthopedia (otp),innexin-3 (inx3)*	RT-PCR, *in situ* hybridization	Berberine	(Balestrini et al. 2014)
			DMSO	(Stevens et al. 2015)
Stem cell proliferation and maintenance	Phospho-histone H3, *pcna, innexin -11 (inx-11),minichromosome maintenance-2 (mcm2), bruno*	Immunohistochemistry, RT-PCR	Berberine	(Balestrini et al. 2014)
			DMSO	(Stevens et al. 2015)
Cancer	*DNA mismatch repair (msh2), epidermal growth factor-1 (egfr1),forkhead box O(foxo), nour-darake (ndk)*	RT-PCR	DMSO	(Stevens et al. 2015)

Together, these techniques provide rapid insight into the mechanisms underlying the observed toxicity. By comparing morphological and behavioral readouts with biochemical and molecular readouts, we can begin to unravel how toxicants manifest their toxic effects.

To better extrapolate findings in planarians to understand how toxicants may affect human health, it must be determined whether planarians metabolize these xenobiotics similarly to humans. Planarians primarily absorb chemicals in the water by epithelial diffusion although chemicals can also be taken in by the pharynx (Balestrini et al., 2014; Kapu and Schaeffer, 1991). Several studies have demonstrated that a variety of toxicants are indeed absorbed by planarians. However, studies thus far have primarily looked at toxicants which are easily detected, such as berberine which is naturally fluorescent (Balestrini et al., 2014) or heavy metals which can be detected by atomic absorption spectrophotometry (Wu et al., 2012b). The distribution and bioaccumulation of xenobiotics within the planarian body appears to be chemical-specific, even among the same class, as cadmium was found to accumulate in the head while copper was evenly distributed throughout the planarian body (Wu et al., 2012b). As many chemicals are metabolically activated or converted after uptake, it remains to be determined whether planarians metabolize toxicants through similar mechanisms as humans. However, a few examples, particularly studies on the organophosphate chlorpyrifos (Hagstrom et al., 2015) and tobacco-specific nitrosamines (Wu et al., 2012a), exist demonstrating that metabolism and/or activation of certain chemicals occurs in planarians similarly to in humans.

In humans, a large portion of xenobiotic metabolism is performed by cytochrome P450s (Raunio et al., 2015). Analysis of the *S. mediterranea* genome (Robb et al., 2008) shows that these enzymes are present in planarians, although it remains to be determined how similar these enzymes are to their human homologs.

In conclusion, planarians are a powerful system to investigate mechanisms of toxicity, particularly those specific to neurodevelopment. Importantly, the availability of both behavioral and molecular tools allows effects on the molecular and cellular levels to be linked to their functional effect on behavior.

CHALLENGES AND OPPORTUNITIES: PLANARIAN NEUROTOXICOLOGY IN THE 21ST CENTURY

While planarian toxicology has led to important insights and the development of tools with broad applicability for planarian research, it faces several limitations to meet the growing needs of modern neurotoxicology. In our view, at least three challenges need to be met if planarians are to play a significant role in the future: screening throughput and robustness, unification of methodology and mechanistic analysis.

Challenge 1: Screening throughput and robustness

The main limitation to existing planarian toxicology studies is the lack of fully automated assays. Because most of the employed techniques rely on manual visual inspection of worms and are thus labor intensive, they have been largely applied to a single chemical (cadmium, phenol, DMF, DMSO or ammonia (Alonso and Camargo, 2011; Grebe and Schaeffer, 1991; Wu et al., 2012a; Zhang et al., 2013)), the interaction of two chemicals (DMSO + toxicant (Stevens et al., 2015), caffeine + guarana (Moustakas et al., 2015)) or, rarely, to a single class of chemicals (surfactants (Li, 2012), pain relievers (Wu and Li, 2015)). As a result, our current understanding of the effect of environmental toxicants on planarians is very limited. Recently, we have analyzed nine known neurotoxicants (Hagstrom et al., 2015), spanning from pesticides to surfactants and alcohols, which to our knowledge is the broadest quantitative toxicology study performed in planarians to date.

To achieve the necessary throughput, full automation of experimental assays and data analysis, with minimal human intervention, are indispensable. To achieve robustness, two conditions need to be met: (1) the number of endpoints must be large enough to enable distinction between classes of neurotoxicants and (2) there must be enough replicates to eliminate false positives and experimental artefacts (Hsieh et al., 2015). The need for replicates will be easily met once automation is realized. To achieve the required repertoire of screening endpoints, we must both automate existing manual readouts and look for novel readouts that are accessible to quantification and automation. To date, the planarian community collectively has built up an array of valuable endpoints, including both morphological (e.g. pharynx extrusion, C-shape, hyperkinesia, eye defects) as well as behavioral (e.g. thermotaxis, phototaxis, chemotaxis, scrunching, environmental familiarity) readouts that are amenable to automated quantification via image analysis. The execution of the experiments leading to these measurements, however, remains largely manual or semi-automated. Therefore, a major effort will be required to find engineering solutions to integrate these assays into a fully automated screening platform. Not all assays will be amenable to such an automated approach. It is therefore important to determine which "array of assays" will provide the necessary coverage of readouts and can be standardized across research groups through automated solutions or agreed-upon protocols for semi-automated setups.

Challenge 2: Unification of methodology

It is challenging, if not impossible, to compare results on the same neurotoxicant from existing studies, because various research groups use different planarian species – most commonly *Dugesia dorotocephala* (Best et al., 1981a; Kapu and Schaeffer, 1991; Villar et al., 1993), *Dugesia tigrina* (Knakievicz and Ferreira, 2008; Moustakas et al., 2015; Ramakrishnan et

al., 2014), *Schmidtea mediterranea* (Lowe et al., 2015; Plusquin et al., 2012; Stevens et al., 2015) and *Dugesia japonica* (Hagstrom et al., 2015; Li, 2012; Yuan et al., 2012; Zhang et al., 2013) - and different species may have different susceptibilities and behavioral responses (Rivera and Perich, 1994). There also exists a lack of uniformity in the field with research groups applying different methods and using only some of the described readouts of the GS- and Wu scoring systems, particularly lethality and overall activity (measured by pLMV) (Alonso and Camargo, 2011; Pagán et al., 2006; Pagán et al., 2009). Additionally, researchers have assessed varying durations of exposure, spanning from several minutes (Pagán et al., 2006) to over a month (Alonso and Camargo, 2011). As we have shown (Hagstrom et al., 2015), acute and chronic compound toxicity can differ, but it is difficult to predict these differences a priori. This heterogeneity makes direct comparisons of results on the same toxicants basically impossible. Thus, one of the major challenges for the future is to standardize a battery of tests and one or two species for conducting toxicology studies. The zebrafish community faces similar difficulties, whereby labs have developed independent screening criteria and methodologies and the exact experimental details are often not reported (Padilla et al., 2011). Since, for planarian toxicology, tool development is an ongoing effort, we have the possibility to streamline procedures at an early stage within the planarian community.

Challenge 3: Mechanistic analysis

While HTS of compounds for toxicological profiling is valuable by itself, an animal model greatly gains in value if it can also shed light on the molecular mechanism underlying a compound's neurotoxicity. In principle, the planarian system promises to allow for such mechanistic insight because the planarian CNS remains tractable on the cellular level and molecular pathways are likely to be simpler than in higher vertebrates. Very few examples exist

(Balestrini et al., 2014; Stevens et al., 2015; Yuan et al., 2012), however, which link the phenotypic readouts of toxicants to an underlying molecular mechanism. Although several of the core pathways commonly affected by toxicants are conserved in planarians, more studies need to be conducted investigating whether toxicants' targets and metabolism in planarians are comparable to those affected in mammals. This would be most easily achieved by studying well-characterized toxicants, such as the ToxCast Phase I chemicals (http://www.epa.gov/chemical-research/toxicity-forecasting), to determine if developmental neurotoxicity in planarians correlates with developmental neurotoxicity in humans and other mammals and occurs through similar mechanisms. Such studies would provide a framework to classify chemicals with unknown toxicity and validate the relevancy of toxicology screens in planarians to provide a first indication of potential toxicity in humans.

In addition, modern technologies such as RNA-seq, which is already applied to the planarian system for stem cell studies (Scimone et al., 2014; van Wolfswinkel et al., 2014), need to be tested in the context of toxicological screening to assay their value for identifying molecular targets. Currently applied techniques for studying the molecular mechanisms underlying toxicity, such as in situ hybridization and immunohistochemistry, albeit necessary for gaining insight into possible anatomical changes to the nervous system, are not amenable to HTS. In the interim, quantitative RT-PCR is being used by some as an intermediate throughput solution (Balestrini et al., 2014; Stevens et al., 2015).

In summary, if we are able to meet these three challenges, even partially, exciting pay-offs and opportunities await, some of which go well beyond the field of neurotoxicology. For example, HTS behavioral screening will be an important and indispensable tool for planarian pharmacology. Finally, robust behavioral readouts are necessary to characterize RNAi

phenotypes. To date, most of these studies have remained qualitative. Having access to a battery of fast and reliable quantitative tests to assert the animal's behavior following gene knockdown will accelerate and improve accuracy in phenotype descriptions and shed new light on planarian biology.

The future of planarian neurotoxicology is bright, but there is a lot of work to be done if we are up to the challenge.

ACKNOWLEDGEMENTS

Chapter 1, in full, is a reprint of the material as it appears in Hagstrom, Danielle; Cochet-Escartin, Olivier; and Collins, Eva-Maria S. “Planarian brain regeneration as a model system for developmental neurotoxicology”, Regeneration, vol. 3, 2016. The final version is available online at: https://onlinelibrary.wiley.com/doi/full/10.1002/reg2.52. The authors retain copyright of this manuscript, which is an open access article permitting the use herein. Danielle Hagstrom, Olivier Cochet-Escartin, and Eva-Maria S. Collins co-wrote and edited the manuscript. Danielle Hagstrom was the primary investigator and author of this paper.

REFERENCES

Agata, K., Soejima, Y., Kato, K., Kobayashi, C., Umesono, Y. and Watanabe, K. (1998). Structure of the planarian central nervous system (CNS) revealed by neuronal cell markers. *Zoolog. Sci.* **15**, 433–440.

Alonso, A. and Camargo, J. A. (2011). The freshwater planarian Polycelis felina as a sensitive species to assess the long-term toxicity of ammonia. *Chemosphere* **84**, 533–7.

Balestrini, L., Isolani, M. E., Pietra, D., Borghini, A., Bianucci, A. M., Deri, P. and Batistoni, R. (2014). Berberine exposure triggers developmental effects on planarian regeneration. *Sci. Rep*. **4**, 4914.

Best, J. B. and Morita, M. (1982). Planarians as a model system for in vitro teratogenesis studies. *Teratog. Carcinog. Mutagen*. **2**, 277–91.

Best, J. B., Morita, M. and Abbotts, B. (1981a). Dugesia dorotocephala, to chlordane. *Bull. Environm. Contam. Toxicol* **26**, 502–507.

Best, J. B., Morita, M. and Abbotts, B. (1981b). Acute toxic responses of the freshwater planarian, Dugesia dorotocephala, to Chlordane. *Bull. Environm. Contam. Toxicol* **26**, 502–507.

Block, R. A. and McConnell, J. V (1967). Classically conditioned discrimination in the planarian, Dugesia dorotocephala. *Nature* **215**, 1465–6.

Buchanan, J. W. (1935). An analysis of physiological states responsible for antero-posterior disintegration in Planaria dorotocephala. *Protoplasma* **22**, 497–512.

Buttarelli, F. R., Pontieri, F. E., Margotta, V. and Palladini, G. (2000). Acetylcholine/dopamine interaction in planaria. *Comp. Biochem. Physiol. C. Toxicol. Pharmacol.* **125**, 225–31.

Buttarelli, F. R., Pontieri, F. E., Margotta, V. and Palladini, G. (2002). Cannabinoid-induced stimulation of motor activity in planaria through an opioid receptor-mediated mechanism. *Prog. Neuro-Psychopharmacology Biol. Psychiatry* **26**, 65–68.

Buttarelli, F. R., Pellicano, C. and Pontieri, F. E. (2008). Neuropharmacology and behavior in planarians: translations to mammals. *Comp. Biochem. Physiol. C. Toxicol. Pharmacol.* **147**, 399–408.

Carter, J. A., Lind, C. H., Truong, M. P. and Collins, E.-M. S. (2015). To each his own. J. *Stat. Phys.* **161**, 250–272.

Cebrià, F. (2007). Regenerating the central nervous system: how easy for planarians! *Dev. Genes Evol.* **217**, 733–748.

Cebrià, F. and Newmark, P. A. (2005). Planarian homologs of netrin and netrin receptor are required for proper regeneration of the central nervous system and the maintenance of nervous system architecture. *Development* **132**, 3691–703.

Cebrià, F., Nakazawa, M., Mineta, K., Ikeo, K., Gojobori, T. and Agata, K. (2002). Dissecting planarian central nervous system regeneration by the expression of neural-specific genes. *Dev. Growth Differ.* **44**, 135–46.

Child, C. M. (1909). The regulatory change of shape in Planaria dorotocephala. *Biol. Bull.* **16**, 277–296.

Child, C. M. (1911). Experimental control of morphogenesis in the regulation of planaria. *Biol. Bull.* **20**, 309–331.

Cochet-Escartin, O., Mickolajczk, K. J. and Collins, E.-M. S. (2015). Scrunching: a novel escape gait in planarians. *Phys. Biol.* **12**, 055001.

Currie, K. W. and Pearson, B. J. (2013). Transcription factors lhx1/5-1 and pitx are required for the maintenance and regeneration of serotonergic neurons in planarians. *Development* **140**, 3577–88.

Farrell, M. S., Gilmore, K., Raffa, R. B. and Walker, E. A. (2008). Behavioral characterization of serotonergic activation in the flatworm Planaria. *Behav. Pharmacol.* **19**, 177–82.

Grebe, E. and Schaeffer, D. J. (1991). Planarians in toxicology, standardization of a rapid neurobehavioral toxicity test using phenol in a crossover study. *Bull. Environ. Contam. Toxicol.* **46**, 866–70.

Hagstrom, D., Cochet-Escartin, O., Zhang, S., Khuu, C. and Collins, E.-M. S. (2015). Freshwater planarians as an alternative animal model for neurotoxicology. *Toxicol. Sci.* **147**, 270–85.

Hsieh, J.-H., Sedykh, A., Huang, R., Xia, M. and Tice, R. R. (2015). A data analysis pipeline accounting for artifacts in Tox21 quantitative high-throughput screening assays. *J. Biomol. Screen.* **20**, 887–97.

Inoue, T., Kumamoto, H., Okamoto, K., Umesono, Y., Sakai, M., Sánchez Alvarado, A. and Agata, K. (2004). Morphological and functional recovery of the planarian photosensing system during head regeneration. *Zoolog. Sci.* **21**, 275–83.

Inoue, T., Yamashita, T. and Agata, K. (2014). Thermosensory signaling by TRPM is processed by brain serotonergic neurons to produce planarian thermotaxis. *J Neurosci.* **34**, 5701–14.

Inoue, T., Hoshino, H., Yamashita, T., Shimoyama, S. and Agata, K. (2015). Planarian shows decision-making behavior in response to multiple stimuli by integrative brain function. *Zool. Lett.* **1**, 1–7.

Jeanray, N., Marée, R., Pruvot, B., Stern, O., Geurts, P., Wehenkel, L. and Muller, M. (2015). Phenotype classification of zebrafish embryos by supervised learning. *PLoS One* **10**, e0116989.

Kapu, M. M. and Schaeffer, D. J. (1991). Planarians in toxicology. Responses of asexual Dugesia dorotocephala to selected metals. *Bull. Environ. Contam. Toxicol.* **47**, 302–7.

Kartry, A. L., Keith-Lee, P. and Morton, W. D. (1964). Planaria: Memory transfer through cannibalism reexamined. *Science* **146**, 274–275.

Knakievicz, T. (2014). Planarians as invertebrate bioindicators in freshwater environmental quality: the biomarkers approach. *Ecotoxicol. Environ. Contam*. **9**, 1–12.

Knakievicz, T. and Ferreira, H. B. (2008). Evaluation of copper effects upon Girardia tigrina freshwater planarians based on a set of biomarkers. *Chemosphere* **71**, 419–28.

Kustov, L., Tiras, K., Al-Abed, S., Golovina, N. and Ananyan, M. (2014). Estimation of the toxicity of silver nanoparticles by using planarian flatworms. *Altern. Lab. Anim.* **42**, 51–8.

Lambrus, B. G., Cochet-Escartin, O., Gao, J., Newmark, P. A., Collins, E.-M. S. and Collins, J. J. (2015). Tryptophan hydroxylase is required for eye melanogenesis in the planarian Schmidtea mediterranea. *PLoS One* **10**, e0127074.

Lein, P., Silbergeld, E., Locke, P. and Goldberg, A. M. (2005). In vitro and other alternative approaches to developmental neurotoxicity testing (DNT). *Environ. Toxicol. Pharmacol.* **19**, 735–44.

Li, M.-H. (2008). Effects of nonionic and ionic surfactants on survival, oxidative stress, and cholinesterase activity of planarian. *Chemosphere* **70**, 1796–803.

Li, M.-H. (2012). Survival, mobility, and membrane-bound enzyme activities of freshwater planarian, Dugesia japonica, exposed to synthetic and natural surfactants. *Environ. Toxicol. Chem*. **31**, 843–50.

Lowe, J. R., Mahool, T. D. and Staehle, M. M. (2015). Ethanol exposure induces a delay in the reacquisition of function during head regeneration in Schmidtea mediterranea. *Neurotoxicol. Teratol.* **48**, 28–32.

McConnell, J. V (1962). Memory transfer through cannibalism in planarians. *J. Neuropsychiatr.* **3**, 542–548.

McConnell, J. V, Jacobson, A. L. and Kimble, D. P. (1959). The effects of regeneration upon retention of a conditioned response in the planarian. *J. Comp. Physiol. Psychol.* **52**, 1–5.

Mineta, K., Nakazawa, M., Cebria, F., Ikeo, K., Agata, K. and Gojobori, T. (2003). Origin and evolutionary process of the CNS elucidated by comparative genomics analysis of planarian ESTs. *Proc. Natl. Acad. Sci. U. S. A.* **100**, 7666–71.

Moustakas, D., Mezzio, M., Rodriguez, B. R., Constable, M. A., Mulligan, M. E. and Voura, E. B. (2015). Guarana provides additional stimulation over caffeine alone in the planarian model. *PLoS One* **10**, e0123310.

Newmark, P. A. and Sánchez Alvarado, A. (2002). Not your father's planarian: a classic model enters the era of functional genomics. *Nat. Rev. Genet*. **3**, 210–219.

Nishimura, K., Kitamura, Y., Taniguchi, T. and Agata, K. (2010). Analysis of motor function modulated by cholinergic neurons in planarian dugesia japonica. *Neuroscience* **168**, 18–30.

Nishimura, K., Inoue, T., Yoshimoto, K., Taniguchi, T., Kitamura, Y. and Agata, K. (2011). Regeneration of dopaminergic neurons after 6-hydroxydopamine-induced lesion in planarian brain. *J. Neurochem.* **119**, 1217–1231.

Padilla, S., Hunter, D. L., Padnos, B., Frady, S. and MacPhail, R. C. (2011). Assessing locomotor activity in larval zebrafish: Influence of extrinsic and intrinsic variables. *Neurotoxicol. Teratol.* **33**, 624–30.

Pagán, O. R., Rowlands, A. L. and Urban, K. R. (2006). Toxicity and behavioral effects of dimethylsulfoxide in planaria. *Neurosci. Lett.* **407**, 274–8.

Pagán, O. R., Coudron, T. and Kaneria, T. (2009). The flatworm planaria as a toxicology and behavioral pharmacology animal model in undergraduate research experiences. *J. Undergrad. Neurosci. Educ.* **7**, A48-52.

Pagán, O. R., Baker, D., Deats, S., Montgomery, E., Tenaglia, M., Randolph, C., Kotturu, D., Tallarida, C., Bach, D., Wilk, G., et al. (2012). Planarians in pharmacology: parthenolide is a specific behavioral antagonist of cocaine in the planarian Girardia tigrina. *Int. J. Dev. Biol.* **56**, 193–6.

Passarelli, F., Merante, A., Pontieri, F. E., Margotta, V., Venturini, G. and Palladini, G. (1999). Opioid–dopamine interaction in planaria: a behavioral study. *Comp. Biochem. Physiol. Part C Pharmacol. Toxicol. Endocrinol.* **124**, 51–55.

Plusquin, M., Stevens, A.-S., Van Belleghem, F., Degheselle, O., Van Roten, A., Vroonen, J., Blust, R., Cuypers, A., Artois, T. and Smeets, K. (2012). Physiological and molecular characterisation of cadmium stress in Schmidtea mediterranea. *Int. J. Dev. Biol.* **56**, 183–91.

Prá, D., Lau, A. H., Knakievicz, T., Carneiro, F. R. and Erdtmann, B. (2005). Environmental genotoxicity assessment of an urban stream using freshwater planarians. *Mutat. Res.* **585**, 79–85.

Raffa, R. and Rawls, S. eds. (2008). Planaria: A model for drug action and abuse. Austin: Landes Bioscience.

Raffa, R. B. and Desai, P. (2005). Description and quantification of cocaine withdrawal signs in Planaria. *Brain Res.* **1032**, 200–2.

Raffa, R. B. and Valdez, J. M. (2001). Cocaine withdrawal in Planaria. *Eur. J. Pharmacol.* **430**, 143–145.

Raffa, R. B., Holland, L. J. and Schulingkamp, R. J. (2001). Quantitative assessment of dopamine D2 antagonist activity using invertebrate (Planaria) locomotion as a functional endpoint. *J. Pharmacol. Toxicol. Methods* **45**, 223–226.

Raffa, R. B., Stagliano, G. W. and Umeda, S. (2003). kappa-Opioid withdrawal in Planaria. *Neurosci. Lett.* **349**, 139–42.

Ramakrishnan, L., Amatya, C., DeSaer, C. J., Dalhoff, Z. and Eggerichs, M. R. (2014). Galantamine reverses scopolamine-induced behavioral alterations in Dugesia tigrina. *Invert. Neurosci.* **14**, 91–101.

Raunio, H., Kuusisto, M., Juvonen, R. O. and Pentikäinen, O. T. (2015). Modeling of interactions between xenobiotics and cytochrome P450 (CYP) enzymes. *Front. Pharmacol.* **6**, 123.

Rivera, V. R. and Perich, M. J. (1994). Effects of water quality on survival and reproduction of four species of planaria (Turbellaria: Tricladida). *Invertebr. Reprod. Dev.* **25**, 1–7.

Robb, S. M. and Sánchez Alvarado, A. (2002). Identification of immunological reagents for use in the study of freshwater planarians by means of whole-mount immunofluorescence and confocal microscopy. *Genesis* **32**, 293–8.

Robb, S. M. C., Ross, E. and Sánchez Alvarado, A. (2008). SmedGD: the Schmidtea mediterranea genome database. *Nucleic Acids Res.* **36**, D599-606.

Ross, K. G., Omuro, K. C., Taylor, M. R., Munday, R. K., Hubert, A., King, R. S. and Zayas, R. M. (2015). Novel monoclonal antibodies to study tissue regeneration in planarians. *BMC Dev. Biol.* **15**, 2.

Schaeffer, D. J. (1993). Planarians as a model system for in vivo tumorigenesis studies. *Ecotoxicol. Environ. Saf.* **25**, 1–18.

Scimone, M. L., Kravarik, K. M., Lapan, S. W. and Reddien, P. W. (2014). Neoblast specialization in regeneration of the planarian Schmidtea mediterranea. *Stem cell reports* **3**, 339–52.

Shomrat, T. and Levin, M. (2013). An automated training paradigm reveals long-term memory in planarians and its persistence through head regeneration. *J. Exp. Biol.* **216**, 3799–810.

Stevens, A.-S., Pirotte, N., Plusquin, M., Willems, M., Neyens, T., Artois, T. and Smeets, K. (2015). Toxicity profiles and solvent-toxicant interference in the planarian Schmidtea mediterranea after dimethylsulfoxide (DMSO) exposure. *J. Appl. Toxicol.* **35**, 319–26.

Talbot, J. and Schötz, E.-M. (2011). Quantitative characterization of planarian wild-type behavior as a platform for screening locomotion phenotypes. *J. Exp. Biol.* **214**, 1063–1067.

Thompson, R. and McConnell, J. (1955). Classical conditioning in the planarian, Dugesia dorotocephala. *J. Comp. Physiol. Psychol.* **48**, 65–8.

Umesono, Y., Tasaki, J., Nishimura, K., Inoue, T. and Agata, K. (2011). Regeneration in an evolutionarily primitive brain--the planarian Dugesia japonica model. *Eur. J. Neurosci.* **34**, 863–9.

van Wolfswinkel, J. C., Wagner, D. E. and Reddien, P. W. (2014). Single-cell analysis reveals functionally distinct classes within the planarian stem cell compartment. *Cell Stem Cell* **15**, 326–39.

Venturini, G., Stocchi, F., Margotta, V., Ruggieri, S., Bravi, D., Bellantuono, P. and Palladini, G. (1989). A pharmacological study of dopaminergic receptors in planaria. *Neuropharmacology* **28**, 1377–1382.

Villar, D., Li, M. H. and Schaeffer, D. J. (1993). Toxicity of organophosphorus pesticides to Dugesia dorotocephala. *Bull. Environ. Contam. Toxicol.* **51**, 80–7.

Wählby, C., Kamentsky, L., Liu, Z. H., Riklin-Raviv, T., Conery, A. L., O'Rourke, E. J., Sokolnicki, K. L., Visvikis, O., Ljosa, V., Irazoqui, J. E., et al. (2012). An image analysis toolbox for high-throughput C. elegans assays. *Nat. Methods* **9**, 714–716.

Walker, D. R. and Milton, G. A. (2013). Memory transfer vs. sensitization in cannibal planarians. *Psychon. Sci.* **5**, 293–294.

Wilson, M. P. and Schwarzman, M. R. (2009). Toward a new U.S. chemicals policy: rebuilding the foundation to advance new science, green chemistry, and environmental health. *Environ. Health Perspect.* **117**, 1202–9.

Wu, J.-P. and Li, M.-H. (2015). Inhibitory effects of pain relief drugs on neurological enzymes: implications on their potential neurotoxicity to aquatic animals. *Environ. Toxicol. Pharmacol.* **39**, 898–905.

Wu, J.-P., Li, M.-H., Chen, J.-S. and Lee, H.-L. (2012a). In vivo and in vitro metabolism of tobacco-specific nitrosamine, 4-(methylnitrosamino)-1-(3-pyridyl)-1-butanone (NNK), by the freshwater planarian, Dugesia japonica. *Chemosphere* **87**, 1341–7.

Wu, J.-P., Chen, H.-C. and Li, M.-H. (2012b). Bioaccumulation and toxicodynamics of cadmium to freshwater planarian and the protective effect of N-acetylcysteine. *Arch. Environ. Contam. Toxicol.* **63**, 220–9.

Yamin, H. G., Stern, E. A. and Cohen, D. (2013). Parallel processing of environmental recognition and locomotion in the mouse striatum. *J. Neurosci.* **33**, 473–84.

Yuan, Z., Zhao, B. and Zhang, Y. (2012). Effects of dimethylsulfoxide on behavior and antioxidant enzymes response of planarian Dugesia japonica. *Toxicol. Ind. Health* **28**, 449–57.

Zhang, J., Yuan, Z., Zheng, M., Sun, Y., Wang, Y. and Yang, S. (2013). Effects of N,N-dimethylformamide on behaviour and regeneration of planarian Dugesia japonica. *Toxicol. Ind. Health* **29**, 753–60.

Zhang, X., Zhang, B., Yi, H. and Zhao, B. (2014). Mortality and antioxidant responses in the planarian (Dugesia japonica) after exposure to copper. *Toxicol. Ind. Health* **30**, 123–31.

Zhang, H.-C., Shi, C.-Y., Sun, L.-Q., Wang, F. and Chen, G.-W. (2015). Toxic effects of ionic liquid 1-octyl-3-methylimidazolium bromide on the antioxidant defense system of freshwater planarian, Dugesia japonica. *Toxicol. Ind. Health.* **32**, 1675-1683.

Chapter 2: Freshwater planarians as an alternative animal model for neurotoxicology

Reprinted from: Hagstrom, Danielle; Cochet-Escartin, Olivier; Zhang, Siqi; Khuu, Cindy; and Collins, Eva-Maria S. "Freshwater planarians as an alternative animal model for neurotoxicology", Toxicological Sciences, vol. 147, 2015.

Supplementary materials can be accessed online at:

https://academic.oup.com/toxsci/article/147/1/270/1642148#supplementary-data

ABSTRACT

Traditional toxicology testing has relied on low-throughput, expensive mammalian studies; however, timely testing of the large number of environmental toxicants requires new *in vitro* and *in vivo* platforms for inexpensive medium to high-throughput screening. Herein, we describe the suitability of the asexual freshwater planarian *Dugesia japonica* as a new animal model for the study of developmental neurotoxicology. As these asexual animals reproduce by binary fission, followed by regeneration of missing body structures within approximately one week, development and regeneration occur through similar processes allowing us to induce neurodevelopment "at will" through amputation. This short time-scale and the comparable sizes of full and regenerating animals enable parallel experiments in adults and developing worms to determine development-specific aspects of toxicity. Because the planarian brain, despite its simplicity, is structurally and molecularly similar to the mammalian brain, we are able to ascertain neurodevelopmental toxicity which is relevant to humans. As a proof of concept, we developed a five-step semi-automatic screening platform to characterize the toxicity of nine known neurotoxicants (consisting of common solvents, pesticides, and detergents) and a neutral agent, glucose, and quantified effects on viability, stimulated and unstimulated behavior, regeneration, and brain structure. Comparisons of our findings with other alternative toxicology animal models, namely zebrafish larvae and nematodes, demonstrated that planarians are comparably sensitive to the tested chemicals. Additionally, we found that certain compounds induced adverse effects specifically in developing animals. We thus conclude that planarians offer new, complementary opportunities for developmental neurotoxicology animal models.

INTRODUCTION

The "Tox21" initiative (http://epa.gov/ncct/Tox21/), a multi-agency partnership was launched in 2008 to establish a new area in toxicology testing, away from low-throughput, high-cost mammalian models, toward *in vitro* and alternative non-mammalian animal systems amenable to low-cost, high-throughput screens (HTS) (Vliet, 2011). To achieve this, the ToxCast program (http://www.epa.gov/ncct/toxcast/) was launched, using a large-scale *in vitro* HTS robotic approach to evaluate thousands of chemicals for a variety of potential molecular and cellular toxicity effects (Judson et al., 2010). However, the inherently artificial environment and lack of biological complexity in *in vitro* HTS makes them difficult to directly connect with organism-level toxicity (Knight et al., 2009). Therefore, as the second component of the Tox21 agenda, medium-throughput-screening (MTS) animal models were introduced to complement HTS assays (Collins et al., 2008). Because each animal model has specific strengths and weaknesses, in terms of throughput, cost, and homology to humans, any one system is insufficient to cover all aspects of toxicity in humans, making comparative analyses across diverse animals important for the proper prioritization of toxicants for further study and development of human exposure guidelines.

In this study, we establish the suitability of freshwater planarians, famous for their regenerative capabilities due to a large population of adult pluripotent stem cells (Cebrià, 2007; Reddien and Sánchez Alvarado, 2004; Rink, 2013; Scimone et al., 2014; Wagner et al., 2011), as a new model for MTS toxicology studies. In terms of organismal complexity, planarians occupy an intermediate position, between the newly developed alternative toxicology animal models zebrafish and nematodes (Boyd et al., 2012; Peterson et al., 2008; Selderslaghs et al., 2009; Sipes et al., 2011; Truong et al., 2014) and possess unique features that make them especially well-

suited for developmental neurotoxicology. Like zebrafish and nematodes, freshwater planarians are small, inexpensive and easy to breed, sensitive to chemicals in the water, and develop quickly (in approximately 1 week). For the asexual *Dugesia japonica* species used in this study, development and regeneration are similar processes as these animals reproduce by transverse fission creating a head and a tail piece, each subsequently regenerating all missing body structures (Sakurai et al., 2012). We can thus induce development "at will" by amputation in a purely clonal population.

What renders freshwater planarians unique and particularly well-suited for developmental neurotoxicology is our ability to simultaneously study genetically identical adult and developing animals, allowing us to directly compare the effect of potential toxicants on the adult and developing brain, without possible complications from the variability of genetic factors. In addition, the planarian nervous system, consisting of a bi-lobed cephalic ganglion (brain) and ventral nerve cords, is much more complex than that of nematodes, but simpler than that of zebrafish. It remains tractable on the cellular level (~10000 neurons) while having sufficient complexity and homology, sharing the same neuronal subpopulations and neurotransmitters as the mammalian brain, to be relevant to human studies (Buttarelli et al., 2008; Cebrià, 2007; Cebrià et al., 2002). In fact, the planarian brain is thought to be more similar to the vertebrate brain than to other invertebrate brains in terms of structure and function (Buttarelli et al., 2008). Most notably, 95% of nervous system related genes in *Dugesia japonica* have homologs in humans (Mineta et al., 2003). Thus, by studying planarian brain development, we can gain insight into key mechanisms for human brain development.

As a result, various species of freshwater planarians have previously been used for pharmacological and toxicological studies (Lowe et al., 2015; Pagán et al., 2006; Stevens et al.,

2014; Talbot and Schötz, 2011). These studies, albeit primarily focused on a single compound, low-throughput, and largely qualitative in nature, demonstrated that planarians are highly sensitive to certain chemicals and that toxicity can be assessed via behavioral and morphological readouts.

In this study, we evaluated the potential of the planarian system as a new model for MTS toxicology studies by studying nine known neurotoxicants and the neutral compound, glucose. Using a proof-of-concept screen, we determined and characterized, for these compounds, the lethal dose, systemic and behavioral effects, and neurotoxicity, resulting from exposure in adult and developing animals. We show that *D. japonica* has comparable sensitivity to other model systems, as evaluated by a quantitative comparison of our data with data from zebrafish and nematodes. Furthermore, by studying full and developing animals simultaneously, we detected toxicity specific to the developing brain. Based on these results, we conclude that planarians are well-suited for screening potential developmental neurotoxicants and allow for the addition of a new alternative animal model to the field of neurotoxicology.

MATERIALS AND METHODS

Test animals

Freshwater planarians of the species *Dugesia japonica* were used for all tests. Planarians were stored in 1x planarian water (Cebrià and Newmark, 2005) in Tupperware containers at 20°C in a Panasonic refrigerated incubator in the dark. Animals were fed organic beef liver once a week and cleaned twice a week when not used for experiments (Dunkel et al., 2011). Test animals were randomly selected from a healthy population. For all experiments, only fully regenerated worms which had not been fed within one week and which were found gliding normally in the container were used. Worms were manually selected to fall within a certain range of sizes and we found them, after automated size measurement, to be 3.4mm +/- 0.7mm (mean +/- SD) in length. To study regenerating animals, on day 1, intact worms were amputated with an ethanol-sterilized razor blade no more than 3 hours before an assay was started.

Test compounds

The following were tested and reconstituted according to manufacturer guidelines as described below: dimethyl sulfoxide (DMSO, Sigma Aldrich, D2650), permethrin (Sigma Aldrich, 44-2748), chlorpyrifos (Fluka Analytical, 45395), dichlorvos (Chem Service, N-11675), ethanol (Roptec, V1001), methanol (Fisher Scientific, A454), TritonX-100 (Alfa Aesar, A16046), sodium dodecyl sulfate (SDS, Promega, H5113), acrylamide (Tokyo Chemical Industry, A1132), and D-glucose (Sigma-Aldrich, D9434). All solutions were prepared in 1x planarian water. Chemicals which were soluble in water, *i.e.* DMSO, dichlorvos, ethanol, methanol, TritonX-100, SDS, acrylamide, and D-glucose, were added directly to planarian water to obtain the desired concentrations. Stocks of 500mM chlorpyrifos and 100mM permethrin were prepared in 100% DMSO such that, in the final working solutions, the DMSO concentration did

not exceed 0.1%. All solutions were checked with a pH-meter and were found to fall within a reasonable range (pH 7.39 – 7.75). Working solutions were stored at room temperature. DMSO, acrylamide, and permethrin solutions were stored in the dark. To mitigate diminishing effects due to evaporation, all ethanol solutions were replaced daily. Table 2.1 summarizes tested chemicals and concentrations.

Table 2.1. Chemicals and concentration ranges tested.

Compound	**CAS**	**Source**	**Purity (%)**	**Concentration range tested**
Acrylamide	79-06-1	Tokyo Chemical Industry	98.0	10μM-100mM
Chlorpyrifos	2921-88-2	Fluka Analytical	99.7	0.1-500μM
Dichlorvos	62-73-7	Chem Service	97.8	10nM-8μM
DMSO	67-68-5	Sigma Aldrich	99.7	0.05-15%
Ethanol	64-17-5	Roptec	100	0.01%-15%
Glucose	50-99-7	Sigma-Aldrich	99.5	55μM-550mM
Methanol	67-56-1	Fisher Scientific	99.9	0.5%-7%
Permethrin	52645-53-1	Sigma-Aldrich	N/A	10-1000μM
SDS	151-21-3	Promega	99.5	0.2-6mg/L
TritonX-100	9002-93-1	Alfa Aesar	N/A	5-50mg/L

Lethality assay

The first step in determining the toxicity of a compound was a broad range screen on its effect on planarian health and regeneration. Small planarians were selected as described above and distributed into a 48-well plate (Falcon) such that each well contained one worm. Each row was filled with half full and half recently amputated (less than 3h) animals. Once a plate was

completely filled with worms, the planarian water was removed and 200µL of the appropriate chemical solution was added to each well. For each concentration of a chemical, at least two independent experiments with 8 full worms and 8 regenerating worms were performed as biological replicates, thus at least 16 full and regenerating animals were assayed for each condition.

Animals were stored in the plate for 15 days at room temperature in the dark. Worms which did not move even after gentle prodding or agitation of the water were considered dead. Deaths were manually inspected and tallied in Microsoft Excel. The resulting data was manually imported into MATLAB (Mathworks) for plotting and analysis. The fraction of dead worms as a function of concentration at days 2, 4, 8, and 15 was plotted and fitted using (Selderslaghs et al., 2009):

$$y = \left(\frac{1}{1 + 10^{(\log LC_{50} - x) \times \text{ Hill slope}}}\right)$$

with *y* the fraction of dead individuals, *x* the logarithm of the chemical concentration to obtain the LC_{50} and *Hill slope* is the slope factor of the dose-response curve. The two asymptotes of the original Hill equation were forced to be 0 and 1 since most of our ranges were sufficient to cover these two asymptotes. In one instance, we did not calculate a LC_{50} value due to lack of death and in two instances with insufficient data to cover these asymptotes this choice lead to an increased uncertainty in the LC_{50} measurements.

Unstimulated behavioral assays

For each toxicant concentration tested, 24 planarians were placed in two 12-well plates (Falcon), with a single worm placed in each well, and their locomotion was determined using automated center-of-mass (COM) tracking (Supplementary Figure S1A-B). Once both plates were filled, the planarian water was removed and 500µl of the appropriate concentration of

chemical was added to each well. For evaluation of acute toxicity, plates were imaged within five minutes of adding the chemical. These same worms were also imaged after eight days of exposure. To assay the locomotion of regenerating worms, for each concentration, 24 planarians were amputated using an ethanol-sterilized razor blade and immediately stored in a 48-well plate, with a single worm in each well containing 200µl of the appropriate chemical. On day 8, the regenerating worms were transferred to two 12-well plates containing a single worm and 500µl of the respective chemical per well. Regenerating worms were imaged eight and fifteen days after amputation and chemical exposure. Except during imaging, the plates were stored at 20°C in the dark.

The imaging system consisted of a ring stand with a CCD camera (PointGrey Flea3 1.3MP Mono USB 3.0) equipped with a 16mm lens (Tamron M118FM16 Megapixel Fixed-focal Industrial Lens). The plates were illuminated from below using a cold LED panel (Amazon.com). Image acquisition was controlled through a custom LabVIEW (National Instruments) script. The two plates were imaged at 5 frames per second (fps) for 10 minutes, following our previously established protocol for characterizing behavioral phenotypes in response to drug exposure (Talbot and Schötz, 2011). Image analysis was performed using custom made scripts in MATLAB. An average intensity projection image was first generated from the entire movie and subtracted from each picture in the stack. The resulting images were thresholded to obtain the worm's outline and each worm was automatically assigned a well number while its center of mass, length, and area were recorded. Worm tracks were sometimes truncated when worms were lost at the well edges. Only tracks longer than 2s were analyzed. Instantaneous speeds (in mm/s) were calculated for all tracks at 2s intervals to improve the signal to noise ratio (Talbot and Schötz, 2011).

We distinguished between three different behaviors: resting, swimming, and gliding. A speed below 0.3mm/s was considered as the worm's resting or wiggling speed. To distinguish swimming from gliding, we defined a dynamic cutoff as follows: the speed distribution of the entire population of 24 worms was computed and fitted by the sum of two Gaussians and a constant value (Supplementary Figure S1C) according to:

$$a_1 e^{\frac{-(x-\mu_1)^2}{\sigma_1^2}} + a_2 e^{\frac{-(x-\mu_2)^2}{\sigma_2^2}} + c$$

The fit was performed using the built-in MATLAB fit function and non-linear least square method. The fit output was shown graphically on top of the raw data. In case of poor fit results, the user could manually determine the relevant parameters instead. Worms were considered as gliding at any time point for which the speed was larger than $\mu_2 - 1.5\sigma_2$, a value that was adapted by hand to represent the behavior of control populations. The worms were declared swimming at time points for which the speed was between the absolute resting cutoff and this dynamic gliding cutoff (Supplementary Figure S1C).

From this population level classification, each worm was assigned a fraction of time spent in each of the three behaviors for all time points tracked. To remove bias due to differences in worm size, we scaled the animal's speed by its aspect ratio, calculated as the ratio of the worm's length squared to the worm area, l^2/lw or l^2/A, to reduce noise in the measurement. Based on control populations and the MATLAB built-in power law fit tool, we found that the gliding speed scaled with the power 2/3 of this aspect ratio (Supplementary Figure S1D). We therefore defined a scaled gliding speed as the absolute gliding speed divided by that measurement. All measurements were averaged over the entire population (n=24) and error bars were calculated as the standard error of the mean. Of note, the contribution of each worm to the mean was not weighed by the time for which it was tracked, thus treating all worms equal.

Thermotaxis assay

For every tested concentration, twenty worms were amputated and allowed to regenerate for 15 days in the respective concentration of chemical. After this period, the regenerating worms were placed in a single 100mm Petri dish filled with 20mL of planarian water. The dish was placed atop a kimwipe on top of a custom 10.5cm wide circular Peltier cooler with a central 3cm wide square cold plate surrounded by a circular heat sink. This cooler was powered by a DC regulated power supply (BK Precision) set to 5V. During the assay, the temperature was initially homogenous at 20°C (gradient off) and then displayed a gradient between 15°C in the center to 20°C at the edges (gradient on). Similar values were previously used to induce negative thermotaxis (motion towards cold regions) in planarians (Inoue et al., 2014).

Per experiment, two trials were run to compare the behavior of the worms with the gradient turned on and off. Imaging was performed with the same set-up as the behavior assay for 10 minutes at 1fps. Heat maps were generated from the resulting movies by subtracting a background picture without worms and computing the standard deviation projection of the resulting stack in ImageJ (National Institutes of Health). To quantify the amount of thermotaxis, each heatmap was first rescaled to have a mean intensity of 1 to account for possible differences in background lighting. We then computed the ratio of the resulting intensity in the cold region with gradient over the same region without gradient. Thus, ratios greater than one signify increased grouping of the worms towards the center of the dish, indicating successful negative thermotaxis.

Regeneration assay

For each chemical, a regeneration assay was set up with a minimum of n=10 similarly sized planarians at selected nonlethal concentrations. On day 1, planarians were imaged and

amputated with an ethanol-sterilized razor blade. Within 3 hours post-amputation, planarians were transferred to 48-well plates, one worm per well, and 200µL of the appropriate concentration of chemical was added to each well. Except during imaging, all worms were stored at 20ºC in the dark. Because little regenerative tissue (blastema) is discernible during the first few days, imaging began on day 4. Worms were imaged on days 4-7 on a MZ16FA stereo microscope (Leica), using a SPOT RT3 camera (Model 25.1, Diagnostics Instruments) controlled by SPOT Basic 5.1 software (SPOT Imaging Solutions). The appearance of eyes was manually scored during imaging.

Image analysis of head regeneration dynamics was carried out using a custom semi-automatic MATLAB script in which the area of the blastema was determined using thresholding techniques (Supplementary Figure S1E-F) based on two images independently analyzed by two people (i.e. average of four data points). Multiple images were analyzed to account for possible variability in analysis. Only worms which remained intact over the course of the experiment, *i.e.* were not damaged due to manual manipulation or did not undergo asexual reproduction via fission, were used for analysis. If this occurred, a biological replicate was performed and the data from all replicates were combined. To eliminate any bias based on the size of the worm, for each worm, the average blastema area was normalized by the square of the worm's width (Supplementary Figure S1E), as measured from two images taken on day 1. The rationale behind this normalization is a correlation between blastema size and wound cross-sectional area. Because we do not have access to the worm thickness in our measurements, but thickness scales proportionally to worm width (Supplementary Figure S1G), we approximated the cross-sectional area using width squared. Widths were manually measured in ImageJ. The normalized blastema growth rate (1/days, denoted as γ) was determined as the slope of the linear regression of the

normalized blastema area for the entire population (including independent experiments) over days 4-7 (Supplementary Figure S1H). Error bars represent the 99% confidence intervals.

Immunohistochemistry (IHC) experiments

To analyze effects on brain structure and regeneration, IHC was performed on full worms which had incubated in the respective chemical for 8 days or regenerated therein for 15 days. Following each experiment described above, worms were washed three times in 1x planarian water and transferred to a 1.5ml microcentrifuge tube, with approximately eight worms per tube. Planarians were fixed using a modified version of a previously published protocol (Umesono et al., 2013), with all solutions prepared in phosphate buffered saline. In brief, worms were incubated in 2% hydrochloric acid for 5 minutes and 4% paraformaldehyde/5% methanol for 3 hours, both at 4°C with rotation. Worms were then transferred to room temperature and washed twice quickly with 0.3% Triton-X 100, followed by a 15 minute incubation with reduction solution (50mM dithiothreitol, 1% NP-40, and 0.5% SDS) to increase permeabilization. Worms were subsequently washed in 50% methanol for 10 minutes and stored in 100% methanol at -20°C.

Fixed samples were bleached under bright white light for 5-6 hours in 6% hydrogen peroxide, followed by overnight blocking at 4°C in antibody blocking buffer (1% DMSO, 10% fetal bovine serum, 0.1% Tween-20, and 0.3% TritonX-100). To visualize brain structure, worms were subsequently incubated with mouse α-synapsin antibody (Developmental Studies Hybridoma Bank, 3C11, anti-SYNORF1, deposited to the DSHB by Buchner, Erich) diluted 1:500 in antibody blocking buffer, overnight at 4°C. The samples were washed with 0.1% Tween-20 and 0.3% TritonX-100 five times for 20-30 minutes and incubated overnight at 4°C with Alexa Fluor 488 Goat Anti-Mouse IgG (H+L) secondary antibody (Life Technologies, A-

11001), diluted 1:1000 in antibody blocking solution. Worms were washed five times for 20-30 minutes at room temperature with 0.1% Tween-20 and 0.3% TritonX-100 before mounting and imaged on an inverted IX81 spinning disc confocal microscope (Olympus DSU) using an ORCA-ER camera (Hamamatsu Photonics) and Slidebook software (version 5, Intelligent Imaging Innovations, Inc). As worms could be lost or damaged during the course of staining, IHC was performed on at least two biological replicates of treated worms to obtain n greater than or equal to 10.

To analyze the relative size of the brain, we quantified the fraction of the width of the brain over the width of the head (Supplementary Figure S1I). Quantification was manually performed in ImageJ by analyzing the maximum intensity projections of z-stacks taken with a 10X objective independently by two researchers who did not know which images he or she was analyzing, thus ensuring that experimenter bias could not influence the analysis. Measurement data was compiled and analyzed in Microsoft Excel and MATLAB.

Potency measurement

To summarize our results, we determined the lowest concentrations of each toxicant at which an effect was seen (lowest observed effect level, LOEL), converted to μM, on 17 quantitative read-outs: LC_{50} for full and regenerating worms at four different time points, mean scaled gliding speeds for full and regenerating worms at two different time points, blastema growth rate, eye regeneration, brain structure for full and regenerating worms, and proper thermotaxis. To compare these concentrations over wide ranges, we defined potency as $-log_{10}(\text{concentration in } \mu\text{M})$.

Statistical Testing

To determine statistical significance in the obtained results for the various assays, we performed a student t-test for pair wise comparison between toxicant population and controls after verification that the data was normally distributed. All statistical analyses were performed in MATLAB. As this was a pilot study to establish the sensitivity of planarians for toxicological screening, we empirically determined the number of samples used in each assay. Using a *post hoc* power analysis with Gpower (Erdfelder et al., 1996), we determined that the sample sizes used in unstimulated behavior, regeneration, and brain structure assays were sufficient to detect effects of one standard deviation at the 1% level at a statistical power of 85%, 75% and 62%, respectively.

RESULTS

Overview

The primary objective of this study was to evaluate whether the asexual freshwater planarian *Dugesia japonica* is a suitable animal model for studying environmental toxicants, particularly developmental neurotoxicants. Therefore, to assess the usefulness of the system, we evaluated the toxicity of ten well-studied substances: dimethyl sulfoxide (DMSO), a classic solvent and known neurotoxicant; pesticides commonly used in agriculture: two organophosphates, chlorpyrifos and dichlorvos, and one pyrethroid, permethrin, because of their relevance for human health and their known toxic mechanisms inhibiting the enzyme acetylcholinesterase and disrupting neuronal sodium channels, respectively (Amitai et al., 1998; Bradberry et al., 2005); the detergents TritonX-100 and sodium dodecyl sulfate (SDS), commonly used in cleaning products and with characterized detrimental effects on fish and other aquatic organisms (Abel, 1974); the most common alcohols, ethanol and methanol, which are well-established to cause developmental neurotoxicity; acrylamide, a widely used industrial chemical also commonly found as a food contaminant (Parzefall, 2008), with known effects as a potential neurotoxicant (LoPachin, 2004); and glucose, expected to be inert to neurodevelopment but potentially affecting other pathways, particularly in metabolism, to establish how effects other than neurotoxicity could be assessed in our system.

We used these compounds to determine (a) how sensitive planarians were to these toxicants when compared to other animal models, and (b) whether a detectable difference existed in the response of adult versus developing planarians, with particular interest in changes in brain structure. To this end, we developed a 5-step semi-automated screening platform that enabled us to first determine the LC_{50} and then the lowest observed effect level (LOEL) for each compound,

using four additional readouts at sublethal concentrations: unstimulated behavior, stimulated behavior, regeneration dynamics, and structural brain defects, as outlined in Figure 2.1.

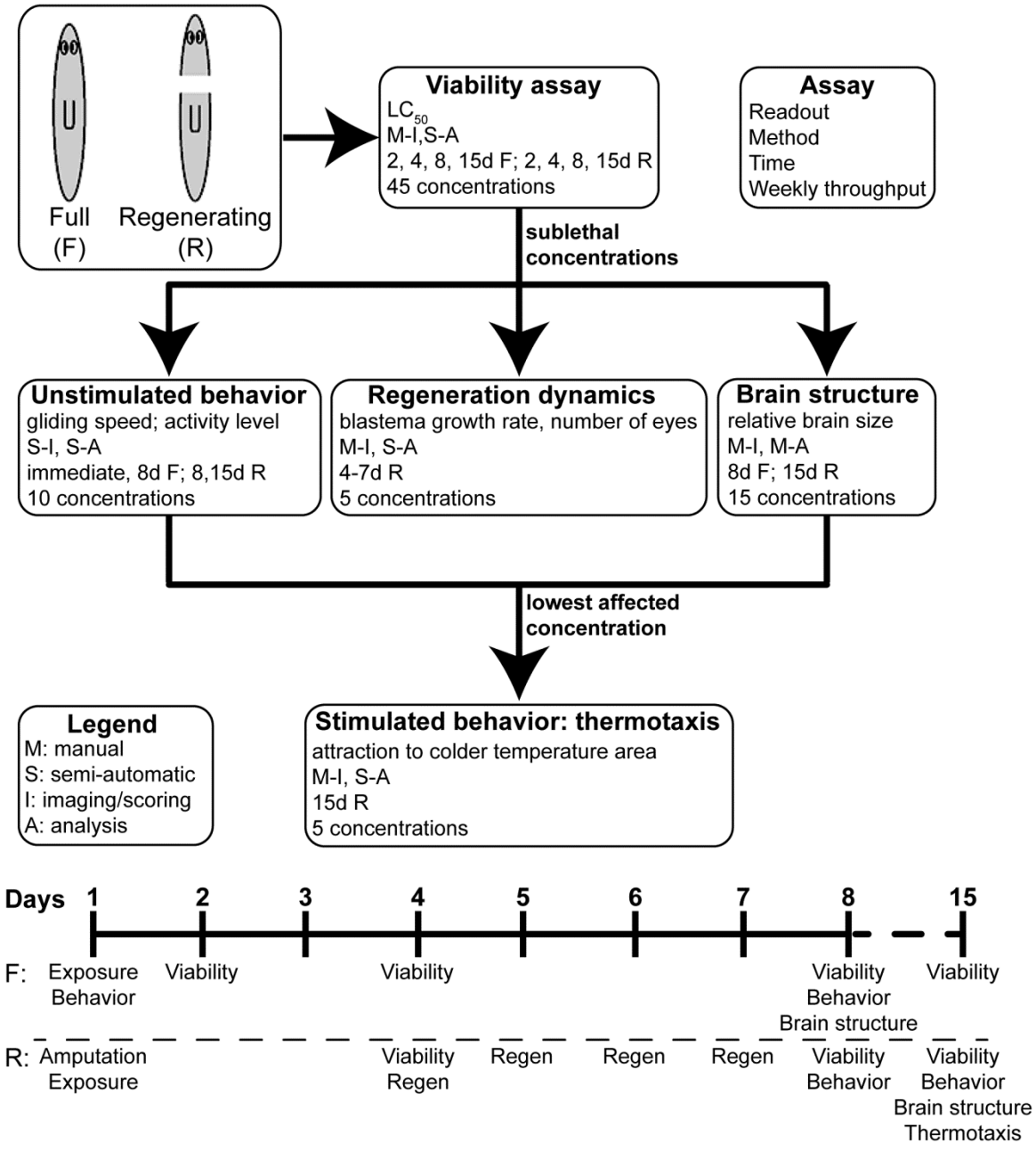

Figure 2.1. Overview of assay. Description of experiments performed with readout, method, times tested, and average weekly throughput listed for each. With the exception of thermotaxis, full and regenerating tail pieces were used for all assays. A timeline is given to describe the screening experimental procedure.

Viability

The first step in our screening platform was to determine the lethal concentration of each compound. Selection of several of the initial broad concentration ranges were guided using previously published reports of lethality and toxicity in planarians (Li, 2008; Pagán et al., 2006; Yuan et al., 2012) and zebrafish (Bichara et al., 2014; DeMicco et al., 2010; Maes et al., 2012; Watson et al., 2014). Since lethality does not solely depend on toxicant concentration but also on the length of exposure, we assessed lethality after 2, 4, 8, and 15 days of exposure (Figure 2.2). Also, we compared the survival of full (adult) and regenerating worms, exposed within 3h post-amputation, over this time scale to assess whether some chemicals were more potent during development. Each chemical was therefore attributed a LC_{50} at four different time points for both full and regenerating worms (n=16 each, from two independent experiments, Table 2.2). As expected, the LC_{50} decreased with the length of exposure. For our other assays, we retained the 15 day LC_{50} as the maximum concentration to be used.

Surprisingly, we found that regenerating worms were slightly more resilient than full worms in the same conditions, with the notable exception of SDS. This effect was most apparent with the pyrethroid permethrin, (Figure 2.2, Table 2.2), where, after 15 days of exposure, the LC_{50} value for regenerating worms (382μM) was found to be almost three times greater than that for full worms (139μM). A possible explanation for this difference in sensitivity may be that regenerating worms are generally more stationary than full worms, potentially reflecting a difference in metabolism.

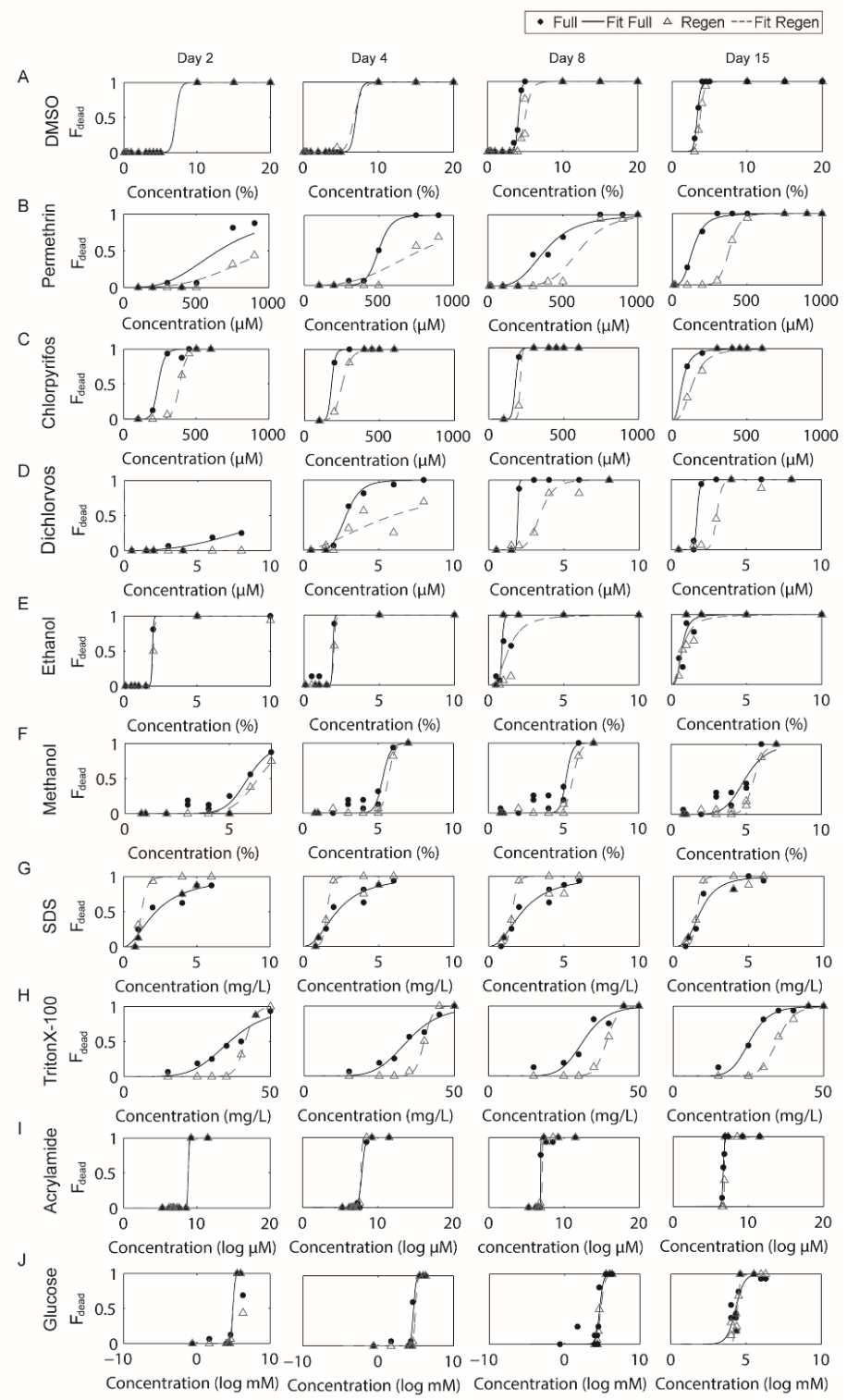

Figure 2.2. Viability of full and regenerating worms. The lethality of each chemical is shown as the fraction of dead worms (F_{dead}) after 2, 4, 8, or 15 days of exposure to (A) DMSO, (B) permethrin, (C) chlorpyrifos, (D) dichlorvos, (E) ethanol, (F) methanol, (G) SDS, (H) TritonX-100, (I) acrylamide, and (J) glucose for full (black) and regenerating (red) worms. Solid black and red dashed lines show the result of the fit, as described in methods, for full and regenerating worms, respectively.

Table 2.2. LC_{50} values after 2, 4, 8, or 15 days of exposure for full and regenerating worms.

Chemical	Worm condition	Day 2	Day 4	Day 8	Day 15
Acrylamide	Full	6787µM	2720µM	991µM	785µM
	Regen	6787µM	1462µM	1208µM	904µM
Chlorpyrifos	Full	238µM	181µM	177µM	67µM
	Regen	386µM	252µM	209µM	135µM
Dichlorvos	Full	11.9µM	2.86µM	1.92µM	1.73µM
	Regen	N/A	6.07uM	3.40uM	3.04uM
DMSO	Full	7.08%	7.03%	4.13%	3.35%
	Regen	7.06%	6.80%	5.03%	3.75%
Ethanol	Full	1.94%	1.92%	0.90%	0.70%
	Regen	2.00%	1.98%	1.34%	0.75%
Glucose	Full	139mM	110mM	105mM	74mM
	Regen	144mM	143mM	125mM	83mM
Methanol	Full	5.88%	5.31%	5.18%	4.92%
	Regen	6.38%	5.68%	5.63%	5.51%
Permethrin	Full	653µM	500µM	384µM	139µM
	Regen	1000µM	784µM	609µM	382µM
SDS	Full	2.22mg/L	2.26mg/L	2.26mg/L	1.82mg/L
	Regen	1.24mg/L	1.57mg/L	1.57mg/L	1.57mg/L
TritonX-100	Full	36mg/L	34mg/L	31mg/L	25mg/L
	Regen	41mg/L	40mg/L	39mg/L	35mg/L

[i] LC_{50} was quantified using a modified Hill's equation (see Materials and Methods)
[ii] N/A indicates no deaths were observed.

Notably, we observed a 100-fold difference in LC_{50} values between the two organophosphates, chlorpyrifos and dichlorvos. This difference is potentially due to the differences in the structure and metabolism of these two compounds. Dichlorvos and chlorpyrifos are dimethyl and diethyl organophosphates, respectively; thus, they could potentially have different affinities for planarian acetylcholinesterase. Furthermore, dichlorvos is already in its toxic oxon form whereas chlorpyrifos must be metabolically converted into its oxon by proteins of the cytochrome P450 family to be able to inhibit acetylcholinesterase (Tang et al., 2001), potentially reflecting the observed decreased sensitivity to chlorpyrifos, in comparison to dichlorvos.

Overall, the observed values are comparable to data from zebrafish and *C. elegans* (see Discussion) demonstrating that planarians are not unusually sensitive or resilient to any of these compounds.

Unstimulated behavior

For the sublethal concentrations determined above, we assayed possible defects in unstimulated planarian behavior induced by the different toxicants through quantification of the gliding speed and overall activity level of individual worms (Figure 2.3). Proper gliding requires both a constant production of mucus and coordinated cilia beating. Even recently regenerating worms are capable of gliding, albeit at a reduced speed until 12-13 days of regeneration (Supplementary Figure S2), showing that gliding does not require a fully functional brain but more likely depends on the function of the ventral nerve cords and proper metabolism.

First, we tested the toxicants' acute general toxicity by measuring the mean gliding speed of full worms immediately after exposure to different sublethal concentrations. Then, to determine the subchronic toxicity of these toxicants, we measured gliding speeds of both full and

regenerating worms after 8 days of exposure to distinguish subchronic toxic effects that affected either full or regenerating worms and thus identify possible effects specific to development. Finally, we tested regenerating worms after 15 days of exposure to assess possible delays in the return of normal gliding speeds following amputation.

Acute toxicity was observed as a reduction in gliding speed in 200μM permethrin (Figure 2.3B), 100nM and 500nM dichlorvos (Figure 2.3D), and 0.5mg/L and 1mg/L SDS (Figure 2.3G). As expected, these concentrations also caused decreased gliding speeds on longer time scales in both full and regenerating worms. In addition, acute toxicity was also observed by a decrease in the worms' activity for 1% and 2% DMSO (Supplementary Figure S3A) and 200μM and 500μM acrylamide (Supplementary Figure S3B). Here again, similar effects were observed at longer time scales in these conditions.

All tested chemicals displayed subchronic toxicity, demonstrating the sensitivity of our unstimulated behavioral assay. Of the ten tested chemicals, five (DMSO, permethrin, SDS, TritonX-100, and glucose) showed subchronic toxicity in all conditions with slight differences in threshold concentrations between regenerating and full worms. The fact that subchronic exposure to glucose resulted in perturbed behavior was expected given its central role in metabolism, which directly affects unstimulated behavior. More specifically, of these five chemicals, all except TritonX-100, displayed lower threshold concentrations in regenerating worms, indicating possible increased sensitivity of developing planarians to these chemicals. However, the other five toxicants had more surprising toxicity profiles.

Figure 2.3. Unstimulated behavior of toxicant-exposed full and regenerating worms. Semi-log plot of mean scaled gliding speeds as a function of concentration during exposure to (A) DMSO, (B) permethrin, (C) chlorpyrifos, (D) dichlorvos, (E) ethanol, (F) methanol, (G) SDS, (H) TritonX-100, (I) acrylamide, and (J) glucose. Different colors correspond to the different time points and situations tested: immediate reaction of full worms (black), 8 days reaction of full worms (red) and reaction of regenerating worms at both 8 (purple) and 15 days (blue). Errors bars are SE of populations of n=24 worms. Stars of different colors indicate statistical relevance at the 1% level for the corresponding time point when compared to control worms.

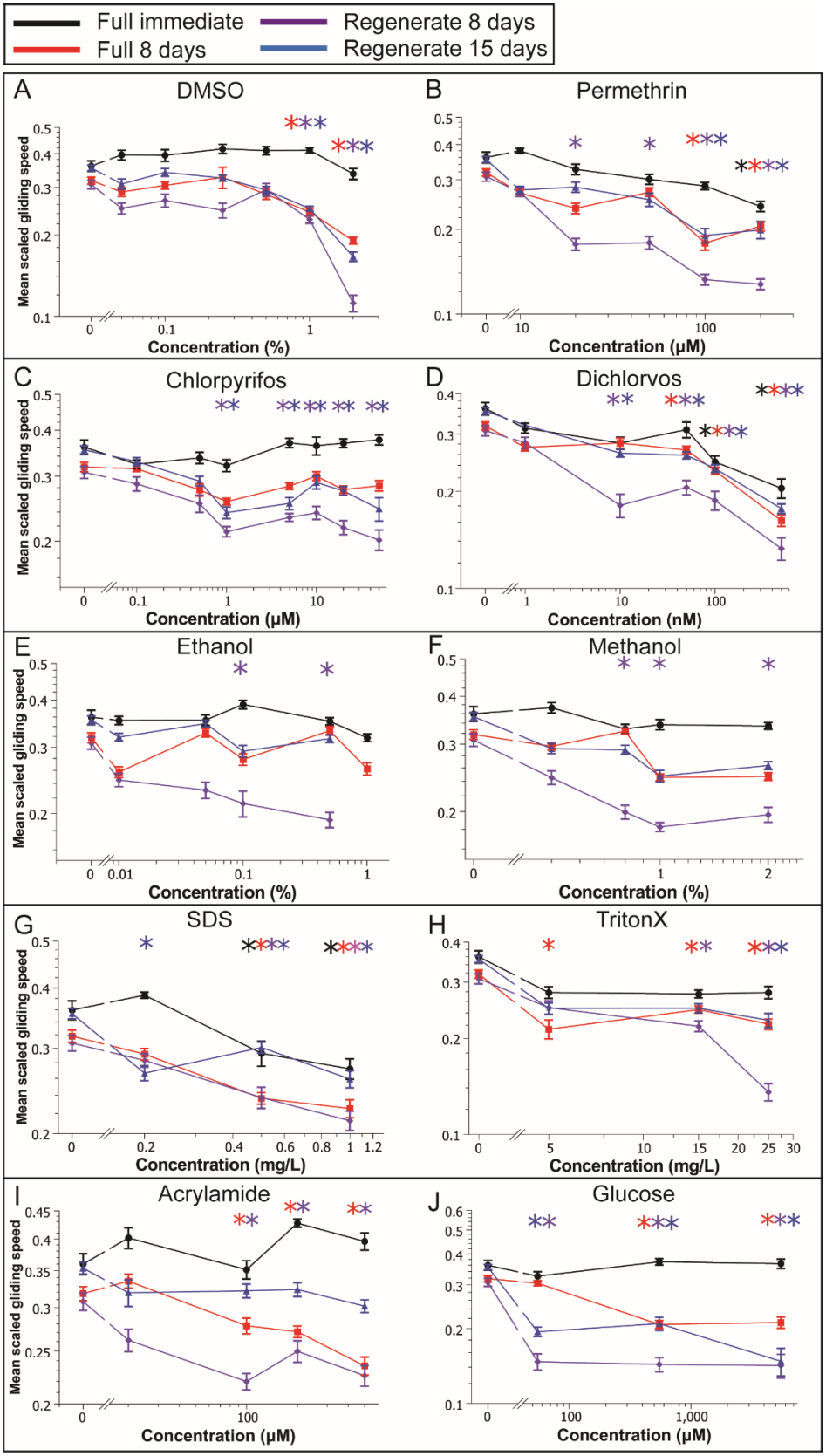
Full immediate
Full 8 days
Regenerate 8 days
Regenerate 15 days
A
DMSO
Mean scaled gliding speed
Concentration (%)
B
Permethrin
Concentration (µM)
C
Chlorpyrifos
Concentration (µM)
D
Dichlorvos
Concentration (nM)
E
Ethanol
Concentration (%)
F
Methanol
Concentration (%)
G
SDS
Concentration (mg/L)
H
TritonX
Concentration (mg/L)
I
Acrylamide
Concentration (µM)
J
Glucose
Concentration (µM)

The alcohols, methanol and ethanol, were peculiar in the sense that they only affected 8 days regenerating worms (above 0.8% and 0.1%, respectively) but neither full nor 15 days regenerating worms (Figure 2.3E-F), suggesting that these concentrations induced a slight delay in the retrieval of locomotion function during regeneration but did not impair these functions altogether.

The organophosphates, chlorpyrifos and dichlorvos, were particularly interesting since regenerating worms showed a higher sensitivity to these class of toxicants when compared to full worms (either immediately or after 8 days of exposure). Chlorpyrifos was the most striking with concentrations as low as 1μM inducing reduced gliding speeds in both 8 days and 15 days regenerating worms whereas none of the tested concentrations showed any effect on full worms (Figure 2.3C). In addition, qualitative differences in the worm's trajectories were visible in chlorpyrifos with an increased frequency of sharp turns and head wiggles (Supplementary Figure S3C-D), similar to reports of a zigzag swimming pattern seen in zebrafish larvae exposed to chlorpyrifos (Watson et al., 2014). Similarly, regenerating worms were more sensitive to dichlorvos than full worms (Figure 2.3D). These results support the hypothesis that organophosphates might have developmental specific neurotoxic effects (Bjørling-Poulsen et al., 2008; Richendrfer et al., 2012) whose mechanisms remain to be understood.

Finally, acrylamide only showed subchronic toxicity on 8 days full and regenerating worms at concentrations higher than 100μM (Figure 2.3I). However, this effect was coupled to a clear reduction of activity levels (seen as the increased fraction of time spent resting, see Supplementary Figure S3B) in full and regenerating worms, at both 8 and 15 days. These results suggest a more subtle effect of acrylamide on unstimulated behavior with potential effects on both the type of behavior adopted by the worms and their ability to perform gliding normally.

Altogether, these results show the ability of our semi-automated setup to reveal subtle effects on passive behavior due to toxicant exposure. We were able to distinguish acute and subchronic toxicity as well as reveal defects specific to developing brains. This emphasizes the strength of the opportunity offered by planarians to study, in parallel and at medium throughput, both adult and regenerating organisms.

Regeneration/development dynamics

Since we are using asexual *D. japonica* planarians, regeneration of a new brain after amputation is comparable to the typical development of a new planarian brain after "birth", which is the generation of a tail piece during binary fission (Sakurai et al., 2012). Thus, by assaying brain regeneration, we are, in a way, simultaneously assaying brain development. To test whether any of the chemicals had adverse effects on regeneration dynamics and therefore development, amputated planarians were exposed to our pre-determined sublethal range of concentrations for each chemical for 7 days, during which regeneration dynamics and eye reappearance were quantified as outlined in Material and Methods (see Supplementary Figure S1J-L for example images). Since proper regeneration requires the coordination of many different processes, including stem cell proliferation, differentiation, and re-establishment of polarity (Reddien, 2013; Umesono et al., 2013), possible toxic effects on this process are likely due to mechanisms of general developmental toxicity. Moreover, while equally regulated by the same processes as general regeneration, eye regeneration, is coordinated by specific neuronal populations (Dong et al., 2012; Mannini et al., 2004) and is therefore a more sensitive endpoint to assay possible specific neurotoxic effects. Therefore, this combined quantitative analysis of regeneration allowed us to simultaneously assess general physiological developmental toxicity as well as specific neuronal toxicity.

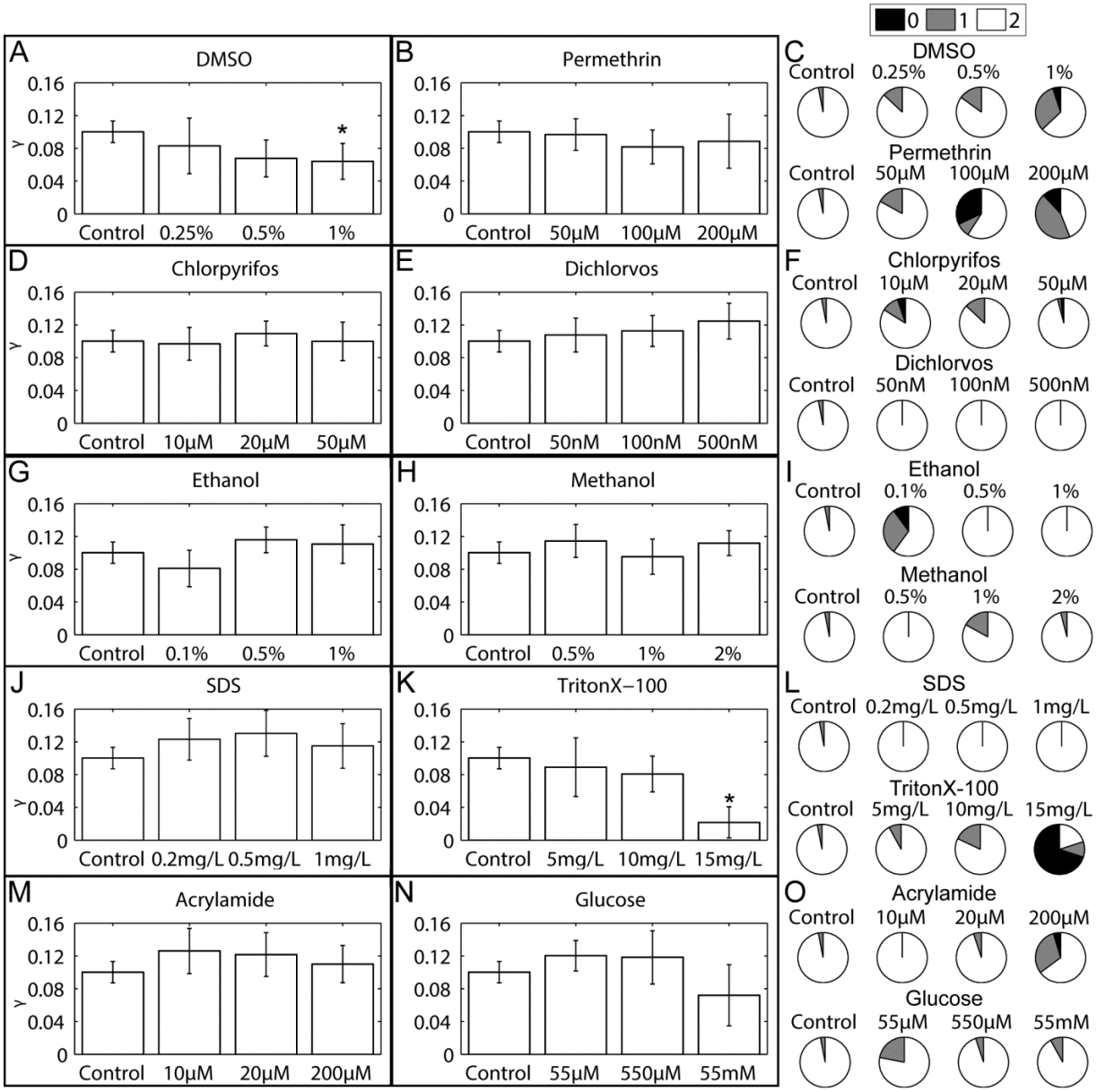

Figure 2.4. Regeneration is generally unaffected by toxicant exposure. Effects of the various chemicals on regeneration were quantified by the population blastema growth rate over days 4-7, normalized by the worm width squared, (γ), and the percent of worms with 0, 1, or 2 eyes at day 7 for (A-C) DMSO (n=15, 20, and19) and permethrin (n=12, 22, and 9), (D-F) chlorpyrifos (n=19, 31, 34) and dichlorvos (n=12, 20, and 11), (G-H) ethanol (n=20, 24, and 11) and methanol (n=11, 12, and 24), (J-K) SDS (n=12, 12, and 10) and TritonX-100 (n=12, 11, and 10), and (M-N) acrylamide (n=20, 20, and 10) and glucose (n=18, 20, and 12) compared to controls (n=58). Error bars represent the 99% confidence intervals of the fit. * denotes the confidence intervals do not overlap with those of controls.

Surprisingly, most of the tested chemicals did not have a significant effect on either the normalized blastema growth rate (γ) or the number of eyes detected at day 7 (Figure 2.4). Of the tested chemicals and concentrations, only 1% DMSO and 15mg/L TritonX-100 (Supplementary Figure SIK) caused a significant delay in blastema growth. Similarly, at these same concentrations, more worms were found to have delays in eye regeneration, as a large number of worms had only one or no eyes at day 7, whereas the majority of controls had regenerated both eyes (Figure 2.4C and L).

Interestingly, although no significant effect on blastema growth was found, worms regenerated in 100μM and 200μM permethrin and 200μM acrylamide showed a delay in eye regeneration (Figure 2.4C, O, and S1L), suggesting that the effects of permethrin and acrylamide may be more specifically neurotoxic rather than generally toxic. This is consistent with the known effects of pyrethroids on neuronal voltage-gated sodium channels (Bradberry et al., 2005) and acrylamide on axonal swelling and demyelination (LoPachin, 2004; Parng et al., 2007).

In general, we found that the majority of the tested toxicants were not toxic to the overall physiology of the regenerating planarian. This suggests that, at the concentrations tested, any adverse effects seen in the toxicant-treated regenerating worms may be due to more targeted effects on specific pathways, rather than an effect of general toxicity.

Brain structure

A powerful tool of alternative model organisms, such as zebrafish, nematodes, and planarians, is the ability to probe toxicity at different levels, from the organismal level down to the cellular and molecular level. To evaluate whether subchronic exposure to sublethal concentrations of the tested chemicals could lead to obvious morphological changes in the planarian brain, indicating possible brain defects resulting from toxicant exposure, we visualized

the nervous system by immunohistochemistry with a pan-neuronal marker, α-synapsin. To account for differences in worm size, the relative brain size was calculated as the ratio of the width of the brain to the width of the head at the same location (Supplementary Figure S1I). Importantly, through this quantitative analysis, we were able to detect neurotoxicity manifested by large scale defects in the gross anatomy of the brain; however, more subtle neurotoxicity at the cellular level could be missed including defects in specific neurodevelopmental processes, such as neurite outgrowth or synaptogenesis.

We compared the relative brain size of full and regenerating worms exposed to different concentrations for 8 and 15 days, respectively (Figure 2.5). These time-scales were chosen as behavioral defects were detectable after 8 days for both full and regenerating animals (Figure 2.3). However, for regenerating animals, toxicant exposure could potentially slow brain reformation. To specifically analyze toxic effects on brain morphology, rather than developmental delays, regenerating worms were assayed after 15 days of exposure to allow for complete nervous system regeneration. Full worms were tested to allow for comparison with regenerating worms to determine whether the toxicants were specific to either the developing or mature brain or were general to both.

Generally, after toxicant exposure, brain morphology was more sensitively affected in regenerating worms than in full worms treated with the same concentrations. Development-specific defects in brain size, wherein regenerating but not full worms were affected, were detected after exposure to DMSO, permethrin, chlorpyrifos, ethanol, methanol, and TritonX-100 (Figure 2.5).

Figure 2.5. Effects on brain morphology. Quantification of relative brain size as brain width/head width comparing controls (n= 20 full and 30 regenerating worms) to animals exposed to (A) DMSO (n=11, 14, 13; 13, 15, 10), (B) permethrin (n=13, 13, 13; 15, 11, 13), (C) chlorpyrifos (n=10, 11, 16; 14, 21, 11), (D) dichlorvos (n=12, 13, 16, 12; 17, 16, 10, 11), (E) ethanol (n=19, 13, 10; 16, 19, 11), (F) methanol (n=12, 22, 20; 11, 11, 13), (G) SDS (n=12, 12, 11; 17, 15, 11), (H) TritonX-100 (n=14, 19, 13; 16, 10, 15), (I) acrylamide (n=15, 14, 19, 15, 12; 19, 16, 12, 14, 13) and (J) glucose (n=13, 17, 13; 19, 13, 13). n listed as (full; regenerated worm) in increasing concentration order. Error bars denote SE and * denotes $p<0.01$ when compared to controls of the same worm type.

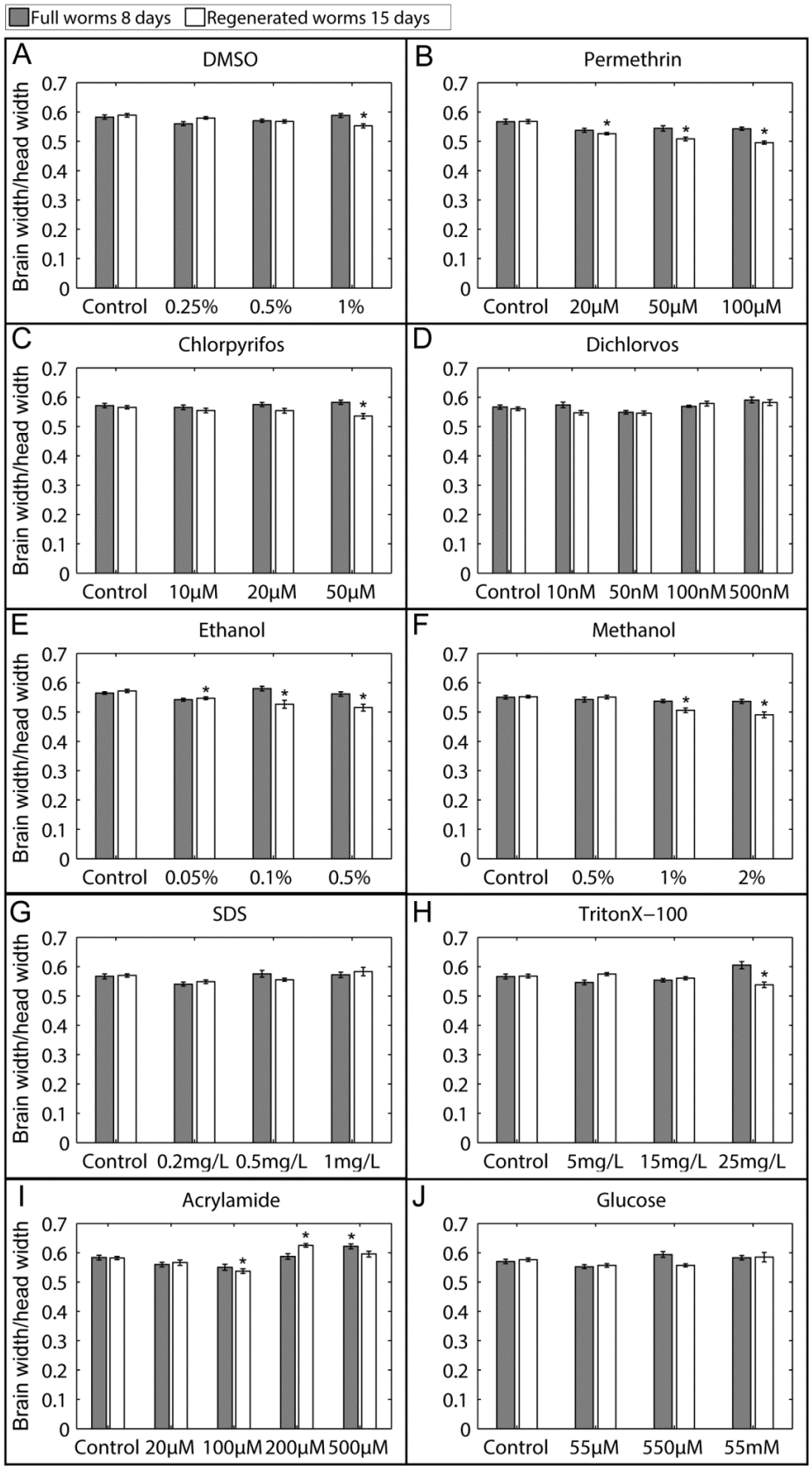
Full worms 8 days
Regenerated worms 15 days
A
DMSO
Brain width/head width
0.7
0.6
0.5
0.4
0.3
0.2
0.1
0
Control
0.25%
0.5%
1%
B
Permethrin
Control
20µM
50µM
100µM
C
Chlorpyrifos
Control
10µM
20µM
50µM
D
Dichlorvos
Control
10nM
50nM
100nM
500nM
E
Ethanol
Control
0.05%
0.1%
0.5%
F
Methanol
Control
0.5%
1%
2%
G
SDS
Control
0.2mg/L
0.5mg/L
1mg/L
H
TritonX−100
Control
5mg/L
15mg/L
25mg/L
I
Acrylamide
Control
20µM
100µM
200µM
500µM
J
Glucose
Control
55µM
550µM
55mM

This increased sensitivity displayed by regenerating worms was especially evident in worms exposed to permethrin, ethanol, and methanol, wherein a significant decrease in brain size was detected at multiple tested concentrations, although, even at the highest tested sublethal concentrations, no changes in the full worm brain morphology were found. Notably, although no quantitative differences in brain size were detected for regenerated worms treated with dichlorvos, qualitative differences in brain density were observed (Supplementary Figure S4), indicating possible neurotoxicity which would require more in-depth analysis at the molecular or cellular level. Overall, the chemicals we tested were more potent on developing brains than on adult ones underlying the need for specific guidelines controlling exposure of infants and pregnant women to various toxicants.

Compared to exposure to the other chemicals, which resulted in classical dose-dependent changes in regenerated brain size, exposure to acrylamide was special with a seemingly biphasic effect on brain size. In fact, we found that exposure to lower concentrations of acrylamide (notably,100μM) led to a significant decrease in regenerated brain size; however, exposure to high concentrations (200μM) resulted in an increase in regenerated brain size compared to non-treated controls (Figure 2.5I). Upon inspection of the respective images associated with these brains, this effect was clearly visible as developing brains incubated in 200μM acrylamide seemed to have a swollen and wider distribution of neurons, compared to control and lower concentrations of acrylamide (Supplementary Figure S4). This effect is consistent with the previously described ability of acrylamide to cause axonal swelling (Parng et al., 2007). Furthermore, of all the tested concentrations in the various chemicals, only 500μM acrylamide caused significant morphological changes in the adult brain. Similar to the effects with high concentrations of acrylamide on regenerating brains, this concentration induced an increase in

brain size compared to controls, suggesting similar mechanisms of toxicity are occurring in the developing and adult brain, although with different sensitivities.

Full or regenerating worms exposed to sublethal concentrations of SDS did not display significant changes in brain morphology (Figure 2.5G); however, more subtle effects on brain structure or function (see below) could be present which we would be unable to discern by this large-scale morphological approach. This was similarly seen for the non-toxic, neutral chemical, glucose (Figure 2.5J), wherein we did not expect to find any structural changes in the brain.

Overall, quantitative comparison of relative brain sizes in regenerating and full worms allowed us to detect large-scale developmental-specific effects of neurotoxicity as exposure at the same concentrations specifically affected the brain size of regenerating animals.

Stimulated behavior: thermotaxis

Since the neuronal processes involved in unstimulated behavior are likely limited, evidenced by the ability of regenerating worms without a fully reformed brain to glide (Supplementary Figure S2), we analyzed the ability of worms exposed to the various toxicants to perform temperature sensing as a more subtle readout of neuronal function (Figure 2.6). It has been previously shown (Inoue et al., 2014) that wild-type planarians exhibit a strong preference for colder temperatures; therefore, we tested for proper brain function using the worms' negative thermotaxis, *i.e.* their ability to move towards regions of lower temperature. The neuronal mechanisms underlying planarian thermotaxis involve temperature sensing by receptors of the transient receptor potential family, signal processing by serotoninergic neurons in the brain, and behavioral output mediated by cholinergic motor neurons (Inoue et al., 2014). The ability of a worm to perform negative thermotaxis is thus a good readout of the proper function of these specific sensory and processing neurons. We tested thermotaxis on worms that were allowed to

regenerate for 15 days in the presence of the different toxicants. Because these tests were conducted manually, as described in Material and Methods, we only tested one concentration per chemical using either the lowest concentration found to induce defects in brain morphology or found to induce behavioral abnormalities for 15 days regenerating animals.

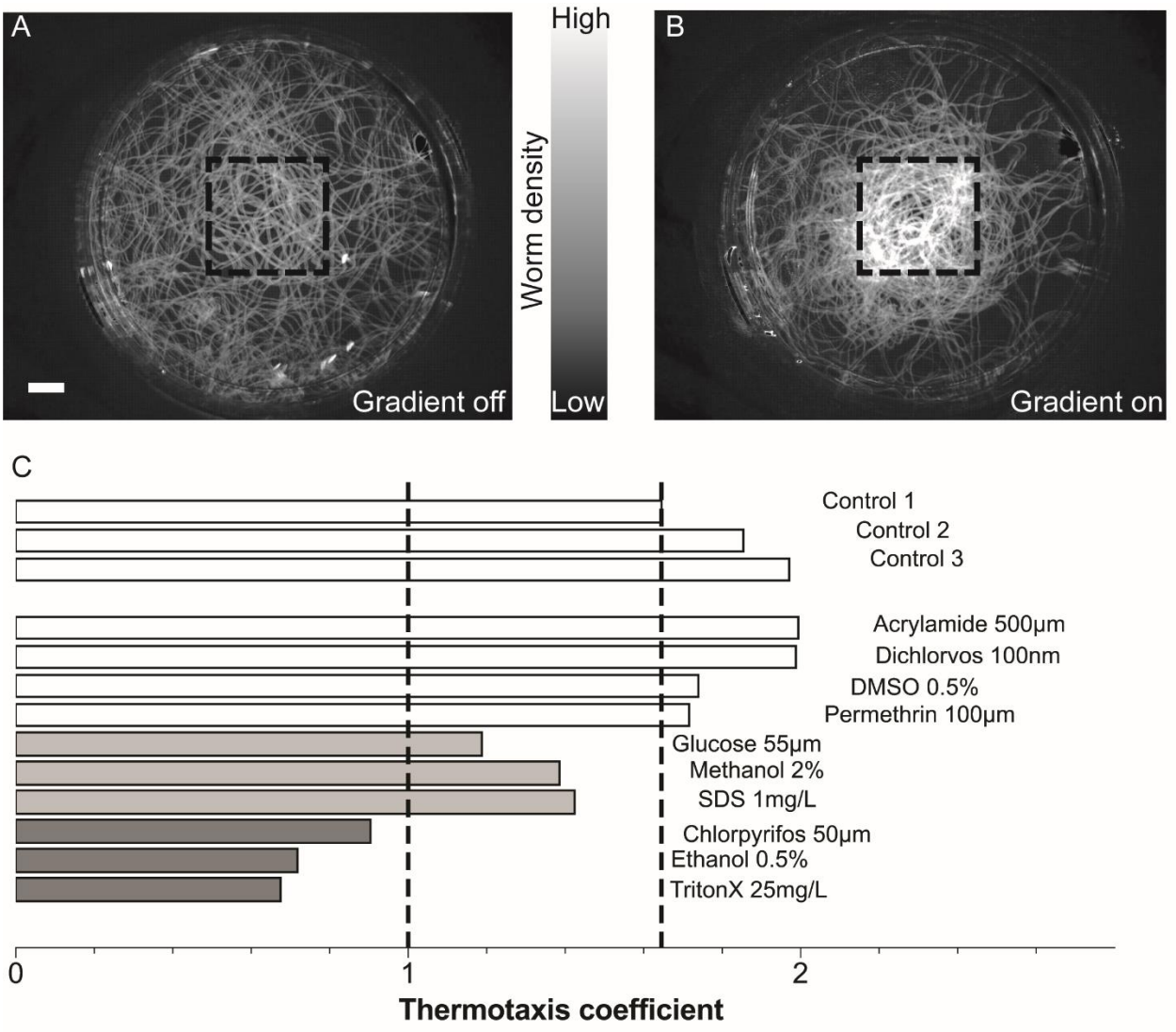

Figure 2.6. Temperature sensing assay. (A) Wild type worms (n=20) density heatmap over a 10min course in the absence or (B) presence of a thermal gradient. Black dotted line shows the area of the cold spot in the center of the dish and grey levels indicate higher worm density in that region in presence of the gradient. Scale bar: 1cm (C) Thermotaxis coefficient for worm populations (n=20 for each) exposed to different toxicants. The black dotted lines indicate the level of absence of any reaction (thermotaxis coefficient of 1) and the lowest measurement of three control populations. The different conditions are further classified based on these two cutoffs as normal thermotaxis (white bars), impaired thermotaxis (light grey bars) and no thermotaxis (dark grey bars).

Through quantification of the worms' response and visual inspection of the density heat maps (Figure 2.6A-B, Supplementary Figure S5), we found that thermotactic ability was entirely suppressed after exposure to 0.5% ethanol, 50μM chlorpyrifos, and 25mg/L TritonX-100 (dark grey bars in Figure 6C). In addition, we found that this behavior was impaired but not entirely suppressed after exposure to 55μM glucose, 2% methanol, and 1mg/L SDS (light grey bars in Figure 2.6C).

Of these six toxicants, four (ethanol, methanol, chlorpyrifos, and TritonX-100) were already shown to induce large scale defects in brain morphology (Figure 2.5), likely explaining this impaired behavior. On the other hand, the structural defects induced by DMSO, permethrin, and acrylamide did not impair thermotaxis and, therefore, are likely targeted at different neuronal populations, not involved in this type of behavior. Finally, at the tested concentrations, neither glucose nor SDS induced visible changes in brain morphology but still impaired thermotaxis. This effect of glucose could potentially be explained by its role in the insulin pathway which has been shown to play a role in thermotaxis and memory in *C. elegans* (Li et al., 2013). In addition, both glucose and SDS were found to have effects on locomotion (Figure 2.3) which could also alter the worms' thermotactic response which, ultimately, requires proper motility.

Overall, these results show how planarians can be used in large scale, population experiments which, in concordance with our other assays, reveal subtler effects on neuronal functions. In the future, similar tests could be conducted using the worm's photo- or chemo-tactic responses which require different neuronal subpopulations to further refine the neurotoxicity profiles of various toxicants.

DISCUSSION

As shown in Figure 2.7, all of the tested toxicants displayed some form of toxicity demonstrated through either unstimulated or stimulated behavior, regeneration dynamics, or brain structure indicating that planarians are an appropriately sensitive animal model for toxicology studies. Importantly, the tested toxicants displayed differential toxicity with different levels of effect on the various endpoints, suggesting these endpoints are specific to various types of toxicity, ranging from general physiological toxicity (regeneration dynamics) to toxicity towards specific neuronal subpopulations (thermotaxis).

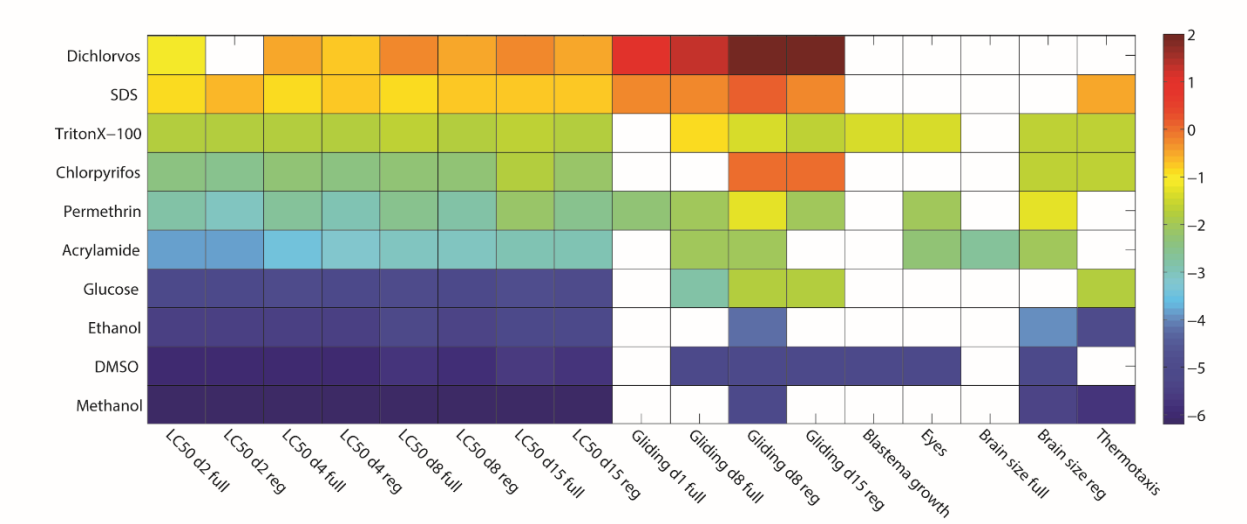

Figure 2.7. Effect and potency of all toxicants on ten quantitative endpoints: LC_{50} for full and regenerating worms at four different time points, mean scaled gliding speeds for full and regenerating worms, blastema growth rate, eye regeneration, brain structure for full and regenerating worms and, finally, proper thermotaxis. The colorbar represents potency defined as $-log_{10}(LOEL\ in\ \mu M)$ (see Material and Methods) while white squares are used when no effects were detected.

Moreover, comparison with other toxicology model organisms, such as zebrafish and nematodes, shows that planarians generally displayed comparable sensitivity to the tested toxicants, with LC_{50} and LOEL values on the same order of magnitude (Tables 2.3-4). However, species-specific differences in sensitivity do exist, most strikingly in the case of permethrin. Although, in terms of lethality, planarians were 1000 fold less sensitive than zebrafish to

permethrin, it has been shown that fish are particularly sensitive to pyrethroid exposure, with a 1000 fold higher sensitivity than mammals (Bradbury and Coats, 1989). This emphasizes the need for a comparative analysis of toxicology across diverse model organisms to better represent possible effects on humans and to find the appropriate threshold concentrations.

Table 2.3. Comparison of LC_{50} values for planarians with zebrafish and nematodes. LC_{50} values of 8 day full and regenerating planarians, from Table 2.2, are compared to values found in zebrafish larvae and nematodes. When necessary, concentrations were converted for better comparison.

Chemical	**Full planarians**	**Regenerating planarians**	**Zebrafish**	**Nematodes**	**References**
DMSO	4.13%	5.03%	1.8%-2.5%		(Bichara et al., 2014; Maes et al., 2012)
permethrin	384μM	609μM	800nM		(DeMicco et al., 2010)
chlorpyrifos	177μM	209μM	1μM	2.76μM	(Roh and Choi, 2008; Watson et al., 2014)
dichlorvos	1.92μM	3.40μM	17μM	39μM	(Rajini et al., 2008; Watson et al., 2014)
ethanol	0.9%	1.34%	1.2%	5%	(Bichara et al., 2014; Yu et al., 2011)
methanol	5.18%	5.63%			
SDS	2.26mg/L	1.57mg/L	16.1mg/L		(Bichara et al., 2014)
TritonX-100	31mg/L	39mg/L			
acrylamide	785μM	904μM	~6.25mM	3.4mM	(Fei et al., 2010; Li et al., 2015)
glucose	105mM	125mM			

Table 2.4. Comparison of LOEL values of tested chemicals in planarians with previous studies in zebrafish and nematodes. LOEL determined as the lowest concentration which elicited a statistically significant effect compared to controls. When necessary, concentrations were converted for better comparison.

Chemical	Planarians	Zebrafish	Nematodes	References
DMSO	1%	0.01%- 2%	1%	(Chen et al., 2011; Maes et al., 2012; Selderslaghs et al., 2009; Sprando et al., 2009)
permethrin	20μM	130nM		(DeMicco et al., 2010)
chlorpyrifos	1μM	0.01μM-0.1μM	0.029μM	(Richendrfer et al., 2012; Roh and Choi, 2008; Watson et al., 2014)
dichlorvos	10nM	0.1μM	1.2nM	(Rajini et al., 2008; Watson et al., 2014)
ethanol	0.05%	0.01%-1%	0.1%	(Chen et al., 2011; Chromcova et al., 2012; Dhawan et al., 1999; Maes et al., 2012)
methanol	0.8%	1%	2%	(Chromcova et al., 2012; Katiki et al., 2011; Maes et al., 2012)
SDS	0.2mg/L	6.4nM (~1.8mg/L)		(Truong et al., 2014)
TritonX-100	5mg/L			
acrylamide	100μM		141μM	(Li et al., 2015)
glucose	55μM	>55mM	250mM	(Mondoux et al., 2011; Selderslaghs et al., 2009)

Species-related sensitivities may reflect differences in toxicokinetics in these different animal models, including toxicant uptake and metabolism. In planarians, the toxicants reach their target tissue by absorption through the skin and diffusion; however, future studies are needed to precisely determine the amount of chemicals taken up and processed by the animal.

In summary, we have shown that the freshwater planarian *D. japonica* is a suitable alternative animal model for developmental neurotoxicology. While planarians do not have the

morphological richness of zebrafish larvae (Truong et al., 2014), thus limiting morphological readouts, they have other unique features that make them a relevant model system: (1) the ability to test adult and developing animals, in parallel, allows us unprecedented insight into development specific effects of toxicants whose molecular and cellular basis remains to be explored in mechanistic studies and (2) because planarians are invertebrates but still possess significant neuronal complexity and homology to the human brain (Buttarelli et al., 2008), they allow us to conduct MTS studies to assess the toxicity of new compounds in a relevant context without the ethical dilemma that comes from working with vertebrate animals. To achieve the necessary throughput and specificity, our current assay clearly needs to be modified in two ways: (1) the different manual components must be integrated into an automated plate handling and scoring platform, and (2) additional readouts, *e.g.* phototaxis, chemotaxis, etc., must be added to the screen and quantitatively evaluated. Now that we have established the suitability of freshwater planarians as an animal model for developmental neurotoxicology, we plan on starting this second phase of system development.

ACKNOWLEDGEMENTS

Chapter 2, in full, is a reformatted reprint of the material as it appears in Hagstrom, Danielle; Cochet-Escartin, Olivier; Zhang, Siqi; Khuu, Cindy; and Collins, Eva-Maria S. "Freshwater planarians as an alternative animal model for neurotoxicology", Toxicological Sciences, vol. 147, 2015. The version of record is available online at: https://academic.oup.com/toxsci/article/147/1/270/1642148. Use of this manuscript in the dissertation herein is covered by the rights permitted to the authors by Oxford Journals. Danielle Hagstrom, Olivier Cochet-Escartin, and Eva-Maria S. Collins designed the experiments and co-wrote the manuscript. Danielle Hagstrom, Olivier Cochet-Escartin, and Siqi Zhang designed and performed the experiments, analyzed and interpreted the data. Cindy Khuu helped with experiments and data analysis. Danielle Hagstrom and Olivier Cochet-Escartin were the primary investigators and authors of this material.

REFERENCES

Abel, P. D. (1974). Toxicity of synthetic detergents to fish and aquatic invertebrates. *J. Fish Biol.* **6**, 279–298.

Amitai, G., Moorad, D., Adani, R. and Doctor, B. P. (1998). Inhibition of acetylcholinesterase and butyrylcholinesterase by chlorpyrifos-oxon. *Biochem. Pharmacol.* **56**, 293–299.

Bichara, D., Calcaterra, N. B., Arranz, S., Armas, P. and Simonetta, S. H. (2014). Set-up of an infrared fast behavioral assay using zebrafish (Danio rerio) larvae, and its application in compound biotoxicity screening. *J. Appl. Toxicol.* **34**, 214–9.

Bjørling-Poulsen, M., Andersen, H. R. and Grandjean, P. (2008). Potential developmental neurotoxicity of pesticides used in Europe. *Environ. Health* **7**, 50.

Boyd, W., Smith, M. and Freedman, J. (2012). Caenorhabditis elegans as a model in developmental toxicology. In *Developmental Toxicology* (ed. Harris, C.) and Hansen, J. M.), pp. 15–24. Totowa, NJ: Humana Press.

Bradberry, S. M., Cage, S. A., Proudfoot, A. T. and Vale, J. A. (2005). Poisoning due to pyrethroids. *Toxicol. Rev.* **24**, 93–106.

Bradbury, S. P. and Coats, J. R. (1989). Comparative toxicology of the pyrethroid insecticides. *Rev. Environ. Contam. Toxicol.* **108**, 133–177.

Buttarelli, F. R., Pellicano, C. and Pontieri, F. E. (2008). Neuropharmacology and behavior in planarians: Translations to mammals. *Comp. Biochem. Physiol. - C Toxicol. Pharmacol.* **147**, 399–408.

Cebrià, F. (2007). Regenerating the central nervous system: how easy for planarians! *Dev. Genes Evol.* **217**, 733–48.

Cebrià, F. and Newmark, P. A. (2005). Planarian homologs of netrin and netrin receptor are required for proper regeneration of the central nervous system and the maintenance of nervous system architecture. *Development* **132**, 3691–703.

Cebrià, F., Nakazawa, M., Mineta, K., Ikeo, K., Gojobori, T. and Agata, K. (2002). Dissecting planarian central nervous system regeneration by the expression of neural-specific genes. *Dev. Growth Differ.* **44**, 135–46.

Chen, T.-H., Wang, Y.-H. and Wu, Y.-H. (2011). Developmental exposures to ethanol or dimethylsulfoxide at low concentrations alter locomotor activity in larval zebrafish: implications for behavioral toxicity bioassays. *Aquat. Toxicol.* **102**, 162–6.

Chromcova, L., Stepanova, S., Plhalova, L., Praskova, E. and Svobodova, Z. (2012). Effect of four selected carrier solvents on embryonal stages of Danio rerio. *Neuro Endocrinol. Lett.* **33 Suppl 3**, 60–5.

Collins, F. S., Gray, G. M. and Bucher, J. R. (2008). Transforming environmental health protection. *Science* **319**, 906–7.

Demicco, A., Cooper, K. R., Richardson, J. R. and White, L. A. (2009). Developmental neurotoxicity of pyrethroid insecticides in zebrafish embryos. *Toxicol. Sci.* **113**, 177–186.

Dhawan, R., Dusenbery, D. B. and Williams, P. L. (1999). Comparison of lethality, reproduction, and behavior as toxicological endpoints in the nematode Caenorhabditis elegans. *J. Toxicol. Environ. Health. A* **58**, 451–62.

Dong, Z., Yuwen, Y., Wang, Q., Chen, G. and Liu, D. (2012). Eight genes expression patterns during visual system regeneration in Dugesia japonica. *Gene Expr. Patterns* **12**, 1–6.

Dunkel, J., Talbot, J. and Schötz, E.-M. (2011). Memory and obesity affect the population dynamics of asexual freshwater planarians. *Phys. Biol.* **8**, 026003.

Erdfelder, E., Faul, F. and Buchner, A. (1996). GPOWER: A general power analysis program. *Behav. Res. Methods, Instruments, Comput.* **28**, 1–11.

Fei, X.-C., Song, C. and Gao, H.-W. (2010). Transmembrane transports of acrylamide and bisphenol A and effects on development of zebrafish (Danio rerio). *J. Hazard. Mater.* **184**, 81–8.

Inoue, T., Yamashita, T. and Agata, K. (2014). Thermosensory signaling by TRPM is processed by brain serotonergic neurons to produce planarian thermotaxis. *J. Neurosci.* **34**, 15701–14.

Judson, R. S., Houck, K. A., Kavlock, R. J., Knudsen, T. B., Martin, M. T., Mortensen, H. M., Reif, D. M., Rotroff, D. M., Shah, I., Richard, A. M., et al. (2010). In vitro screening of environmental chemicals for targeted testing prioritization: the ToxCast project. *Environ. Health Perspect.* **118**, 485–92.

Katiki, L. M., Ferreira, J. F. S., Zajac, A. M., Masler, C., Lindsay, D. S., Chagas, A. C. S. and Amarante, A. F. T. (2011). Caenorhabditis elegans as a model to screen plant extracts and compounds as natural anthelmintics for veterinary use. *Vet. Parasitol.* **182**, 264–8.

Knight, A. W., Little, S., Houck, K., Dix, D., Judson, R., Richard, A., McCarroll, N., Akerman, G., Yang, C., Birrell, L., et al. (2009). Evaluation of high-throughput genotoxicity assays used in profiling the US EPA ToxCast chemicals. *Regul. Toxicol. Pharmacol.* **55**, 188–99.

Li, M.-H. (2008). Effects of nonionic and ionic surfactants on survival, oxidative stress, and cholinesterase activity of planarian. *Chemosphere* **70**, 1796–803.

Li, Y., Zhao, Y., Huang, X., Lin, X., Guo, Y., Wang, D., Li, C. and Wang, D. (2013). Serotonin control of thermotaxis memory behavior in nematode Caenorhabditis elegans. *PLoS One* **8**, e77779.

Li, J., Li, D., Yang, Y., Xu, T., Li, P. and He, D. (2015). Acrylamide induces locomotor defects and degeneration of dopamine neurons in Caenorhabditis elegans. *J. Appl. Toxicol.*

LoPachin, R. M. (2004). The changing view of acrylamide neurotoxicity. *Neurotoxicology* **25**, 617–30.

Lowe, J. R., Mahool, T. D. and Staehle, M. M. (2015). Ethanol exposure induces a delay in the reacquisition of function during head regeneration in Schmidtea mediterranea. *Neurotoxicol. Teratol.* **48**, 28–32.

Maes, J., Verlooy, L., Buenafe, O. E., de Witte, P. A. M., Esguerra, C. V and Crawford, A. D. (2012). Evaluation of 14 organic solvents and carriers for screening applications in zebrafish embryos and larvae. *PLoS One* **7**, e43850.

Mannini, L., Rossi, L., Deri, P., Gremigni, V., Salvetti, A., Saló, E. and Batistoni, R. (2004). Djeyes absent (Djeya) controls prototypic planarian eye regeneration by cooperating with the transcription factor Djsix-1. *Dev. Biol.* **269**, 346–59.

Mineta, K., Nakazawa, M., Cebria, F., Ikeo, K., Agata, K. and Gojobori, T. (2003). Origin and evolutionary process of the CNS elucidated by comparative genomics analysis of planarian ESTs. *Proc. Natl. Acad. Sci. U. S. A.* **100**, 7666–71.

Mondoux, M. A., Love, D. C., Ghosh, S. K., Fukushige, T., Bond, M., Weerasinghe, G. R., Hanover, J. A. and Krause, M. W. (2011). O-linked-N-acetylglucosamine cycling and insulin signaling are required for the glucose stress response in Caenorhabditis elegans. *Genetics* **188**, 369–82.

Pagán, O. R., Rowlands, A. L. and Urban, K. R. (2006). Toxicity and behavioral effects of dimethylsulfoxide in planaria. *Neurosci. Lett.* **407**, 274–278.

Parng, C., Roy, N. M., Ton, C., Lin, Y. and McGrath, P. (2007). Neurotoxicity assessment using zebrafish. *J. Pharmacol. Toxicol. Methods* **55**, 103–12.

Parzefall, W. (2008). Minireview on the toxicity of dietary acrylamide. *Food Chem. Toxicol.* **46**, 1360–4.

Peterson, R. T., Nass, R., Boyd, W. A., Freedman, J. H., Dong, K. and Narahashi, T. (2008). Use of non-mammalian alternative models for neurotoxicological study. *Neurotoxicology* **29**, 546–55.

Rajini, P. S., Melstrom, P. and Williams, P. L. (2008). A Comparative Study on the Relationship Between Various Toxicological Endpoints in Caenorhabditis elegans Exposed to Organophosphorus Insecticides. *J. Toxicol. Environ. Health. A* **71**, 1043–1050.

Reddien, P. W. (2013). Specialized progenitors and regeneration. *Development* **140**, 951–7.

Reddien, P. W. and Sánchez Alvarado, A. (2004). Fundamentals of planarian regeneration. *Annu. Rev. Cell Dev. Biol.* **20**, 725–57.

Richendrfer, H., Pelkowski, S. D., Colwill, R. M. and Créton, R. (2012). Developmental sub-chronic exposure to chlorpyrifos reduces anxiety-related behavior in zebrafish larvae.

Neurotoxicol. Teratol. **34**, 458–65.

Rink, J. C. (2013). Stem cell systems and regeneration in planaria. *Dev. Genes Evol.* **223**, 67–84.

Roh, J.-Y. and Choi, J. (2008). Ecotoxicological evaluation of chlorpyrifos exposure on the nematode Caenorhabditis elegans. *Ecotoxicol. Environ. Saf.* **71**, 483–9.

Sakurai, T., Lee, H., Kashima, M., Saito, Y., Hayashi, T., Kudome-Takamatsu, T., Nishimura, O., Agata, K. and Shibata, N. (2012). The planarian P2X homolog in the regulation of asexual reproduction. *Int. J. Dev. Biol.* **56**, 173–82.

Scimone, M. L., Kravarik, K. M., Lapan, S. W. and Reddien, P. W. (2014). Neoblast specialization in regeneration of the planarian Schmidtea mediterranea. *Stem Cell Reports* **3**, 339–352.

Selderslaghs, I. W. T., Van Rompay, A. R., De Coen, W. and Witters, H. E. (2009). Development of a screening assay to identify teratogenic and embryotoxic chemicals using the zebrafish embryo. *Reprod. Toxicol.* **28**, 308–20.

Sipes, N. S., Padilla, S. and Knudsen, T. B. (2011). Zebrafish—As an integrative model for twenty-first century toxicity testing. *Birth Defects Res. Part C Embryo Today Rev.* **93**, 256–267.

Sprando, R. L., Olejnik, N., Cinar, H. N. and Ferguson, M. (2009). A method to rank order water soluble compounds according to their toxicity using Caenorhabditis elegans, a Complex Object Parametric Analyzer and Sorter, and axenic liquid media. *Food Chem. Toxicol.* **47**, 722–8.

Stevens, A. S., Pirotte, N., Plusquin, M., Willems, M., Neyens, T., Artois, T. and Smeets, K. (2014). Toxicity profiles and solvent-toxicant interference in the planarian Schmidtea mediterranea after dimethylsulfoxide (DMSO) exposure. *J. Appl. Toxicol.* **35**, 319–326.

Talbot, J. and Schötz, E.-M. (2011). Quantitative characterization of planarian wild-type behavior as a platform for screening locomotion phenotypes. *J. Exp. Biol.* **214**, 1063–7.

Tang, J., Cao, Y., Rose, R. L., Brimfield, A. A., Dai, D., Goldstein, J. A. and Hodgson, E. (2001). Metabolism of chlorpyrifos by human cytochrome P450 isoforms and human, mouse, and rat liver microsomes. *Drug Metab. Dispos.* **29**, 1201–4.

Truong, L., Reif, D. M., St Mary, L., Geier, M. C., Truong, H. D. and Tanguay, R. L. (2014). Multidimensional in vivo hazard assessment using zebrafish. *Toxicol. Sci.* **137**, 212–33.

Umesono, Y., Tasaki, J., Nishimura, Y., Hrouda, M., Kawaguchi, E., Yazawa, S., Nishimura, O., Hosoda, K., Inoue, T. and Agata, K. (2013). The molecular logic for planarian regeneration along the anterior-posterior axis. *Nature* **500**, 73–6.

Vliet, E. van (2011). Current standing and future prospects for the technologies proposed to transform toxicity testing in the 21st century. *ALTEX* **28**, 17–44.

Wagner, D. E., Wang, I. E. and Reddien, P. W. (2011). Clonogenic neoblasts are pluripotent adult stem cells that underlie planarian regeneration. *Science* **332**, 811–6.

Watson, F. L., Schmidt, H., Turman, Z. K., Hole, N., Garcia, H., Gregg, J., Tilghman, J. and Fradinger, E. A. (2014). Organophosphate pesticides induce morphological abnormalities and decrease locomotor activity and heart rate in Danio rerio and Xenopus laevis. *Environ. Toxicol. Chem.* **33**, 1337–45.

Yu, X., Zhao, W., Ma, J., Fu, X. and Zhao, Z. J. (2011). Beneficial and harmful effects of alcohol exposure on Caenorhabditis elegans worms. *Biochem. Biophys. Res. Commun.* **412**, 757–62.

Yuan, Z., Zhao, B. and Zhang, Y. (2012). Effects of dimethylsulfoxide on behavior and antioxidant enzymes response of planarian Dugesia japonica. *Toxicol. Ind. Health* **28**, 449–457.

Chapter 3: Multi-behavioral endpoint testing of an 87-chemical compound library in freshwater planarians

Reprinted from: Zhang, Siqi; Hagstrom, Danielle; Hayes, Patrick; Graham, Aaron; and Collins, Eva-Maria S. "Multi-behavioral endpoint testing of an 87-chemical compound library in freshwater planarians", Toxicological Sciences, kfy145, 2018 (in press).
Supplementary materials can be accessed online at: https://academic.oup.com/toxsci/advance-article/doi/10.1093/toxsci/kfy145/5034903?guestAccessKey=3ddabc3c-f78a-4814-914b-0469e0d3f7d4

ABSTRACT

There is an increased recognition in the field of toxicology of the value of medium-to-high-throughput screening methods using *in vitro* and alternative animal models. We have previously introduced the asexual freshwater planarian *Dugesia japonica* as a new alternative animal model and proposed that it is particularly well-suited for the study of developmental neurotoxicology. In this paper, we discuss how we have expanded and automated our screening methodology to allow for fast screening of multiple behavioral endpoints, developmental toxicity, and mortality. Using an 87-compound library provided by the National Toxicology Program (NTP), consisting of known and suspected neurotoxicants, including drugs, flame retardants, industrial chemicals, polycyclic aromatic hydrocarbons (PAHs), pesticides and presumptive negative controls, we further evaluate the benefits and limitations of the system for medium-throughput screening, focusing on the technical aspects of the system. We show that, in the context of this library, planarians are the most sensitive to pesticides with 16/16 compounds causing toxicity and the least sensitive to PAHs, with only 5/17 causing toxicity. Furthermore, while none of the presumptive negative controls were bioactive in adult planarians, 2/5, acetaminophen and acetylsalicylic acid, were bioactive in regenerating worms. Notably, these compounds were previously reported as developmentally toxic in mammalian studies. Through parallel screening of adults and developing animals, planarians are thus a useful model to detect such developmental-specific effects, which was observed for 13 chemicals in this library. We use the data and experience gained from this screen to propose guidelines for best practices when using planarians for toxicology screens.

INTRODUCTION

It has been nearly a decade since the launch of the "Toxicology Testing in the 21st century" (Tox21; www.tox21.gov) federal initiative to transform toxicology testing in the United States. Its ongoing goal is to dramatically increase the coverage of chemical testing by replacing traditional mammalian models with alternative testing strategies amenable to high-throughput screening (HTS) (Collins et al., 2008). Since its inception, thousands of chemicals have been screened *in vitro* using HTS robotic systems to identify mechanisms of action and prioritize chemicals for further targeted testing. However, connecting those HTS data to their *in vivo* relevancy to be predictive of effects on human health remains challenging as important aspects of biology, such as xenobiotic metabolism and interactions between cell types, are inherently missing in these *in vitro* systems. In addition, although these assays often focus on key molecular and cellular targets underlying known toxicity pathways, more knowledge is needed to connect these molecular and cellular effects to functional consequences on organismal health to discern their significance. Realizing this need and the urgency of the matter, the development of medium-throughput screening (MTS)-amenable alternative animal models, such as zebrafish and nematodes, was encouraged as part of the Tox21 initiative. These animal models are attractive MTS toxicology systems due to their ease of breeding and chemical administration, low cost, small size, short developmental time, and genetic tractability (Boyd et al., 2012; Boyd et al., 2015; Hill et al., 2005; Tejeda-Benitez and Olivero-Verbel, 2016; Truong et al., 2014). Moreover, each system provides unique advantages. For example, the transparency of zebrafish larvae, which develop externally, allows for a breadth of morphological assessments of the development of internal structures in living animals (Kimmel et al., 1995; Truong et al., 2014). However, despite these advantages, the toxicology community remains divided on the added

value of these alternative systems, particularly as each has its own drawbacks, species-specific sensitivities and discrepancies with humans, as with any system (Boyd et al., 2015; Scholz, 2013).

A battery approach using multiple complementary testing platforms allows for comparative analyses to find concordance between systems and produce more weight of evidence for reliable and relevant predictions of effects on human health, as demonstrated by a recent battery screen on organophosphorus flame retardants (Behl et al., 2015). These predictions can then be verified by targeted testing in mammalian models, which, although not without caveats, are still considered the gold standard in toxicology, particularly for regulatory decisions (Tsuji and Crofton, 2012).

We have previously introduced the freshwater planarian *Dugesia japonica* as a new alternative animal model for developmental neurotoxicology and shown that it possesses comparable sensitivity to other, more established alternative models (Hagstrom et al., 2015). In addition, the planarian system offers the unique advantage to study adult and regenerating/developing animals in parallel with the same assays, because in this asexual species the sole form of neurodevelopment is neuroregeneration of a head from a tail piece following fission. Finally, planarians have a large behavioral repertoire that can be quantified and assessed in a fully automated fashion, providing multiple distinct endpoints of neuronal function. Importantly, the planarian nervous system contains most of the same neurotransmitters as the mammalian brain and is considered more structurally similar to the vertebrate brain than other invertebrate brains (Buttarelli et al., 2008; Cebrià, 2007; Mineta et al., 2003; Ross et al., 2017; Umesono et al., 2011). A brief review of the planarian nervous system and of neuroregeneration can be found in Supplementary Information, Section 1. Moreover, we have recently reviewed

the history, challenges and benefits of planarians as a model for neurotoxicology (Hagstrom et al., 2016).

While our previous work demonstrated the potential of *D. japonica* for toxicology screens, it was limited in scope (10 compounds, including controls) (Hagstrom et al., 2015). Most of the experiments and analysis were conducted manually, which limited throughput and scalability. Our screening platform has since been greatly expanded and optimized to incorporate more behavioral endpoints that are all assayed in a fully automated fashion.

In this study, we evaluate the capabilities and limitations of this improved planarian MTS platform by testing a library of 87 compounds provided by the National Toxicology Program (NTP), consisting of known and suspected developmental neurotoxicants and negative controls. This compound library, which has also been tested in other alternative systems, including zebrafish and *in vitro* cell culture systems (see other articles in this special issue), gives us a unique opportunity to test the robustness and relevancy of the planarian system as a whole and of the specific endpoints we have developed to assay different neuronal functions. We focus on evaluating the technical aspects of our expanded screening platform and the utility of the planarian model system for toxicology screens, setting clear standards and challenges that need to be addressed for the field going forward. A direct comparison of the results of this planarian screen with a zebrafish model, and with available mammalian data, are the focus of a companion paper (Hagstrom et al.).

MATERIALS AND METHODS

Test animals

Freshwater planarians of the species *D. japonica*, originally obtained from Shanghai University, China, and cultivated in our lab >5 years, were used for all tests. Planarians were stored in 1x Instant Ocean (IO, Blacksburg, VA) in Tupperware containers at 20°C in a Panasonic refrigerated incubator in the dark. Animals were fed organic chicken or beef liver purchased from a local butcher twice a week. Planarian containers were cleaned 3 times a week per standard protocols (Dunkel et al., 2011). Animals were starved for at least 5 days before being used for experiments and their containers were cleaned immediately prior to worm selection for experiments. Test worms were manually selected to fall within a certain range of sizes and we found full worm length, after automated size measurement, to be 7.3mm +/- 2.3mm (mean +/- SD), and tail worm length to be 7.3mm +/- 2.7mm (mean +/- SD). Slightly larger intact planarians (~1-2 mm larger to account for the size of the head) were chosen for regenerating tail experiments such that the final sizes of the amputated tail pieces were similar to the full/adult test planarians. Some animals were recovered after the screen and reintroduced into the normal population after a minimum of 4 weeks of separate care. As planarians undergo dynamic turnover of all cell types within a few weeks (Rink, 2013) and as we observed no qualitative differences in behavior between recovered and wild-type animals, these recovered worms were considered functionally wild-type. For all experiments, only fully regenerated worms which had not been fed within one week and which were found gliding normally in the container were used. To study regenerating animals, on day 1, intact worms were amputated, by cutting posterior to the auricles and anterior to the pharynx with an ethanol-sterilized razor blade, no more than 3 hours before the compounds were added. During the course of the screen, some

animals underwent fission producing at least 2 pieces (a head and a tail piece) (see below and Supplementary Information, Section 4). To obtain full and tail worms of comparable size, we amputate slightly larger worms to obtain the tail pieces. Since fission probability increases with worm size (Carter et al., 2015; Yang et al., 2017) and decapitation (Bronsted, 1955; Hori and Kishida, 1998; Morita and Best, 1984), fission primarily occurred for tail worms. For these cases, only the head piece was considered in all morphological and behavioral analyses, as this would represent the first regenerated brain.

Test compounds

The 87-compound library (summarized in Supplementary Table 1) was provided by the NTP and included 5 categories: pesticides, flame retardants, drugs, industrial compounds and polycyclic aromatic hydrocarbons (PAHs) (Behl et al., 2018). Five negative controls were also included. The compounds were provided as ~20mM stocks (or lower) in 100% dimethyl sulfoxide (DMSO, Gaylord Chemicals, Slidell, LA) in a 96-well plate. The master library was stored at -80ºC.

Chemical preparation and screen setup

The 87-chemical library was separated into 5 "Chemical Sets" of 18 (sets 1-4) or 15 (set 5) chemicals (Supplementary Table 1). Chemicals in the same Chemical Set were tested on the same day, i.e. the same experiment. All chemicals, regardless of provided concentration, were treated the same. 0.5% DMSO was used as solvent control, because we have previously shown that there are no effects on planarian morphology or behavior at this concentration (Hagstrom et al., 2015). To keep the final DMSO concentration constant at 0.5%, the highest concentration tested in the screening process was a 200-fold dilution of the original provided chemical stock. Subsequent concentrations were a 10-fold dilution of the previous. Thus, each compound was

tested at 5 concentrations, generally ranging from 10nM to 100µM (with some exceptions, see Supplementary Table 1). Each 48-well screening plate assayed n=8 planarians in a 0.5% DMSO control, and n=8 worms each per concentration of chemical (5 test concentrations per plate in total) (Figure 3.1). Experiments were performed in triplicate (independent experiments performed on different days, final n=24) with the concentrations shifted down two rows (one row in run D, see raw data in the Dryad Digital Repository (doi: 10.5061/dryad.mk6m608)) with each replicate to control for edge effects. For each chemical and each experiment, 2 plates, one containing full (intact) planarians and one containing regenerating tails, were assayed. Screening was performed on day 7 and day 12.

Plate setup and storage

200X stock plates of the tested chemicals were prepared ahead of time by transferring 50µl of the provided chemical stock into one well of a 48-well plate (Genesee, San Diego, CA). 10-fold serial dilutions were performed in DMSO in the same plate using a multi-pipettor to create the remaining stock concentrations. The control well contained DMSO only. These plates were sealed with foil seals (Thermo Scientific, Waltham, MA) and stored at -20°C. On the day of plate set-up, the 200X stock plates were thawed at room temperature for approximately 30 minutes. 10X stocks plates were then made by diluting the 200X stocks 20X in IO water. Dilutions were mixed by rotation on an orbital shaker for approximately 10 minutes before use. The highest concentration of some chemicals, noted in Supplementary Table 1, precipitated out of solution in the 10X stock plates due to low solubility in water.

Screening plates were prepared by transferring individual full planarians or amputated tail pieces into the wells of a 48-well plate with 200µl of IO water using a P1000 pipet with a cut-off tip. A multi-pipettor was used to remove 20µl of IO water from each well and add 20µl

of the appropriate 10X stock solution. The plates were sealed with ThermalSeal RTS seals (Excel Scientific, Victorville, CA) to prevent evaporation and gas exchange with the environment. The plates were stored, without their lids, in stacks in the dark at room temperature when not being screened. Prepared plates were only moved to the screening platform when screened at day 7 and day 12.

Screening platform

We have further automated and expanded the custom-built planarian screening platform introduced in (Hagstrom et al., 2015). The new platform consists of a commercial robotic microplate handler (Hudson Robotics, Springfield Township, NJ), two custom-built imaging systems and multiple assay stations (Figure 3.1). One imaging system is specifically used to image individual planarians at high spatial resolution to allow for quantification of lethality, morphology and eye regeneration. It consists of 4 monochromatic Flea USB3 cameras (FLIR Systems Inc., Wilsonville, OR), each equipped with a fixed-focal (16mm) optical lens (Tamron, Saitama, Japan) and 5mm spacer (Edmund Optics, Santa Monica, CA). Each camera is used to image a single well, thus 4 wells are imaged simultaneously and the entire plate is scanned in the x- and y- directions. The second imaging system consists of one monochromatic Flea USB3 camera, equipped with a fixed-focal (25mm) double-gauss lens (Edmund Optics) and red filter (Roscolux, Stamford, CT), which is used to image the whole plate from above for all behavioral assays. To prevent angular distortion on the edge of the wells, a Fresnel lens (MagniPros, South El Monte, CA) is placed on top of the plate when imaging with the single camera. All cameras are mounted on a custom rail platform (Inventables Inc., Chicago, IL), which enables x-, y- and linear motion. All assays were imaged at a frame rate of 5 frames per second. Different assay stations were designed specifically for different assays, as explained below. The imaging

systems, assay stations and plate handler were controlled by the computer. The stimuli and illuminations in the assays were mainly controlled via Arduino (Arduino, Somerville, MA). Image acquisition was controlled through custom LabVIEW scripts. All assays were performed in the following order, whereby the notation in brackets indicates on which day(s) the assay was performed: phototaxis (d7/d12), unstimulated locomotion (d7/d12), lethality/regeneration (d7/d12), thermotaxis (d12) and scrunching (d12) (see also Figure 3.1). Any data analysis which had to be cross-checked manually was performed blinded by a single investigator, who was not given the chemical identity of the plates. The raw data are provided in the Dryad Digital Repository (doi:10.5061/dryad.mk6m608).

Lethality assay

To assay planarian lethality and eye regeneration, high-resolution imaging of each individual well was performed. Since planarians tend to rest on the edge of the well, prior to imaging each set of 4 wells, the screening plate was placed on a microplate orbital shaker (Big Bear Automation, Santa Clara, CA) and shaken for 1 second at 800 rotations per minute (rpm) to force the worms to the center of the well. Each well was then imaged for 10 seconds. The plate was illuminated from above by red LED strings (Amazon, Seattle, WA) attached around the camera lens.

Semi-automatic analysis was performed on the image sequence of each single planarian to determine whether the animal was alive or dead. Death was determined by the absence of the worm or the presence of a disintegrating body, using the fact that a dead planarian usually disintegrates (Buchanan, 1935). An alive planarian was marked as ‘0’and a dead one as ‘1’ (Figure 3.2A-B). If the worm “suicides” by leaving the water and thus drying out, the respective well would be marked as ‘10’ and discarded in the data analysis.

Lethality was calculated as

$$lethality = \frac{total\ number\ of\ dead\ planarians}{total\ number\ of\ planarians}$$

Where "total number of planarians" excludes any suicides. For compounds which showed significant lethality in the concentration range tested (see Statistical Testing section below), the fraction of dead planarians as a function of concentration at days 7 and 12 was fitted as described in (Hagstrom et al., 2015) using a Hill equation to obtain the LC_{50} (Supplementary Figure S1). Of note, fissioned planarians in a single well were marked as one unit. If any fissioned piece was alive in one well, this well was considered to contain an alive worm and marked as '1'.

Eye regeneration assay

Eye regeneration data was also collected from the high-resolution imaging performed in the lethality assay (described above). Image analysis was performed with a custom Python-based machine learning algorithm using a transfer learning neural network (Pan and Yang, 2010). A custom pre-processing program was used in Python to crop 100 x 100 pixel^2 images of a planarian's head region from the original images. The cropped images were imported into the neural network, which categorized the worms based on a prediction of the number of eyes in the images: normal (2 eyes), abnormal (0, 1 eye or >2 eyes), and invalid (for example, when the worm was on the edge of the well, flipped over, or the head region was not properly cropped) (Figure 3.2D-G). The neural network was trained using a training set consisting of 2206 images of normal eyes, 1047 images of abnormal eyes and 6703 images with undetectable quality. The training set was labeled semi-manually with a customized computer program. The prediction results of each image for each alive planarian were integrated using a custom MATLAB script to make the final decision of the number of eyes in this regenerating animal. If more than 1 image frame predicted normal eyes, the planarian was determined to have normal eyes. If more than 1

image frame predicted abnormal eyes, but no image frame predicted normal eyes, the worm was determined to have abnormal eyes. In all other cases, the image sequence was an invalid case, due to lack of analyzable images resulting from worm positioning in the well which obscured the eyes, see Figure 3.2G), and discarded in the following analysis. Since the prediction of the "abnormal" category was often inaccurate because of the small training set and large variability in data, we manually double checked all results predicted to be "abnormal" and invalid. For planarians which underwent fission during the course of the screen, resulting in more than 1 animal in a well, the number of regenerated eyes in the head piece was scored manually. The eye regeneration rate was calculated as

$$eye\ regeneration\ rate = \frac{number\ of\ planarians\ with\ 2\ eyes\ regenerated}{number\ of\ analyzable\ planarians}$$

Unstimulated behavioral assay

As planarians tend to rest when stored in the dark, screening plates were firstly shaken for 6 seconds at 900rpm on the microplate shaker used in the lethality assay, to encourage motion before imaging. The screening plate was then moved by the automatic plate handler onto a transparent plate holder. There it was imaged for 3 min by the single camera, with a cold LED panel (B&H Photo Video, New York, NY) equipped with a red filter (Roscolux, Stamford, CT) placed under the transparent plate holder to provide illumination for tracking.

Image analysis was performed using a custom MATLAB script, based on center of mass (COM) tracking. To accurately determine the COM of each planarian, the tracking analysis was specifically optimized for fissioned worms (see Supplementary Information, Section 4). This assay provided 2 readouts: the fraction of time spent resting and the instantaneous speed of locomotion. The instantaneous speeds were calculated for all tracks over 2-second intervals to increase the signal-to-noise ratio (Hagstrom et al., 2015). An empirically determined absolute

speed cutoff was used to distinguish the planarians' moving and resting behaviors (see Supplementary Information, Section 5). Instantaneous speeds less than 0.5 mm/s were considered to represent resting and were disregarded in speed calculations. The fraction of time spent resting was calculated as the amount of time resting divided by the total time tracked. Speed values > 0.5 mm/s represent planarian locomotion and were averaged to calculate the mean speed for each planarian. Of note, this speed includes instances of both swimming and gliding behaviors and thus differs from our previously used measure ((Hagstrom et al., 2015), Supplementary Information, Section 5). Planarians with no tracking data (i.e. tracking was lost for worms moving at the edge of the well due to low contrast) were considered non-analyzable and excluded for further analysis. In <4% of day 7 plates and <12% of day 12 plates (full animal and regenerating tails), 1 or 2 animals were non-analyzable. In ~1% of the day 12 plates, 3-5 animals were excluded. For fissioned worms, when the head and tail pieces were distinguishable, analysis was only performed on the head piece. Otherwise, when the head and tail pieces were indistinguishable, analysis was only performed on the fastest piece, as heads generally move faster.

Phototaxis

For this assay, the same transparent plate holder was used as for the unstimulated behavioral assay. Planarians are negative phototactic to blue light and insensitive to red light (Paskin et al., 2014). To study negative phototactic behavior, blue LED lights (SuperNight, Portland, OR) surrounding the screening plate were used to provide the blue light stimulus. Additionally, red backlighting underneath the plate holder provided light for tracking throughout the assay. Similar to photomotor response studies in zebrafish larvae (Kokel and Peterson, 2011; Truong et al., 2014), we used a combination of dark-light-dark-light cycles. First, the plate was

imaged for 30 seconds using red light (dark condition) and then imaged for 30 seconds with both red and blue lights (light condition) (Figure 3.5A). This sequence was then repeated. The red filter on the single camera blocks the blue light, which optimizes the imaging of this assay. Because it was only found after screening was complete that the second dark cycle was too short for animals to adapt, we compared the planarians' behavior in the first dark cycle with that in cycles 2-4 (1^{st} light cycle, 2^{nd} dark cycle and 2^{nd} light cycle) instead of analyzing each dark/light cycle sequence separately.

Image analysis was automated using a custom MATLAB script. The instantaneous speeds were calculated as in the unstimulated assay. The instantaneous speed was averaged in cycle 1 and cycles 2-4. Any average speed value < 0.01 mm/s (background noise level) was set to 0.01 mm/s. Speed cutoffs were set as the mean speed of the control populations in DMSO measured in the unstimulated behavioral assay, for Day 7/Day 12 full worms and regenerating tails. In the test concentrations, planarians with a mean speed in cycle 1 lower than the speed cutoff were excluded due to their relatively high background activity, which would cause false positives in the phototaxis assay. Otherwise, the mean speed in cycles 2-4 was normalized by the mean speed in cycle 1 (background activity). Planarians with a normalized mean speed in cycles 2-4 higher than 1 were defined as having reacted to the light stimulus, and marked as "1". If the normalized mean speed in cycles 2-4 did not exceed 1, the planarian was considered to have no reaction, and marked as "0". If the planarian was dead or had high background activity, it was discarded and marked as "NaN". The phototaxis response rate was calculated as

$$phototaxis\ response\ rate = \frac{total\ number\ of\ worms\ reacting\ to\ light}{total\ number\ of\ analyzable\ worms}$$

Thermotaxis assay

The plate was placed on a custom setup with 12 peltiers (15mm x 15mm) (Digi-key, Thief River Falls, MN) that are evenly spaced and embedded in an aluminum heat sink. The peltiers are arranged in a matrix of 3 rows x 4 columns (i.e. 4 wells share one peltier) and powered by an AC to DC power supply (Genssi, Las Vegas, NV) (Figure 3.5B). This setup, which is controlled automatically through an Arduino board, creates an identical heat gradient with a temperature difference of 3-4°C in each well of the screening plate. During the assay, the plate was imaged without the heat gradient (ambient temperature) for 2 minutes, and then imaged with the heat gradient for 4 minutes by the single camera. The plate was illuminated from the top by a custom-made red LED ceiling light which does not obscure the view of the camera.

Image analysis was performed using a custom, automated MATLAB script. The COM of each planarian was tracked over time and used to calculate the fraction of time the animal spent in the cold area in the well when the gradient is on. Since it takes time to establish a stable heat gradient across the well, we only accounted for the fraction of time the worm spent in the cold area during the last two minutes of the assay. The cold area in each well was defined as the area of a sector with central angle of 120° (Figure 3.5B). Since the image analysis worked poorly on fissioned planarians, since it expects one object per well, we manually calculated the fraction of time the head piece spent in the cold area.

Scrunching assay

Scrunching is a musculature-driven escape gait in planarians, which can be triggered by multiple external stimuli, including amputation, high heat, electric shock and low pH. It is characterized by asymmetric elongation-contraction cycles (with elongation time > contraction

time), and a species-specific frequency and amplitude (Cochet-Escartin et al., 2015). To induce scrunching in the screening platform, the screening plate was placed on a peltier plate (TE Technology Inc., Traverse City, MI), which was controlled by the computer through a temperature controller board (TE Technology Inc.), to increase the aquatic temperature in the wells. The temperature of the peltier plate was initially set to 65°C for the first 30 seconds to quickly heat up the plate from room temperature. Then, the temperature was gradually decreased to 43°C to stabilize the aquatic temperature across the plate at around 32°C for 4 minutes (Supplementary Figure S3), which was sufficient to induce wild-type *D. japonica* to scrunch. The plate was imaged by the single camera and illuminated by the same type of custom red LED light used in thermotaxis (see above).

Image analysis was performed using a custom, automated MATLAB script. The COM and length of each planarian were tracked over time. The worm's length over time was plotted and smoothed to detect instances of scrunching. We extracted body length oscillations in the smoothed plot which fulfilled the scrunching criteria mentioned above (asymmetric cycles, characteristic frequency) to determine instances of scrunching (Figure 3.5C). We defined such oscillations consisting of >3 consecutive peaks in the body length versus time plot as scrunching and marked the planarian as "1". If no such characteristic oscillations were found, the worm was marked as "0" for no scrunching. If the planarian was dead or not properly detected (not enough tracking data), it was discarded and marked as "NaN". The automated image analysis was not possible with fissioned planarians and thus these animals were scored manually. Scrunching rate was calculated as

$$scrunching\ rate = \frac{total\ number\ of\ scrunching\ worms}{total\ number\ of\ analyzable\ worms}$$

Statistical testing

All data from the triplicate runs were compiled before performing any statistical test. For lethality, eye regeneration, phototaxis and scrunching endpoints, significant effects were determined using a one-tailed Fisher's exact test to compare the rates determined for each chemical concentration with the rate of its own DMSO controls. For thermotaxis and unstimulated behavioral endpoints, Tukey's interquartile test was first used to remove any outliers, with at most 5% (e.g. 1 out of 24 worms) of the data removed. Since the distribution of the thermotaxis data was highly skewed and variable, a non-parametric one-tailed Mann Whitney U-test was used to compare the distributions of the fraction of time in the cold area for each chemical concentration with the respective distribution of its own control. For speed and fraction of time resting from the unstimulated behavior assay, Lilliefors test was first used to test the normality of the samples. Depending on whether the sample distributions were normal or not, we performed either a parametric two-tailed t-test or a nonparametric two-tailed Mann-Whitney U-test, respectively. For all endpoints, any condition with a p-value less than 0.05 was considered statistically different from the controls. However, we observed that due to low variance in some individual plate control populations (and high variability across plates), some statistically relevant hits were likely not biologically meaningful (see Supplementary Information Section 2 and Supplementary Figure S6). Examples such as this resulted in a large number of dose-independent hits and hits in the negative controls, together suggesting these may be false positives. Thus, to reduce potential false positives, we disregarded hits that had a smaller effect than determined by a "biological relevance" cutoff based on the variability of the DMSO controls in each assay. These cutoffs were meant to disregard hits that fell within the variability of the DMSO controls across all plates and were thus based on the distribution of the compiled

control values for each chemical (n=87) and endpoint (Supplementary Figure S4). High variability within animal behavior endpoints has also been observed in zebrafish (Zhang et al., 2017). For endpoints where the distribution of the compiled control values was normal (unstimulated behavior and phototaxis), cutoffs were based on mean +/- 2 or 3 SD (see Supplementary Information), respectively. For endpoints where the distribution of the compiled control values was not normal (day 12 lethality, thermotaxis, and scrunching), cutoffs were set as the 5^{th} and 95^{th} quantiles. These cutoffs were empirically determined to encompass the variability of the DMSO controls and to minimize dose-independent hits (see Supplementary Information Section 2 for more details). Similar approaches to creating assay-specific noise threshold levels has been described previously (Behl et al., 2015). Of note, the distributions of control values in the day7 lethality and eye regeneration endpoints were so narrow (Supplementary Figure S4) that biological relevancy cutoffs were not appropriate. However, because controls exhibited few deaths at day 7, some chemical concentrations were designated as statistically significant hits for day 7 lethality but not day 12. These cases were excluded as artifacts. Moreover, we checked for inconsistency in the data to find instances where a single plate was responsible for designating a "hit". Inconsistent hits were defined as instances with only 1 replicate outside of the biological relevancy cutoff range and two replicates within the control variability. These hits were therefore excluded (see Supplementary Figure S5 for the statistical workflow). Other groups have reportedly dealt with similar issues with plate-to-plate variability by rerunning inconsistent plates (Zhang et al., 2017), whereas we have decided to keep all data. The lowest observed effect level (LOEL) was determined as the lowest concentration which showed a significant effect (i.e. statistically significant and passed inconsistency and biological relevancy tests, Supplementary

Figure S5) in any endpoint. All statistical analyses were performed in MATLAB (see Table 3.1 for a summary).

To determine the observed power of each of the tested endpoints, we performed post-hoc power analysis using G*power (Faul et al., 2007) (Table 3.1). For some endpoints our distributions were highly skewed and/or multi-modal (unstimulated behavior and thermotaxis assays) and we were unable to transform them into normal distributions. Thus, in these cases power analysis could not be performed, since G-power expects a normal distribution as input.

Table 3.1. Summary of statistical testing.

Assay	**Endpoints**	**Statistical test**	**Median observed power**
Lethality	Lethality rate	One-tailed Fisher's exact test	1
Morphology	Eye regeneration rate	One-tailed Fisher's exact test	0.99
Unstimulated behavior	Speed	Two-tailed T-test or Mann Whitney U-test	N/D*
	Fraction of time resting	Two-tailed T-test or Mann Whitney U-test	N/D*
Phototaxis	Phototaxis response rate	One-tailed Fisher’s exact test	0.75
Thermotaxis	Fraction of time in cold area	One-tailed Mann Whitney U-test	N/D*
Scrunching	Scrunching rate	One-tailed Fisher's exact test	0.98

* N/D: not determined

RESULTS

To evaluate the strengths and weaknesses of the planarian system for toxicology MTS, we screened an 87-compound library, provided by the NTP, consisting of known and suspected developmental neurotoxicants and five negative controls (Supplementary Table 1). Each chemical was tested at 5 concentrations, generally ranging from 10nM to 100μM, in both full (intact) planarians and regenerating tail pieces (n=8 each) (Figure 3.1), with a 0.5% DMSO solvent control population (n=8) in each plate. Six chemicals (BDE-153, Chrysene and Dibenz(a,h)anthracene, Bis(tributyltin) oxide, Benzo[g,h,i]perylene, and 2,3,7,8-Tetrachlorodibenzo-p-dioxin) were provided at lower than 20mM due to low solubility in DMSO and were thus tested at lower concentrations (see Supplementary Table 1 for concentrations). On day 7, when regenerating animals start to develop their photosensing system and regain motility (Hagstrom et al., 2015; Inoue et al., 2004), adult and regenerating planarians were assessed for viability, regeneration, locomotion and phototactic behavior. On day 12, all of these endpoints, except for regeneration, were tested again. In addition, on day 12, we evaluated the effects on two more stimulated behaviors: thermotaxis and scrunching. Screening on both days 7 and 12 allows us to evaluate the temporal dynamics of possible subchronic toxic effects and effects on regeneration (Figure 3.1). Raw data are available from the Dryad Digital Repository (doi: 10.5061/dryad.mk6m608).

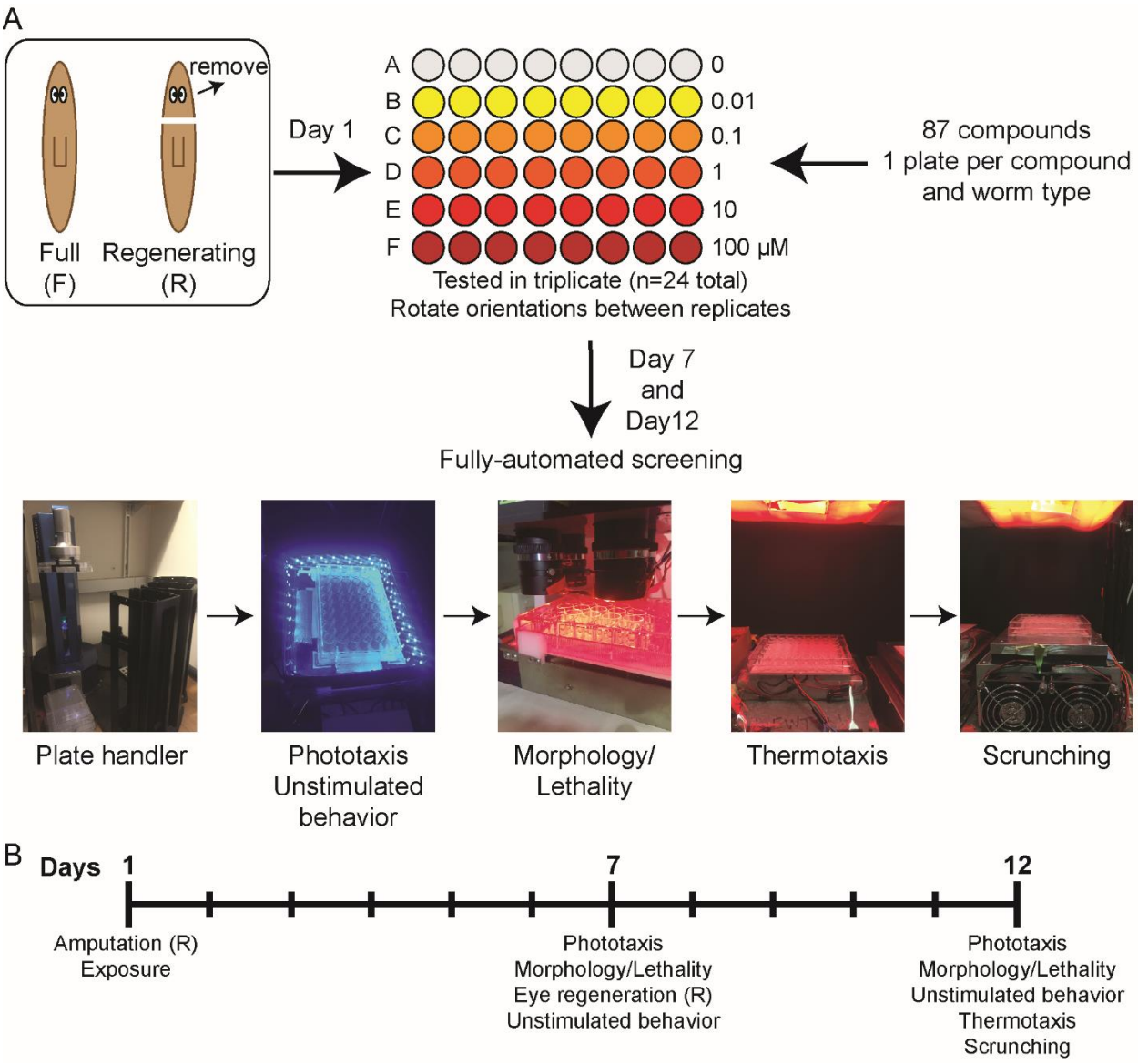

Figure 3.1. Overview of planarian screening platform. (A) Schematic of screening workflow. On day 1, for each chemical, one plate each is filled with either full planarians (F) or regenerating tail pieces (R). 5 test concentrations and 1 control concentration (0.5% DMSO) are placed in each row with n=8 animals per concentration. Plate orientation is altered between replicates. Screening is performed on days 7 and 12. (B) The timeline shows which assays are performed on which screening days.

Lethality and eye regeneration

To evaluate whether the chemicals have an effect on planarian viability (Figure 3.2A-B), we performed statistical tests for all chemicals and, when appropriate, calculated the LC_{50} for chemicals with significant lethality (Supplementary Figure Sl and Supplementary Table 2). Over the entire 12 days of screening, 29 of the 87 tested chemicals (33%) were significantly lethal for at least one concentration, with 27 of them already being lethal by Day 7. No significant lethality was found in any of the negative controls at the tested concentrations. While lethality was found in at least one chemical from each chemical class tested, the majority of lethal compounds (18 of 29, 62%) consisted of either flame retardants or pesticides (9 lethal chemicals each). As there are only 15 or 16 chemicals comprising each of these classes in the library, respectively, this also means that the majority of the chemicals in these classes (56-60%) were lethal to planarians. Full worms tended to be more sensitive to the lethal effects of some chemicals, as 6 chemicals caused significant day 12 lethality at lower concentrations in full worms than in regenerating tails. This difference was the most striking with the flame retardant 3,3',5,5'-Tetrabromobisphenol A as significant lethality was observed in full planarians at 1μM but in regenerating tails at 100μM. We attribute this difference in sensitivity of full and tail worms, which was also observed in a previous screen (Hagstrom et al., 2015), partially to the generally lower motility and potentially lower level of metabolism in regenerating tail pieces. In contrast, only two chemicals, the drug Diazepam and the industrial chemical Auramine O had lower day 12 lethality LOELs in regenerating tails than in full animals.

Figure 3.2. Lethality and eye regeneration endpoints. High-resolution imaging of each well was used to determine whether a planarian was (A) alive or (B) dead. (C) Distributions of lethal chemicals and their day 12 LOEL by chemical class for full worms (F, top row) and regenerating tails (R, bottom row). Chemicals which were not found to be lethal at the tested concentrations are marked as N/D for "not determined". (D-F) High-resolution imaging of day 7 regenerating tails was used to evaluate whether the eyes had regenerated. A custom neural network was used to automatically detect whether the planarian had (D) 2 eyes (normal), or abnormal eyes, (either (E) 1 eye or (F) no eyes) as described in Materials and Methods. Insets show cropped and zoomed-in head regions. Arrows point to the eyes. (G) In some cases, it was impossible to correctly determine the number of eyes. Such cases were classified as invalid and discarded in the analysis. Black scale bars: 1mm. White scale bars: 0.2mm. (H-P) Eye regeneration rate (percentage of planarians with 2 regenerated eyes) shown for each replicate (dots) and for all combined data (bars) as a function of concentration for chemicals in which defects were seen in the absence of significant lethality. If no individual replicate data is shown, all animals were dead in this sample. Significant defects in eye regeneration are in black bars. Concentrations corresponding to the day 12 regenerating tail lethality LOELs for each chemical are in red text. No red text signifies no significant lethality was found in the range of concentrations tested. Chemicals shown are flame retardants (H) 3,3',5,5'-Tetrabromobisphenol A, (I) Firemaster 500 and (J) tris(2-Chloroisopropyl)phosphate (TCPP), pesticides (K) Bis(tributyltin)oxide, (L) Heptachlor and (M) Rotenone, (N) industrial Bisphenol A, (O) PAH Pyrene and (P) negative control Acetylsalicylic acid.

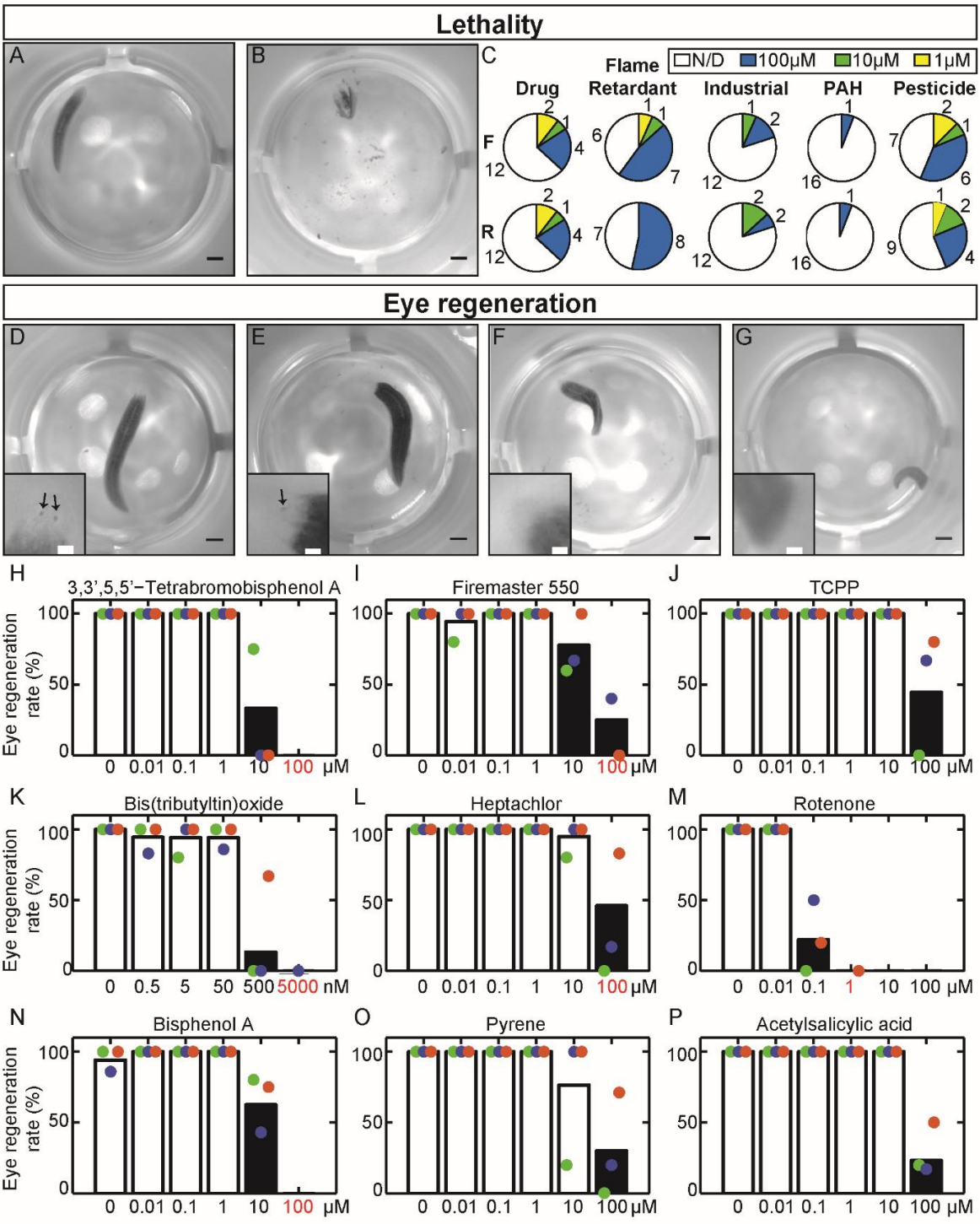
Lethality
A
B
C
Flame
N/D
100μM
10μM
1μM
Drug
Retardant
Industrial
PAH
Pesticide
F
R
Eye regeneration
D
E
F
G
H
3,3',5,5'−Tetrabromobisphenol A
I
Firemaster 550
J
TCPP
K
Bis(tributyltin)oxide
L
Heptachlor
M
Rotenone
N
Bisphenol A
O
Pyrene
P
Acetylsalicylic acid
Eye regeneration rate (%)
0 0.01 0.1 1 10 100 μM
0 0.5 5 50 500 5000 nM
0 0.01 0.1 1 10 100 μM

Eye regeneration was categorized as normal (2 eyes), abnormal (0 or 1 eye) or invalid (could not be analyzed) (Figure 3.2D-G). 21 chemicals (~24%) showed significant defects in eye regeneration. In the majority of these chemicals (12 of 21), regeneration defects may have been a consequence of overt systemic toxicity as effects occurred at day 12 significantly lethal concentrations (Figure 3.7). However, 9 of these 21 chemicals showed selective effects with the eye regeneration LOEL being less than that of the day 12 tail lethality LOEL. These selective chemicals consisted of 3 pesticides, 3 flame retardants, 1 industrial chemical, 1 PAH, and 1 negative control (Acetylsalicylic acid, Figure 3.2H-P).

Unstimulated behavior

We evaluated whether the chemicals perturbed planarian unstimulated behavior by quantifying the worms' fraction of time resting and mean speed during the assay (Figure 3.3). Together, these endpoints demonstrate whether the exposed planarians were moving and if so, whether they were moving normally. Control animals, regenerating tails and full worms, were found to move at a mean speed of approximately 1mm/s, and rest little of the time, in agreement with previous studies on planarian locomotion (Hagstrom et al., 2015). For simplicity and because these endpoints complemented each other (Supplementary Figure S7), a chemical was classified as a hit if there was a defect in either speed or fraction of time resting.

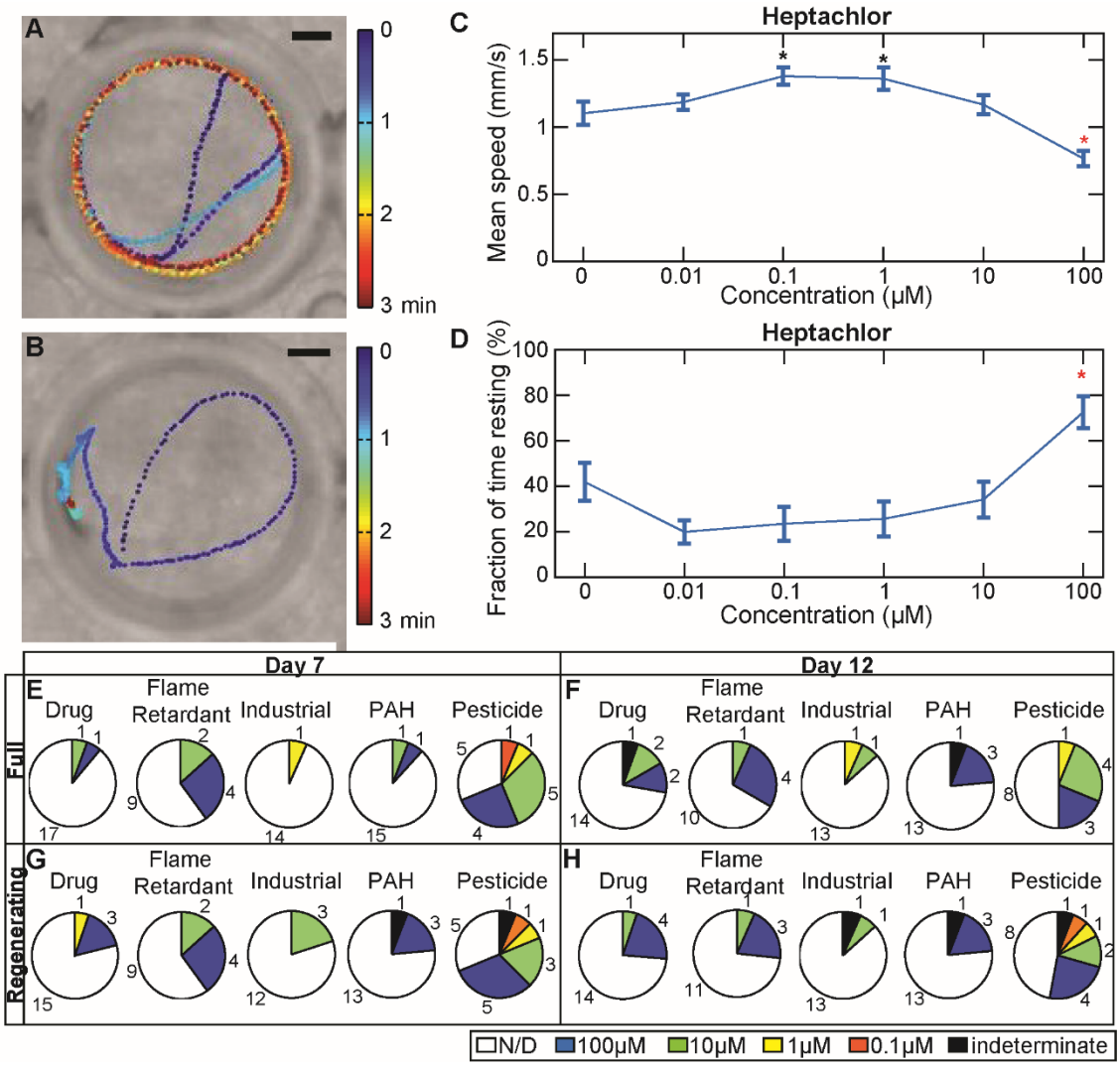

Figure 3.3. Unstimulated behavior: gliding and resting. (A) Representative center of mass (COM) track of one gliding planarian color-coded by time. (B) Representative color-coded COM track of a planarian which started to rest after approximately 1 minute. Scale bars: 2mm. (C-D) Example of dose-response curves of (C) mean speed and (D) mean fraction of time spent resting with standard error as error bars, for same groups of regenerating tails in Heptachlor at Day 12. Stars indicate significant differences from controls ($p<0.05$), showing either hyper- (black, increased locomotor activity) or hypo-activity (red, decreased locomotor activity). (E-F) Distributions of chemicals with defects in unstimulated behavior and their LOEL by chemical class for full worms (E-F, top row) and regenerating tails (G-H, bottom row) at day 7 (left) or day 12 (right). Chemicals which were not found to have an effect on unstimulated behaviors at the tested concentrations are marked as N/D for "not determined". Chemicals with non-monotonic dose-response curves are marked as "indeterminate".

Considering both endpoints together, 43 chemicals (49%) caused decreased locomotion in at least one worm type (full worms or regenerating tails) and time point. The majority of these chemicals (31 of 43) caused behavioral effects at nonlethal concentrations (Figure 3.7 and Supplementary Table 3). Overall, pesticides comprised the most hits on unstimulated behavior (11 chemicals each for day 7 full and regenerating planarians, and 8 chemicals each for day 12 full and regenerating planarians) (Figure 3.3E-H). In fact, considering the entire library, planarian unstimulated behavior was the most sensitive to the effects of the pesticide rotenone with defects as low as 101nM in full worms at day 7 and in regenerating tails at days 7 and 12. Interestingly, rotenone-exposed day 12 full worms did not display defects in unstimulated behavior, suggesting potential transient toxicity or adaptation over time. Loss or gain of hits between day 7 and day 12 were found with several other chemicals (Figure 3.4A). Moreover, although the majority of chemicals affected both full worms and regenerating tails, some effects were worm type-specific (Figure 3.4B). Together, these demonstrate the power of assaying toxicity at multiple endpoints and developmental stages to discern the temporal dynamics of toxicity.

In addition to hits which caused decreased activity (due to decreased speed and/or increased time resting), in 8 instances we observed one or two chemical concentrations with induced hyperactivity (due to increased speed and/or decreased time resting compared to controls) (Supplementary Table 4). In fact, the pesticide heptachlor caused hyper-activity in lower concentrations but hypo-activity in higher concentrations in day 12 regenerating tails (Figure 3.3C).

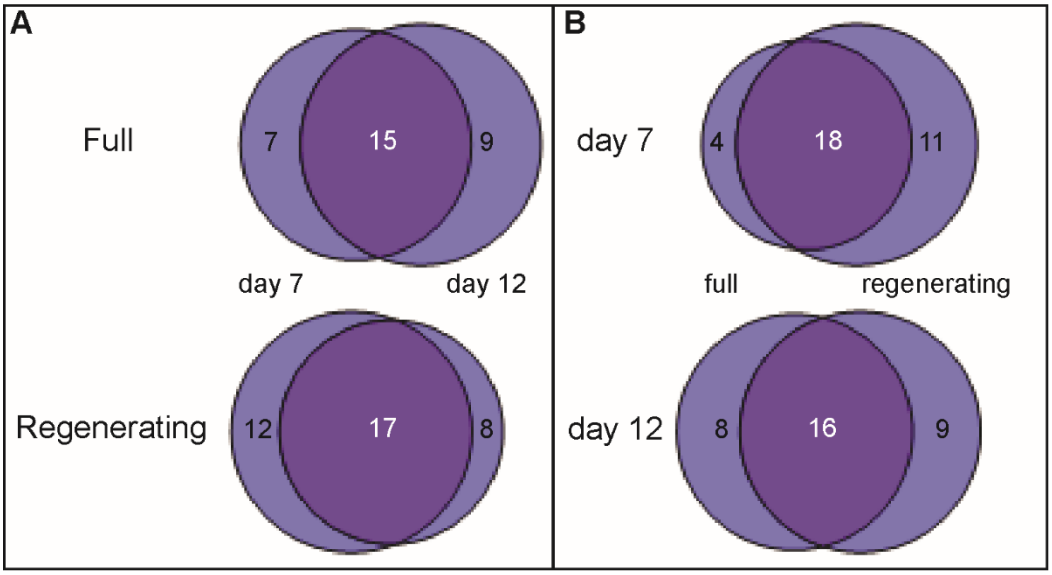

Figure 3.4. Comparison of time-points and worm types for unstimulated behavior hits. (A) Considering both unstimulated behavioral endpoints together, comparison of hits that were conserved between day 7 and day 12 in either full worms (top) or regenerating tails (bottom). (B) Considering both unstimulated behavioral endpoints together, comparison of hits that were conserved between full worms and regenerating tails at either day 7 (top) or day 12 (bottom). All comparisons are performed per chemical, irrespective of concentration.

Stimulated behaviors: phototaxis, thermotaxis and scrunching

Planarians are known to be sensitive to a variety of environmental stimuli, including light and low and high temperatures (Birkholz and Beane, 2017; Cochet-Escartin et al., 2015; Inoue et al., 2004; Inoue et al., 2014; Lambrus et al., 2015; Paskin et al., 2014). For some of these stimuli, it has been shown that different neuronal subpopulations are involved in the animal's characteristic responses to the stimuli (Currie and Pearson, 2013; Inoue et al., 2014; Nishimura et al., 2010). We, therefore, assayed three different stimulated behaviors (phototaxis, thermotaxis and scrunching; Figure 3.5) to potentially differentiate between specific and general neurotoxicity.

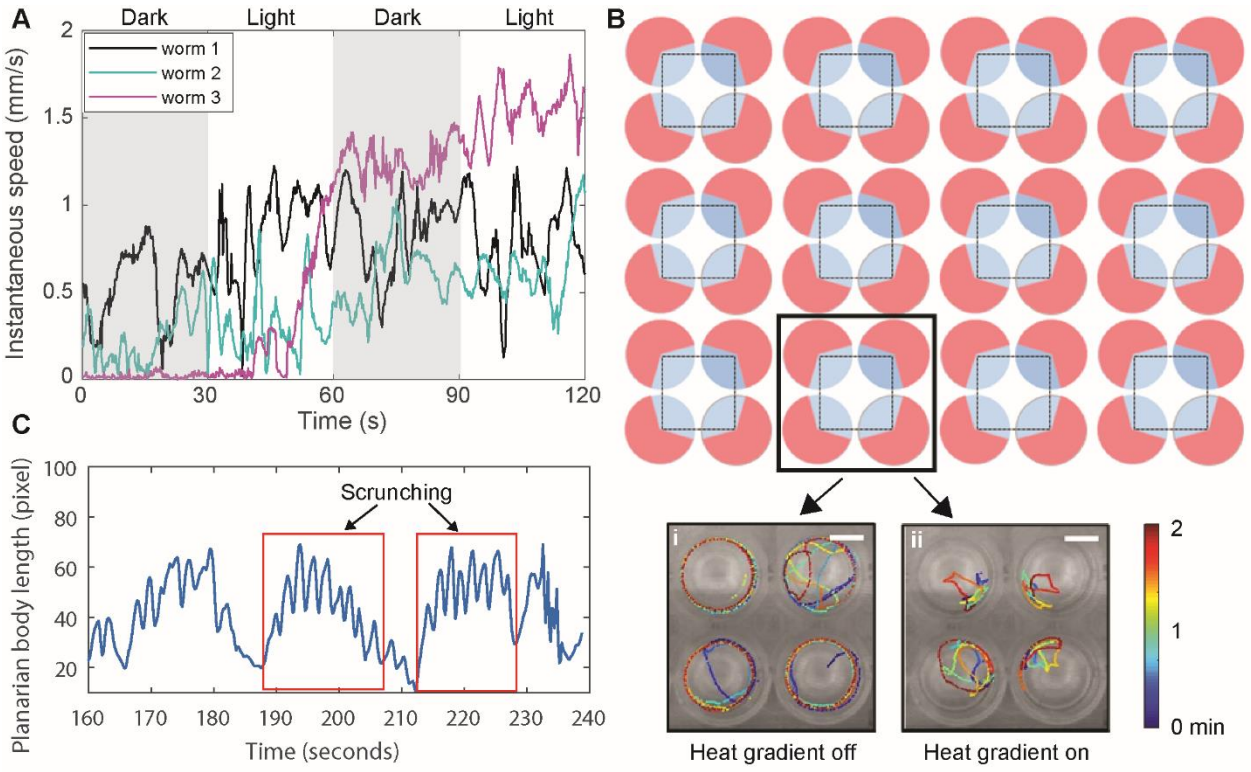

Figure 3.5. Stimulated behaviors. (A) Planarians exhibiting phototaxis respond to alternating light and dark cycles with increasing speed. Examples of 3 full worms in DMSO controls at day 7 were plotted. (B) Schematic of thermotaxis. 12 peltier elements (squares) were evenly distributed to create a heat gradient across each well. The cold area (blue sectors) in each well was defined as the area of a sector of 120° in the analysis. Insets show tracks, color-coded by time, of representative planarian responses to the heat gradient. Both images show the motion of 4 planarians in 4 wells over 2 minutes with either the heat gradient (i) off or (ii) on. Scale bar: 5mm. (C) Representative plot of planarian body length over a short time period (160-240 seconds) in the scrunching assay. The body length oscillations which fulfilled the scrunching criteria in the plot are in a red box. The observed low-frequency oscillations are mostly the worm's turns and head wiggling.

First, we tested the planarians response to light (phototaxis). Planarians demonstrate negative phototaxis to blue light while being insensitive to red light (Paskin et al., 2014). Inspired by zebrafish photomotor response assays (Kokel and Peterson, 2011; Truong et al., 2014), we exposed planarians to bright light and compared behavior before (background activity) and after the light stimulus (Figure 3.5A). We then scored the number of planarians which demonstrated phototaxis. We found 15 chemicals induced phototaxis defects in at least one worm type (full or regenerating planarian) and one time point (day 7 or 12), making this the least

sensitive of the tested endpoints. However, the majority of these chemicals (9) caused effects at nonlethal concentrations (Supplementary Table 5). The most hits were found in day 7 regenerating tails. Day 7 regenerating hits were found to largely overlap with hits in eye regeneration and unstimulated behavior (Figure 3.6A), suggesting these animals have significant regeneration delays. This is exemplified by the chemical Bis(tributyltin)oxide, which showed the most potent effects on planarian phototaxis, with a LOEL of 0.5μM in both worm types and time points. At this concentration, regenerating tails also had defects in eye regeneration, unstimulated behavior (day 7 and 12) and scrunching, in the absence of lethality, suggesting a strong defect in regeneration. Similar defects were also found in full animals, but in the presence of lethality. The majority of hits at either day were not shared between full animals and regenerating tails (Supplementary Figure S8B).

We also evaluated how the chemicals affected the planarians' ability to react to a temperature gradient (thermotaxis, Figure 3.5B). The gradient was established using a custom peltier setup to induce individual temperature gradients in each well, thus incorporating our previous manual screening setup (Hagstrom et al., 2015) into the automated screening of 48-well plates. 16 (~18%) of the tested chemicals demonstrated defects in thermotaxis. These active chemicals were mostly evenly distributed among the chemical classes, consisting of 5 industrial chemicals, 4 drugs, 3 flame retardants, 3 pesticides and 1 PAH. In addition, we observed that adults and regenerating animals were often affected differently, with some chemicals only affecting one worm type and not the other, with regenerating tails generally showing greater sensitivity (Supplementary Figure S8C). Moreover, the majority of these effects (10 of the 16 chemicals, ~63%) showed specific neurotoxic effects at nonlethal concentrations (Figure 3.7 and Supplementary Table 6) suggesting that this is a sensitive endpoint to discern sublethal

neurotoxicity, particularly in developing animals. Planarian thermotaxis was most sensitive to the drug Tetraethylthiuram disulfide and the pesticide Aldicarb with LOELs of ~10μM for regenerating tails and full worms, respectively. However, at the same concentration, Aldicarb also caused hypoactivity in the unstimulated behavior assay, suggesting the thermotaxis defect may be a consequence of decreased locomotion. Tetraethylthiuram disulfide, on the other hand, caused thermotaxis defects in the absence of locomotion defects, suggesting defects in thermoreception.

Lastly, we evaluated the planarians' ability to react to noxious stimuli. Scrunching is a musculature-driven escape gait in planarians, characterized by asymmetric elongation-contraction cycles (Cochet-Escartin et al., 2015) (Figure 3.5C). This gait can be induced by a variety of noxious stimuli, such as heat, amputation and pH. In our screening platform, scrunching is induced by heating the aquatic temperature of the wells by placing the screening plate on a peltier plate. 38 (~44%) of the tested chemicals caused planarians to be unable to scrunch properly. Similar to lethality, active chemicals in this endpoint were dominated by pesticides (12 chemicals) and flame retardants (10 chemicals). Interestingly, we observed this endpoint to often be affected differentially in the full and regenerating animals, with a slight bias towards regenerating tail pieces, as 14 (37%) chemicals showed increased sensitivity in the regenerating tails and 9 (24%) showed increased sensitivity in the full worms, with 15 toxicants (39%) affecting both worm types at the same concentrations (Supplementary Figure S8D). Among the 38 chemicals that caused scrunching defects, 29 (~76%) showed a scrunching defect with a scrunching LOEL lower than the respective lethality LOEL, for at least one worm type (Figure 3.7 and Supplementary Table 7), suggesting that scrunching is a sensitive endpoint for sublethal neurotoxicity. For example, the most sensitive scrunching defect was seen with the

industrial chemical 1-ethyl-3-methylimidazolium diethylphosphate with a LOEL of 101 nM for regenerating tails. This chemical was not found to be lethal to planarians up to the maximum concentration tested (101 μM).

Because the tested endpoints are not necessarily independent from each other, we evaluated the extent of agreement between endpoints that may be correlated. For example, phototaxis and thermotaxis responses rely on animal locomotion to respond to the respective stimuli. Moreover, defects in eye regeneration could be expected to be correlated with defects in phototaxis. We don't, however, expect all hits to be concordant, since the blue light, which was used in the phototaxis assay, can be sensed by photoreceptors in the eyes and pigment in the body epithelium (Birkholz and Beane, 2017). While the majority of phototaxis hits in the regenerating tails were also hits in eye regeneration and/or unstimulated behavior (Figure 3.6A), 1 hit was found in phototaxis alone, suggesting that this assay does add additional sensitivity beyond the other endpoints. Similarly, in full worms, 2 hits were found which were not hits in the unstimulated behavior assay (Supplementary Figure S8A). Moreover, in both thermotaxis and scrunching (Figure 3.6B-C), a large proportion of hits were found to overlap with unstimulated behavior hits, though endpoint-specific effects were found in all cases. Together, these comparisons demonstrate the value of the large repertoire of planarian behaviors to be able to discern subtler neurotoxic effects from general systemic toxicity or gross motor defects.

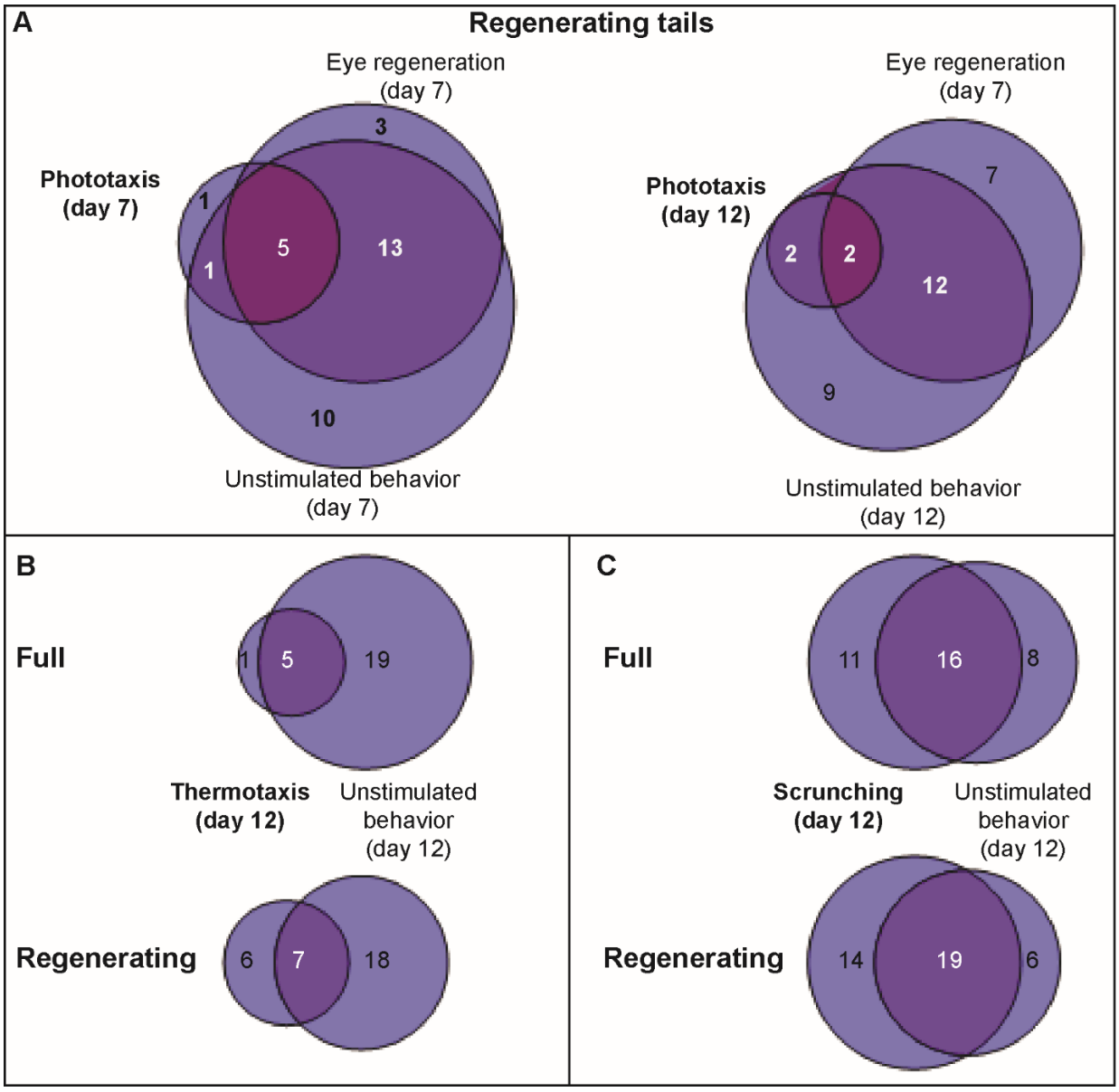

Figure 3.6. Comparison of shared hits in stimulated vs unstimulated behaviors. (A) Venn diagram of overlap of hits in day 7 eye regeneration, with day 7 (left) or day 12 (right) phototaxis and unstimulated behavior assays in regenerating tails. (B) Venn diagram of hits in thermotaxis and unstimulated behavior at day 12 for full worms (top) and regenerating tails (bottom). (C) Venn diagram of hits in scrunching and unstimulated behavior at day 12 for full worms (top) and regenerating tails (bottom).

Sensitivity of endpoints and global response

Through the discussion of the individual assays, we have shown that the different endpoints possess different sensitivities to different toxicities of the tested chemical compounds. Figure 3.7 provides a visual summary of these findings in the case of the regenerating tails (see Supplementary Figure S9 for full worms), allowing for direct comparison of the endpoint sensitivities and selectivity. Furthermore, we applied Ward's method of clustering to summarize the hits of all active compounds (49) for regenerating tails (Figure 3.8) and full worms (47 chemicals) across all endpoints (Figure 3.9), similar to (Truong et al., 2014). Endpoints were clustered into 3 major groups: lethality/morphology endpoints, unstimulated behavior/scrunching and phototaxis/thermotaxis, suggesting endpoints in the same cluster might be functionally related. Some of these clusters seem to represent particular toxic signatures for the different chemical classes (Table 3.2). For example, the majority of pesticides were active in the lethality, unstimulated behavior and scrunching assays. Interestingly, while full worms exposed to pesticides showed more hits (higher class concordance) in lethality, the regenerating tails had more hits in scrunching, suggesting differential effects on the adult and developing nervous system. There was also concordance of endpoints in full worms exposed to flame retardants, with most of the flame retardants being hits in lethality and scrunching. These were also the most concordant endpoints for the regenerating tails exposed to flame retardants, but with slightly less concordance. No obvious signatures were found for any of the other chemical classes, which also generally showed less activity across all planarian endpoints.

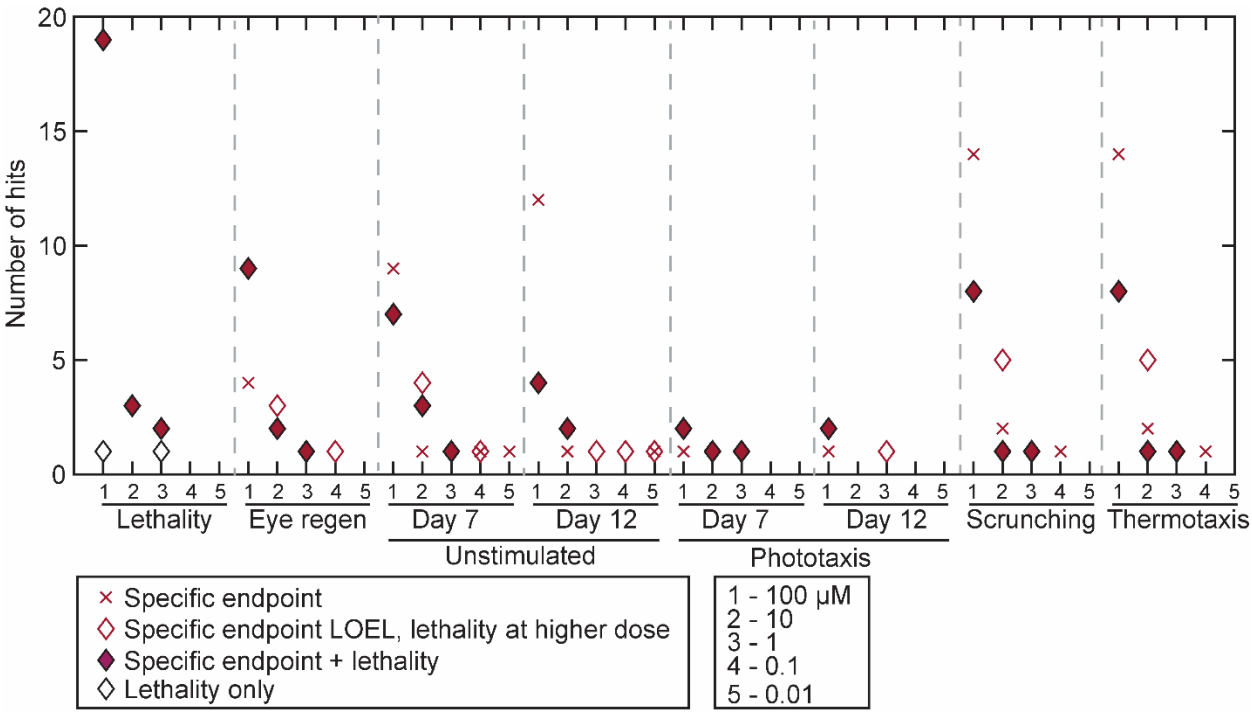

Figure 3.7. Analysis of LOEL by endpoint. Regenerating tail LOELs for each endpoint, separated into 5 concentration classes, listed highest to lowest (1-5). Most chemicals were tested in the range of 0.01-100µM (see legend). However, BDE-153, Chryene and Dibenz(a,h)anthracene were tested at 0.005-50µM, Bis(tributyltin) oxide at 0.5-5000nM, Benzo[g,h,i]perylene at 0.4-4000 nM, and 2,3,7,8-Tetrachlorodibenzo-p-dioxin at 0.04 – 400 nM, due to low solubility in DMSO. Each endpoint LOEL is categorized and counted (y-axis) based on the co-occurrence of lethality at the same or higher concentrations.

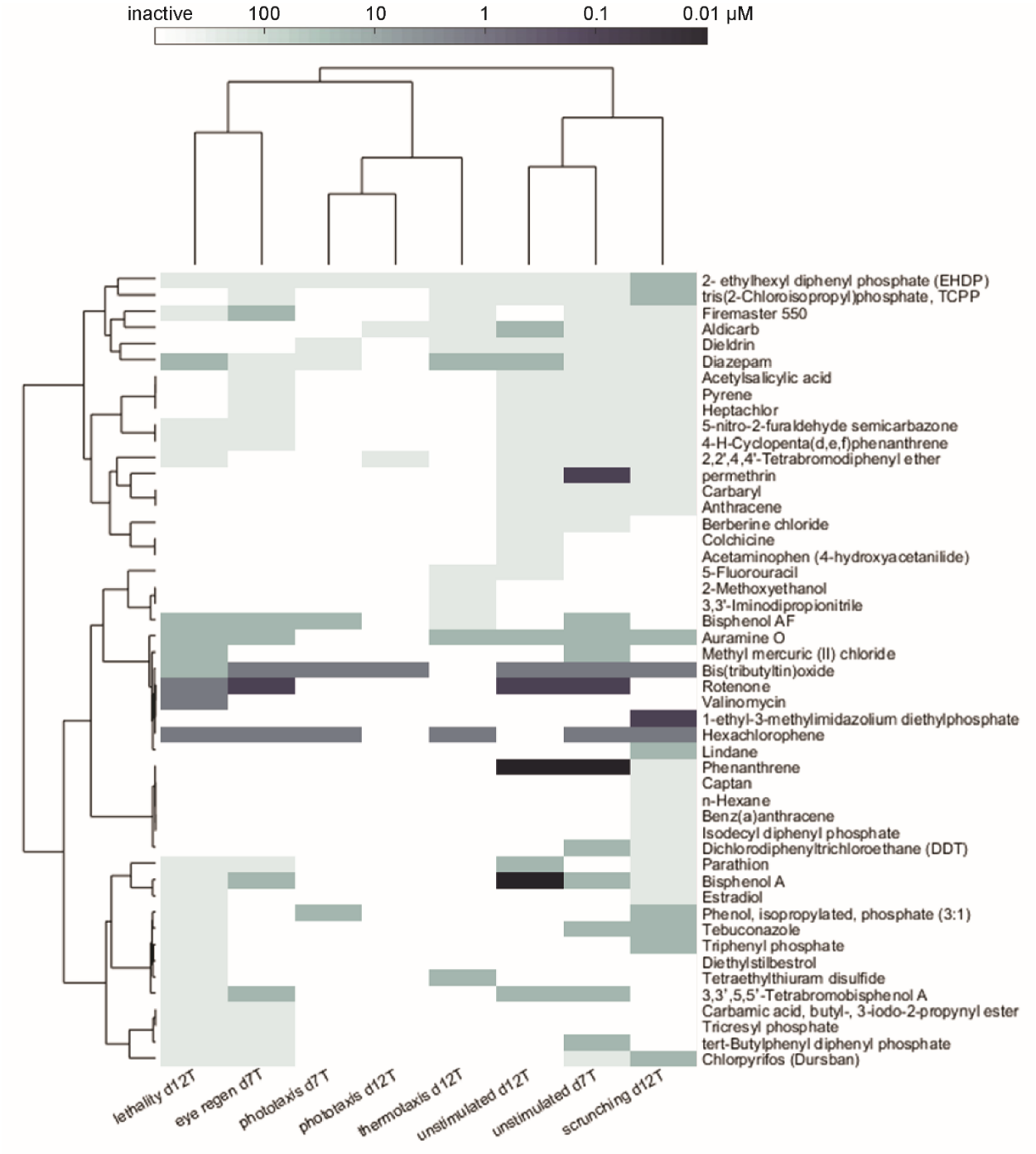

Figure 3.8. Summary of screening results for regenerating tail. Bicluster heat map of chemicals affecting at least one endpoint in regenerating tails with LOEL color-coded. The hits were clustered using Ward's method by calculating Euclidean distance between LOELs.

Figure 3.9. Summary of screening results in full planarians. Bicluster heat map of chemicals affecting at least one endpoint in full planarians with LOEL color-coded. The hits were clustered using Ward's method by calculating Euclidean distance between LOELs.

Table 3.2. Summary of percentage of actives observed in different toxicant classes in all endpoints for either full worms (F) or regenerating tails (R). Percentages are based on the total number of chemicals in the respective class.

Endpoints	Day	Drug (19)		Flame retardant (15)		Industrial(15)		PAH(17)		Pesticide (16)		Negative(5)	
		F	R	F	R	F	R	F	R	F	R	F	R
Lethality	12	37%	37%	60%	53%	20%	20%	6%	6%	56%	44%	0%	0%
Eye	7	NA	16%	NA	40%	NA	20%	NA	12%	NA	38%	NA	20%
Unstimulated	7	11%	21%	40%	40%	7%	20%	12%	24%	69%	69%	0%	20%
	12	26%	26%	33%	27%	13%	13%	24%	24%	50%	50%	0%	0%
Phototaxis	7	0%	11%	7%	13%	0%	7%	0%	0%	25%	13%	0%	0%
	12	11%	0%	13%	13%	7%	0%	0%	0%	25%	13%	0%	0%
Thermotaxis	12	5%	21%	0%	20%	7%	27%	6%	0%	19%	13%	0%	0%
Scrunching	12	21%	21%	67%	47%	13%	27%	24%	29%	44%	75%	0%	20%

When comparing active versus inactive compounds, we found that 41 of the active chemicals are shared hits between full planarians and regenerating tails. When comparing potency, we found 13 chemicals were developmentally selective with lower overall LOELs in regenerating tails than that in full worms (Table 3.2). Our ability to directly compare the effect of chemicals on the brain of adult (full/intact) and developing (regenerating) animals is a unique strength of the planarian system.

Table 3.3. Developmentally selective chemicals. Chemicals which had overall lower LOELs in regenerating tails than in full planarians.

Class	**Chemical**	**Selective endpoints**
Drug	Colchicine	Unstimulated day 12
Industrial	1-ethyl-3-methylimidazolium diethylphosphate	Scrunching
	2-Methoxyethanol	Thermotaxis
	3,3'-Iminodipropionitrile	Thermotaxis
	Bisphenol A	Unstimulated day 12*
	n-Hexane	Scrunching
PAH	Anthracene	Unstimulated day 7/12, Scrunching
	Phenanthrene	Unstimulated day 7* /12*
Pesticide	Chlorpyrifos (Dursban)	Scrunching
	Lindane	Scrunching
	Permethrin	Unstimulated day 7*
Negative	Acetaminophen	Unstimulated day 12
	Acetylsalicylic acid	Unstimulated day 7/12, Scrunching

* dose was non-monotonic

DISCUSSION

Robustness of screen and best practices

Robustness and reliability of screening are major concerns in the evaluation and verification of toxicology models (Judson et al., 2013). One aspect is reproducibility of results between independent experimental runs (technical replicates). Therefore, in our screen, we assayed each chemical concentration in 3 independent runs and provide the data for direct comparison of the replicates in Supplementary File 1. The majority of hits were reproducible with significant activity in all 3 runs, with on average 73% shared for all runs for all endpoints with full and regenerating planarians (Supplementary Table 8). However, variability among runs was evident in some cases potentially due to technical artifacts and variability among animal populations, as described below.

First, technical issues in the scrunching assay contributed to the observed spread in the data for this endpoint. Specifically, in 3.8% of the screened plates (N=522 plates), the contact between the plate and the peltier used for administering the noxious heat stimulus was inadequate, causing variability in the scrunching response. However, the same dose-dependent trends seen in the replicates with properly functioning peltier contact was still evident in these malfunctioning replicates (Supplementary Figure S11).

Next, to account for possible effects of well position within a single plate, we rotated the position of the different chemical concentrations among runs by shifting each concentration down 2 rows with each replicate. This revealed the existence of an “edge effect”, whereby planarians located at the outermost rows of the plate displayed a relatively higher lethality rate when compared to the planarians located in the plate interior at the same concentration (Supplementary Figure S10). We thus conclude, as others have previously (Truong et al., 2014),

that alteration of well position for a given chemical concentration between replicates is an important aspect of ensuring reliability of results and thus enhancing screen robustness.

Finally, the planarian's diet turned out to be a significant source of biological variability affecting planarian fitness and behavior. Varying quality of food batches caused a measurable influence on the animals' sensitivity to chemical exposure (see Supplementary Information Section 3 for details) and calls for standardization of food quality to eliminate this source of variability within and between experiments and labs.

To minimize the effects of inter-run variability arising from any of these factors, we excluded hits that were determined through a single run and did not have consistent effects across the triplicates (see Material and Methods and Supplementary Figure S5).

Negative controls

The NTP 87-compound library contained 5 compounds indicated as negative controls (acetaminophen, acetylsalicylic acid, D-glucitol, L-ascorbic acid and saccharin sodium salt hydrate). All negative controls were inactive in full planarians. In contrast, in regenerating tails, while 3 of the 5 negative controls (D-glucitol, L-ascorbic acid and saccharin) showed no effects, at least one endpoint was affected by acetaminophen and acetylsalicylic acid. Acetaminophen caused decreased unstimulated speed in day 12 regenerating tails at the highest concentration tested (103μM). However, this hit was right at the biological relevance cutoff (see Materials and Methods), so it is possible that it is a false positive or potentially mild effect.

Acetylsalicylic acid caused defects in eye regeneration, unstimulated behavior (day 7 and 12) and scrunching in regenerating tails (but not full worms) at the highest tested concentration (99.5μM) suggesting developmental defects. While these chemicals were selected by the NTP to be inactive controls at the tested concentrations, toxicity has been observed with these

compounds previously. Data collected by the NTP from different public databases shows that acetaminophen and acetylsalicylic acid have been reported to have “other” and developmental/other toxicity, respectively (https://sandbox.ntp.niehs.nih.gov/neurotox/). Moreover, these 2 compounds have been associated with toxicity in multi-generation and developmental mammalian guideline studies, respectively, reported on ToxRefDB (Hagstrom et al.) For example, oral exposure of 1% (1.43 mg/kg body weight) acetaminophen to Swiss CD-1 mice for 14 weeks caused multi-generational effects on reproduction and growth (Reel et al., 1992), while single dose oral exposure to 500 mg/kg acetylsalicylic acid caused teratogenesis in rats (DePass and Weaver, 1982). Thus, these findings point toward a potential toxic effect of these compounds on developmental processes in various animal systems.

Comparison of hits with existing planarian toxicology data

For some of the chemicals tested in this screen, previous largely manual toxicology studies on planarians exist. We therefore compared our results with the published literature to evaluate concordance (Table 3.4). Of note, while we studied chronic exposure in both full and regenerating planarians, most of the previous studies evaluated either only regeneration and/or acute exposure. Direct comparisons between different experiments are difficult to make because of differences in experimental methods (chemical concentrations tested, exposure conditions and duration, worm type (full/regenerating), data and statistical analysis, number of replicates, etc.), and differences in planarian species used, which may have differing sensitivity. Together, this experimental heterogeneity emphasizes the need for uniform testing guidelines going forward. The zebrafish community faces similar challenges, for example see (Truong et al., 2014), with different labs using different experimental methodologies.

Table 3.4. Comparison of results with previous planarian studies. As necessary, concentrations were converted to μM for ease of comparison.

	This screen		Previously published				
Chemical	**LOEL (μM)**	**Endpoints affected**	**Species**	**LOEL (μM)**	**Endpoints affected**	**Exposure duration**	**Reference**
6-Hydroxydopamine hydrochloride	0.1*	Unstimulated behavior (d12F)	*Dugesia gonocephala*	~120†	Mobility	7 days	(Caronti et al., 1999)
Acetaminophen	100	Unstimulated behavior (d12R)	*D. japonica*	1000§	Lethality	4 days	(Li, 2013a)
Acetylsalicylic acid	100	Eye regeneration, unstimulated behavior (d7R, d12R), scrunching (d12R)	*D. japonica*	520§	Lethality	4 days	(Li, 2013a)
Acrylamide	N/D	none	*D. japonica*	100	Gliding speed, brain regeneration	8,15 days	(Hagstrom et al., 2015)¶
Benz(a)anthracene	100	Scrunching (d12F/R)	*D. dorotocephala*	Not available	Lethality	3 months	(Best and Morita, 1982)
Berberine chloride	10	Unstimulated behavior (d7F/R, d12F/R)	*D. japonica*	50	Eye regeneration, mobility	7 days	(Balestrini et al., 2014)
Bisphenol A	0.01*	Lethality (F/R), eye regeneration, unstimulated behavior (d7R, d12F/R), scrunching (d12R)	*D. japonica*	~20§ 2	Lethality Regeneration	4 days 7 days	(Li, 2013b) (Li, 2014)
Carbaryl	100	Unstimulated behavior (d7F/R, day12F/R), scrunching (day12F/R)	*Dugesia tigrina*	1	Mobility	2h	(Feldhaus et al., 1998)
Chlorpyrifos	10	Lethality (F/R), eye regeneration, unstimulated behavior (d7R), scrunching (d12R)	*D. japonica; D. dorotocephala*	1 5	Lethality, unstimulated behavior, brain regeneration, thermotaxis; lethality, acute behavior, head regeneration	8,15 days 7 days	(Hagstrom et al., 2015)¶ (Villar et al., 1993)
Colchicine	100	Unstimulated behavior (d12F)	*D. dorotocephala*	200	Regeneration	10 days	(McWhinnie, 1955)

Table 3.4. Comparison of results with previous planarian studies. Continued.

	This screen		Previously published				
Chemical	**LOEL (µM)**	**Endpoints affected**	**Species**	**LOEL (µM)**	**Endpoints affected**	**Exposure duration**	**Reference**
Dichlorodiphenyltrichloroethane (DDT)	10	Lethality (F), unstimulated behavior (d7F,d12F/T), scrunching (d12F/T), thermotaxis (d12T)	*Polycelis feline, Creobia alpina*	1	Regeneration, mobility	14 days	(Kouyoumjian and Villeneuve, 1979)
Diethylstilbestrol	10	Lethality (F/R), unstimulated behavior (d12F)	*D. japonica*	2§ 2	Lethality Regeneration	4 days 7 days	(Li, 2013b) (Li, 2014)
Estradiol	100	Lethality (F/R), scrunching (d12R)	*D. japonica*	6§ 9	Lethality Regeneration	4 days 7 days	(Li, 2013b) (Li, 2014)
Methyl mercuric (II) chloride	10	Lethality (F/R), Unstimulatd behavior (d7F)	*D. dorotocephala; Polycelis tenuis and Dugesia lugubris*	0.3	Lethality, morphology, regeneration, behavior	5h-10 days	(Best et al., 1981)
Parathion	10	Lethality (F/R), eye regeneration, unstimulated behavior (d12F/T), scrunching (d12T)	*Schmidtea mediterranea*	50	Lethality, regeneration, mobility	1 – 4 days, 7 days, 12 days	(Poirier et al., 2017)
Permethrin	0.1*	Unstimulated behavior (d7F/R, d12R), scrunching (d12R)	*D. japonica*	20	Lethality, gliding speed, eye regeneration, brain regeneration	8,15 days	(Hagstrom et al., 2015)¶
Rotenone	0.1	Lethality (F/R), eye regeneration, unstimulated behavior (d7F/R, d12R)	*D. japonica*	0.01	Lethality, acute behavior	4 days	(Kitamura et al., 2003)
Thalidomide	N/D	none	*D. tigrina*	232	Eye regeneration	5 day exposure, assayed at day 7	(Best and Morita, 1982)

*dose response was non-monotonic
†only 1 tested concentration
§LC_{50}
¶see Supplementary Information Section 6 for more details

Strengths and current limitations of the planarian as a model for developmental neurotoxicity

The performance of this 87-compound screen revealed both the strengths and weaknesses of the planarian screening platform, as summarized in Table 3.5. As with any toxicology system, the planarian system has its limitations. However, when appropriately utilized, this system can add value to the existing testing pipeline through its unique strengths, such as the ability to screen adults and developing animals in parallel with the same assays to delineate developmental-specific effects and differentiate between DNT and general neurotoxicity (Table 3.2). For example, of the 38 known developmental neurotoxicants in this library (Supplementary Table 1, (Ryan et al., 2016)), 10 (1 drug, 5 industrial, and 4 pesticides) had greater effects in regenerating planarians, with lower overall LOELs than full planarians.

Table 3.5. Summary of the strengths and weaknesses of the planarian toxicology system.

Strengths	**Weaknesses**
• Cost- and time-effective screen within 12 days compared to months in mammalian systems • Invertebrate system • Amenable to full automation • Easy administration of compounds in the water • Many different behavioral readouts, some with known cellular/molecular pathways • Ability to study adult and developing animals in parallel with the same assays • Allows for multi-generational studies	• Limited morphological endpoints due to simple anatomy • May be missing some relevant toxicological targets • Potential water solubility issues and loss of toxicants into the environment • Unknown PK/PD parameters (e.g. internal concentrations and xenobiotic metabolism); • Single route of exposure (absorption) • Clonal animals, no genetic diversity

Another strength of the planarian system is the large repertoire of quantitative behavioral readouts that allow coverage of a wide spectrum of neuronal functions that are currently not assayed in other medium-throughput animal systems, such as zebrafish larvae. Moreover, the molecular mediators of some of these behaviors have been characterized (Birkholz and Beane,

2017; Inoue et al., 2014; Nishimura et al., 2010), allowing for insight into mechanisms of neurotoxicity. For example, 10 μM Tetraethylthiuram disulfide was found to selectively disrupt thermotaxis in regenerating tails, but not full planarians, in the absence of other affected endpoints. Planarian thermotaxis has been shown to be mediated by Transient Receptor Potential (TRP) channels (Inoue et al., 2014), and Tetraethylthiuram disulfide has been found to be a selective agonist for human TRPA1 *in vitro* (Maher et al., 2008). Additionally, regenerating planarians were found to be highly sensitive to rotenone, a pesticide and mitochondrial disruptor. We observed significant defects in full and regenerating tails unstimulated behavior and eye regeneration at concentrations as low as 101nM. In rodent models, the effects of rotenone on retinal neurodegeneration and locomotor activity have been well documented (Alam et al., 2004; Normando et al., 2016; Rojas et al., 2008). The similarity of these affected endpoints in both models suggests that similar molecular pathways are targeted in the same way. Together, these demonstrate the utility of the range of planarian morphological and behavioral endpoints to connect adverse functional outcomes with mechanisms, which are likely conserved in higher organisms, including mammals and humans.

In the NTP 87-compound library, 38 chemicals were denoted as known developmental neurotoxicants (Supplementary Table 1) from previous *in vivo* and *in vitro* studies (Ryan et al., 2016) and 23 (~61%) were active in planarian regenerating tails. Concordance varied by class from most to least: pesticide (13/14), industrial (4/10), and drug (6/14). No PAHs or flame retardants were listed as known developmental neurotoxicants. Moreover, in our companion paper (Hagstrom et al.), we found that of the 28 chemicals in this library with associated quality mammalian guideline studies available on the U.S. EPA Toxicity Reference Database, 20 (71%) were active in regenerating planarians. Some of these false negatives may be due to absence of

the relevant biological targets in planarians. For example, the inactivity of thalidomide, an infamous teratogen with suggested effects on angiogenesis (Stephens et al., 2000), in planarians may not be surprising given their lack of a circulatory system.

Other factors need to be taken into account when evaluating concordance, such as the extent of uptake and bioavailability in the animals. The reported concentrations in this study are nominal water concentrations and the internal concentrations within the planarians are unknown. Thus, it is uncertain whether inactivity is due to loss of chemical to the plastic, lack of absorption into the planarian, insufficient metabolic machinery, or other pharmacokinetic (PK) differences. For example, since chemical uptake in planarians occurs through the skin or pharynx (Balestrini et al., 2014; Kapu and Schaeffer, 1991) and planarians possess a protective mucus coating (Martin, 1978; Pedersen, 2008), certain chemical classes may be unable to effectively penetrate into the animal. Future research will have to determine the PK and pharmacodynamics (PD) of this system, and identify which compounds are bioavailable, to be able to connect activity with the relevant exposure in mammals and humans. While this study focused on the planarian system, a companion study in this special issue (Hagstrom et al.) performs a direct comparison using this NTP 87-compound library between the planarian and zebrafish systems, and available mammalian data. Together, both studies demonstrate the added value of comparative screening in multiple complementary models to assay a larger swath of chemical and biological space.

ACKNOWLEDGEMENTS

Chapter 3, in full, is a reformatted reprint of the material as it appears in Zhang, Siqi; Hagstrom, Danielle; Hayes, Patrick; Graham, Aaron; and Collins, Eva-Maria S. "Multi-behavioral endpoint testing of an 87-chemical compound library in freshwater planarians," Toxicological Sciences, kfy145, 2018 (in press). The version of record is available online at: https://academic.oup.com/toxsci/advance-article/doi/10.1093/toxsci/kfy145/5034903?guestAccessKey=3ddabc3c-f78a-4814-914b-0469e0d3f7d4. Use of this manuscript in the dissertation herein is covered by the rights permitted to the authors by Oxford Journals. Danielle Hagstrom, Siqi Zhang, and Eva-Maria S. Collins designed the experiments and coauthored the manuscript. Danielle Hagstrom set up the chemicals and experiments, and analyzed and interpreted the data. Siqi Zhang built the automatic screening platform, performed the screening experiments and analyzed and interpreted the data. Patrick Hayes and Aaron Graham developed the neural network platform to analyze eye regeneration. Danielle Hagstrom and Siqi Zhang were the primary investigators and authors of this material.

REFERENCES

Alam, M., Mayerhofer, A. and Schmidt, W. J. (2004). The neurobehavioral changes induced by bilateral rotenone lesion in medial forebrain bundle of rats are reversed by L-DOPA. *Behav. Brain Res.* **151**, 117–124.

Alves, S. N. and de Melo, A. L. (2013). Effects of benzodiazepine and ivermectin on Girardia tigrina (Platyhelminthes: Turbellaria). *Biosci. J.* **29**, 209–215.

Balestrini, L., Isolani, M. E., Pietra, D., Borghini, A., Bianucci, A. M., Deri, P. and Batistoni, R. (2014). Berberine exposure triggers developmental effects on planarian regeneration. *Sci. Rep.* **4**, 4914.

Behl, M., Hsieh, J. H., Shafer, T. J., Mundy, W. R., Rice, J. R., Boyd, W. A., Freedman, J. H., Hunter, E. S., Jarema, K. A., Padilla, S., et al. (2015). Use of alternative assays to identify and prioritize organophosphorus flame retardants for potential developmental and neurotoxicity. *Neurotoxicol. Teratol.* **52**, 181-193.

Behl, M., Ryan, K., Hsieh, J.-H., Parham, F., Shapiro, A., Collins, B. J., Birnbaum, L. S., Bucher, J. R., Walker, N. J., Foster, P. M., et al. (2018). Screening for developmental neurotoxicity (DNT) at the National Toxicology Program: The future is now! *Toxicol. Sci.*

Best, J. B. and Morita, M. (1982). Planarians as a model system for in vitro teratogenesis studies. *Teratog. Carcinog. Mutagen.* **2**, 277–91.

Best, J. B., Morita, M., Ragin, J. and Best, J. (1981). Acute toxic responses of the freshwater planarian, Dugesia dorotocephala, to methylmercury. *Bull. Environ. Contam. Toxicol.* **27**, 49–54.

Birkholz, T. R. and Beane, W. S. (2017). The planarian TRPA1 homolog mediates extraocular behavioral responses to near-ultraviolet light. *J. Exp. Biol.* **220**, 2616–2625.

Boyd, W., Smith, M. and Freedman, J. (2012). Caenorhabditis elegans as a model in developmental toxicology. In *Developmental Toxicology* (ed. Harris, C.) and Hansen, J. M.), pp. 15–24. Totowa, NJ: Humana Press.

Boyd, W. A., Smith, M. V., Co, C. A., Pirone, J. R., Rice, J. R., Shockley, K. R. and Freedman, J. H. (2015). Developmental effects of the ToxCast™ phase I and phase II chemicals in Caenorhabditis elegans and corresponding responses in zebrafish, rats, and rabbits. *Environ. Health Perspect.* **124**, 586–93.

Bronsted, H. V. (1955). Planarian regeneration. *Biol. Rev.* **30**, 65–126.

Buchanan, J. W. (1935). An analysis of physiological states responsible for antero-posterior disintegration in Planaria dorotocephala. *Protoplasma* **22**, 497–512.

Buttarelli, F. R., Pellicano, C. and Pontieri, F. E. (2008). Neuropharmacology and behavior in planarians: Translations to mammals. *Comp. Biochem. Physiol. - C Toxicol. Pharmacol.*

147, 399–408.

Caronti, B., Margotta, V., Merante, A., Pontieri, F. E. and Palladini, G. (1999). Treatment with 6-hydroxydopamine in planaria (Dugesia gonocephala s.l.): Morphological and behavioral study. *Comp. Biochem. Physiol. - C Pharmacol. Toxicol. Endocrinol.* **123**, 201–207.

Carter, J. A., Lind, C. H., Truong, M. P. and Collins, E.-M. S. (2015). To each his own. *J. Stat. Phys.* **161**, 250–272.

Cebrià, F. (2007). Regenerating the central nervous system: how easy for planarians! *Dev. Genes Evol.* **217**, 733–48.

Cochet-Escartin, O., Mickolajczk, K. J. and Collins, E.-M. S. (2015). Scrunching: a novel escape gait in planarians. *Phys. Biol.* **12**, 055001.

Collins, F. S., Gray, G. M. and Bucher, J. R. (2008). Transforming environmental health protection. *Science* **319**, 906–7.

Currie, K. W. and Pearson, B. J. (2013). Transcription factors lhx1/5-1 and pitx are required for the maintenance and regeneration of serotonergic neurons in planarians. *Development* **140**, 3577–88.

DePass, L. R. and Weaver, E. V. (1982). Comparison of teratogenic effects of aspirin and hydroxyurea in the Fischer 344 and Wistar strains. *J. Toxicol. Environ. Health* **10**, 297–305.

Dunkel, J., Talbot, J. and Schötz, E.-M. (2011). Memory and obesity affect the population dynamics of asexual freshwater planarians. *Phys. Biol.* **8**, 026003.

Faul, F., Erdfelder, E., Lang, A.-G. and Buchner, A. (2007). G*Power 3: A flexible statistical power analysis program for the social, behavioral, and biomedical sciences. *Behav. Res. Methods* **39**, 175–191.

Feldhaus, J. M., Feldhaus, A. J., Ace, L. N. and Pope, C. N. (1998). Interactive effects of pesticide mixtures on the neurobehavioral responses and AChE levels of planaria. In *Environmental Toxicology and Risk Assessment* - (ed. Little, E. E.), DeLonay, A. J.), and Greenberg, B. M.), pp. 140–149. American Society for Testing and Materials.

Hagstrom, D., Truong, L., Zhang, S., Tanguay, R. L. and Collins, E.-M. S. Comparative analysis of zebrafish and planarian model systems for developmental neurotoxicity screens using an 87-compound library Title. *Toxicol. Sci.*(in revision).

Hagstrom, D., Cochet-Escartin, O., Zhang, S., Khuu, C. and Collins, E.-M. S. (2015). Freshwater planarians as an alternative animal model for neurotoxicology. *Toxicol. Sci.* **147**, 270–285.

Hagstrom, D., Cochet-Escartin, O. and Collins, E.-M. S. (2016). Planarian brain regeneration as a model system for developmental neurotoxicology. *Regeneration* **3**, 65–77.

Hill, A. J., Teraoka, H., Heideman, W. and Peterson, R. E. (2005). Zebrafish as a model

vertebrate for investigating chemical toxicity. *Toxicol. Sci.* **86**, 6–19.

Hori, I. and Kishida, Y. (1998). A fine structural study of regeneration after fission in the planarian Dugesia japonica. *Hydrobiologia* **383**, 131–136.

Inoue, T., Kumamoto, H., Okamoto, K., Umesono, Y., Sakai, M., Alvarado, A. S. and Agata, K. (2004). Morphological and functional recovery of the planarian photosensing system during head regeneration. *Zoolog. Sci.* **21**, 275–283.

Inoue, T., Yamashita, T. and Agata, K. (2014). Thermosensory signaling by TRPM is processed by brain serotonergic neurons to produce planarian thermotaxis. *J. Neurosci.* **34**, 15701–14.

Judson, R., Kavlock, R., Martin, M., Reif, D., Houck, K., Knudsen, T., Richard, A., Tice, R. R., Whelan, M., Xia, M., et al. (2013). Perspectives on validation of high-throughput assays supporting 21st century toxicity testing. *ALTEX* **30**, 51–56.

Kapu, M. M. and Schaeffer, D. J. (1991). Planarians in toxicology. Responses of asexual Dugesia dorotocephala to selected metals. *Bull. Environ. Contam. Toxicol.* **47**, 302–7.

Kimmel, C. B., Ballard, W. W., Kimmel, S. R., Ullmann, B. and Schilling, T. F. (1995). Stages of embryonic development of the zebrafish. *Dev. Dyn.* **203**, 253–310.

Kitamura, Y., Inden, M., Sanada, H., Takata, K., Taniguchi, T., Shimohama, S., Orii, H., Mochii, M., Agata, K. and Watanabe, K. (2003). Inhibitory effects of antiparkinsonian drugs and caspase inhibitors in a Parkinsonian flatworm model. *J. Pharmacol. Sci. J Pharmacol Sci* **92**, 137–142.

Kokel, D. and Peterson, R. T. (2011). Using the zebrafish photomotor response for psychotropic drug screening. *Methods Cell Biol.* **105**, 517–524.

Kouyoumjian, H. H. and Villeneuve, J. P. (1979). Further studies on the toxicity of DDT to planaria. *Bull. Environ. Contam. Toxicol.* **22**, 109–112.

Lambrus, B. G., Cochet-Escartin, O., Gao, J., Newmark, P. A., Collins, E.-M. S. and Collins, J. J. (2015). Tryptophan hydroxylase is required for eye melanogenesis in the planarian Schmidtea mediterranea. *PLoS One* **10**, e0127074.

Li, M. H. (2013a). Acute toxicity of 30 pharmaceutically active compounds to freshwater planarians, Dugesia japonica. *Toxicol. Environ. Chem.* **95**, 1157–1170.

Li, M. H. (2013b). Acute toxicity of industrial endocrine-disrupting chemicals, natural and synthetic sex hormones to the freshwater planarian, Dugesia japonica. *Toxicol. Environ. Chem.* **95**, 984–991.

Li, M. H. (2014). Effects of bisphenol A, two synthetic and a natural estrogens on head regeneration of the freshwater planarians, Dugesia japonica. *Toxicol. Environ. Chem.* **96**, 1174–1184.

Maher, M., Ao, H., Banke, T., Nasser, N., Wu, N.-T., Breitenbucher, J. G., Chaplan, S. R. and Wickenden, A. D. (2008). Activation of TRPA1 by farnesyl thiosalicylic acid. *Mol. Pharmacol.* **73**, 1225–1234.

Martin, G. G. (1978). A new function of rhabdites: Mucus production for ciliary gliding. *Zoomorphologie* **91**, 235–248.

McWhinnie, M. A. (1955). The effect of colchicine on reconstitutional development in Dugesia dorotocephala. *Biol. Bull.* **108**, 54–65.

Mineta, K., Nakazawa, M., Cebria, F., Ikeo, K., Agata, K. and Gojobori, T. (2003). Origin and evolutionary process of the CNS elucidated by comparative genomics analysis of planarian ESTs. *Proc. Natl. Acad. Sci. U. S. A.* **100**, 7666–71.

Morita, M. and Best, J. B. (1984). Effects of photoperiods and melatonin on planarian asexual reproduction. *J. Exp. Zool.* **231**, 273–282.

Nishimura, K., Kitamura, Y., Taniguchi, T. and Agata, K. (2010). Analysis of motor function modulated by cholinergic neurons in planarian Dugesia japonica. *Neuroscience* **168**, 18–30.

Normando, E. M., Davis, B. M., De Groef, L., Nizari, S., Turner, L. A., Ravindran, N., Pahlitzsch, M., Brenton, J., Malaguarnera, G., Guo, L., et al. (2016). The retina as an early biomarker of neurodegeneration in a rotenone-induced model of Parkinson's disease: Evidence for a neuroprotective effect of rosiglitazone in the eye and brain. *Acta Neuropathol. Commun.* **4**, 86.

Pan, S. J. and Yang, Q. (2010). A survey on transfer learning. *IEEE Trans. Knowl. Data Eng.* **22**, 1345–1359.

Paskin, T. R., Jellies, J., Bacher, J. and Beane, W. S. (2014). Planarian phototactic assay reveals differential behavioral responses based on wavelength. *PLoS One* **9**, e114708.

Pedersen, K. J. (2008). Sliime-secreting cells of planarians. *Ann. N. Y. Acad. Sci.* **106**, 424–443.

Poirier, L., Brun, L., Jacquet, P., Lepolard, C., Armstrong, N., Torre, C., Daudé, D., Ghigo, E. and Chabrière, E. (2017). Enzymatic degradation of organophosphorus insecticides decreases toxicity in planarians and enhances survival. *Sci. Rep.* **7**, 15194.

Reel, J. R., Lawton, A. D. and Lamb, J. C. (1992). Reproductive toxicity evaluation of acetaminophen in Swiss CD-1 mice using a continuous breeding protocol. *Fundam. Appl. Toxicol.* **18**, 233–239.

Rink, J. C. (2013). Stem cell systems and regeneration in planaria. *Dev. Genes Evol.* **223**, 67–84.

Rojas, J. C., Saavedra, J. A. and Gonzalez-Lima, F. (2008). Neuroprotective effects of memantine in a mouse model of retinal degeneration induced by rotenone. *Brain Res.* **1215**, 208–217.

Ross, K. G., Currie, K. W., Pearson, B. J. and Zayas, R. M. (2017). Nervous system development and regeneration in freshwater planarians. *Wiley Interdiscip. Rev. Dev. Biol.* **6**, e266.

Ryan, K. R., Sirenko, O., Parham, F., Hsieh, J. H., Cromwell, E. F., Tice, R. R. and Behl, M. (2016). Neurite outgrowth in human induced pluripotent stem cell-derived neurons as a high-throughput screen for developmental neurotoxicity or neurotoxicity. *Neurotoxicology* **53**, 271–281.

Scholz, S. (2013). Zebrafish embryos as an alternative model for screening of drug-induced organ toxicity. *Arch. Toxicol.* **87**, 767–769.

Stephens, T. D., Bunde, C. J. and Fillmore, B. J. (2000). Mechanism of action in thalidomide teratogenesis. *Biochem. Pharmacol.* **59**, 1489–99.

Tejeda-Benitez, L. and Olivero-Verbel, J. (2016). Caenorhabditis elegans, a biological model for research in toxicology. In *Reviews of Environmental Contamination and Toxicology* (ed. de Voogt, W.), pp. 1–35. Springer, Cham.

Truong, L., Reif, D. M., St Mary, L., Geier, M. C., Truong, H. D. and Tanguay, R. L. (2014). Multidimensional in vivo hazard assessment using zebrafish. *Toxicol. Sci.* **137**, 212–33.

Tsuji, R. and Crofton, K. M. (2012). Developmental neurotoxicity guideline study: Issues with methodology, evaluation and regulation. *Congenit. Anom. (Kyoto).* **52**, 122–128.

Umesono, Y., Tasaki, J., Nishimura, K., Inoue, T. and Agata, K. (2011). Regeneration in an evolutionarily primitive brain--the planarian Dugesia japonica model. *Eur. J. Neurosci.* **34**, 863–9.

Villar, D., Li, M. H. and Schaeffer, D. J. (1993). Toxicity of organophosphorus pesticides to Dugesia dorotocephala. *Bull. Environ. Contam. Toxicol.* **51**, 80–87.

Yang, X., Kaj, K. J., Schwab, D. J. and Collins, E.-M. S. (2017). Coordination of size-control, reproduction and generational memory in freshwater planarians. *Phys. Biol.* **14**, 036003.

Zhang, G., Truong, L., Tanguay, R. L. and Reif, D. M. (2017). A new statistical approach to characterize chemical-elicited behavioral effects in high-throughput studies using Zebrafish. *PLoS One* **12**, e0169408.

Chapter 4: Comparative analysis of zebrafish and planarian model systems for developmental neurotoxicity screens using an 87-compound library

Reprinted from: Hagstrom, Danielle; Truong, Lisa; Zhang, Siqi; Tanguay, Robert L; and Collins, Eva-Maria S. “Comparative analysis of zebrafish and planarian model systems for developmental neurotoxicity screens using an 87-compound library”, Toxicological Sciences (in revision).

ABSTRACT

There is a clear need to establish and validate new methodologies to more quickly and efficiently screen chemicals for potential toxic effects, particularly on development. The emergence of alternative animal systems for rapid toxicology screens presents valuable opportunities to evaluate how systems complement each other. In this article, we compare a chemical library of 87-compounds in two such systems, developing zebrafish and freshwater planarians, by screening for developmental neurotoxic effects. We show that the systems' toxicological profiles are complementary to each other, with zebrafish yielding more detailed morphological endpoints and planarians more behavioral endpoints. Overall, zebrafish was more sensitive to this chemical library, yielding 86/87 hits, compared to 50/87 hits in planarians. The difference in sensitivity could not be attributed to molecular weight, Log K_{ow} or the bioconcentration factor. Of the 87 chemicals, 28 had previously been evaluated in mammalian developmental neuro- (DNT), neuro- or developmental toxicity studies. Of the 28, 20 were hits in the planarian, and 27 were hits in zebrafish. Eighteen of the 28 had previously been identified as DNT hits in mammals and were highly associated with activity in zebrafish and planarian behavioral assays in this study. Only 1 chemical (out of 28) was a false negative in both zebrafish and planarian systems. Differences in endpoint coverage and system sensitivity illustrate the value of a dual systems approach to rapidly query a large chemical-bioactivity space and provide weight-of-evidence for prioritization of chemicals for further testing.

INTRODUCTION

There is increasing recognition in the field of toxicology that the high expense, low throughput, and uncertainty of traditional rodent testing are inadequate to evaluate the ever-growing number of environmental chemicals. Alternative integrated systems, such as zebrafish, nematodes, and planarians, have emerged to fill these gaps because they are small, easy to breed and maintain, comparatively inexpensive, and develop quickly (Boyd et al., 2012; Boyd et al., 2015; Hagstrom et al., 2016; Hill et al., 2005; Tejeda-Benitez and Olivero-Verbel, 2016; Truong et al., 2014). Use of these models, with their own unique strengths and limitations, is an effective bridge between *in vitro* and whole animal/mammalian testing methods, allowing for rapid exploration of adverse outcome pathways. Comparative screening in multiple such animal models covers more chemical-biological space, thus providing greater weight of evidence for prioritization of chemical hazards.

Recently, the NIEHS National Toxicology Program (NTP) initiated a collaboration wherein different labs studying a variety of alternative models, including *in vitro* cell culture systems, zebrafish, and planarians, screened a library of 87 unique compounds, allowing for cross-system comparisons (Behl et al., 2018). This library consisted of known and suspected developmental neurotoxicants and 5 designated negative control chemicals, expanded from a previously tested library of 80 compounds (Ryan et al., 2016). Here we compare the results of screening this library in a developmental zebrafish model and freshwater planarian system. Zebrafish embryos and larvae have become a popular animal model for developmental (Linney et al., 2004) and neurotoxicity studies (Bailey et al., 2013; He et al., 2014) because this system strikes an optimal balance among model complexity and tractability. This system is amenable to high-throughput whole animal screening (Geier et al., 2018a; Noyes et al., 2015; Truong et al.,

2014) and maintains strong developmental and physiological similarity to higher vertebrates. In particular, the external development and optical transparency of zebrafish embryos allows for detailed morphological studies. Moreover, 84% of genes that have been associated with a human disease have an obvious orthologue in zebrafish (Howe et al., 2013).

The asexual freshwater planarian *Dugesia japonica* has recently emerged as a high-throughput, alternative whole animal model for developmental neurotoxicology (Hagstrom et al., 2015; Hagstrom et al., 2016). Planarians have a high capacity to regenerate, which allows them to reproduce asexually by binary fission (Malinowski et al., 2017) and fully regenerate a centralized nervous system (Cebrià, 2007; Rink, 2013). In this asexual species, neurodevelopment is achieved through neuroregeneration and can be induced by decapitation. Because of the similar sizes of adult and regenerating/developing animals, the planarian system offers the unique ability to screen both life stages in parallel with the same assays to identify potential effects specific to development. Moreover, planarians possess a large repertoire of quantifiable behaviors, many of which can be assayed in a fully automated fashion, including thermotaxis, phototaxis, and a characteristic escape response, providing distinct readouts of neuronal function (Cochet-Escartin et al., 2015; Hagstrom et al., 2016; Inoue et al., 2014; Paskin et al., 2014; Zhang et al., 2018).

Because the systems differ in their developmental timeline, we compared the chemical effects at two different stages: 1) early development (24 hours post fertilization (hpf) in the zebrafish and day 7 in the planarian), when the animals begin to form major anatomical structures, and 2) late development (day 5 or 120 hpf in the zebrafish and day 12 in the planarian), when the animals have essentially completed development. We assayed for developmental delays, morphological abnormality, mortality and altered behavioral endpoints.

Eighty-six out of 87 chemicals were bioactive in the zebrafish, while 50 were bioactive in regenerating planarians. Physicochemical properties (e.g. molecular weight, log K_{ow} and bioconcentration factor (BCF)) did not account for bioactivity differences between the models. Of the 87 chemicals, 28 were previously associated with high quality mammalian toxicity data in ToxRefDB. The regenerating planarian responses to 20 of these 28 chemicals (~71%) and the zebrafish responses to 27 of the 28 (96%) were concordant with mammalian outcomes. By utilizing both model systems, the field might rapidly query more chemical-bioactivity space for guided prioritization of testing in mammals using mechanistic insight gained from the breadth of morphological and behavioral endpoints jointly provided by the two systems.

MATERIALS AND METHODS

Chemical library

Supplementary Table 1 lists the chemicals composing the NTP 87-compound library, consisting of 5 chemical classes (drugs, industrial chemicals, flame retardants, polycyclic aromatic hydrocarbons (PAHs), and pesticides) as well as 5 intended negative control chemicals. More details on the composition of the library can be found in Behl et al, the introduction of this special issue (Behl et al., 2018). Chemicals were provided as ~20 mM stocks, dissolved in dimethyl sulfoxide (DMSO). Four duplicate chemicals were provided in the 91-compound library tested in the zebrafish study but were not provided in the planarian library.

Planarian studies

Asexual *D. japonica* were used for the planarian screen. Details of the experimental procedures and data analysis, as well as the analyzed data for each endpoint can be found in (Zhang et al., 2018). In brief, 3 replicates of n=8 (n=24 in total) developing/regenerating and adult/intact planarians were each screened for every chemical of the library, generally at 10 nM, 100 nM, 1 μM, 10 μM and 100 μM. Exposure began on day 1, after the amputation of regenerating planarians, and the planarians were kept in sealed 48-well plates (Genesee Scientific, San Diego, CA) for 12 days, with screening occurring on days 7 and 12 (Figure 4.1). The DMSO levels were kept constant at 0.5% and n=8 control populations exposed to the 0.5% DMSO solvent control were included in every plate. We have previously shown this DMSO concentration has no effect on planarian morphology or behaviors (Hagstrom et al., 2015). All raw data associated with the screen are available on the Dryad Digital Repository (doi: 10.5061/dryad.mk6m608).

Zebrafish studies

Tropical 5D wildtype adult zebrafish were housed at Oregon State University, Sinnhuber Aquatic Research Laboratory (SARL) in standard 14h light/10h dark-light cycle. Embryos were collected, cleaned and staged prior to dechorionation at 4 hpf. The chorions were enzymatically removed and at 6 hpf, one embryo was placed per well in round bottom 96-well plates prefilled will 100 µL of embryo media. The chemicals were digitally dispensed directly from the 20 mM stocks into the test wells using a Hewlett Packard D300e, and all wells normalized to 0.64% DMSO (vol/vol). Each chemical was tested at 0, 1, 2, 4.5, 9, 18, 34, and 67 µM and sealed with parafilm to minimize evaporation and shaken gently overnight at 235 rpm (Truong et al., 2016). Ten chemicals (2,3,7,8-Tetrachlorodibenzo-p-dioxin, Bis(tributyltin)oxide, Benzo[g,h,i]perylene, hexachlorophene, rotenone, tetraethylthiuram disulfide, deltamethrin, methyl mercury (II) chloride, saccharin sodium salt hydrate, and valinomycin) were retested at lower concentrations as the first assessment resulted in 100% mortality or morbidity in all concentrations. A list of the concentrations can be found in Supplementary Table 2. Developmental toxicity was assessed by evaluating mortality, developmental progression, spontaneous movement, and notochord distortion at 24 hpf. Behavioral assessments were conducted at 24 hpf (Embryo photomotor response, EPR) using the Photo-motor Response Assessment Tool (Reif et al., 2016) and at 120 hpf using Viewpoint LifeScience Zebraboxes (Truong et al., 2014; Zhang et al., 2017). At 120 hpf, additional developmental and morphological toxicity endpoints were assessed including: mortality, yolk sac edema, curved or bent body axis in either direction, missing or smaller/larger than normal eye, shortened or malformed snout, malformed jaw, malformed or missing otic vesicle, pericardial edema, malformation or necrosis of the brain, malformed, missing or disorganized somites, malformed or missing pectoral fin, malformed or missing caudal fin, lack

of pigment or over pigmentation, lack of circulation, truncated body, failure of swim bladder to inflate, bent notochord and/or tail, and response to touch. After chemical exposure, embryos were not exposed to visible light until administration of the EPR test at 24 hpf (Reif et al., 2016). The test consisted of 30 s of darkness (IR light, Background); first 1 s pulse of intense VIS light, 9 s darkness (Excitation); second pulse of VIS light, 10 s darkness (Refractory) (Truong et al., 2014). Statistical significance was calculated for each interval using a Kolmogorov-Smirnov test (K-S) with a threshold of $p < 0.01$. The 120 hpf larval photomotor response assay (LPR) was conducted just prior to morphological evaluation. In the LPR, larvae experience a total of 4 light cycles, each cycle consisting of 3 min of alternating light and dark. Wells with mortality or malformed animals were excluded from the subsequent analysis. An entropy score was calculated for each interval and compared to the control to compute a relative ratio, as described in (Zhang et al., 2017). Statistical significance was determined using a K-S test ($p < 0.01$) and a relative ratio of $> 10\%$ or $< 10\%$. All analyses were conducted using custom R scripts previously described (R Core Team, 2016). All zebrafish morphological dose response plots are available in Supplementary Materials (Supplementary Figure 2).

Meta-analysis

Supplementary File 1 contains the lowest effect levels (LELs) identified for each endpoint in both the zebrafish and planarian screens. Incidences of endpoint abnormality (hit detection) in the two systems were compared based on whether the chemical was deemed active or not, irrespective of concentration. Each chemical was scored in MATLAB (Mathworks, Nattick, MA) as either active in planarians, active in zebrafish, active in both, or inactive. We did not consider the concentration which elicited a response due to differences in the concentrations tested and because of the unknown relationships between the nominal aquatic concentrations and

the internal dose within the animals. As such, we have no available information to determine the actual amount of toxicants inside the animals, making direct comparisons of dose inappropriate. Therefore, the data was converted to binary data: hit or no hit (Supplementary Table 3). The endpoints were organized into classes (Table 4.1) to compare similar endpoints between the two systems. Furthermore, to compare similar developmental stages, endpoints at 24 hpf in the zebrafish studies were compared with endpoints at day 7 in the planarian studies and 120 hpf (day 5) zebrafish endpoints with day 12 planarian endpoints. Comparisons were also made at the system level, considering any affected endpoint.

Table 4.1. Classes of endpoints used in the two systems.

Endpoint Class	Zebrafish endpoints	Planarian endpoints
Mortality	Mortality (24 hpf, 120 hpf)	Lethality (day 7, day 12)
Morphology	Developmental progress (24 hpf) Spontaneous movement (24 hpf) Notochord distortion (24 hpf) Curved/bent axis (120 hpf) Brain malformation or necrosis (120 hpf) Malformed or missing caudal fin (120 hpf) No circulation or blood flow (120 hpf) Eyes malformed, missing or abnormal sized (120 hpf) Heart malformation, pericardial edema (120 hpf) Malformed jaw (120 hpf) Malformed or missing otic (120 hpf) Malformed or missing pectoral fin (120 hpf) Lack of pigmentation or over pigmentation (120 hpf)	Eye regeneration (day 7)
Behavior	Embryo photomotor response (EPR: 24hpf) Larval photomotor response (LPR: 120hpf)	Unstimulated behavior (day 7 and 12) Phototaxis (day 7 and 12) Scrunching (day 12) Thermotaxis (day 12)

The physicochemical and *in vivo* animal data analysis was completed using custom R scripts (R Core Team, 2016). The chemical-physical property log octanol/water partition coefficient (log K_{ow}) and bioconcentration factor (BCF) was obtained using EPISuite v4.11 (http://www.epa.gov/opptintr/exposure/pubs/episuite.htm). The CAS was input into EPISuite and the experimental log K_{ow} and BCF values were used when available. The molecular weight and CAS were provided by the NTP.

To compare the results of the zebrafish and planarian screens with *in vivo* animal data, the publicly available animal data were downloaded from the US Environmental Protection Agency's Toxicity Reference Database (ToxRefDB) (https://www.epa.gov/chemical-research/toxicity-forecaster-toxcasttm-data). The August 2014 data release of the study treatment file ("toxrefdb_study_tg_effect_endpoint_AUG2014_FOR_PUBLIC_RELEASE") and the summary file ("toxrefdb_nel_lel_noael_loael_summary_AUG2014_FOR_PUBLIC_RELEASE") were used. The studies used in this analysis were those that fit the usability criteria of "Acceptable guideline (post -1998), "Acceptable Guideline (pre-1998)", and "Acceptable Non-guideline". As the 87 compounds were selected to be potential developmental or developmental neurotoxicants, the study types were filtered to developmental (DEV), multi-generational (MGR), neurotoxicity (NEU) and developmental neurotoxicity (DNT). There was no filter on the species used. One point to consider is that the current version of ToxRefDB only houses chemicals that cause adverse effects in animal studies. The 59 other chemicals found in this 87-compound library could either have been in ToxRefDB but with studies that did not follow guideline protocols (which we deemed not usable for these analyses) or were negatives. For these reasons, the concordance study was benchmarked to the 28 active chemicals. Concordance analysis was

conducted using a custom R script, and the R package, circlize. DEV and MGR study types were mapped to zebrafish and planarian mortality and morphology, while NEU and DNT were mapped to zebrafish EPR and LPR and planarian early and late behavior.

RESULTS

Screening the NTP 87-compound library in both systems

Each of the chemicals of the NTP 87-compound library (Behl et al., 2018; Ryan et al., 2016) were classified as either generally developmentally toxic, developmentally neurotoxic, neurotoxic, or unknown due to limited data (https://sandbox.ntp.niehs.nih.gov/neurotox/). The chemicals were structure and use classified as drug, flame retardant, industrial, PAH, pesticide, or inactive (as defined by the NTP). As Supplemental Figure 1 illustrates, the largest class in the library consisted of drugs (19 of 87; 22%). There were 5 chemicals selected as inactive negative controls by the NTP library curators.

Figure 4.1 shows an overview of the different experimental schemes used for the zebrafish and planarian screens. In both studies, developing animals (either dechorionated 6 hpf zebrafish embryos or amputated planarian tails) were statically exposed to multiple concentrations of each chemical in multi-well plates. For planarian studies, both adult (intact) animals and decapitated animals regenerating a new brain (regenerating tail pieces) were assayed. For ease of comparison to the developing zebrafish, we focused on data associated with the regenerating planarians. The comparison with adult worms can be found in Supplementary Figure 3. Chemical bioactivity was assayed in early development (24 hpf zebrafish and day 7 planarian) and late development (120 hpf zebrafish and day 12 planarian) (Figure 4.1). Dual system screening yielded a significantly larger coverage of endpoints, with zebrafish contributing most of the morphological endpoints (13 vs. 1 in planarians) and the planarian system contributing more behavioral endpoints, covering different behavioral stimuli (light, temperature, noxious heat) and general locomotion compared to photoresponse behaviors, (6 vs. 2 in zebrafish).

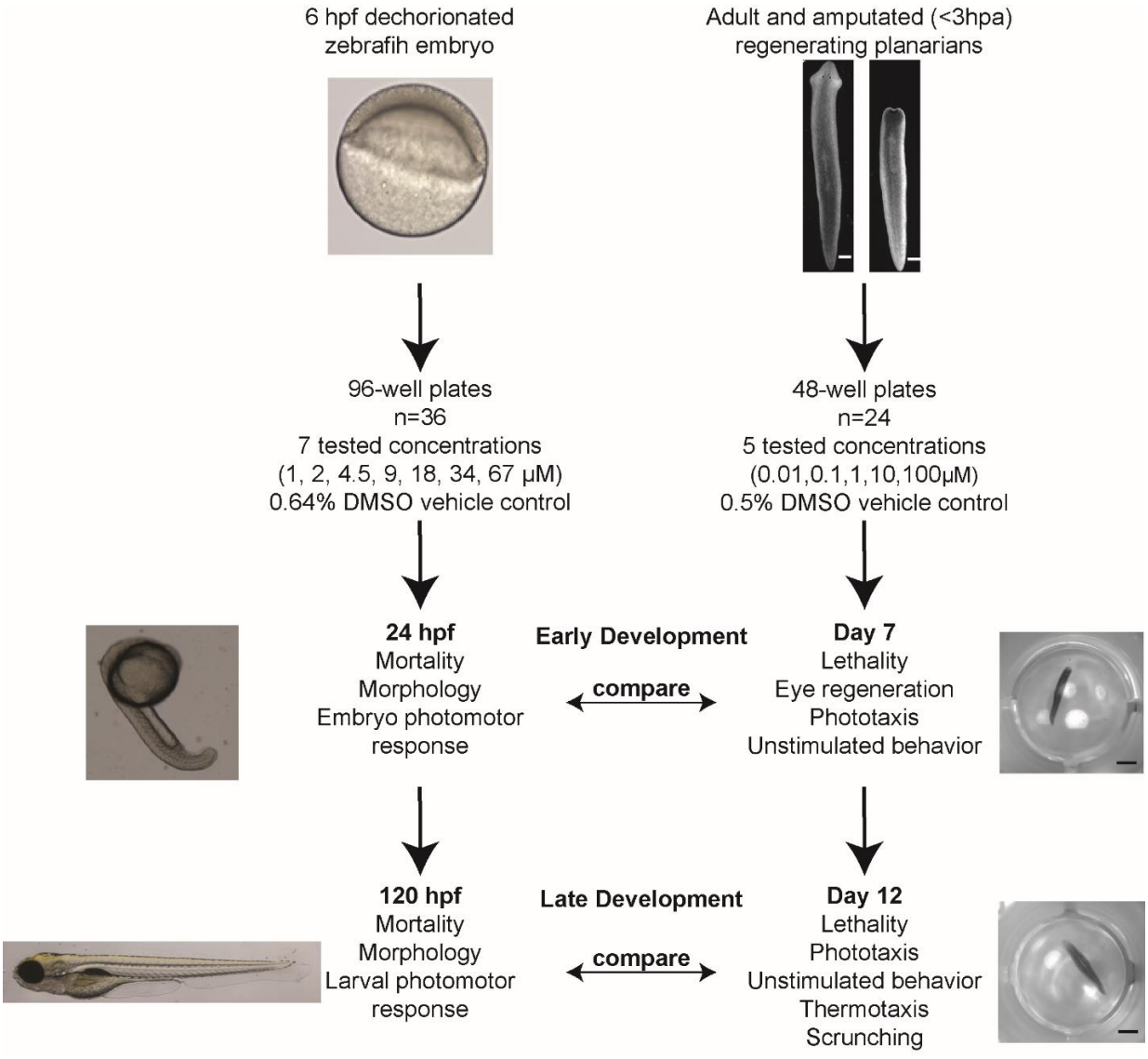

Figure 4.1. Comparison of screening schemes in the zebrafish and planarian systems. Details of the two screens including testing conditions and endpoints by time-point. Table 4.1 summarizes the different morphological endpoints assayed in the zebrafish system. Hpa: hours post-amputation. Scales are as follows: white scale bars: 0.5mm, black scale bars: 2mm; Zebrafish 6 hpf embryo is ~0.7 mm diameter; 24 hpf is1.9 mm long; 120 hpf is 3.9 mm long (https://zfin.org/zf_info/zfbook/stages/index.html).

Concordance of active chemicals between zebrafish and planarians

Considering any assay endpoint, zebrafish were more sensitive indicators of bioactivity, i.e., 86 of 87 (99%) unique chemicals were bioactive (Figure 4.2A). Thirty-two chemicals were hits in morphological endpoints, 49 in the EPR, and 66 in the LPR. Fifteen chemicals were bioactive in all 4 assays.

Additionally, 50 of the 87 chemicals (57%) were bioactive at any endpoint in regenerating (developing) planarians and 48 (55%) in adult worms (see Supplementary Figure 3). In regenerating planarians, 21 chemicals were hits for eye regeneration (morphology), 31 for at least one early behavior, and 45 for at least one late behavior (Figure 4.2B). Thus, the majority of bioactivity in the planarian system (47 of 50 chemicals, 90%) was detected by behavioral endpoints and almost ¼ (12 of 50) with behavior alone. It should be noted that 6 chemicals showed dose-independent effects (i.e. active at a lower but not higher concentrations) on unstimulated behavior in regenerating planarians (marked in red in Supplementary File 1). However, for 5 of these, effects were still seen at higher concentrations in other endpoints. For one chemical, Chrysene, the only observed effect was dose-independent hyper-activity in the unstimulated behavior assay. All other hits showed dose-dependence or only caused effects at the highest concentration tested. Thirteen chemicals were active in all 4 endpoint categories in planarians. All of the developing planarian bioactivity hits were also hits in zebrafish, accounting for 58% of the zebrafish bioactivity hits. The only chemical inactive in both screens was the drug hydroxyurea.

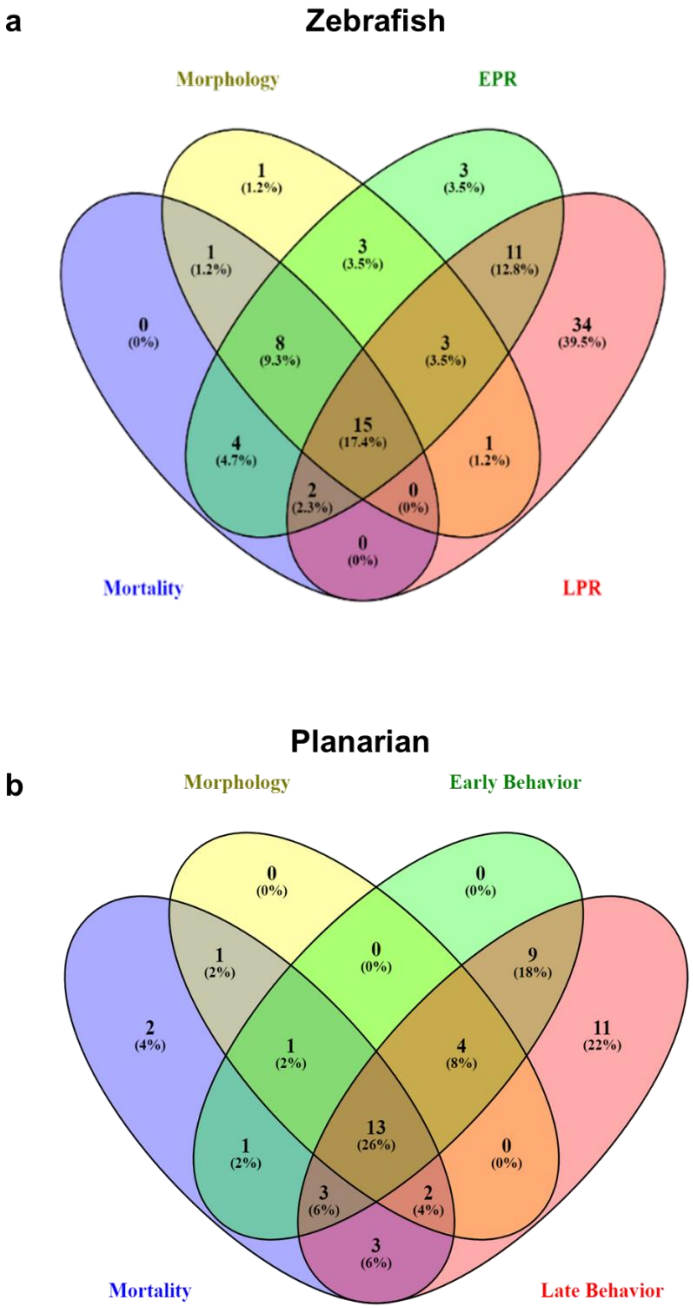

Figure 4.2. **Summary of (A) zebrafish and (B) planarian hits in each endpoint class**. Both model systems were exposed to the 87 chemicals and assessed in 4 assays: morphology, mortality, (A) EPR and LPR in zebrafish, and (B) early and late behavior in planarians.

Similar endpoints - mortality, morphology, behavior – were assessed in each model; thus, we compared the chemical hit rate for each endpoint class (Table 4.1 and Figure 4.3). Because of the similar developmental timelines, early and late endpoints were compared across models and concordance was based on the number of shared hits out of the total in zebrafish. Similar numbers of chemicals were found to be lethal in the two systems, with approximately 70% of these mortality hits being concordant (15/21 and 21/30 for early and late time points, respectively). In addition, 15/32 chemicals were concordant for morphological effects (47%). In both systems, the majority of chemical hits were detected in the behavior endpoints with 25/49 (51%) and 36/66 (55%) chemicals concordant at the early and late time-points, respectively. Similar trends were also found when comparing developing zebrafish to adult planarians, albeit with slightly less concordance, particularly for behavioral endpoints (Supplementary Figure 3).

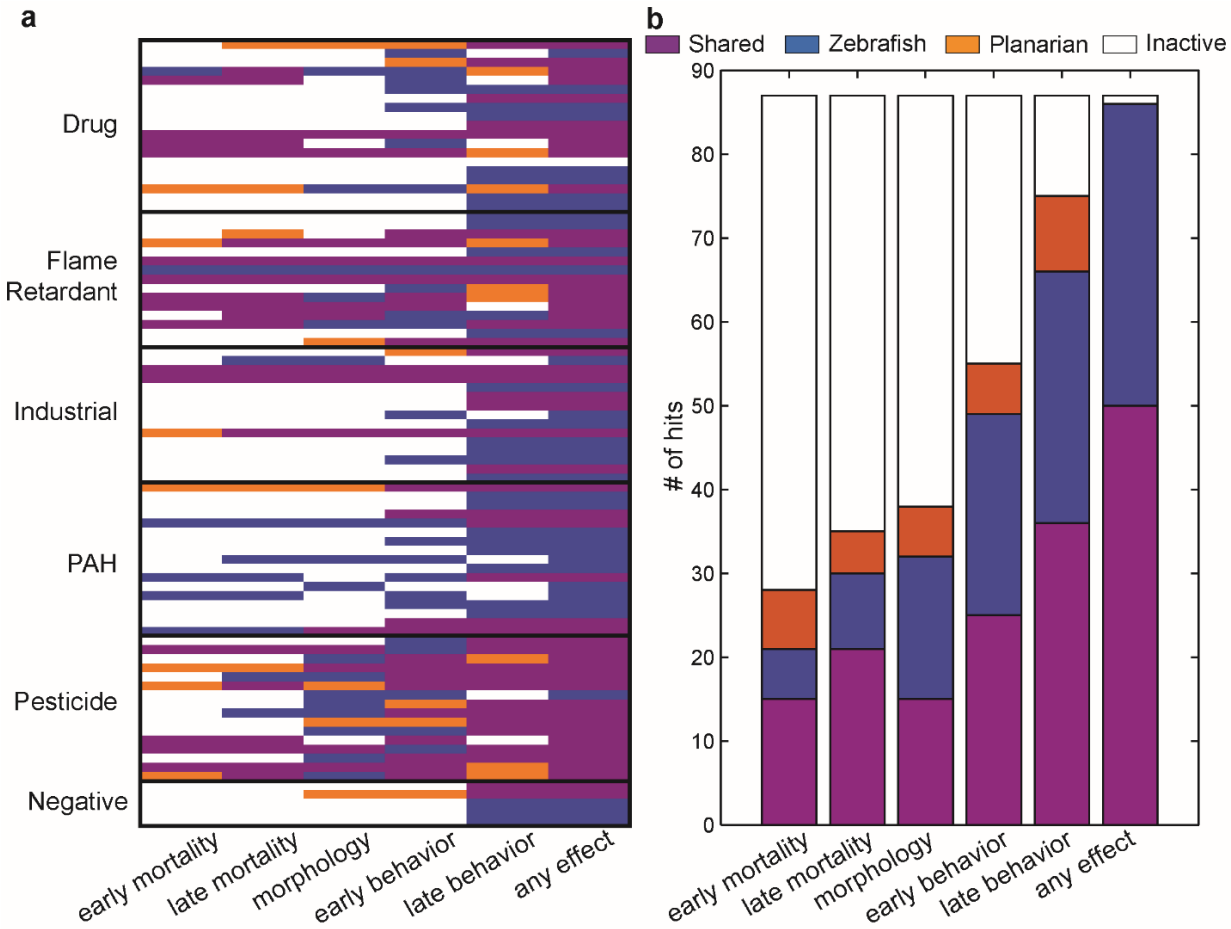

Figure 4.3. Comparison of active hits in the zebrafish and regenerating planarian screens. (A) Classification of hits for each chemical (rows), organized by chemical class, whether it was active in both systems (purple), zebrafish only (blue), regenerating planarians only (orange), or inactive (white) in each endpoint class (columns). See Table 4.1 for a description of the endpoints within classes. (B) Number of hits in each endpoint classification used in (A).

Comparison to physicochemical properties

The NTP 87-compound library consists of chemicals with a range of physicochemical properties. We focused on properties of putative high relevance to a waterborne exposure paradigm: molecular weight (MW), Log K_{ow} (log of the octanol/water partition coefficient) and BCF (bioconcentration factor). We found that neither MW, Log K_{ow}, nor BCF was entirely predictive of a response for both model systems. The single inactive chemical in the zebrafish screen, hydroxyurea, was not due to high molecular weight (Figure 4.4A), log K_{ow} (Figure 4.4C), or BCF (Figure 4.4E). Similarly, high molecular weight did not explain the instances of negative chemicals in the planarian model (Figure 4.4B) as they were all below 600 g/mol. Log K_{ow} and BCF (Figures 4.4D, F, respectively) were also not readily associated with instances of chemical inactivity. Thus, the overall association of physicochemical parameters with whole animal chemical bioactivity was weak.

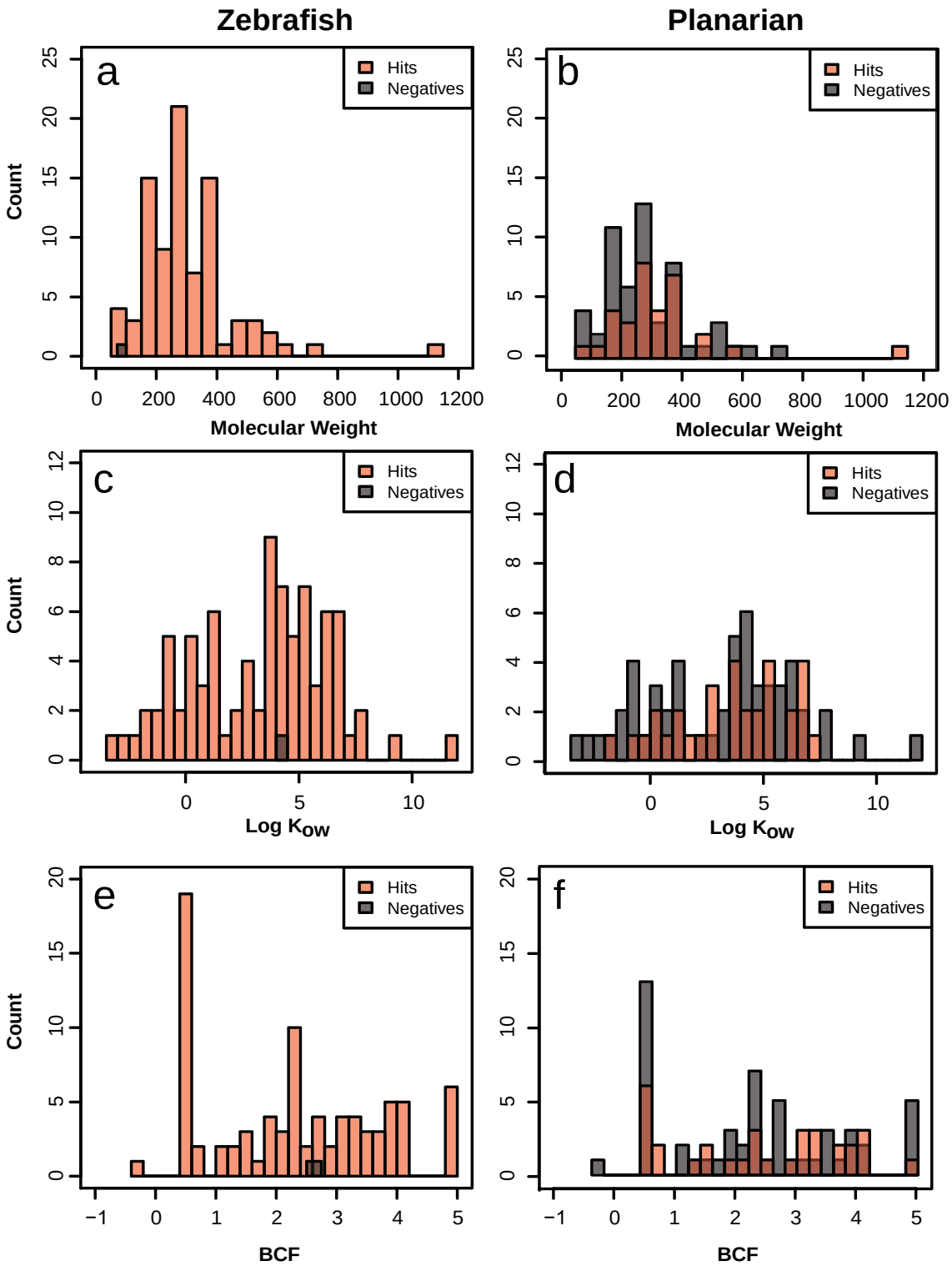

Figure 4.4. **Physicochemical properties of the NTP 87-compound library.** Comparing the (A, B) molecular weight, (C, D) Log K_{ow}, and (E, F) BCF of the inactives and the biological actives in zebrafish (left) and planarian (right).

Concordance with available animal data

The US EPA Toxicity Reference Database (ToxRefDB) houses *in vivo* studies from over 1,000 chemicals and thousands of animal toxicity studies in rat, rabbit, mouse, primate, dog, guinea-pig, hamster, and mink. We found that 28 chemicals in ToxRefDB (Supplementary Table 4) were also common to the NTP 87-compound library. Of note, this shared chemical set mainly consisted of pesticides (12 chemicals), drugs (8 chemicals), and industrial chemicals (5 chemicals) as well as 2 of the designated negative controls and 1 PAH.

By way of dataset comparison, we filtered the 28 ToxRefDB chemicals by adverse response category: 16 were identified in ToxRefDB as developmentally toxic (DEV), 18 as developmentally neurotoxic (DNT), 1 as a neurotoxic (NT) and 15 as multi-generationally toxic (MGR), in their respective studies (Supplementary Table 4).

Among the 28 chemicals common to this study and ToxRefDB, the overall, any effect, hit concordance was 27 of 28 (96%) for zebrafish bioactivity (Figure 4.5A) and 20 of 28 (71%) for regenerating planarian bioactivity (Figure 4.5B). For the 16 chemicals associated with general developmental toxicity in ToxRefDB, using morphology and mortality endpoints, 11 (69%) were hits in zebrafish, 7 (44%) were hits in the regenerating planarian, and 6 (37.5%) were hits in both. Four developmentally toxic chemicals did not show activity in our dual screen in either morphology or mortality: 2-methyloxyethanol, captan, Di(2-ethylhexyl) phthalate, and naphthalene. For the 15 multi-generationally toxic chemicals, 12 (80%) were hits in zebrafish, 6 (40%) were hits in the regenerating planarian, and 6 (40%) were hits in both systems when considering only morphology and mortality. Three of the 15 were inactive: 6-propyl-2-thiouracil, acetaminophen and Di(2-ethylhexyl)phthalate. Eighteen of the 28 shared chemicals had DNT studies, indicating that the 28 chemicals (and the NTP 87-compound library itself) were enriched

with developmental neurotoxicants. For the 18 developmentally neurotoxic chemicals, 17 (95%) were also hits in zebrafish behavior (both EPR and LPR), and 10 (56%) were hits in early and/or late planarian behavior, with all 10 of these being hits in both models. Neither model in the present study detected bioactivity for hydroxyurea. Only one chemical, carbamic acid, had a neurotoxicity study and was a hit in both the zebrafish and planarian. We note that 5 chemicals of the NTP 87-compound library were previously classified as negatives by the library's curators, but 2, acetaminophen and acetylsalicylic acid, were hits in ToxRefDB in MGR and DEV studies, respectively.

For a summary perspective of how the 28 chemicals interacted with the zebrafish and planarian endpoints, we created a chord diagram (Figure 4.5), which links the chemicals to ToxRefDB study types and zebrafish/planarian endpoints. The width of each endpoint or chemical indicates the number of interactions. In the zebrafish chord plot, LPR and morphology had the most interactions and were on par with the ToxRefDB DNT study type (Figure 4.5A). For the planarian, this trend is similar with late behavior being a highly linked endpoint (Figure 4.5B). The chord diagram for both models' endpoint classes (4 each) and the 4 ToxRefDB toxicity types is shown in Figure 4.5C. Both the zebrafish LPR and planarian late behavior endpoints had the most interactions (associated bioactivity with the largest width) with the subset of 28 chemicals, supporting the utility and predictivity of the systems' behavioral endpoints for classifying DNT.

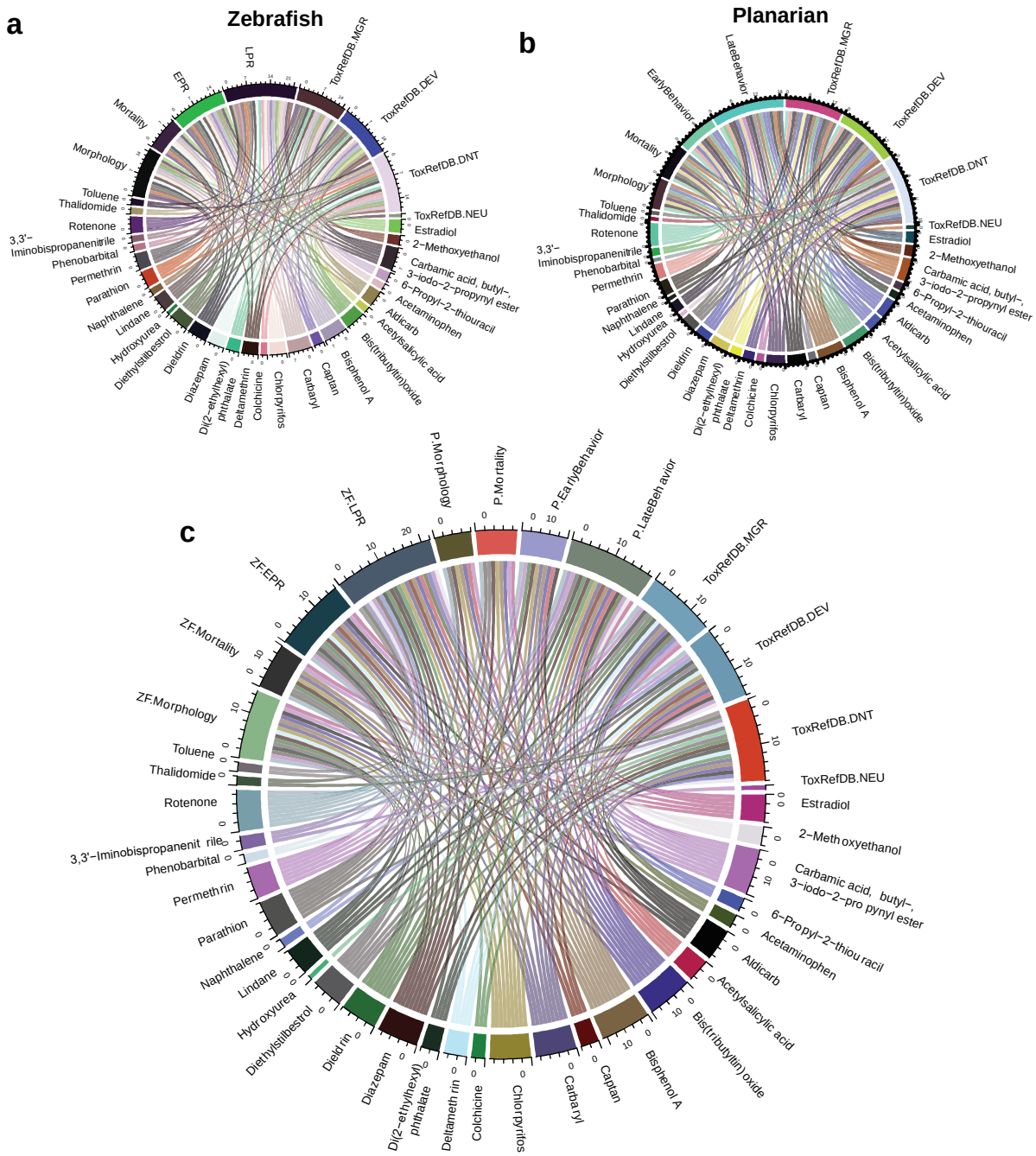

Figure 4.5. Inter-relationship between 28 chemicals, zebrafish and planarian assay endpoints and study types in ToxRefDB. A total of 28 chemicals had *in vivo* animal studies and were linked to (A) 4 zebrafish endpoints, (B) 4 planarian endpoints and (C) study types in ToxRefDB (DEV: Developmental, MGR: multigeneration, DNT: developmental neurotoxicity or NEU: neurotoxicity), zebrafish (morphology, mortality, EPR or LPR) and planarian assay endpoints (morphology, mortality, early and late behavior). Each color represents one of these parameters, and the line indicates the relationship between two parameters. The width of each parameter is a count of the number of relationships.

DISCUSSION

Trends by chemical class

Differences were observed in the sensitivity of the two systems to the various chemical classes in the NTP 87-compound library. Since almost all chemicals were bioactive in the zebrafish screen, concordance was based on whether a zebrafish hit was also a planarian hit. Concordance (from most to least): pesticides (15/16, planarian/zebrafish; 94%), flame retardants (10/15, 67%), drugs (10/18, 56%), industrial chemicals (7/15, 47%), and PAHs (6/17, 35%). The class of PAHs had the lowest concordance between the two models, which may be due to the absence of known PAH targets and pathways in planarians. Some PAHs activate the aryl hydrocarbon receptor (AHR) to produce toxicity and cancer (Choi et al., 2010; Garcia et al., 2018; Geier et al., 2018b; Knecht et al., 2017b; Qiao et al., 2017). Benzo[a]pyrene, a hit in zebrafish, but not planarians, produces developmental and neurobehavioral deficits dependent on the presence of the AHR2 (Incardona et al., 2011; Knecht et al., 2017a). Thus, lack of conservation of the AHR pathway in planarians may explain the observed insensitivity to PAH exposure.

Molecular weight, log K_{ow}, and BCF values are physicochemical properties proposed to be the most predictive for water exposure. In this study, we found that not to be true as no clear trends emerged for actives and inactives in the planarian system (Figure 4.4). As 86 of the 87 chemicals were hits in the zebrafish model, it was not feasible to assess this trend. However, the one negative, hydroxyurea, did not have any extreme values, supporting the conclusion from the planarian system that the 3 parameters are weakly predictive of bioactivity.

Differences in chemical sensitivity could be due to a variety of factors: route of exposure/ chemical uptake, metabolic activity, etc. It is worth noting that while exposure in both systems is

mainly achieved through epidermal diffusion, other routes (e.g. planarian pharynx) can also be involved, the extent to which may depend on the life-stage of the animal or the chemical itself. Additionally, planarians are covered in a protective mucus barrier, important for defense against infection and injury (Cochet-Escartin et al., 2015; Pedersen, 2008), which may impede uptake of some chemicals.

The NTP 87-compound library curators classified 5 chemicals as inactive in the toxicological screens performed to date under the range of test conditions used: Acetaminophen, acetylsalicylic acid (aspirin), D-glucitol, L-ascorbic acid and saccharin sodium salt hydrate. Two of these (acetaminophen and acetylsalicylic acid) were identified as hits in animal guideline studies (MGR and DEV, respectively). Additionally, they were also found to be bioactive in the zebrafish LPR and in regenerating planarian late behavior (acetaminophen) and morphology and early/late behaviors (acetylsalicylic acid). However, we note that the regenerating planarian behavioral effects of acetaminophen were very mild, being just outside the noise level (biological cutoffs) of the controls (Zhang et al., 2018). Other studies have also observed this bioactivity (Marques et al., 2004; Prášková et al., 2012; Weigt et al., 2010). Both the zebrafish and planarian detected bioactivity for these 2 misclassified DNTs and did so in under 12 days. The remaining 3 NTP-inactives had either limited data (D-glucitol), were a developmental toxicant (L-ascorbic acid), or a known carcinogen (saccharin sodium salt hydrate) (https://sandbox.ntp.niehs.nih.gov/neurotox/). Although these 3 chemicals were not DNT compounds, they were bioactive in the zebrafish assays, likely due to the sensitivity of the developing zebrafish as a biosensor and the fact that highly diverse chemical insults during vertebrate development often manifest as common endpoint readouts. Of note, none of the negative controls were active in adult planarians (Supplementary Figure 3). However, it is

difficult to classify chemicals as being negative when dosimetry is unknown, in any model system. Therefore, the differences in classification could be due to different databases and criteria.

The battery of models approach to screening and its predictive power

Whatever the end goal of a chemical screen might be, the principles of the 3Rs (Replacement, Reduction, and Refinement (Dix et al., 2007)) and good scientific practice collectively necessitate that the simplest yet most informative model that minimizes the number of false negatives and false positives is the preferred choice. However, in reality, no one model is likely to be sufficient to capture all necessary biological space in a time and cost-efficient manner. Thus, battery testing relying on comparative analysis across a range of complementary models (including both *in vitro* and *in vivo* systems) may provide the best option for efficient testing, particularly during early hazard identification and prioritization.

In this study, we showed that the zebrafish and planarian models provide a complementary assessment of biological space making them well-suited for battery-approach screening. The optical transparency of developing zebrafish allows for a wide range of morphological assessments to monitor proper developmental milestones and organ formation, exemplified by the high concordance of bioactivity in zebrafish morphological endpoints and ToxRefDB DEV studies. Additionally, their rapid development allows for integration of the central nervous system and assessment for developmental toxicants. On the other hand, the breadth of quantifiable planarian behaviors, some of which are known to be controlled through distinct neuronal subpopulations (Currie and Pearson, 2013; Inoue et al., 2014; Nishimura et al., 2010), provides insight in the mechanisms of (developmental) neurotoxicity. Moreover, planarians are uniquely suited to allow for direct comparisons between adult and developing

animals to be able to distinguish developmental effects from general (neuro-)toxicity. In fact, we found that 13 of the 50 chemicals active in regenerating planarians were developmentally selective, i.e. toxicity was not found in adult planarians or was found at a higher dose (Zhang et al., 2018).

Moreover, the zebrafish and planarian models were concordant in their bioactivity readouts across the diverse chemical space captured in this NTP 87-compound library (Figure 4.3). Interestingly, when comparing actives in the different endpoint classes, both systems contained hits that were not captured by the other. Thus, although more chemicals of this library were bioactive in zebrafish than in planarians, possibly due to the larger number of morphological endpoints evaluated, the unique endpoint hits in planarians (particularly late behavior, consisting of 4 different endpoints testing both stimulated (in response to light, thermal gradients and noxious heat stimuli) and unstimulated behaviors) may provide greater insight into the phenotypic profiling and mechanisms of neurotoxicity for some chemicals.

Even combined, the zebrafish and planarians models are likely not sufficient to capture all realms of possible human health hazards. For example, both models are aquatic organisms relying on chemical exposure in their aquatic environment. This may lead to inconsistencies in toxic outcomes when compared to the breadth of possible routes of exposure in other systems. Moreover, the relationship between the nominal chemical concentrations and the internal concentrations found in the animals is often lacking and could be affected by various factors (solubility issues, absorption by the plastic, absorption into the animal, instability in water over the course of the screen, metabolism, etc.). The understanding of these factors and the pharmacokinetic/pharmacodynamics in these systems will be essential for further validation.

This will be particularly important to compare and connect activity in these models with the relevant doses/exposure seen in mammals and humans.

The appropriateness and effectiveness of gold standard *in vivo* mammalian, developmental neurotoxicity studies, which can take 130+ days from exposure to evaluation of the neurobehavioral development of the offspring through adulthood (Dubovický et al., 2008; Virginia Moser et al., 2016) is fiercely debated. The time and expense costs of such guideline studies make them inadequate to evaluate the growing list of chemicals of concern (Tsuji and Crofton, 2012). Moreover, there is uncertainty how to accurately extrapolate data from rats to humans. By adapting high throughput alternative models, we can streamline the toxicology pipeline to efficiently prioritize which chemicals should be tested in guideline studies. These alternative models will likely not completely replace guideline studies, which may still be required for decision making, but can provide rapid guidance of which studies are worth pursuing and which toxicants are of the greatest concern. Libraries such as the NTP library tested here, which are enriched in chemicals with known toxicity, are useful tools for model validation to determine whether effects in alternative models are predictive of mammalian, and ultimately, human toxicity. Twenty-seven of the 28 compounds (96%) in the NTP library which had quality guideline studies associated with them in ToxRefDB were bioactive in either the zebrafish or planarian screens, with 20 (71%) bioactive in both, validating the predictivity and relevancy of these models for mammalian toxicity. Using both systems, we are able to provide necessary information to prioritize the chemicals of highest concern, such as in (Behl et al., 2015), and help fill the data gaps of under-represented toxicant classes with potential hazards in a relatively quick manner. The developmental zebrafish assay is completed in 5 days, while the planarian assay requires 12 days. Neither interval is a limitation, especially in light of the cost-, space- and

facility-efficiencies of both models. We thus envision using the zebrafish and planarian models as primary screening tools for vast swathes of chemical space, building big structure-bioactivity datasets from which to prioritize chemicals for further evaluation in the current testing pipeline and potentially predict chemical hazard in the future.

Thus, while a lot of work remains to be done to understand how these and other alternative systems compare to the standard toxicology models, what this and the other studies of the same chemical library in this special issue demonstrate, is the added value alternative models are bringing to modern toxicology. A battery approach that harvests the strengths of each of these systems in combination will ultimately transform the toxicology pipeline.

ACKNOWLEDGEMENTS

Chapter 4, in full, is a reformatted reprint of the material as it appears in Hagstrom, Danielle; Truong, Lisa; Zhang, Siqi; Tanguay, Robert L; and Collins, Eva-Maria S. "Comparative analysis of zebrafish and planarian model systems for developmental neurotoxicity screens using an 87-compound library", which has been submitted for publication at Toxicological Sciences. Use of this manuscript in the dissertation herein is covered by the rights permitted to the authors by Oxford Journals. The original planarian screening data was obtained by Danielle Hagstrom, Siqi Zhang, and Eva-Maria S. Collins as described in Chapter 3. Lisa Truong and Robert Tanguay designed, executed, and analyzed the experiments associated with the zebrafish screening data. Danielle Hagstrom performed the direct system comparisons while Lisa Truong performed the comparisons with available mammalian data and physico-chemical properties. Danielle Hagstrom, Eva-Maria S. Collins, and Lisa Truong co-wrote the manuscript with Robert Tanguay and Siqi Zhang contributing to the editing of the manuscript. Danielle Hagstrom and Lisa Truong were the primary investigators and authors of this material.

REFERENCES

Bailey, J., Oliveri, A. and Levin, E. D. (2013). Zebrafish model systems for developmental neurobehavioral toxicology. *Birth Defects Res. C. Embryo Today* **99**, 14–23.

Behl, M., Hsieh, J. H., Shafer, T. J., Mundy, W. R., Rice, J. R., Boyd, W. A., Freedman, J. H., Hunter, E. S., Jarema, K. A., Padilla, S., et al. (2015). Use of alternative assays to identify and prioritize organophosphorus flame retardants for potential developmental and neurotoxicity. *Neurotoxicol. Teratol.* **52**, 181-193

Behl, M., Ryan, K., Hsieh, J.-H., Parham, F., Shapiro, A., Collins, B. J., Birnbaum, L. S., Bucher, J. R., Walker, N. J., Foster, P. M., et al. (2018). Screening for developmental neurotoxicity (DNT) at the National Toxicology Program: The future is now! *Toxicol. Sci.*

Boyd, W., Smith, M. and Freedman, J. (2012). Caenorhabditis elegans as a model in developmental toxicology. In *Developmental Toxicology* (ed. Harris, C.) and Hansen, J. M.), pp. 15–24. Totowa, NJ: Humana Press.

Boyd, W. A., Smith, M. V., Co, C. A., Pirone, J. R., Rice, J. R., Shockley, K. R. and Freedman, J. H. (2015). Developmental effects of the ToxCast^{TM} phase I and phase II chemicals in Caenorhabditis elegans and corresponding responses in zebrafish, rats, and rabbits. *Environ. Health Perspect.* **124**, 586–93.

Cebrià, F. (2007). Regenerating the central nervous system: how easy for planarians! *Dev. Genes Evol.* **217**, 733–48.

Choi, H., Harrison, R., Komulainen, H. and Delgado Saborit, J. M. (2010). Polycyclic aromatic hydrocarbons. In *WHO guidelines for indoor air quality: selected pollutants*, pp. 289–345. Bonn, Germany: World Health Organization.

Cochet-Escartin, O., Mickolajczk, K. J. and Collins, E.-M. S. (2015). Scrunching: a novel escape gait in planarians. *Phys. Biol.* **12**, 055001.

Currie, K. W. and Pearson, B. J. (2013). Transcription factors lhx1/5-1 and pitx are required for the maintenance and regeneration of serotonergic neurons in planarians. *Development* **140**, 3577–88.

Dix, D. J., Houck, K. A., Martin, M. T., Richard, A. M., Setzer, R. W. and Kavlock, R. J. (2007). The Toxcast program for prioritizing toxicity testing of environmental chemicals. *Toxicol. Sci.* **95**, 5–12.

Dubovický, M., Kovačovský, P., Ujházy, E., Navarová, J., Brucknerová, I. and Mach, M. (2008). Evaluation of developmental neurotoxicity: some important issues focused on neurobehavioral development. *Interdiscip. Toxicol.* **1**, 206–10.

Garcia, G. R., Bugel, S. M., Truong, L., Spagnoli, S. and Tanguay, R. L. (2018). AHR2 required for normal behavioral responses and proper development of the skeletal and reproductive systems in zebrafish. *PLoS One* **13**, e0193484.

Geier, M. C., Chlebowski, A. C., Truong, L., Massey Simonich, S. L., Anderson, K. A. and Tanguay, R. L. (2018a). Comparative developmental toxicity of a comprehensive suite of polycyclic aromatic hydrocarbons. *Arch. Toxicol.* **92**, 571–586.

Geier, M. C., Chlebowski, A. C., Truong, L., Massey Simonich, S. L., Anderson, K. A. and Tanguay, R. L. (2018b). Comparative developmental toxicity of a comprehensive suite of polycyclic aromatic hydrocarbons. *Arch. Toxicol.* **92**, 571–586.

Hagstrom, D., Cochet-Escartin, O., Zhang, S., Khuu, C. and Collins, E.-M. S. (2015). Freshwater planarians as an alternative animal model for neurotoxicology. *Toxicol. Sci.* **147**, 270–285.

Hagstrom, D., Cochet-Escartin, O. and Collins, E.-M. S. (2016). Planarian brain regeneration as a model system for developmental neurotoxicology. *Regeneration* **3**, 65–77.

He, J.-H., Gao, J.-M., Huang, C.-J. and Li, C.-Q. (2014). Zebrafish models for assessing developmental and reproductive toxicity. *Neurotoxicol. Teratol.* **42**, 35–42.

Hill, A. J., Teraoka, H., Heideman, W. and Peterson, R. E. (2005). Zebrafish as a model vertebrate for investigating chemical toxicity. *Toxicol. Sci.* **86**, 6–19.

Howe, K., Clark, M. D., Torroja, C. F., Torrance, J., Berthelot, C., Muffato, M., Collins, J. E., Humphray, S., McLaren, K., Matthews, L., et al. (2013). The zebrafish reference genome sequence and its relationship to the human genome. *Nature* **496**, 498–503.

Incardona, J. P., Linbo, T. L. and Scholz, N. L. (2011). Cardiac toxicity of 5-ring polycyclic aromatic hydrocarbons is differentially dependent on the aryl hydrocarbon receptor 2 isoform during zebrafish development. *Toxicol. Appl. Pharmacol.* **257**, 242–249.

Inoue, T., Yamashita, T. and Agata, K. (2014). Thermosensory signaling by TRPM is processed by brain serotonergic neurons to produce planarian thermotaxis. *J. Neurosci.* **34**, 15701–14.

Knecht, A. L., Truong, L., Simonich, M. T. and Tanguay, R. L. (2017a). Developmental benzo[a]pyrene (B[a]P) exposure impacts larval behavior and impairs adult learning in zebrafish. *Neurotoxicol. Teratol.* **59**, 27–34.

Knecht, A. L., Truong, L., Marvel, S. W., Reif, D. M., Garcia, A., Lu, C., Simonich, M. T., Teeguarden, J. G. and Tanguay, R. L. (2017b). Transgenerational inheritance of neurobehavioral and physiological deficits from developmental exposure to benzo[a]pyrene in zebrafish. *Toxicol. Appl. Pharmacol.* **329**, 148–157.

Linney, E., Upchurch, L. and Donerly, S. (2004). Zebrafish as a neurotoxicological model. In *Neurotoxicology and Teratology*, pp. 709–718.

Malinowski, P. T., Cochet-Escartin, O., Kaj, K. J., Ronan, E., Groisman, A., Diamond, P. H. and Collins, E.-M. S. (2017). Mechanics dictate where and how freshwater planarians fission. *Proc. Natl. Acad. Sci. U. S. A.* **114**, 10888–10893.

Marques, C. R., Abrantes, N. and Gonçalves, F. (2004). Life-history traits of standard and

autochthonous cladocerans: I. Acute and chronic effects of acetylsalicylic acid. *Environ. Toxicol.* **19**, 518–526.

Nishimura, K., Kitamura, Y., Taniguchi, T. and Agata, K. (2010). Analysis of motor function modulated by cholinergic neurons in planarian Dugesia japonica. *Neuroscience* **168**, 18–30.

Noyes, P. D., Haggard, D. E., Gonnerman, G. D. and Tanguay, R. L. (2015). Advanced morphological-behavioral test platform reveals neurodevelopmental defects in embryonic zebrafish exposed to comprehensive suite of halogenated and organophosphate flame retardants. *Toxicol. Sci.* **145**, 177–195.

Paskin, T. R., Jellies, J., Bacher, J. and Beane, W. S. (2014). Planarian phototactic assay reveals differential behavioral responses based on wavelength. *PLoS One* **9**, e114708.

Pedersen, K. J. (2008). Sliime-secreting cells of planarians. *Ann. N. Y. Acad. Sci.* **106**, 424–443.

Prášková, E., Živná, D., Štěpánová, S., Ševčíková, M., Blahová, J., Maršálek, P., Široká, Z., Voslářová, E. and Svobodová, Z. (2012). Acute toxicity of acetylsalicylic acid to juvenile and embryonic stages of Danio rerio. *Neuroendocrinol. Lett.* **33**, 72–76.

Qiao, Y., Li, Q., Du, H.-Y., Wang, Q.-W., Huang, Y. and Liu, W. (2017). Airborne polycyclic aromatic hydrocarbons trigger human skin cells aging through aryl hydrocarbon receptor. *Biochem. Biophys. Res. Commun.* **488**, 445–452.

R Core Team (2016). *R: A language environment for statistical computing*. Vienna, Austria.

Reif, D. M., Truong, L., Mandrell, D., Marvel, S., Zhang, G. and Tanguay, R. L. (2016). High-throughput characterization of chemical-associated embryonic behavioral changes predicts teratogenic outcomes. *Arch. Toxicol.* **90**, 1459–1470.

Rink, J. C. (2013). Stem cell systems and regeneration in planaria. *Dev. Genes Evol.* **223**, 67–84.

Ryan, K. R., Sirenko, O., Parham, F., Hsieh, J. H., Cromwell, E. F., Tice, R. R. and Behl, M. (2016). Neurite outgrowth in human induced pluripotent stem cell-derived neurons as a high-throughput screen for developmental neurotoxicity or neurotoxicity. *Neurotoxicology* **53**, 271–281.

Tejeda-Benitez, L. and Olivero-Verbel, J. (2016). Caenorhabditis elegans, a biological model for research in toxicology. In *Reviews of Environmental Contamination and Toxicology* (ed. de Voogt, W.), pp. 1–35. Springer, Cham.

Truong, L., Reif, D. M., St Mary, L., Geier, M. C., Truong, H. D. and Tanguay, R. L. (2014). Multidimensional in vivo hazard assessment using zebrafish. *Toxicol. Sci.* **137**, 212–33.

Truong, L., Bugel, S. M., Chlebowski, A., Usenko, C. Y., Simonich, M. T., Simonich, S. L. M. and Tanguay, R. L. (2016). Optimizing multi-dimensional high throughput screening using zebrafish. *Reprod. Toxicol.* **65**, 139–147.

Tsuji, R. and Crofton, K. M. (2012). Developmental neurotoxicity guideline study: Issues with methodology, evaluation and regulation. *Congenit. Anom. (Kyoto).* **52**, 122–128.

Virginia Moser, Raffaele, K., Crofton, K., Gilbert, M., Bowers, W. and Bailey, F. (2016). *NAFTA Technical working group on pesticides (twg): Developmental neurotoxicity study (DNT) guidance document*.

Weigt, S., Huebler, N., Braunbeck, T., von Landenberg, F. and Broschard, T. H. (2010). Zebrafish teratogenicity test with metabolic activation (mDarT): Effects of phase I activation of acetaminophen on zebrafish Danio rerio embryos. *Toxicology* **275**, 36–49.

Zhang, G., Roell, K. R., Truong, L., Tanguay, R. L. and Reif, D. M. (2017). A data-driven weighting scheme for multivariate phenotypic endpoints recapitulates zebrafish developmental cascades. *Toxicol. Appl. Pharmacol.* **314**, 109–117.

Zhang, S., Hagstrom, D., Hayes, P., Graham, A. and Collins, E.-M. S. (2018). Multi-behavioral endpoint testing of an 87-chemical compound library in freshwater planarians. *Toxicol. Sci.*

Chapter 5: Planarian cholinesterase: *in vitro* characterization of an evolutionarily ancient enzyme to study organophosphorus pesticide toxicity and reactivation

Reprinted from: Hagstrom, Danielle; Hirokawa, Hideto; Zhang, Limin; Radić, Zoran; Taylor, Palmer; and Collins, Eva-Maria S. "Planarian cholinesterase: in vitro characterization of an evolutionarily ancient enzyme to study organophosphorus pesticide toxicity and reactivation", Archives of Toxicology, vol. 91, 2017.

Supplementary materials can be accessed online at:

https://link.springer.com/article/10.1007%2Fs00204-017-2130-7

ABSTRACT

The freshwater planarian *Dugesia japonica* has recently emerged as an animal model for developmental neurotoxicology and found to be sensitive to organophosphorus (OP) pesticides. While previous activity staining of *D. japonica*, which possess a discrete cholinergic nervous system, has shown acylthiocholine catalysis, it is unknown whether this is accomplished through an acetylcholinesterase (AChE), butyrylcholinesterase (BChE), or a hybrid esterase and how OP exposure affects esterase activity. Here, we show that the majority of *D. japonica* cholinesterase (DjChE) activity departs from conventional AChE and BChE classifications. Inhibition by classic protonable amine and quaternary reversible inhibitors (ethopropazine, donepezil, tacrine, edrophonium, BW284c51, propidium) shows that DjChE is far less sensitive to these inhibitors than human AChE, suggesting discrete differences in active center and peripheral site recognition and structures. Additionally, we find that different OPs (chlorpyrifos oxon, paraoxon, dichlorvos, diazinon oxon, malaoxon) and carbamylating agents (carbaryl, neostigmine, physostigmine, pyridostigmine) differentially inhibit DjChE activity *in vitro*. DjChE was most sensitive to diazinon oxon and neostigmine and least sensitive to malaoxon and carbaryl. Diazinon oxon inhibited DjChE could be reactivated by the quaternary oxime, pralidoxime (2-PAM), and the zwitterionic oxime, RS194B, with RS194B being significantly more potent. Sodium fluoride (NaF) reactivates OP-DjChE faster than 2-PAM. As one of the most ancient true cholinesterases, DjChE provides insight into the evolution of a hybrid enzyme before the separation into distinct AChE and BChE enzymes found in higher vertebrates. The sensitivity of DjChE to OPs and capacity for reactivation validate the use of planarians for OP toxicology studies.

INTRODUCTION

Acetylcholinesterase (AChE) is a serine hydrolase of the α,β-hydrolase-fold family catalyzing hydrolysis of the neurotransmitter acetylcholine (ACh) that controls various central nervous system (CNS) cognitive, peripheral autonomic, and somatic motor functions. AChE regulates cholinergic neurotransmission by catalyzing the hydrolysis of released synaptic ACh in a sub-millisecond to second time frame (Quinn, 1987; Rosenberry, 1975; Taylor, 2017). Because of this crucial role, AChE has long been an important pharmacological and toxicological target. For example, carbamylating AChE inhibitors, such as physostigmine and neostigmine, have been used pharmacologically to treat CNS disorders such as Alzheimer's disease and peripheral autonomic disorders, affecting secretion and smooth muscle tone, and somatic motor disorders (myasthenia gravis) (King and Aaron, 2015; Pope et al., 2005).

Moreover, AChE is the primary target of organophosphorus and carbamylating pesticides, the most commonly used classes of insecticides worldwide (Grube et al., 2011; King and Aaron, 2015; Pope et al., 2005; Russom et al., 2014). OPs inhibit AChE through alkylphosphorylation of the active site serine, thus leading to ACh accumulation and cholinergic overstimulation, resulting in decreased heart and respiration rates, muscle tremors, and eventually paralysis and death (King and Aaron, 2015; Russom et al., 2014; Taylor, 2017). A most insidious use of certain OPs has been in terrorism by rogue terrorist groups and despotic regimes (King and Aaron, 2015; Ohbu et al., 1997; Okumura et al., 1996).

Apart from lethal acute toxicity at high doses, the wide use and availability of OPs in agricultural and domestic use raise questions about the safety of long-term exposure at the currently approved levels (Gatto et al., 2009; González-Alzaga et al., 2014; Muñoz-Quezada et al., 2013; Shelton et al., 2014). In particular, recent studies have suggested developmental toxic

manifestations that may be linked not only to cholinesterases, but related serine hydrolases or other protein targets (González-Alzaga et al., 2014; Muñoz-Quezada et al., 2013; Pancetti et al., 2007; Pope, 1999; Pope et al., 2005).

We have recently shown that the freshwater planarian *Dugesia japonica* is a valuable in vivo model for neurotoxicity studies (Hagstrom et al., 2015; Hagstrom et al., 2016). The planarian's capacity to regenerate after asexual reproduction or amputation - due to its large population of stem cells - make it well suited to study perturbations in neurodevelopment (Hagstrom et al., 2016). Because full and regenerating worms are of similar size, the planarian system allows for a direct comparison of the effects of neurotoxicants on brain development and function using the same behavioral endpoints (Hagstrom et al., 2015; Hagstrom et al., 2016). Using a custom planarian screening platform (Hagstrom et al., 2015), we found that planarians are sensitive to OPs. Exposure to chlorpyrifos or dichlorvos at sub-lethal concentrations elicits behavioral phenotypes with reduced rates of locomotion. We observed that planarians exposed to chlorpyrifos exhibited an increased frequency of sharp turns and head motions (Hagstrom et al., 2015) suggestive of altered neuromuscular communication through OP-mediated cholinesterase inhibition. Regenerating worms displayed increased sensitivity compared to full/intact animals, suggesting additional neurodevelopmental effects of these OPs (Hagstrom et al., 2015).

Cholinergic neurons contribute to control of motor functions in *D. japonica*. When exposed to physostigmine, planarians contract (Nishimura et al., 2010). This suggests that planarians use cholinesterase to regulate ACh levels at neuromuscular junctions and perhaps also at sites within the CNS. Further support for this hypothesis comes from activity staining using an acetylthiocholine (ATCh) substrate, which revealed specific localization in the planarian nervous system (Zheng et al., 2011). To be a suitable model for mammalian and aquatic organism

toxicity, the molecular, structural, and biochemical properties of the planarian cholinesterase(s) and related targets require thorough investigation.

Here, we characterize the cholinesterase activity of D. japonica tissue homogenates and find that the predominant D. japonica cholinesterase (DjChE) activity has recognition and catalytic properties characteristic of an AChE-BChE hybrid. To compare the properties of DjChE with mammalian AChE and thus gain insight into structural differences, we probe how DjChE activity is inhibited by classic reversible inhibitors, OPs, and carbamylating agents. Finally, we study oxime (the quaternary, 2-PAM, and the zwitterion, RS194B) and fluoride mediated reactivation after inhibition by diazinon oxon. We find a greater potency for RS194B and enhanced fluoride mediated reactivation after inhibition with the OP. As an ancient true cholinesterase, DjChE provides insight into the evolution of distinct AChE and BChE enzymes from a hybrid enzyme ancestor.

MATERIALS AND METHODS

Planarian culture

Freshwater planarians of the species *Dugesia japonica* were used for all experiments. Planarians were stored in 1x Instant Ocean (Instant Ocean, Blacksburg, VA) in Tupperware containers at 20°C in a Panasonic refrigerated incubator in the dark. Animals were fed organic chicken liver once or twice a week and cleaned twice a week when not used for experiments. Animals were starved for at least 5 days before homogenization.

Preparation of planarian homogenates

To prepare homogenates, approximately 2 ml of suspended planarians were transferred to a 50 ml conical tube and placed on ice. All water was removed and replaced with 1 ml cold 1X Phosphate buffered saline containing 1% TritonX-100 (Sigma-Aldrich, St. Louis, MO). The worms were homogenized using a handheld electric homogenizer (Tissuemeiser, Fisher Scientific, Hampton, NH) until a homogeneous slurry was formed. The homogenate was incubated on ice for approximately 30 min and transferred to a pre-chilled 1.5 ml microcentrifuge tube to be centrifuged at 21,000 x *g* for 30 min at 4°C. The supernatant was removed and used for experiments. This clarified homogenate was stored at 4°C and used within one week of preparation.

Cholinesterase activity assays

Cholinesterase activity was measured using an Ellman assay (Ellman et al., 1961) wherein planarian homogenate was added to the Assay Buffer (0.01% BSA (Sigma-Aldrich), 0.3 mM 5,5'-dithio-bis-[2-nitrobenzoic acid] (DTNB, Sigma-Aldrich) in 0.1 M phosphate buffer, pH 7.4). Thiocholine substrates, acetylthiocholine (ATCh) or butyrylthiocholine (BTCh), both from Sigma-Aldrich, were added last. No background reaction of the homogenate with DTNB was

observed under these conditions. Absorbance was immediately measured continuously for 1 min at 412 nm using a CARY 1E UV-Vis Spectrophotometer (Agilent Technologies, Santa Clara, CA). The slope of the absorbance was taken as the activity (min^{-1}) of the sample. For all experiments, the planarian homogenate was diluted with 1% TritonX-100 in PBS to achieve an activity of approximately 0.2-0.4 min^{-1} when measured with 1 mM ATCh as substrate. All experiments were conducted at room temperature.

Detection of ATCh or BTCh catalysis in fixed worms was performed as previously described (Zheng et al., 2011).

Chemicals

Tetraisopropyl pyrophosphoramide (iso-OMPA) was purchased from Sigma-Aldrich and prepared in ethanol. BW284c51, ethopropazine, 2-PAM (pyridine-2-aldoxime), sodium fluoride (NaF) and donepezil were purchased from Sigma-Aldrich and prepared in deionized water. Edrophonium was purchased from Santa Cruz Biotechnology (Dallas, TX) and stocks were prepared in water. Tacrine hydrochloride (Spectrum Chemical, New Brunswick, NJ) stocks were prepared in phosphate buffer. RS194B was synthesized and purified as previously described (Radić et al., 2012). The OPs (chlorpyrifos oxon, diazinon oxon, dichlorvos, malaoxon, and paraoxon) and carbamylating agents (carbaryl, physostigmine (eserine), pyridostigmine, and neostigmine) were purchased from Sigma-Aldrich with the exception of chlorpyrifos oxon and diazinon oxon, which were purchased from Chem Service (West Chester, PA). Stocks were prepared in ethanol and further diluted in water or buffer, with the exception of physostigmine which was prepared in dimethyl sulfoxide (DMSO, Sigma-Aldrich). Solvent (ethanol or DMSO) content in inhibition or reactivation reactions was never above 1% in the samples and controls.

Reversible inhibition

To determine the effects of classic reversible inhibitors on planarian cholinesterase activity, diluted homogenate and inhibitor were added to Assay Buffer and incubated for 5 min at room temperature. Substrate (ATCh or BTCh) was then added and the absorbance measured. Percent activities are reported as the ratio of activity in the inhibited sample over the activity in a control sample incubated with buffer or appropriate solvent. Data are reported as the means $\pm$ standard deviation (SD) of at least two independent experiments, with activities measured in technical triplicates for each experiment. IC_{50} values were calculated by fitting with a four parameter logistic fit using the Standard Curve Analysis tool in SigmaPlot (Systat Software Inc., San Jose, CA). K_d's were calculated from the IC_{50} values according to $K_d = \frac{IC_{50}}{1+\frac{[S]}{K_m}}$, where [S] is the substrate concentration.

Irreversible inhibition

The kinetics of inhibition with irreversible inhibitors reacting covalently with the cholinesterases (OPs and carbamylating agents) was determined by incubating the planarian homogenate with a 10% volume of inhibitor at room temperature (e.g. 10 µl 10X inhibitor to 90 µl homogenate). At the indicated time points, a 10 µl aliquot was taken from the inhibitor-homogenate mix and added to 980 µl Assay Buffer. Substrate was immediately added and the absorbance was measured. ATCh was used at a final concentration of 1 mM. Residual activity is reported as the percent activity of the average activity of a solvent control measured multiple times over the same inhibition time course. In SigmaPlot, the percent activity remaining over time was fit to the exponential decay formula $y = ae^{-(kobs)x}$ to determine k_{obs} (for example, see Supplementary Figure S1A). Where necessary, when inhibition was not complete at steady-state, a y0 parameter was added to provide a more accurate fit. For each inhibitor, the bimolecular rate

constant, k_r, was determined from the slope of the linear regression of k_{obs} versus concentration (Supplementary Figure S1 and S2). For each inhibitor, at least 4 different concentrations were tested from at least 2 biologically independent samples.

Reactivation of OP inhibited cholinesterase

Homogenates were inhibited with diazinon oxon, chlorpyrifos oxon, or paraoxon to achieve at least 95% inhibition in 30 min or less. Inhibited homogenates in 0.1 ml volume were passed over a spin column (Sit et al., 2011) to separate the conjugated enzyme from excess inhibitor. Samples were further diluted 10-fold and reactivating quaternary oxime (2-PAM), zwitterionic oxime (RS194B), or NaF were added in the specified concentration. Aliquots of 0.01 ml were removed at various times and added to 1.0 ml of Assay Buffer and 1 mM ATCh and the activity immediately read. Determination of the rate of reactivation, k_{obs}, were performed as described in (Kovarik et al., 2004).

RESULTS

D. japonica shows ChE activity distinguishable from AChE and BChE

Cholinesterase activity was measured in homogenates (Ellman et al., 1961) to compare hydrolysis of ATCh versus BTCh substrates over a range of substrate concentrations (Figure 5.1A). Catalysis of the BTCh substrate occurred at approximately half the rate of ATCh. The Km's were found to be 123 ± 6 and 59 ± 4 μM (mean ± SE of 6 independent experiments) for the ATCh and BTCh substrates, respectively. Hydrolysis of ATCh shows marginal substrate inhibition at 100 mM substrate, whereas hydrolysis of BTCh is constant at concentrations of 1-100 mM. This is dissimilar to the characteristic marked substrate inhibition by ATCh (ACh) and substrate activation seen at high concentrations of BTCh (BCh) typically found in mammalian AChE and BChE, respectively (Augustinsson, 1948; Radić et al., 1993). Staining of DjChE activity using ATCh and BTCh substrates after fixation of whole animals confirms that both activities are found in vivo and are localized to the CNS (Figure 5.1B).

AChE and BChE catalyze the hydrolysis of ATCh, whereas in mammals appreciable catalysis of the larger BTCh substrate molecule requires BChE (Taylor and Radić, 1994). Therefore, to determine what extent of ATCh and BTCh are catalyzed by a possible BChE-like enzyme, activity was measured after inhibition with a bulky organophosphate anhydride, iso-OMPA, that at low concentrations inhibits mammalian BChE but not AChE (Radić et al., 1993; Vellom et al., 1993). We found that incubation with up to 1 mM iso-OMPA was unable to significantly inhibit either ATCh or BTCh hydrolysis (Figure 5.1C) and only slow inhibition was seen at 5 mM iso-OMPA. Differential inhibition for ATCh and BTCh catalysis was not evident. Hence, DjChE does not seem to carry classical BChE inhibition parameters. Notably, since we measure enzyme activity in planarian homogenates, we cannot distinguish whether DjChE

activity is performed by a single enzyme or multiple enzymes with very similar catalytic parameters.

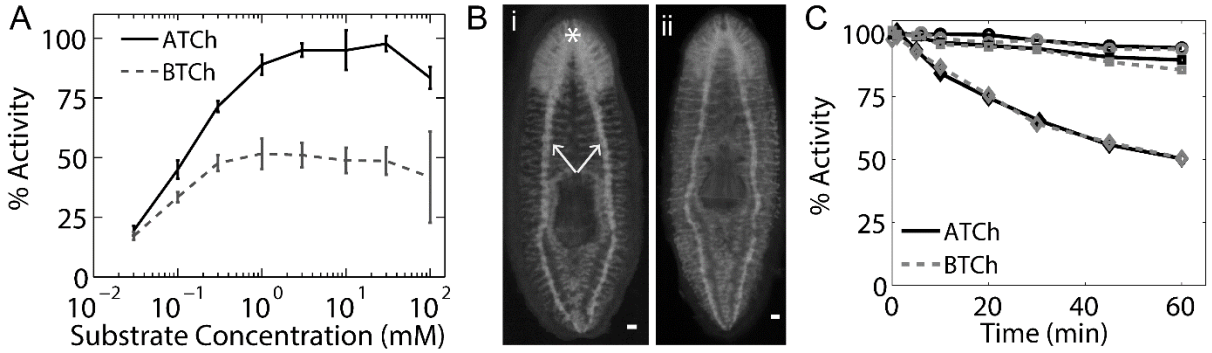

Figure 5.1. DjChE shows kinetic characteristics intermediate to mammalian AChE and BChE. (A) Activity of DjChE was determined using an Ellman assay over a range of ATCh (solid black line) and BTCh (dashed gray line) concentrations. Activity is reported as the percent of the maximum activity in that experiment using ATCh as a substrate. Error bars represent the standard deviation (SD) of 6 independent experiments. (B) Staining of DjChE activity in fixed *D. japonica* using ATCh (i) and BTCh (ii) substrates show activity is localized to the nervous system (* indicates the cephalic ganglion or brain and arrows indicate the ventral nerve cords) without clear spatial discrimination between the two activities. (C) Inhibition kinetics from 500 µM (circles), 1 mM (squares), and 5 mM (diamonds) iso-OMPA on DjChE activity using 1mM ATCh (black solid line) and BTCh (gray dashed line) as substrates. Activity is reported as the percent of the mean activity in the solvent control samples.

DjChE is far less sensitive to classic reversible inhibitors than human AChE

We measured the extent of inhibition on DjChE activity incurred by classic quaternary (BW284c51, edrophonium, and propidium) and amine reversible inhibitors (ethopropazine, donepezil, and tacrine) (Figure 5.2). To determine if these inhibitors act competitively, as described for AChE of other species (Taylor and Radić, 1994; Taylor et al., 1995), activity was compared using ATCh substrate at concentrations slightly below (0.1 mM) or above (1 mM) the Km. Because ethopropazine and BW284c51 are known to be specific inhibitors of mammalian BChE and AChE, respectively (Radić et al., 1993; Taylor and Radić, 1994; Vellom et al., 1993), we also compared DjChE activity using 0.1 or 1 mM BTCh as substrate. In agreement with our

results for iso-OMPA, differential inhibition was not evident between the ATCh and BTCh substrates when inhibiting with ethopropazine or BW284c51 (Figure 5.2A-B).

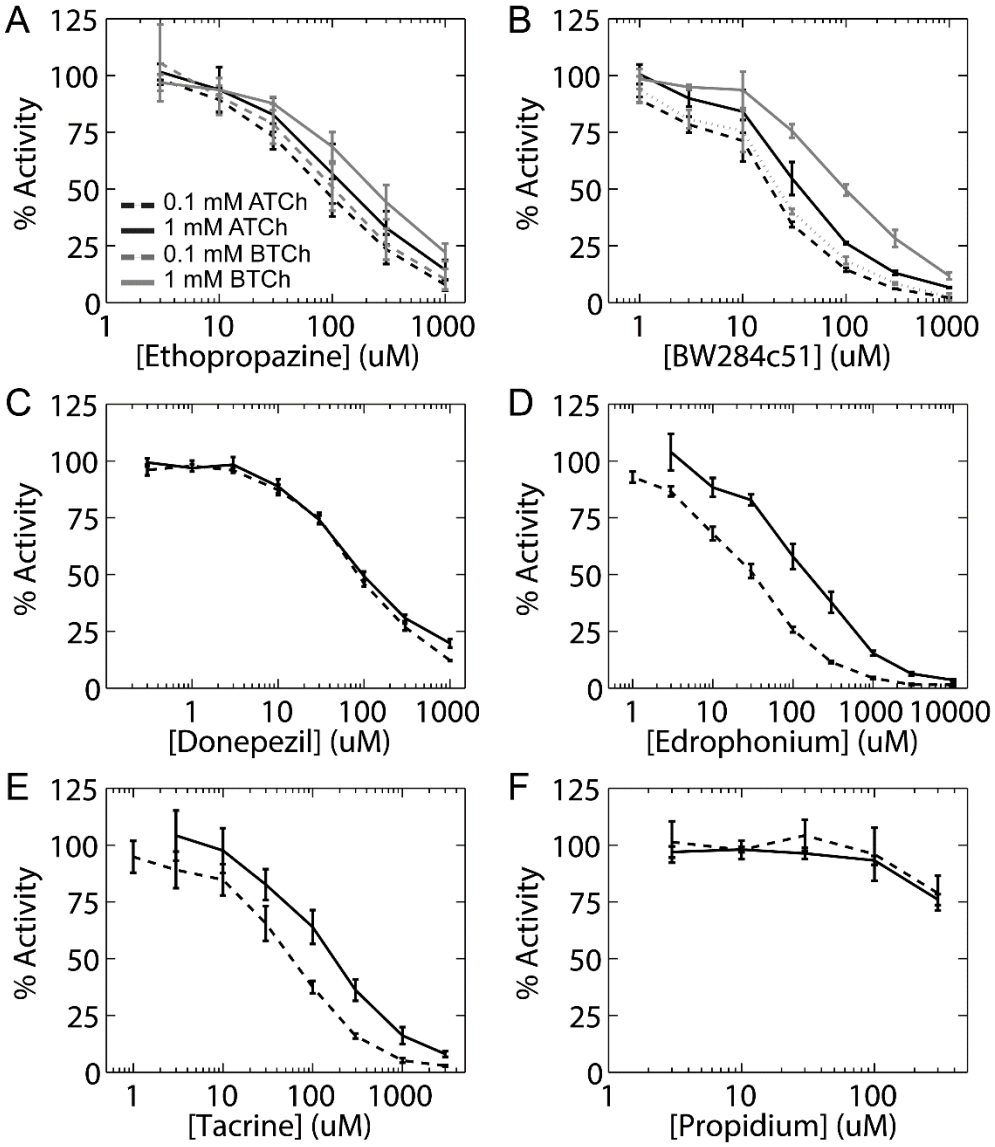

Figure 5.2. Inhibition by classic reversible quaternary and uncharged amine inhibitors. Panels show the percent of DjChE activity remaining in the samples after 5 min incubation with the reversible inhibitors ethopropazine (A), BW284c51 (B), donepezil (C), edrophonium (D), tacrine (E), and propidium (F) using 0.1 (dashed line) or 1 mM (solid line) ATCh (black) or BTCh (gray) substrates. Error bars indicate the SD of at least 2 independent experiments.

DjChE ATCh hydrolytic activity was found to be resistant to inhibition by up to 300 µM propidium (Figure 5.1F). The calculated IC_{50} values for these inhibitors at the various substrate concentrations are shown in Table 5.1. Corresponding K_d values are provided in Supplementary Table 1. Generally, DjChE was found to be far less sensitive to these reversible inhibitors than reported previously for human AChE (Supplementary Table 2) (Atack et al., 1989; Giacobini, 2000; Giacobini, 2001; Taylor, 2017).

Table 5.1. IC_{50} (M) of reversible inhibitors for 0.1 and 1 mM ATCh and BTCh.

	Substrate			
Inhibitor	*0.1 mM ATCh*	*1 mM ATCh*	*0.1 mM BTCh*	*1 mM BTCh*
Ethopropazine	$9.3 \pm 3.1 \times 10^{-5}$	$1.3 \pm 0.5 \times 10^{-4}$	$9.1 \pm 2.1 \times 10^{-5}$	$2.2 \pm 0.7 \times 10^{-4}$
BW284c51	$2.0 \pm 0.3 \times 10^{-5}$	$3.2 \pm 0.3 \times 10^{-5}$	$2.3 \pm 0.3 \times 10^{-5}$	$8.9 \pm 0.3 \times 10^{-5}$
Donepezil	$8.9 \pm 0.6 \times 10^{-5}$	$6.9 \pm 0.2 \times 10^{-5}$	ND[a]	ND[a]
Edrophonium	$3.1 \pm 0.1 \times 10^{-5}$	$1.6 \pm 0.2 \times 10^{-4}$	ND[a]	ND[a]
Tacrine	$6.2 \pm 0.6 \times 10^{-5}$	$1.4 \pm 0.1 \times 10^{-4}$	ND[a]	ND[a]
Propidium	$>3.0 \times 10^{-4}$	$>3.0 \times 10^{-4}$	ND[a]	ND[a]

IC_{50} values given as the mean ± SE of at least 2 independent experiments (shown in Figure 5.2).
[a]ND, not determined.

DjChE is inhibited by OPs and carbamylating agents

Progressive inhibition rates by the active oxon forms of various common OPs (diazinon oxon, chlorpyrifos oxon, dichlorvos, paraoxon, and malaoxon) were analyzed. Interestingly, bimolecular inhibition rate constants, k_r, for these OPs differed by two orders of magnitude with DjChE being most sensitive to diazinon oxon and least sensitive to malaoxon (Table 5.2). Over the range of concentrations tested, the reaction rate was linear with concentration (Supplementary Figure S1), and limiting rates were not observed.

Table 5.2. Rates of inhibition by OP oxons.

OP	k_r ($M^{-1}min^{-1}$)
Diazinon oxon	$22 \pm 2 \times 10^5$
Dichlorvos	$9.1 \pm 0.9 \times 10^5$
Chlorpyrifos oxon	$3.0 \pm 0.3 \times 10^5$
Paraoxon	$1.7 \pm 0.1 \times 10^5$
Malaoxon	$0.14 \pm 0.01 \times 10^5$

k_r values (bimolecular rate constants) were calculated from at least 5 different OP concentrations and reported as mean ± 95% confidence intervals from at least 2 independent experiments (technical and biological replicates). Raw data are shown in Supplementary Figure S1.

We similarly characterized the inhibition profiles for the carbamylating agents: carbaryl, neostigmine, physostigmine, and pyridostigmine. Carbamates, along with OPs, are used as insecticides due to their transient inhibition of AChE by covalent carbamylation of the active center serine. In contrast to OPs, carbamylation is comparably short-lived, since AChE can be reactivated by cleaving the carbamyl moiety through spontaneous hydrolysis within tens of minutes (Giacobini, 2000; Taylor, 2017). Similar to our results with OPs, inhibition constants varied over several orders of magnitude among these inhibitors, with neostigmine producing the fastest rates of inhibition and carbaryl the slowest (Table 5.3). Values are shown as bimolecular rate constants, since reaction rates were linear over the concentration range studied (Supplementary Figure S2).

Table 5.3. Rates of inhibition by carbamylating agents.

Carbamylating agent	k_r ($M^{-1}\,min^{-1}$)
Neostigmine	$1.3 \pm 0.2 \times 10^5$
Physostigmine	$0.32 \pm 0.02 \times 10^5$
Pyridostigmine	$0.10 \pm 0.01 \times 10^5$
Carbaryl	$0.00064 \pm 0.00008 \times 10^5$

k_r values (bimolecular rate constants) were calculated from at least 4 different carbamate concentrations and reported as mean ± 95% confidence intervals from at least 2 independent experiments (technical and biological replicates). Raw data are shown in Supplementary Figure S2.

Diethylphosphoryl DjChE formed by diazinon oxon is reactivated by the oximes, pralidoxime and RS194B

Since DjChE was found to be sensitive to phosphorylation and carbamylation by OPs and carbamates, respectively, we wondered whether reactivation of OP-inhibited DjChE could be enhanced by common oximes. To this end, we evaluated whether a member of the quaternary pyridinium aldoximes, pralidoxime (2-PAM) and a lead zwitterionic oxime (RS194B), would reactivate DjChE that had been inhibited completely by diazinon oxon (Figure 5.3). Both oximes, at concentrations of 4 mM, were able to reactivate DjChE ATCh hydrolyzing activity. At this concentration, RS194B promoted reactivation significantly faster than 2-PAM. Under these conditions, no significant spontaneous reactivation was observed. As these rates are representative of reactivation of diethylphosphoryl DjChE, reactivation rates should be similar for other OPs forming the same conjugate (paraoxon and chlorpyrifos oxon).

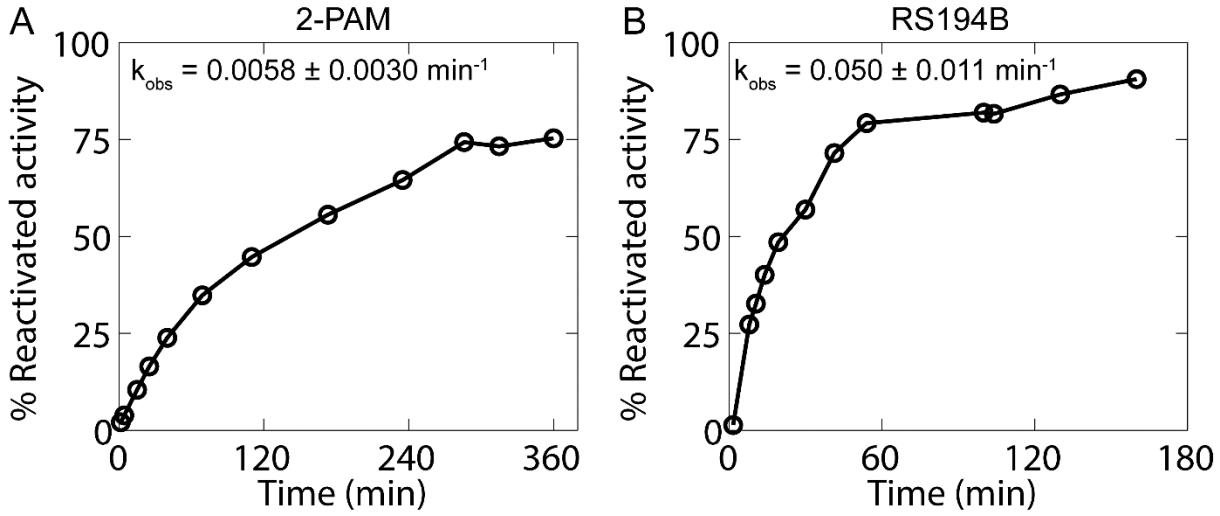

Figure 5.3. Oxime elicited reactivation of diazinon oxon inhibited DjChE activity using (A) 4 mM 2-PAM or (B) RS194B. Percent reactivated activity is based on an uninhibited control measured several times over the course of reactivation. One representative experiment is shown. For each experiment, the k_{obs} was calculated from the first order approach to full or steady-state reactivation and the mean k_{obs} ± SD of 2-3 experiments is shown.

Reactivation of DjChE by NaF

Given the unique features of resistance to inhibition by the classic quaternary and cationic amines and rapid reactivation by a zwitterionic oxime observed with DjChE, we examined a largely hidden finding in cholinesterase research. In early studies on AChE reactivation, Heilbronn and colleagues (Albanus et al., 1965; Heilbronn, 1965) found that fluoride anion will catalyze cholinesterase reactivation, albeit at a slow rate. We found that NaF could reactivate DjChE activity and that the rate of reactivation shows a linear dependence on fluoride concentration (Figure 5.4). Moreover, reactivation was independent of the organophosphate inhibitor (diazinon oxon, paraoxon, and chlorpyrifos oxon), all of which form the diethylphosphoryl enzyme conjugate (Supplementary Figure S3). Interestingly, reactivation of DjChE was significantly more rapid with 10 mM NaF (mean k_{obs} = 0.023 min^{-1}) than with 4 mM 2-PAM (mean k_{obs} =0.0058 min^{-1}).

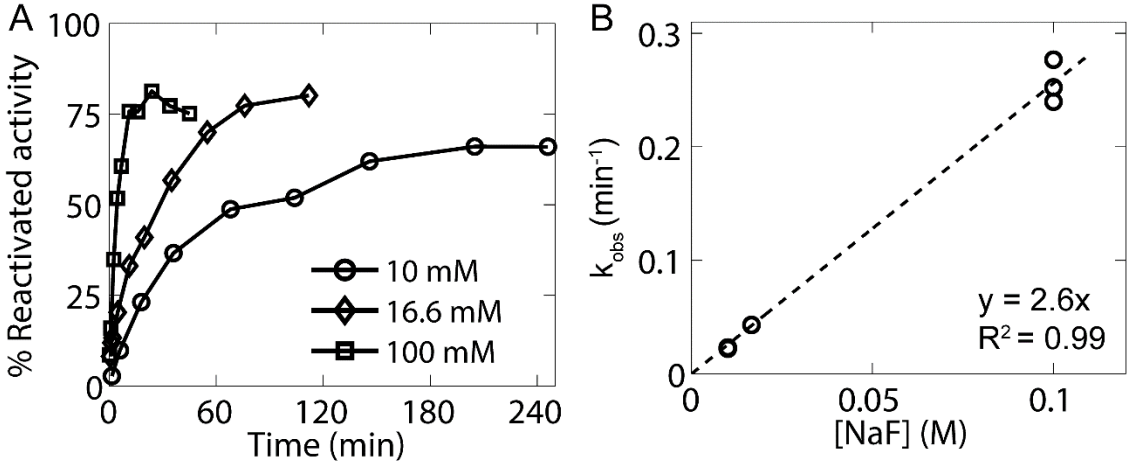

Figure 5.4. DjChE is efficiently reactivated by NaF. (A) Reactivation of diazinon oxon-inhibited DjChE after treatment with 10 (circles), 16.6 (diamonds), or 100 mM (squares) NaF. One representative experiment is shown for each concentration. Percent reactivated activity is based on an uninhibited control measured several times over the course of reactivation. (B) For each experiment, k_{obs} was calculated from the first order approach to full or a steady-state of reactivation (see Materials and Methods). Since k_{obs} appears to have a linear relationship with NaF concentration (dashed line), this represents a bimolecular reactivation where the binding site for F- shows no saturation at these concentrations.

DISCUSSION

Kinetic characteristics of DjChE: catalysis and inhibition.

AChE can be distinguished from BChE in mammalian, avian, and most fish species on the basis of efficient catalysis of acetylcholine and propionyl choline, but marked reduction for butyrylcholine as noted by Augustinsson (Augustinsson, 1948). However, in the case of DjChE activity, the relative difference between acetylcholine and butyrylcholine substrate catalysis, as measured with the thioesters, is only a factor of 2 (Figure 5.1A). This difference is much less than that reported for AChE from various species of *Schistosoma,* which showed approximately 5 times greater acetylcholine catalysis over butyrylcholine catalysis (Bentley et al., 2005). Moreover, the bulky organophosphate, iso-OMPA, is an effective irreversible inhibitor of mammalian BChE, but as shown in Figure 5.1C, does not inhibit DjChE activity up to 1 mM and only shows a slow progressive inhibition at 5 mM.

We note several similarities in substrate catalysis and inhibitor profiles for DjChE compared to cholinesterases from other invertebrate species, including *Schistosoma* (platyhelminths) (Bentley et al., 2005), nematodes (Combes et al., 2001; Johnson and Russell, 1983), teleosts (Pezzementi et al., 2011), and jawless fish (Sanders et al., 1996). With the high turnover substrates, the acylcholine and acylthiocholine esters, mammalian AChEs exhibit substrate inhibition. For mammalian BChE, an enzyme that effectively catalyzes esters with a longer acyl chain length, higher concentrations of substrate lead to activation. Substrate inhibition is thought to be due to a second substrate molecule retarding the exchange of substrate and product in the space impacted gorge of AChE. In BChE, that possesses a larger gorge volume at its base (Nicolet et al., 2003; Sussman et al., 1991), the second substrate helps confer a gorge conformation facilitating the commitment to catalysis for initial substrate binding. By

contrast, substrate inhibition or activation of DjChE is minimal and occurs at far higher concentrations (100 mM) (Figure 5.1A). This mirrors what has been found with other invertebrate ChEs, including the closely related *Schistosoma* blood fluke (Bentley et al., 2005; Pezzementi et al., 2011; Sanders et al., 1996), and, while common to many invertebrate and some vertebrate animal species, is sometimes referred to as an atypical cholinesterase (Pezzementi et al., 2011).

A discrete peripheral site has been proposed for AChE, based on allosteric actions of gallamine (Changeux, 1966). Direct titration and subsequent characterization of the peripheral site was achieved with the quaternary fluorophore, propidium (Taylor and Lappi, 1975). Extended bisquaternary molecules such as BW284c51 and the neutral molecule donepezil (Kryger et al., 1998) interact with the active center and partially occlude the peripheral site in AChE to varying degrees. The substantially diminished affinity found for DjChE for BW284c51, donepezil, and propidium (Figure 5.2B, C, F) suggests this enzyme lacks or has an altered peripheral site. On the other hand, while the differences in binding energy may not be as dramatic, both edrophonium and tacrine show reduced binding affinities (greater K_d values) for DjChE (Figure 5.2 D-E). Since both of the latter ligands reside at the base of the active center gorge and do not extend to the rim, it seems likely that some differences in binding determinants also reside near the base of the active center gorge. Interestingly, DjChE was notably less sensitive to propidium than *Schistosoma* AChE (Bentley et al., 2005), suggesting structural differences of the peripheral sites.

As expected for serine hydrolases, DjChE is inhibited by OPs and carbamylating agents representing families of pesticides widely used in home and garden as well as large scale agricultural use. Since, in both cases, inhibition is progressive forming a covalent conjugate with

the target cholinesterase, potency is rank ordered in terms of the rate of inhibition. Since the carbamylating agents form a more labile conjugate, inhibition at lower concentrations will not carry the reaction to complete inhibition, rather to a steady state where inhibition and decarbamylation rates are equal. In all cases, analysis was carried out by manual reactant additions. Hence, rate measurements that rank order the covalent reactivity have been analyzed as bimolecular rate constants (k_r), being linear with concentration (Tables 5.2 and 5.3, Supplementary Figure S1 and S2). Generally, DjChE was similarly sensitive to the various OPs as mammalian AChE, with bimolecular rate constants varying within approximately an order of magnitude of that reported for human or mouse AChE (Reiner and Radić, 2000). Not surprisingly, DjChE showed greater sensitivity than mouse AChE to dichlorvos, the non-enzymatic byproduct of metrifonate, a commonly used schistosomiasis drug (Holmstedt et al., 1978). The most potent of the OPs was diazinon oxon. Consequently, it was employed as the lead inhibitor for the reactivation studies. Since chlorpyrifos oxon and paraoxon also form the diethylphosphoryl enzyme, reactivation should occur at the same rate for all of these inhibitors (Supplementary Figure S3).

The inhibitor data also suggest that if two or more cholinesterases were present in *D. japonica*, either their abundance based on catalytic properties is heavily weighted to one or their catalytic and inhibitor susceptibility properties do not vary sufficiently to distinguish two classes of activity. Thus, the most parsimonious explanation would be a single cholinesterase with hybrid properties between BChE and AChE. Analysis by Pezzementi and Chatonnet on the evolutionary history of cholinesterases has suggested that Platyhelminthes, including planarians and *Schistosoma*, contain the earliest true cholinesterases yet described (Pezzementi and Chatonnet, 2010). Thus, the present study helps to elucidate the evolutionary origins of early

cholinesterase structure and activity, which had previously only been described in *Schistosoma.* Interestingly, DjChE behaves more like a true hybrid AChE/BChE enzyme, whereas the *Schistosoma* cholinesterase has more AChE-like characteristics, suggesting potential evolutionary pressures leading to functional divergence in these closely related species. Similar hybrid AChE/BChE enzymes have been cloned and characterized from hagfish (Sanders et al., 1996) and teleosts (Pezzementi et al., 2011), suggesting that early cholinesterase activity in lower vertebrates was accomplished by an enzyme with intermediate AChE and BChE properties, before the gene duplication event leading to the divergent AChE and BChE enzymes found in higher vertebrates (Chatonnet and Lockridge, 1989). Based on parallels in catalytic properties with these other α,β-hydrolase-fold enzymes, we would predict the following sequence characteristics for DjChE: (a) classic catalytic triad resembling Ser200, Glu327 and His440 in the *Torpedo californica* sequence (Schumacher et al., 1986) and three disulfide bonded loops, (b) an acyl pocket corresponding to Phe295 and 297 that contains only a single aromatic residue, (c) a choline binding site dominated by Trp84 which serves a major role in the binding of quaternary inhibitors, (d) the absence or severe disruption of a peripheral anionic site defined by Trp286, Tyr72, and Tyr124, (e) a reduced number of aromatic side chains in the active center gorge compared with AChE, and (f) the absence of a clear distinction between AChE and BChE binding, where ethopropazine is selective for BChE. Future sequence identification and functional characterization of DjChE allow for a direct comparison with the published sequences from Schistosomes (Bentley et al., 2003), hagfish (Sanders et al., 1996), hemichordates (Pezzementi et al., 2015), and nematodes (Combes et al., 2001) to verify these proposed sequence features.

Reactivation of diazinon oxon-inhibited DjChE by common oximes and NaF

Examining the influence of the reactivation kinetics augmented by quaternary and zwitterionic oximes and F^- anion on DjChE could yield new insights into the reactivation process. Moreover, the planarian's capacity to regenerate makes the system well-suited to study not only toxic effects of OPs, but also the control of possible repair mechanisms in stem cells or neuronal precursor cells, necessitating an understanding of the reactivation process in this animal.

We found that diazinon oxon inhibited DjChE could be reactivated by the quaternary oxime 2-PAM, the zwitterion RS194B, and even fluoride ion, provided by NaF. When comparing the lowest concentration of NaF tested (10 mM), more complete and rapid reactivation occurred in the order of RS194B > NaF >2-PAM. These data are similar to studies with human AChE which have shown that RS194B is the most efficient reactivator, able to reactivate human AChE *in vitro* at a rate 2.5 times faster than equimolar 2-PAM (Radić et al., 2013). In mammals, RS194B, but not 2-PAM, crosses the blood-brain barrier and reactivates AChE in the central nervous system (Radić et al., 2012). RS194B can also cross the chorion membrane in zebrafish eggs (Schmidt et al., 2015). Hence, as a zwitterion, with a fraction of the compound existing as a neutral species at physiologic pH, RS194B appears to readily partition across a variety of biological membranes.

Similar to early studies by Heilbronn and colleagues (Albanus et al., 1965; Heilbronn, 1965), we found that NaF could reactivate diethylphosphoryl DjChE. We cannot, however, directly compare our rates to the early studies with human AChE due to the use of different OP inhibitors (sarin vs diazinon oxon), resulting in reactivation of different cholinesterase conjugates. To date, studies have focused largely on oximes as the nucleophiles of choice and the

use of quaternary ammonium cations to site direct the nucleophile. Surprisingly, we found that 10 mM NaF resulted in four times faster reactivation than 4 mM 2-PAM and appears to be more effective in reactivating DjChE than human AChE. Oximes in solution function as general bases in catalysis, but within the cholinesterase active center gorge, they may have unusual properties; the active center gorge may function to facilitate the oxime-oximate abstraction of a proton. Nucleophilicity of fluoride anion is to be expected, but the active center gorge structure reveals a strong dipole in the direction of the gorge base, facilitating the entry of a cationic substrate into the active center (Sussman et al., 1991). Dipole moments may differ among the cholinesterases, and this may also contribute to the diminished affinity of active center quaternary ligands, such as edrophonium. On the other hand, the small atomic size of fluoride may enhance its collisional access in the spatially constrained active center gorge that is further impacted by the conjugated OP. Finally, the potent reactivation of DjChE by fluoride anion and neutral oximes suggests an ancient and conserved reactivation mechanism already present in hybrid AChE/BChE enzymes of invertebrates. However, fluoride concentrations in the mM range are toxic. Accordingly, its value may not lie in its potential as a reactivator in the environment, but in providing mechanistic and kinetic insights for the design of new chemical landscapes for reactivation.

In conclusion, many of the hybrid AChE/BChE characteristics of DjChE seem to parallel those of cholinesterases found in other invertebrates and jawless fish species and may represent an evolutionarily ancient class of cholinesterase before the distinct separation of AChE and BChE activity in vertebrates (Chatonnet and Lockridge, 1989; Pezzementi and Chatonnet, 2010; Pezzementi et al., 2011). Although several aspects of DjChE kinetics, inhibitor binding, rates of reactivation, and thus structure seem to differ from mammalian AChE and BChE, the sensitivity of DjChE to OPs, and ability to reactivate in the presence of oximes and fluoride potentiate the

use of planarians for toxicology studies on these harmful pesticides. As the peripheral site may play a role in aspects of OP toxicity (Kousba et al., 2004), the differences in the DjChE peripheral site, as compared to mammalian AChE, provides an opportunity to distinguish between these effects. The unique regenerative capabilities of planarians allows one not only to compare toxicity on adult and developing animals in parallel (Hagstrom et al., 2016), but also bears the potential to delineate how OP-induced neurological damage could be repaired.

ACKNOWLEDGEMENTS

Chapter 5, in full, is a reformatted reprint of the material as it appears in Hagstrom, Danielle; Hirokawa, Hideto; Zhang, Limin; Radić, Zoran; Taylor, Palmer; and Collins, Eva-Maria S. "Planarian cholinesterase: in vitro characterization of an evolutionarily ancient enzyme to study organophosphorus pesticide toxicity and reactivation", Archives of Toxicology, vol. 91, 2017. The final publication is available at: https://link.springer.com/article/10.1007%2Fs00204-016-1908-3#enumeration. Permission to use this manuscript was granted to Danielle Hagstrom by Springer Nature. Danielle Hagstrom, Zoran Radić, Palmer Taylor, and Eva-Maria Collins designed the experiments, interpreted the data and co-authored the manuscript. Danielle Hagstrom, Hideto Hirokawa, and Limin Zhang performed the experiments. Danielle Hagstrom and Hideto Hirokawa were the primary investigators and authors of this material.

REFERENCES

Albanus, L., Heilbronn, E. and Sundwall, A. (1965). Antidote effect of sodium fluoride in organophosphorus anticholinesterase poisoning. *Biochem. Pharmacol.* **14**, 1375–1381.

Atack, J. R., Yu, Q.-S., Soncrant, T. T., Brossi, A. and Rapoport, S. I. (1989). Comparative inhibitory effects of various physostigmine analogs against acetyl- and butyrylcholinesterases. *J. Pharmacol. Exp. Ther.* **249**, 194–202.

Augustinsson, K.-B. (1948). Cholinesterases. *Nature* **162**, 194–195.

Bentley, G. N., Jones, A. K. and Agnew, A. (2003). Mapping and sequencing of acetylcholinesterase genes from the platyhelminth blood fluke Schistosoma. *Gene* **314**, 103–112.

Bentley, G. N., Jones, A. K. and Agnew, A. (2005). Expression and comparative functional characterisation of recombinant acetylcholinesterase from three species of Schistosoma. *Mol. Biochem. Parasitol.* **141**, 119–123.

Changeux, J.-P. (1966). Responses of acetylcholinesterase from Torpedo marmorata to salts and curarizing drugs. *Mol. Pharmacol.* **2**, 369–392.

Chatonnet, A. and Lockridge, O. (1989). Comparison of butyrylcholinesterase and acetylcholinesterase. *Biochem. J.* **260**, 625–634.

Combes, D., Fedon, Y., Toutant, J.-P. and Arpagaus, M. (2001). Acetylcholinesterase genes in the nematode Caenorhabditis elegans. *Int. Rev. Cytol.* **209**, 207–239.

Ellman, G. L., Courtney, K. D., Andres, V. and Featherstone, R. M. (1961). A new and rapid colorimetric determination of acetylcholinesterase activity. *Biochem. Pharmacol.* **7**, 88–95.

Gatto, N. M., Cockburn, M., Bronstein, J., Manthripragada, A. D. and Ritz, B. (2009). Well-water consumption and Parkinson's disease in rural California. *Environ. Health Perspect.* **117**, 1912–1918.

Giacobini, E. (2000). Cholinesterase inhibitors: from the Calabar bean to Alzheimer therapy. In *Cholinesterases and Cholinesterase Inhibitors* (ed. Ezio Giacobini), pp. 181–219. London: Martin Dunitz Ltd.

Giacobini, E. (2001). Selective inhibitors of butyrylcholinesterase: a valid alternative for therapy of Alzheimer's disease? *Drugs Aging* **18**, 891–898.

González-Alzaga, B., Lacasaña, M., Aguilar-Garduño, C., Rodríguez-Barranco, M., Ballester, F., Rebagliato, M. and Hernández, A. F. (2014). A systematic review of neurodevelopmental effects of prenatal and postnatal organophosphate pesticide exposure. *Toxicol. Lett.* **230**, 104–121.

Grube, A., Donaldson, D., Kiely, T. and Wu, L. (2011). *Pesticides Industry Sales and Usage:*

2006 and 2007 Market Estimates.

Hagstrom, D., Cochet-Escartin, O., Zhang, S., Khuu, C. and Collins, E.-M. S. (2015). Freshwater planarians as an alternative animal model for neurotoxicology. *Toxicol. Sci.* **147**, 270–285.

Hagstrom, D., Cochet-Escartin, O. and Collins, E.-M. S. (2016). Planarian brain regeneration as a model system for developmental neurotoxicology. *Regeneration* **3**, 65–77.

Heilbronn, E. (1965). Action of fluoride on cholinesterase - II. In vitro reactivation of cholinesterases inhibited by organophosphorus compounds. *Biochem. Pharmacol.* **14**, 1363–1373.

Holmstedt, B., Nordgren, I., Sandoz, M. and Sundwall, A. (1978). Metrifonate. Summary of toxicological and pharmacological information available. *Arch. Toxicol.* **41**, 3–29.

Johnson, C. D. and Russell, R. L. (1983). Multiple molecular forms of acetylcholinesterase in the nematode Caenorhabditis elegans. *J. Neurochem.* **41**, 30–46.

King, A. M. and Aaron, C. K. (2015). Organophosphate and carbamate poisoning. *Emerg. Med. Clin. North Am.* **33**, 133–151.

Kousba, A. A., Sultatos, L. G., Poet, T. S. and Timchalk, C. (2004). Comparison of chlorpyrifos-oxon and paraoxon acetylcholinesterase inhibition dynamics: potential role of a peripheral binding site. *Toxicol. Sci.* **80**, 239–48.

Kovarik, Z., Radić, Z., Berman, H. A., Vera, S.-R., Reiner, E. and Taylor, P. (2004). Mutant cholinesterases possessing enhanced capacity for reactivation of their phosphonylated conjugates. *Biochemistry* **43**, 3222–3229.

Kryger, G., Silman, I. and Sussman, J. L. (1998). Three-dimensional structure of a complex of E2020 with acetylcholinesterase from Torpedo californica. *J. Physiol.* **92**, 191–194.

Muñoz-Quezada, M. T., Lucero, B. A., Barr, D. B., Steenland, K., Levy, K., Ryan, P. B., Iglesias, V., Alvarado, S., Concha, C., Rojas, E., et al. (2013). Neurodevelopmental effects in children associated with exposure to organophosphate pesticides: a systematic review. *Neurotoxicology* **39**, 158–168.

Nicolet, Y., Lockridge, O., Masson, P., Fontecilla-Camps, J. C. and Nachon, F. (2003). Crystal structure of human butyrylcholinesterase and of its complexes with substrate and products. *J. Biol. Chem.* **278**, 41141–41147.

Nishimura, K., Kitamura, Y., Taniguchi, T. and Agata, K. (2010). Analysis of motor function modulated by cholinergic neurons in planarian Dugesia japonica. *Neuroscience* **168**, 18–30.

Ohbu, S., Yamashina, A., Takasu, N., Yamaguchi, T., Murai, T., Nakano, K., Matsui, Y., Mikami, R., Sakurai, K. and Hinohara, S. (1997). Sarin poisoning on Tokyo subway. *South. Med. J.* **90**, 587–593.

Okumura, T., Takasu, N., Ishimatsu, S., Miyanoki, S., Mitsuhashi, A., Kumada, K., Tanaka, K. and Hinohara, S. (1996). Report on 640 victims of the Tokyo subway sarin attack. *Ann. Emerg. Med.* **28**, 129–135.

Pancetti, F., Olmos, C., Dagnino-Subiabre, A., Rozas, C. and Morales, B. (2007). Noncholinesterase effects induced by organophosphate pesticides and their relationship to cognitive processes: implication for the action of acylpeptide hydrolase. *J. Toxicol. Environ. Heal. Part B Crit. Rev.* **10**, 623–630.

Pezzementi, L. and Chatonnet, A. (2010). Evolution of cholinesterases in the animal kingdom. *Chem. Biol. Interact.* **187**, 27–33.

Pezzementi, L., Nachon, F. and Chatonnet, A. (2011). Evolution of acetylcholinesterase and butyrylcholinesterase in the vertebrates: An atypical butyrylcholinesterase from the medaka Oryzias latipes. *PLoS One* **6**, e17396.

Pezzementi, L., Geiss, C., King, W., Lenfant, N. and Chatonnet, A. (2015). Molecular characterization of an acetylcholinesterase from the hemichordate Saccoglossus kowalevskii. *Comp. Biochem. Physiol. Part B* **181**, 50–58.

Pope, C. N. (1999). Organophosphorus pesticides: do they all have the same mechanism of toxicity? *J. Toxicol. Environ. Heal. Part B Crit. Rev.* **2**, 161–181.

Pope, C., Karanth, S. and Liu, J. (2005). Pharmacology and toxicology of cholinesterase inhibitors: uses and misuses of a common mechanism of action. *Environ. Toxicol. Pharmacol.* **19**, 433–46.

Quinn, D. M. (1987). Acetylcholinesterase: enzyme structure, reaction dynamics, and virtual transition states. *Chem. Rev.* **87**, 955–979.

Radić, Z., Pickering, N. A., Vellom, D. C., Camp, S. and Taylor, P. (1993). Three distinct domains in the cholinesterase molecule confer selectivity for acetyl- and butyrylcholinesterase inhibitors. *Biochemistry* **32**, 12074–12084.

Radić, Z., Sit, R. K., Kovarik, Z., Berend, S., Garcia, E., Zhang, L., Amitai, G., Green, C., Radić, B., Fokin, V. V, et al. (2012). Refinement of structural leads for centrally acting oxime reactivators of phosphylated cholinesterases. *J. Biol. Chem.* **287**, 11798–11809.

Radić, Z., Sit, R. K., Garcia, E., Zhang, L., Berend, S., Kovarik, Z., Amitai, G., Fokin, V. V, Sharpless, K. B. and Taylor, P. (2013). Mechanism of interaction of novel uncharged, centrally active reactivators with OP-hAChE conjugates. *Chem. Biol. Interact.* **203**, 67–71.

Reiner, E. and Radić, Z. (2000). Mechanism of action of cholinesterase inhibitors. In *Cholinesterases and Cholinesterase Inhibitors* (ed. Giacobini, E.), pp. 103–120. London: Martin Dunitz Ltd.

Rosenberry, T. L. (1975). Acetylcholinesterase. *Adv. Enzymol. Relat. Areas Mol. Biol.* **43**, 103–218.

Russom, C. L., LaLone, C. A., Villeneuve, D. L. and Ankley, G. T. (2014). Development of an adverse outcome pathway for acetylcholinesterase inhibition leading to acute mortality. *Environ. Toxicol. Chem.* **33**, 2157–2169.

Sanders, M., Mathews, B., Sutherland, D., Soong, W., Giles, H. and Pezzementi, L. (1996). Biochemical and molecular characterization of acetylcholinesterase from the hagfish Myxine glutinosa. *Comp. Biochem. Physiol. , Part B Biochem. Mol. Biol.* **115**, 97–109.

Schmidt, H. R., Radić, Z., Taylor, P. and Fradinger, E. A. (2015). Quaternary and tertiary aldoxime antidotes for organophosphate exposure in a zebrafish model system. *Toxicol. Appl. Pharmacol.* **284**, 197–203.

Schumacher, M., Camp, S., Maulet, Y., Newton, M., MacPhee-Quigley, K., Taylor, S. S., Friedmann, T. and Taylor, P. (1986). Primary structure of Torpedo californica acetylcholinesterase deduced from its cDNA sequence. *Nature* **319**, 407–409.

Shelton, J. F., Geraghty, E. M., Tancredi, D. J., Delwiche, L. D., Schmidt, R. J., Ritz, B., Hansen, R. L. and Hertz-Picciotto, I. (2014). Neurodevelopmental disorders and prenatal residential proximity to agricultural pesticides: the CHARGE study. *Environ. Health Perspect.* **122**, 1103–9.

Sit, R. K., Radić, Z., Gerardi, V., Zhang, L., Garcia, E., Katalinić, M., Amitai, G., Kovarik, Z., Fokin, V. V, Sharpless, K. B., et al. (2011). New structural scaffolds for centrally acting oxime reactivators of phosphylated cholinesterases. *J. Biol. Chem.* **286**, 19422–19430.

Sussman, J. L., Harel, M., Frolow, F., Oefner, C., Goldman, A., Toker, L. and Silman, I. (1991). Atomic structure of acetylcholinesterase from Torpedo californica: a prototypic acetylcholine-binding protein. *Science (80-.).* **253**, 872–879.

Taylor, P. (2017). Anticholinesterase agents. In *Goodman and Gilman's The Pharmacological Basis of Therapeutics* (ed. Laurence L Brunton), pp. 239–254. McGraw Hill.

Taylor, P. and Lappi, S. (1975). Interaction of fluorescence probes with acetylcholinesterase. The site and specificity of propidium binding. *Biochemistry* **14**, 1989–1997.

Taylor, P. and Radić, Z. (1994). The cholinesterases: from genes to proteins. *Annu. Rev. Pharmacol. Toxicol.* **34**, 281–320.

Taylor, P., Radić, Z., Hosea, N. A., Camp, S., Marchot, P. and Berman, H. A. (1995). Structural bases for the specificity of cholinesterase catalysis and inhibition. *Toxicol. Lett.* **82**–**83**, 453–458.

Vellom, D. C., Radić, Z., Li, Y., Pickering, N. A., Camp, S. and Taylor, P. (1993). Amino acid residues controlling acetylcholinesterase and butyrylcholinesterase specificity. *Biochemistry* **32**, 12–17.

Zheng, D.-M., Xie, H.-Q., Wang, A.-T. and Wu, C.-C. (2011). The nerve system identificiation by histochemical localization of acetylcholinesterase in planarian Dugesia japonica. *Chinese*

J. Zool. **45**, 68–75.

Chapter 6: Planarian cholinesterase: molecular and functional characterization of an evolutionarily ancient enzyme to study organophosphorus pesticide toxicity

Reprinted from: Hagstrom, Danielle; Zhang, Siqi; Ho, Alicia; Tsai, Eileen S.; Radić, Zoran; Jahromi, Aryo; Kaj, Kelson J.; He, Yingtian; Taylor, Palmer; and Collins, Eva-Maria S. "Planarian cholinesterase: molecular and functional characterization of an evolutionarily ancient enzyme to study organophosphorus pesticide toxicity", Archives of Toxicology, vol. 92, 2018. Supplementary materials can be accessed online at: https://link.springer.com/article/10.1007%2Fs00204-017-2130-7

ABSTRACT

The asexual freshwater planarian *Dugesia japonica* has emerged as a medium-throughput alternative animal model for neurotoxicology. We have previously shown that *D. japonica* are sensitive to organophosphorus pesticides (OPs) and characterized the *in vitro* inhibition profile of planarian cholinesterase (DjChE) activity using irreversible and reversible inhibitors. We found that DjChE has intermediate features of acetylcholinesterase (AChE) and butyrylcholinesterase (BChE). Here, we identify two candidate genes (*Djche1* and *Djche2)* responsible for DjChE activity. Sequence alignment and structural homology modeling with representative vertebrate AChE and BChE sequences confirmed our structural predictions, and show that both DjChE enzymes have intermediate sized catalytic gorges and disrupted peripheral binding sites. *Djche1* and *Djche2* were both expressed in the planarian nervous system, as anticipated from previous activity staining, but with distinct expression profiles. To dissect how DjChE inhibition affects planarian behavior, we acutely inhibited DjChE activity by exposing animals to either an OP (diazinon) or carbamate (physostigmine) at 1µM for 4 days. Both inhibitors delayed the reaction of planarians to heat stress. Simultaneous knockdown of both *Djche* genes by RNAi similarly resulted in a delayed heat stress response. Furthermore, chemical inhibition of DjChE activity increased the worms' ability to adhere to a substrate. However, increased substrate adhesion was not observed in *Djche1/Djche2 (RNAi)* animals or in inhibitor-treated day 11 regenerates, suggesting this phenotype may be modulated by other mechanisms besides ChE inhibition. Together, our study characterizes DjChE expression and function, providing the basis for future studies in this system to dissect alternative mechanisms of OP toxicity.

INTRODUCTION

Organophosphorus pesticides (OP) are among the most agriculturally important and common pesticides used today. In the United States, 20 million pounds of OPs were used in 2012, accounting for 33% of all insecticides used (Atwood and Paisley-Jones, 2017). Similarly, in 2014, Spain, France, Italy, Germany, and Poland, which together make up 72.7% of the European Union's pesticide sales (EUROSTAT, 2016), had a combined usage of 4642 tonnes (~10 million pounds) of OPs according to the Food and Agriculture Organization of the United Nations (http://www.fao.org/faostat/en/#data/RP). The primary shared mode of action of these pesticides is to inhibit the enzyme acetylcholinesterase (AChE), an essential regulator of cholinergic nerve transmission (King and Aaron, 2015; Russom et al., 2014; Taylor, 2017). Inhibition of AChE, which catalyzes the hydrolysis of the neurotransmitter acetylcholine (ACh), results in increased levels of synaptic ACh and subsequent overstimulation of nicotinic and muscarinic ACh receptors. Cholinergic toxicity is clinically manifested by decreased heart and respiration rates, increased secretions (sweating, lacrimation, and salivation), muscle tremors, and eventually paralysis and death (Eleršek and Filipic, 2011; King and Aaron, 2015; Russom et al., 2014; Taylor, 2017). Because of its key role in regulating cognitive, peripheral autonomic, and somatic motor functions, AChE is also a common pharmacological target. For example, Alzheimer's disease, glaucoma, and myasthenia gravis have been treated with carbamate AChE inhibitors, such as physostigmine, and OPs, such as phospholine (echothiophate) iodide (Giacobini, 2000; Pope et al., 2005; Taylor, 2017).

At high doses, OPs are lethal to both insects and humans due to inhibition of AChE and subsequent cholinergic toxicity. However, there have been growing concerns that chronic, low dose exposure to these pesticides can also cause harm. Epidemiological studies have suggested a

correlation between pesticide exposure and neurodegenerative diseases (Sánchez-Santed et al., 2016). Similar correlations have also been found linking prenatal and early life OP exposure to cognitive impairment in children (González-Alzaga et al., 2014; Muñoz-Quezada et al., 2013; Shelton et al., 2014).

In addition to inhibiting AChE function, studies have suggested that some chronic (Ray and Richards, 2001; Terry, 2012) and/or developmental (Timofeeva et al., 2008a; Timofeeva et al., 2008b) toxic outcomes may be independent of OPs' effects on AChE. This idea is corroborated by findings in *in vivo* and *in vitro* rat studies showing that OPs can have effects on a variety of cellular processes, such as cell signaling, oxidative stress, and axonal growth, at concentrations which do not significantly inhibit AChE (Slotkin and Seidler, 2007; Yang et al., 2008). However, the degree that these secondary effects relate to specific toxic endpoints remains unclear.

ACh can also act as a neuromodulator to dynamically regulate the state of neurons, including but not limited to cholinergic neurons, in response to changing conditions (Picciotto et al., 2012). For example, feedback loops exist to regulate the levels of ACh synthesis, release, uptake, and receptor binding. Thus, chronic exposure to OPs may trigger compensatory mechanisms to adapt to chronically elevated Ach levels. The extent that adaptive mechanisms modulate specific toxic outcomes, and whether these mechanisms can be affected by secondary effects of OPs (Pope et al., 2005), warrant further investigation.

The freshwater planarian *Dugesia japonica* has recently emerged as a valuable *in vivo* model for neurotoxicity studies, with particular focus on neurodevelopment (Hagstrom et al., 2015; Hagstrom et al., 2016). This asexual species naturally reproduces through transverse fission. Herein, the worm splits itself into two pieces which, due to a large population of adult

stem cells (Rink, 2013), subsequently regenerate all missing body structures, including the central nervous system (CNS). In these animals, regeneration is the sole mechanism of neurodevelopment and shares fundamental processes with vertebrate neurodevelopment (Cebrià and Newmark, 2005; Cebrià et al., 2002a; Cebrià et al., 2002b; Cowles et al., 2013; Umesono et al., 2011). Distinct from other animal models, the similar sizes of full and regenerating planarians allows for a direct comparison of the effects of neurotoxicants on brain development and function with the same behavioral assays (Hagstrom et al., 2015; Hagstrom et al., 2016). Using a custom planarian screening platform (Hagstrom et al., 2015), we showed that planarians are sensitive to OPs as subchronic exposure to sublethal concentrations of dichlorvos (10-500nM) caused reduced rates of locomotion, with greater effects on regenerating rather than adult animals.

Furthermore, using activity measurements in planarian homogenates, we have recently demonstrated that planarian cholinesterase, DjChE, has intermediate characteristics of AChE and the closely related butyrylcholinesterase (BChE) (Hagstrom et al., 2017). Moreover, DjChE underwent similar rates of inhibition by OPs and carbamates as mammalian AChE, suggesting similar levels of sensitivity. We predicted that the enzyme(s) responsible for DjChE activity would be defined by a conserved catalytic triad and choline binding site, an active site gorge that is larger than that of AChE but smaller than BChE, and a disrupted peripheral anionic site. However, these predictions remained to be verified through structural analysis, and the *in vivo* expression profile of the enzyme(s) was unknown. Moreover, a direct link between *in vivo* inhibition of DjChE activity and the functional consequences on planarian behavior is still missing. Herein, we verify our *in vitro* predictions by identifying and characterizing the expression and function of two candidate genes responsible for DjChE activity *in vivo*.

Using RNA interference (RNAi), we further compared the effects of simultaneous knockdown of both *Djche* genes with those induced by ChE inhibitors (diazinon and physostigmine) on planarian locomotion, the animals' response to heat stress, and substrate adhesion. These endpoints were chosen based on our previous results that OPs can cause decreased planarian locomotion (Hagstrom et al., 2015), findings in nematodes that increased Ach levels caused heat stress tolerance (Furuhashi and Sakamoto, 2016), and the use of hyper-secretions as one of the clinical hallmarks of cholinergic toxicity (Eleršek and Filipic, 2011; Taylor, 2017). Comparison of acute and subchronic developmental exposure of these endpoints suggests the existence of secondary effects on non-ChE targets to modulate the functional outcomes of OP toxicity.

Together, we structurally and functionally characterize DjChE and demonstrate a direct link between *in vivo* inhibition of DjChE activity and functional consequences on planarian behavior. This work therefore lays the foundation for the dissection of the mechanisms underlying OP toxicity in planarians.

MATERIALS AND METHODS

Planarian culture

Freshwater asexual planarians of the species *Dugesia japonica* were used for all experiments. For behavioral experiments, animals used were 5.4 ± 1.1 mm (mean ± standard deviation) in length. Planarians were maintained in 1x Instant Ocean (IO, Blacksburg, VA) in Tupperware containers at 20°C in a Panasonic refrigerated incubator in the dark. Animals were fed organic chicken or beef liver 1-2x/week and cleaned twice a week when not used for experiments. Animals were starved for at least 5 days before experiments.

Identification and cloning of Djche

D. japonica homologs of acetylcholinesterase (AChE) were found using NCBI tBLASTn to query the deduced amino acid sequence of *Schistosoma mansoni* AChE (GenBank AAQ14321.1) (Bentley et al., 2003) against a *D. japonica* transcriptome. The transcriptome was assembled *de novo* from published sequencing data (Qin et al., 2011) using EBARDenovo (Chu et al., 2013). Two potential *ache* homologs were identified in *D. japonica* and crosschecked against the ESTHER protein database (Lenfant et al., 2013) to align most closely with acetylcholinesterase. Since we recently determined that *D. japonica* cholinesterase activity has characteristics of a hybrid AChE/BChE (Hagstrom et al., 2017), we termed these candidate sequences as *Djche1* and *Djche2*. The deduced amino acid sequences were determined from the longest open reading frame found using NCBI ORF finder (https://www.ncbi.nlm.nih.gov/orffinder/). Sequence alignments were performed in JalView (Waterhouse et al., 2009).

RNA was extracted from recently amputated *D. japonica* head fragments using an RNeasy Mini Kit (Qiagen, Germantown, MD). Head cDNA was created using a SuperScript III

First Strand Synthesis Reverse Transcriptase Kit (Invitrogen, Carlsbad, CA). Approximately 700 and 1000 bp fragments of *Djche1* and *Djche2*, respectively, were amplified from this cDNA by PCR using the following primers: Djche1_F: TCGAAACGCTATAATGGAATCCG, Djche1_R: AGGTTGGCAATGTTACTGTACG, Djche2_F: TTGGCAAGCTGATGGAAGTG, Djche2_R: CCAGCCGGTTATAGTTGAAGG. These fragments were subsequently cloned into the pPR-T4P vector.

Homology modeling of DjChE structure

Individual amino acid sequences of the two candidate DjChEs were submitted to Swiss-Model, a homology based 3D structure creation server (https://swissmodel.expasy.org/). The server searched its template library for evolutionary related structures matching the target sequence resulting in identification of several hundred potential templates. Template quality has been predicted from features of the target-template alignment and three of those with the highest quality were then selected for model building (Arnold et al., 2006; Benkert et al., 2011; Biasini et al., 2014). For both DjChE structures, *Torpedo californica* AChE was selected as the template (2cek and 2w6c, respectively). For comparisons in Figure 6.2, the 2w6c structure is shown. Additional details on model building can be found in Supplementary Materials.

In situ hybridization

Anti-sense digoxigenin (DIG) or fluorescein labeled probes were synthesized using T7 RNA polymerase essentially as described in (King and Newmark, 2013). Planarian fixation and subsequent *in situ* hydridization were performed as in (King and Newmark, 2013) with a few modifications: initial mucus removal was performed by treating with 2% hydrochloric acid in phosphate buffered saline (PBS) for 45 seconds with hand-inversion; animals were bleached overnight in 6% hydrogen peroxide in methanol under bright white light and subsequently

rehydrated in 50% MeOH/50% PBSTx (0.3% Triton-X 100 in PBS); and hybridization was performed at 60ºC overnight.

For co-localization experiments, a double fluorescent *in situ* hybridization (FISH) was performed using a combined POD-based tyramide development and AP-based Fast Blue development (Brown and Pearson, 2015). Briefly, hybridization was performed concurrently with both DIG- and fluorescein-labeled riboprobes. Following post-hybridization washes, the samples were blocked in 5% horse serum and 0.5% Roche Western Blocking Reagent (RWBR, Roche, Indianapolis, IN) in MABT (150mM NaCl, 100mM Maleic Acid, 0.1% Tween 20, pH 7.5) at room temperature for 3-4 hours and treated overnight at 4˚C with a mix of anti-fluorescein-POD and anti-DIG-AP antibodies (both from Roche and diluted 1:2000 in 5% horse serum/0.5% RWBR). Following fluorescein tyramide development of the POD antibody, the samples were washed four times for 5-10 minutes with MABT. An AP-based Fast Blue development was then performed for colorimetric and fluorescent (far red) detection of the DIG-labeled riboprobe, as described in (Brown and Pearson, 2015). Samples were mounted on glass slides and imaged on an inverted IX81 spinning disc confocal microscope (Olympus DSU) using an ORCA-ER camera (Hamamatsu Photonics) and Slidebook software (version 5, Intelligent Imaging Innovations, Inc).

Chemical Exposure

To analyze the effects of inhibition of ChE catalytic activity, planarians were exposed to 1μM physostigmine (eserine) or diazinon (both from Sigma-Aldrich, Saint Louis, MO). These concentrations were chosen because preliminary experiments determined they were not systemically toxic or lethal. Lack of systemic toxicity was demonstrated by the absence of lethality or morphological abnormalities for up to 12 days of exposure (Supplementary Figure

S1) and by the absence of regeneration delays (Supplementary Figure S4). Exposure solutions were prepared in IO water from 200X stocks solution in dimethyl sulfoxide (DMSO, Sigma-Aldrich) to have a final concentration of 0.5% DMSO. While others have suggested DMSO concentrations used with planarians should not exceed 0.1% (Pagán et al., 2006), we found 0.5% did not have a significant effect on planarian behavior (Hagstrom et al., 2015). Control animals were treated with 0.5% DMSO. Solutions were replaced daily to keep concentrations constant. During exposure, worms were kept in 12-well plates (Genesee, San Diego, CA) containing one worm and 1ml of chemical per well and stored in the dark at room temperature. Gliding and heat stress assays were performed on day 4 of exposure and stickiness assays on day 5. For experiments with regenerating animals, intact planarians were decapitated with an ethanol-sterilized razor blade. The tail pieces were placed in 12-well plates and exposed to inhibitor solutions within 1 hour of amputation. Gliding and heat stress assays were performed on day 11 of exposure/regeneration and stickiness assays on day 12. Experiments were performed in IO water.

Cholinesterase activity assays

Qualitative detection of ATCh or BTCh catalysis in fixed worms was performed as previously described (Hagstrom et al., 2017; Zheng et al., 2011), except staining incubation was decreased to 3.5 hours to gain the sensitivity needed to detect differences in activity in inhibitor-treated and knockdown animals.

To quantify the extent of ChE inhibition in inhibitor-treated planarians, 30 planarians were exposed to either 0.5% DMSO, 1μM diazinon, or 1μM physostigmine for 5 or 12 days, as described above. At the end of exposure, the planarians were washed three times with IO water and homogenized in 100μl 1% Triton X-100 (Sigma-Aldrich) in PBS as previously described

(Hagstrom et al., 2017). Levels of acetylthiocholine (ATCh) catalysis (ChE activity) were determined by an Ellman assay (Ellman et al., 1961) using 1mM ATCh (Sigma-Aldrich) as a substrate, as previously described (Hagstrom et al., 2017). Activity measurements were performed with at least 3 technical replicates per condition. Activity levels were normalized by protein concentration, determined by a Bradford Assay, and compared to the mean of the normalized levels in the DMSO controls in the same experiment (set as 100% activity). Data are shown as the mean and standard deviation of two independent experiments (biological replicates).

RNA interference (RNAi) experiments

Expression of *Djche1* and *Djche2* were knocked down in combination by feeding planarians organic chicken liver mixed with *in vitro* transcribed dsRNA mixed with food coloring, per standard protocols (Rouhana et al., 2013). Negative control populations, denoted as *control (RNAi)*, were fed organic chicken liver mixed with dsRNA of the *unc22* gene, a non-homologous *C. elegans* gene. All RNAi treated populations were fed twice per week and cleaned three times per week. To speed up knock down, some RNAi worms were injected directly with the respective dsRNA (1μg/μl per gene). Injections were performed on intact animals daily for 4 consecutive days (Takano et al., 2007) using a Pneumatic PicoPump, Model PV 820 (World Precision Instruments, Sarasota, FL). One day after the last injection, the planarians were decapitated using an ethanol-sterilized razor blade. Animals were allowed to regenerate for 11 days before behavioral analysis.

Behavioral assays

Gliding

Six contact lens containers (Wöhlk Contactlinsen, Schönkirchen, Germany) containing one planarian each and 1.5 mL IO water were placed on a LED panel (Amazon, Seattle, WA). The planarians were allowed to glide undisturbed for 10 minutes while imaging from above using a Basler camera (A601f-2, Basler, Germany), mounted on a ring stand. Assays were typically run with n=12 (2 sets of 6) animals per experiment for each condition. At least 2 independent experiments were run per condition. Gliding movies were analyzed as previously described in detail in (Hagstrom et al., 2015).

Heat stress

A single planarian was pipetted into 2 mL IO water into a 35 mm petri dish (CELLTREAT Scientific Products, Pepperell, MA). Of note, we also tried Falcon (Corning, NY) 35 mm petri dishes, but found that planarians in the CELLTREAT brand were easier to image because they spent relatively less time at the container edges. To create a high temperature environment, we used a peltier plate (TE Technology Inc., Traverse City, MI), which was controlled by a temperature controller (TE Technology, Inc.) and powered by an AC to DC power supply (Amazon). The plate was set to 52ºC and six dishes, with one planarian each, were heated for 10 minutes starting from room temperature. Thermistors were used to determine the dynamics of the aquatic temperature in the dishes over the course of the experiment (Supplementary Figure S2). The aquatic temperature stabilized after about 3 minutes to 30ºC and was consistent across all dishes and across multiple trials. The dishes were imaged from above using a Basler camera mounted to a ring stand. Lighting was provided via a red LED string light (Amazon) from above and surrounding the edges of the peltier. Assays were typically run with

n=12 (2 sets of 6) animals per experiment and condition. At least 2 independent experiments were run per condition.

Analysis was performed using a custom MATLAB center-of-mass (COM) tracking script. The displacement of each worm across 12 second intervals was calculated in MATLAB. Displacement was scaled by body length and displacements under 1 body length were empirically determined to correspond to movements which were primarily body shape changes. The proportion of displacements under 1 body length to all tracked displacements was determined and binned across one minute intervals. The median value for each condition is shown, with error bars representing the 25 and 75% quantiles.

Worm Substrate Adhesion ("Stickiness")

The stickiness of planarians was determined based on the worms' ability to adhere to a substrate as described in (Malinowski et al., 2017). In brief, an individual planarian was placed into a 3D printed plastic arena filled with 25ml of IO water and allowed to acclimate for approximately 2 mins. We then introduced a water flow and tested whether it was able to displace the worm from a fixed distance (~ 25mm). If displaced, the current flow rate was recorded with a Hall sensor (Amazon). If not displaced, the flow rate would be increased in discrete steps until displacement occurred.

Regeneration assay

The rate of blastema growth was determined as described in (Hagstrom et al., 2015). For chemical treatment, exposure began immediately (within 1 hour) after decapitation.

Statistical Analysis

Since all data for gliding, heat stress, and substrate adhesion experiments were not normally distributed, statistical analysis was done using the Wilcoxon rank sum test (Mann Whitney test) in MATLAB.

RESULTS

D. japonica has two candidate genes encoding cholinesterase

We assembled a *D. japonica* transcriptome *de novo* using published sequencing data (Qin et al., 2011) as described in Materials and Methods. Two putative transcripts encoding cholinesterase were found using NCBI tBLASTn to query the deduced amino acid sequence of *Schistosoma mansoni* AChE (GenBank AAQ14321.1) (Bentley et al., 2003) against the *D. japonica* transcriptome. We named the two corresponding candidate genes *Djche1* and *Djche2.* The deduced amino acid sequences of these genes were aligned with representative amino acid sequences for vertebrate AChE and BChE from *Torpedo californica* (TcAChE) and human (HsBChE), respectively (Figure 6.1).

Both DjChE amino acid sequences contain essential catalytic residues for cholinesterase function, including the esterase-type catalytic triad (Ser200, Glu327, His440, numbering corresponding to TcAChE, per convention) and choline binding site (Trp84, Glu199, Phe330, Phe331). In agreement with our predictions based on *in vitro* inhibitor data (Hagstrom et al., 2017), both DjChE sequences seem to have intermediate characteristics between AChE and BChE (acyl pocket consisting of one phenylalanine, and an undefined peripheral anionic site at the rim of the gorge).

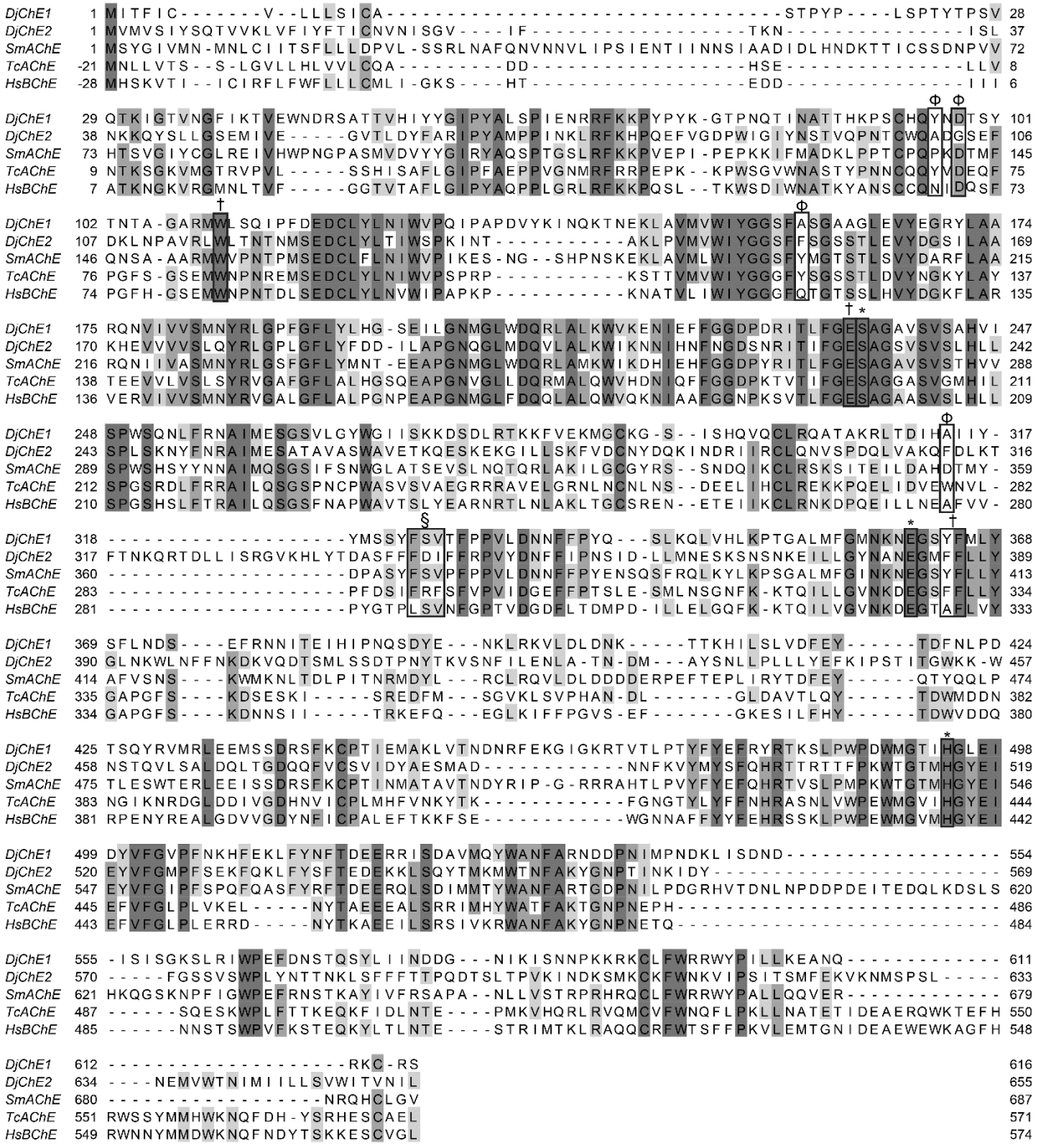

Figure 6.1. Candidate DjChEs show characteristics of both AChE and BChE. Alignment of deduced amino acid sequences of DjChE1 and DjChE2 with a representative vertebrate AChE (TcAChE), vertebrate BChE (HsBChE), and AChE from a related parasitic flatworm, *S. mansoni* (SmAChE). Note: for TcAChE and HsBChE, the leader signal peptide is shown but is not included in the numbering since it is not found in the mature polypeptides. Shading indicates level of conservation. Important structural residues are boxed and labeled: catalytic triad (*), acyl pocket (§), choline binding site (†), and peripheral anionic site (ϕ).

We further evaluated the protein structure of the candidate planarian cholinesterases by performing homology modeling using the published structure of TcAChE (Paz et al., 2009) (Figure 6.2, Supplementary Material). The homology-based structures of DjChE1 and DjChE2 similarly agree with our previous structural predictions (Hagstrom et al., 2017). Particularly, in both DjChE1 and DjChE2 structures, the catalytic triad and choline binding site are well conserved. Conversely, with only one (F288) of two commonly found phenylalanines and the substitution of the Arg289 "anchor" with a smaller side chain, the acyl pocket volume is much larger and more flexible than that of TcAChE. Lastly, several of the largely aromatic residues that define the vertebrate peripheral anionic site (Tyr70, Asp72, Tyr 121, Trp279) have been substituted with smaller aliphatic side chains in the planarian structures resulting in a wider gorge opening. In summary, both planarian cholinesterase candidate genes have hybrid features of both AChE and BChE, similar to other invertebrate cholinesterase (see Discussion) (Bentley et al., 2005; Pezzementi et al., 2011; Sanders et al., 1996).

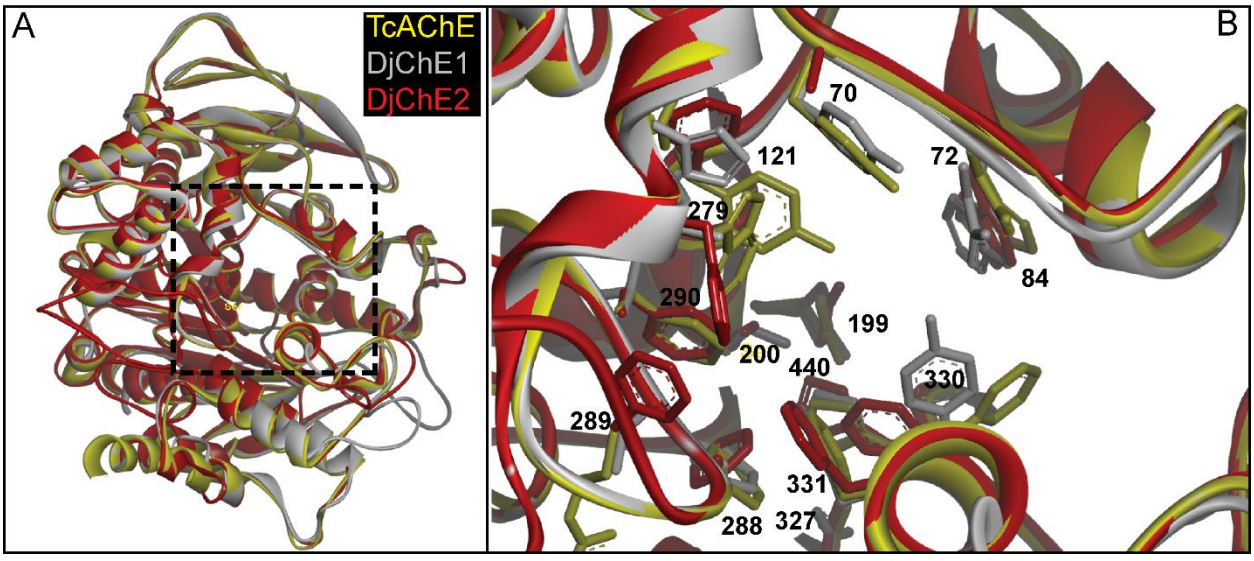

Figure 6.2. Homology modeling of planarian cholinesterase protein structure. (A) Whole protein structures of DjChE1 (grey) and DjChE2 (red) are overlaid with TcAChE (2w6c, yellow). Boxed area denotes the catalytic gorge. (B) Magnified view of boxed area in A. Important structural residues are labeled, with numbering based on TcAChE.

Djche1 and 2 are expressed in the planarian nervous system

Whole-mount fluorescent *in situ* hybridization (FISH) was performed to determine the expression patterns of *Djche1* and *Djche2* (Figure 6.3). Similarly to the cholinergic marker, *Djchat* (Figure 6.3A), *Djche1* is expressed widely throughout the planarian nervous system in both the anterior cephalic ganglion and ventral nerve cords (Figure 6.3B). This mRNA expression profile agrees with cholinesterase activity stains which have shown cholinesterase enzymatic activity distributed throughout the planarian CNS (Hagstrom et al., 2017). *Djche2,* however, was found to be more ubiquitously expressed throughout the planarian body in a punctate pattern, with concentration of some puncta in the head region and along the nerve cords (Figure 6.3C).

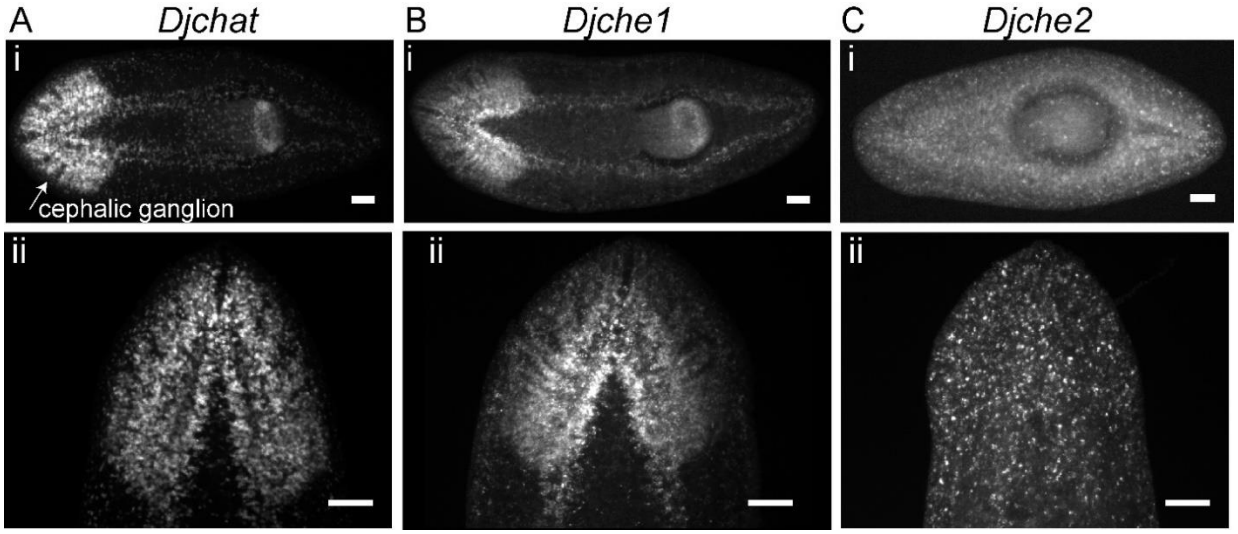

Figure 6.3. Planarian cholinesterases are expressed in the nervous system. Fluorescent *in situ* hybridization of *Djchat* (A), *Djche1* (B), and *Djche2* (C) showing the whole animal (i) or a maximum intensity projection of multiple planes in the head region (ii). Scale bars: 100μm.

Next, we performed multi-color FISH to determine the extent that these important regulators of the cholinergic system co-localize (Figure 6.4). As expected from the single FISH, expression of *Djche1* extensively overlapped with expression of *Djchat* (Figure 6.4A). *Djche2*

also showed partial co-localization with both *Djchat* and *Djche1*, particularly in the medial arc of the cephalic ganglion (Figure 6.4B-C).

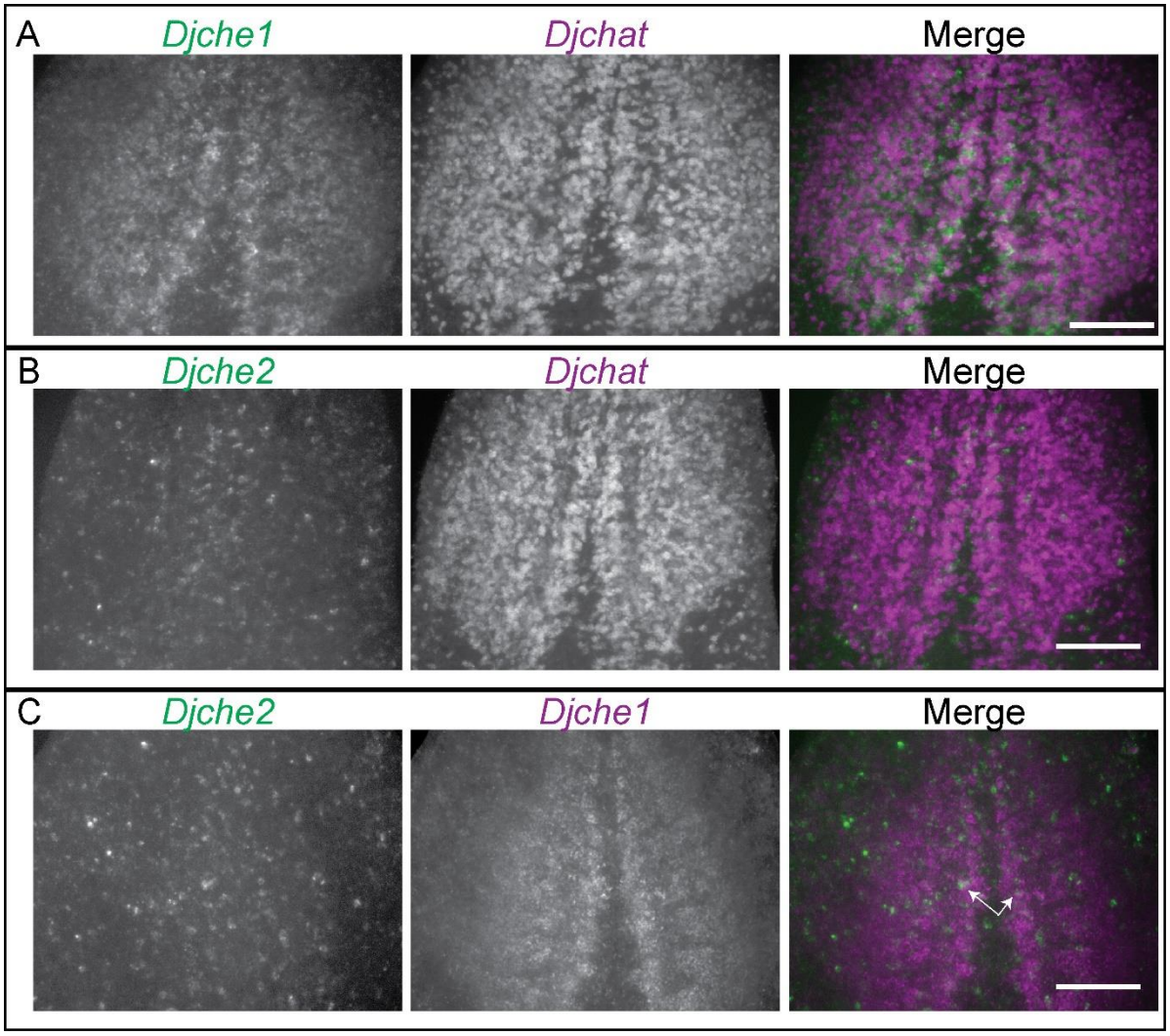

Figure 6.4. Planarian cholinesterases co-localize with each other and *Djchat* in the medial arc of the brain. Multicolor FISH for (A) *Djche1* (green) and *Djchat* (magenta), (B) *Djche2* (green) and *Djchat* (magenta), and (C) *Djche2* (green) and *Djche1* (magenta)**.** Co-localization is indicated by a lighter color where the two channels overlap. Arrows denote examples of co-localization in the medial arc domain. Scale bars: 100μm.

Inhibition of cholinesterase activity decreases sensitivity to heat stress

It has been previously shown in the nematode *Caenorhabditis elegans* that exogenous ACh exposure promotes thermo-tolerance. In these experiments, worms pre-cultured for 24

hours on plates containing ACh solution demonstrated increased survivability compared to controls after 10h incubation at 35°C (Furuhashi and Sakamoto, 2016). Therefore, we assayed whether inhibition of ChE, which would increase synaptic ACh levels, affects planarians' response to heat stress. To this end, the animals' aquatic environment was slowly heated from room temperature to 30°C (Supplementary Figure S2) and the animals' reactions were monitored through video recordings (see Materials and Methods). Being higher than planarians' normal comfortable temperature range, 15-25 °C (Inoue et al., 2014), 30°C should induce heat stress while not induce scrunching, a planarian escape gait induced at 34-36°C (Cochet-Escartin et al., 2015). Solvent control animals (treated with 0.5% DMSO) reacted to the heat stress through frequent turns and head flailing, followed by decreased movement and eventual paralysis (Figure 6.5A, Supplemental Video). This reaction was quantified by the fraction of time that the animals exhibited body shape changes rather than normal gliding behavior (see Materials and Methods). In control animals, the fraction of body shape changes gradually increased over time as the temperature rose and leveled out at approximately 0.9 once the temperature plateaued at 30° after 3 minutes (Figure 6.5B).

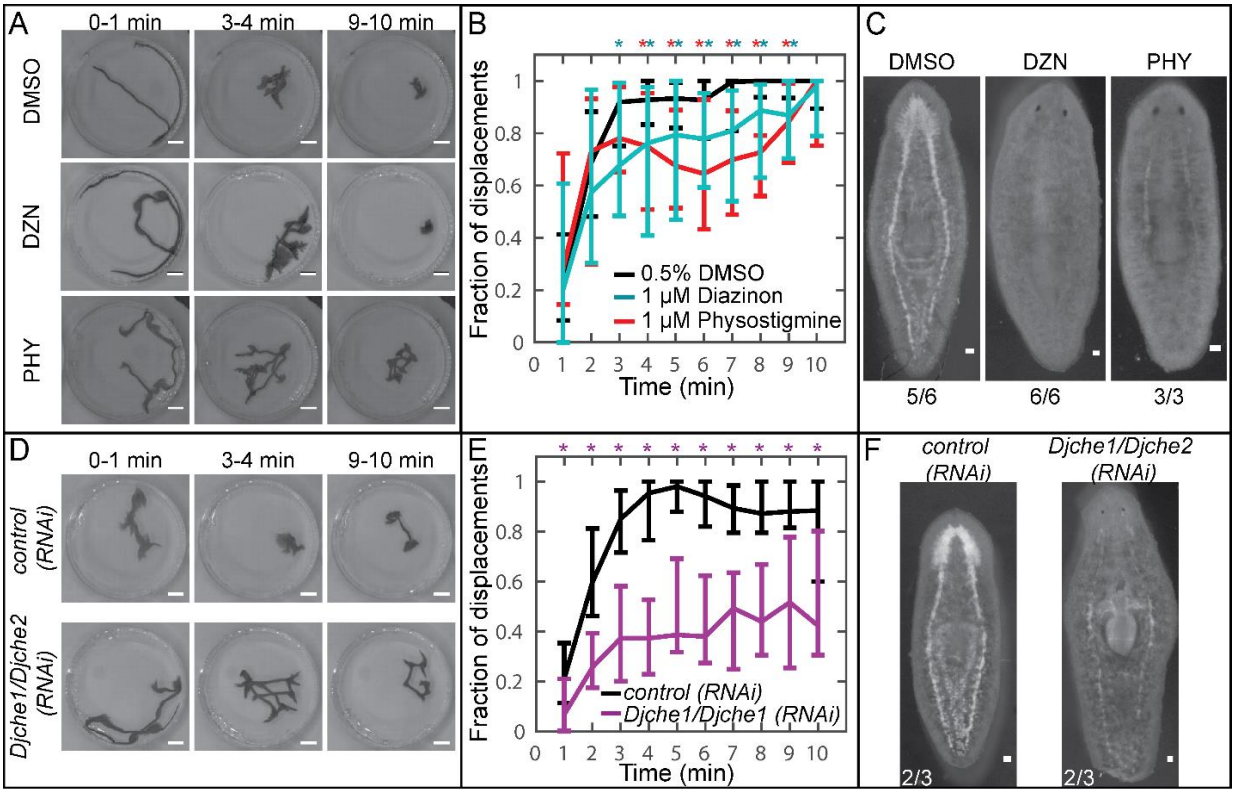

Figure 6.5. Inhibition of DjChE decreases sensitivity to heat stress. (A) Representative minimum intensity projections over 1 minute intervals to show worm tracks of a 0.5% DMSO (DMSO) (top), 1µM diazinon (DZN, middle), and physostigmine (PHY, bottom) treated worm in response to heat stress. Note how during minutes 3-4, the DMSO-treated worm stays in one location with frequent turning (fan-like pattern in track) whereas the DZN and PHY-exposed planarians explore a larger area and have wider turns. (B) Diazinon and physostigmine treated animals undergo fewer and delayed body shape changes (as a fraction of all displacements tracked) than DMSO controls (n= 39, 46, 24 for DMSO, diazinon, and physostigmine, respectively). (C) ChE activity stains show inhibition of DjChE activity in 1µM diazinon and physostigmine treated animals. Numbers indicate how representative the staining is out of the number of animals assayed. (D) Representative minimum intensity projections over 1 minute intervals to show worm tracks of a *control (RNAi)* and *Djche1/Djche2 (RNAi)* animal in response to heat stress. (E) *Djche1/Djche2 (RNAi)* animals undergo fewer and delayed body shape changes (as a fraction of all displacements tracked) than *control (RNAi)* animals (n= 20 and 29 for *control (RNAi)* and *Djche1/Djche2 (RNAi)*, respectively). (F) ChE activity stains show loss of DjChE activity in *Djche1/Djche2 (RNAi)* animals. Numbers indicate how representative the staining is out of the number of animals assayed. Scale bars: 5mm (A, D), 100 µm (C, F). * indicates significant differences at the 5% level.

To acutely inhibit DjChE activity, planarians were treated for 4 days with 1µM diazinon, an OP whose oxon metabolite efficiently inhibits DjChE activity *in vitro* (Hagstrom et al., 2017). Diazinon treated animals exhibited decreased sensitivity to heat stress, manifested in less body shape changes for a longer time (Supplemental Video). They eventually reached control levels

by 10 minutes of heat exposure (Figure 6.5A-B). To determine whether this phenotype was specific to inhibition of ChE activity, we also exposed worms to physostigmine, a carbamate ChE inhibitor that has been previously shown to inhibit planarian ChE activity *in vitro* (Hagstrom et al., 2017). Moreover, acute exposure to at least 3μM physostigmine has been shown to cause planarians to contract (Nishimura et al., 2010). Similarly to diazinon, 4 day exposure to 1μM physostigmine caused a delayed reaction to heat stress (Figure 6.5A-B). Activity stains confirmed that under these exposure conditions, diazinon and physostigmine significantly inhibited DjChE activity (Figure 6.5C). Quantitative measurements of DjChE in homogenates of exposed planarians further confirmed significant inhibition of DjChE compared to solvent controls (Supplementary Figure S3).

To verify that differences in the heat stress response were not due to general motility differences, we assayed the unstimulated locomotion of these animals. At the used concentrations, physostigmine and diazinon caused a significant decrease in gliding speed (Supplementary Figure S4A). Notably, we previously observed a decrease in gliding speed of full planarians after exposure to dichlorvos for 8 days (Hagstrom et al., 2015), suggesting that this may be a shared phenotype of ChE inhibition.

Despite moving at a slower speed, the ChE inhibitor-treated animals had generally higher activity under heat stress than controls. Therefore, the heat stress phenotype is independent of the gliding phenotype.

Knockdown of both Djches causes decreased sensitivity to heat stress

To determine whether the toxic outcomes of the ChE inhibitors were specific to their action on ChE, RNAi was used to simultaneously knockdown expression of both *Djche1* and *Djche2.* At first, RNAi was administered through feeding of dsRNA mixed with chicken liver.

However, this technique remained inefficient at establishing consistent knockdown even after prolonged feedings (greater than 1 year). To increase the efficiency of knockdown, planarians which were previously fed RNAi liver were injected with dsRNA for both genes for 4 consecutive days. The animals were decapitated 1 day after the last injection and allowed to regenerate for 11 days before being assayed for behavioral phenotypes. This protocol was followed, because amputation and subsequent regeneration following dsRNA injection has been shown to increase knockdown efficiency in the newly regenerated tissue in planarians (Takano et al., 2007).

Djche1/Djche2 (RNAi) animals did not display any defects in regeneration when compared to *control (RNAi)* populations (Supplementary Figure S4). However, similarly to chemical inhibition of DjChE activity, *Djche1/Djche2 (RNAi)* animals were less sensitive to heat stress. They underwent dramatically less body shape changes as the temperature increased compared to *control (RNAi)* animals (Figure 6.5D). Although the fraction of body shape changes did gradually increase over time, it never reached the same extent as in *control (RNAi)* animals (Figure 6.5E). In contrast to acute chemical inhibition of DjChE, *Djche1/Djche2 (RNAi)* animals did not display noticeable differences in normal locomotion/gliding speed (Supplementary Figure S4). Knockdown of *Djche1* and *Djche2* mRNA were confirmed by whole-mount ISH (Figure S5). We further confirmed that knockdown of the two putative *Djche* genes is sufficient to functionally knockdown DjChE activity through staining of cholinesterase activity (Figure 6.5F) and an Ellman assay of homogenized RNAi animals (Supplementary Figure S3).

Inhibition but not knockdown of Djche increases worm stickiness

When handling diazinon or physostigmine treated worms, we observed the animals tended to be “stickier” and often adhered to their substrate more strongly than control animals.

Planarians secrete mucus for self-defense and locomotion, the latter of which is accomplished by cilia beating in a layer of secreted adhesive mucus (Martin, 1978). Increased mucus secretion or changes in mucus composition in response to environmental stimuli can increase mucus production (Cochet-Escartin et al., 2015) and the worm's adhesion to its substrate ("stickiness") (Malinowski et al., 2017). To quantify the animals' stickiness, we dispelled a controlled stream of water at the animal and measured the flow rate necessary to dislodge the worm (Malinowski et al., 2017). In agreement with our qualitative assessment of increased stickiness, planarians which had been treated with 1µM diazinon or physostigmine for 5 days required larger flow rates to be dislodged, indicating increased stickiness and adhesion (Figure 6.6A). Of note, although the distributions were significantly different from controls, the stickiness of inhibitor-treated planarians was much more variable than that of controls, possibly due to inter-worm variability in uptake or metabolism.

We next assayed whether *Djche1/Djche2 (RNAi)* animals also displayed increased stickiness to determine if this phenotype is specific to decreased DjChE activity. Unlike animals treated with the chemical inhibitors, *Djche1/Djche2 (RNAi)* animals did not demonstrate increased stickiness compared to *control (RNAi)* animals (Figure 6.6B), suggesting that this effect may be modulated, in part or total, by mechanisms other than solely decreased DjChE activity.

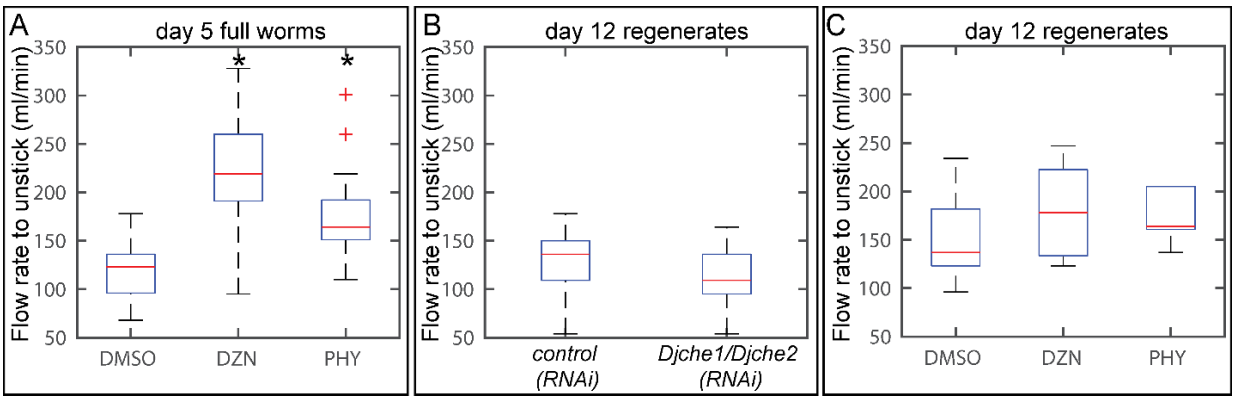

Figure 6.6. Diazinon and physostigmine, but not DjChE knockdown, increase worm adhesion ("stickiness"). Boxplot of the flow rate necessary to unstick worms from a substrate comparing worms exposed for 5 days to either (A) 0.5% DMSO (DMSO, n=46), 1µM diazinon (DZN, n=46), or 1µM physostigmine (PHY, n=23), (B) *control (RNAi)* (n=18) and *Djche1/Djche2 (RNAi)* (n=24) animals, or (C) regenerating tails exposed for 12 days to either 0.5% DMSO (DMSO, n=11), 1µM diazinon (DZN, n=9), or 1µM physostigmine (PHY, n=9). * indicates significant differences at the 5% level.

In summary, while acute chemical inhibition of DjChE activity causes effects on gliding speed, heat stress response, and substrate adhesion, knockdown of *Djche* gene expression only caused effects on the heat stress response. We therefore assayed whether absence of some behavioral effects in *Djche1/Djche2 (RNAi)* animals could be due to adaptation to decreased DjChE activity over time. To this end, we repeated our behavioral analysis on regenerating planarians exposed to either 1µM diazinon or physostigmine for 11-12 days. As with acute chemical inhibition and RNAi treatment, inhibitor-treated regenerating planarians exhibited a less pronounced heat stress response compared to control animals (Supplementary Figure S6) and had substantially less DjChE activity than control animals (Supplementary Figure S3). However, in contrast to acute inhibition, inhibitor-treated regenerating planarians were not significantly stickier than control animals (Figure 6.6C). Particularly for diazinon-treated animals, the flow required to unstick the worms was significantly lower in regenerating animals compared to day 5 full (intact) animals. In addition, inhibitor-treated regenerating animals did not have reduced gliding speeds (Supplementary Figure S6) or any regeneration defects

(Supplementary Figure S4). Thus, chemical inhibition of regenerating planarians recapitulated the effects seen with regenerating RNAi animals, but not those of acutely inhibited animals. Together, these data suggest that planarians may develop adaptive mechanisms to mitigate the effects of long-term cholinergic stimulation.

DISCUSSION

Enzymatic properties of DjChE: sequence and structure

In this study, we have identified two potential gene sequences (*Djche1* and *Djche2*) responsible for cholinesterase activity in *D. japonica.* Our previous work characterizing the catalytic properties and inhibition profile of cholinesterase activity in planarian homogenates demonstrated that DjChE activity has hybrid properties of both AChE and BChE (Hagstrom et al., 2017). Both potential DjChE sequences identified in this study contain the features we previously predicted, namely: (a) classic esterase-type catalytic triad (Ser200, Glu 327 and His440), (b) an acyl pocket containing only one of two Phe (295 and 297), (c) a choline binding site containing Trp84, (d) disruption of a peripheral anionic site defined by Trp286, Tyr72, and Tyr124, and (e) fewer aromatic side chains lining the active center gorge compared to AChE (Figures 6.1 and 6.2). Together these characteristics result in planarian cholinesterases with a larger acyl pocket and a wider gorge opening than vertebrate AChE. This is consistent with our previous observations that DjChE can catalyze the larger butyrylcholine substrate (although less efficiently than acetylcholine) and does not undergo substrate inhibition (Hagstrom et al., 2017). These qualities are common among cholinesterases from many invertebrates, including *Drosophila* (Gnagey et al., 1987), *C. elegans* (Arpagaus et al., 1994), *Schistosoma* (Bentley et al., 2003; Bentley et al., 2005), and some vertebrate species (Pezzementi et al., 2011) and may represent an ancestral cholinesterase before separation into the distinct AChE and BChE enzymes found in vertebrates (Pezzementi and Chatonnet, 2010).

In planarian homogenates, we could not distinguish more than one distinct cholinesterase activity (Hagstrom et al., 2017). However, here we have identified two potential genes responsible for DjChE activity which are both actively expressed in *D. japonica*. Both genes

contain all the key enzymatic features described above, though sometimes achieved in different ways. Thus, they likely have similar catalytic properties and inhibitor affinities preventing us from distinguishing the two activities in crude homogenates. We cannot exclude the possibility, however, that one *Djche* may be much more highly expressed than the other and may account for the majority of the activity. Future experiments using planarian recombinant DNA expressed enzymes would help answer whether there are any significant differences in the enzymatic properties of translated proteins expressed from these two genes.

Expression profiles of Djche

In vertebrates, AChE is encoded by a single gene but is alternatively spliced to produce different isoforms, differing only in their C-termini regions, each with distinct expression profiles and possibly different functions (Camp et al., 2010; Li et al., 1991; Soreq and Seidman, 2001; Taylor and Radić, 1994) Conversely, nematodes have three genes encoding AChE (*ace-1, -2, -3*) with distinct expression profiles and mostly non-redundant functions (Combes et al., 2003; Selkirk et al., 2005). Similarly to nematodes, *Djche1* and *Djche2* were found to have mostly non-overlapping expression profiles. D*jche1* is primarily expressed in the planarian nervous system with extensive co-localization with *Djchat*, suggesting this gene is expressed in cholinergic neurons. Conversely, *Djche2* is much more ubiquitously expressed throughout the planarian body with less spatial compartmentalization than *Djche1*. This spatial segregation could hint that the different *Djche* genes perform distinct functions, such as modulating ACh in the central versus the peripheral nervous systems, or discretely in synapses versus extra-synaptic release.

Interestingly, both *Djche* genes and *Djchat* were found to co-localize in neurons located in the medial arc of the planarian brain (Figure 6.4). Several important regulators of planarian

neurogenesis and patterning are expressed in this region, including netrin (Cebrià and Newmark, 2005; Cebrià et al., 2002a), hedgehog (Rink et al., 2009), and homeodomain transcription factors (Currie et al., 2016). In *Schmidtea mediterranea*, *hedgehog* and the homeodomain transcription factors *arx* and *nkx2.1* were all found to be expressed specifically in ventromedial cholinergic neurons. Knockdown of *arx* reduced the number of ventromedial cholinergic neurons specifically in adult animals, suggesting arx and the hedgehog machinery are necessary for maintenance of these neurons (Currie et al., 2016). Together, these data suggest that ventromedial neurons, such as those that co-express *Djchat* and the *Djche* genes, may be important for formation, patterning, and maintenance of the planarian brain. Studies in several animal models and cell culture systems have suggested that AChE may have morphogenic functions during neurodevelopment, which may or may not depend on catalysis of ACh (Biagioni et al., 2000; Bigbee et al., 2000; Layer et al., 2013; Paraoanu et al., 2006; Sperling et al., 2012; Yang et al., 2008). Consistent with the possibility that DjChE activity may regulate planarian brain formation, we previously found that subchronic exposure to high concentrations of the OP chlorpyrifos led to decreased brain size in regenerating but not full worms (Hagstrom et al., 2015). In this study, we did not observe any regeneration defects in either RNAi worms or chemically-treated worms. However, it is still possible that brain size defects were present, since this would have likely not been picked up by gross analysis of the blastema size. Thus, the role, if any, of DjChEs in planarian neurodevelopment remains to be discovered.

Functional consequences of decreased DjChE activity

Acute toxicity of OPs is primarily due to over-activation of the cholinergic system due to increased synaptic ACh levels and overstimulation of the nicotinic and muscarinic ACh receptors in the central and peripheral nervous systems (King and Aaron, 2015; Pope et al., 2005; Russom

et al., 2014; Taylor, 2017). However, it has long been recognized that these chemicals have other direct and indirect effects. For example, OPs have been shown to directly interact with other targets, including other esterases (e.g. neurotoxic esterase (NTE), carboxylesterase, etc.), and a host of other hydrolase enzymes (e.g. lipases, proteases, acyl peptide hydrolase, etc.) (Clarke et al., 1994; Eleršek and Filipic, 2011; Pancetti et al., 2007; Pope et al., 2005). These targets may also modulate the extent of cholinergic toxicity elicited by OP exposure by up- or down-regulating pre- and post-synaptic components involved in ACh synthesis, uptake, and binding (receptors) (Liu and Pope, 1998; Pope et al., 2005). Importantly, actions on these secondary targets can vary dramatically between different OPs and can occur even at concentrations lower than necessary to inhibit AChE. Thus, it has been suggested that these secondary effects may play an important role in modulating the subacute and chronic effects of OPs, which can vary greatly depending on the inhibitor (Casida and Quistad, 2004; Eleršek and Filipic, 2011; Pope, 1999; Pope et al., 2005). The manner and extent that these secondary effects play in the manifestation of specific toxic endpoints, however, are unclear.

We have previously reported that physostigmine and diazinon-oxon, the oxon metabolite of diazinon, are efficient inhibitors of DjChE activity *in vitro* (Hagstrom et al., 2017). However, *in vitro* inhibition concentrations are not necessarily predictive of *in vivo* inhibition capacity as other factors, such as the amount of inhibitor taken up by the animal, may modulate the actual concentration seen by the enzyme. In this study, we found that planarians acutely exposed for 4-5 days to 1μM diazinon or physostigmine had substantial inhibition of DjChE activity, as seen qualitatively by activity staining (Figure 6.5) and quantitatively by Ellman assays in homogenates of exposed worms (Supplementary Figure S3). Efficient *in vivo* inhibition by diazinon suggests that planarians are capable of bioactivation by cytochrome P450 of diazinon to

diazinon-oxon, which is the active metabolite responsible for AChE inhibition (Mutch and Williams, 2006). Of note, in our hands, quantification of physostigmine-induced inhibition in homogenates underestimated the levels of inhibition when compared to the qualitative activity stains. This is likely due to the instability of the carbamylated enzyme as it can undergo rapid decarbamylation in the absence of physostigmine (Dawson, 1994). For example, it has been reported that single dose exposure to physostigmine in Alzheimer's patients has a BChE inhibition half-life of 84 minutes (Asthana et al., 1995). Thus, during the preparation of the homogenized sample, which takes approximately 1.5 hours, inhibited DjChE may be partially reactivated before activity measurements are made. However, in the activity stain, in which animals are fixed immediately after exposure, inhibition by physostigmine can be accurately captured and demonstrated that substantial loss of DjChE activity had occurred (Figure 6.5). Reactivation was likely a concern in both the day 5 full worms and day 12 regenerating worms, with differences between the two due to increased inhibition in the regenerates compared to the acute exposure (compare Figure 6.5C and Supplementary Figure S3D).

Despite significant loss of activity (greater than 95% in 1μM diazinon treated animals), inhibitor-treated planarians were alive and generally healthy for up to 12 days of exposure with no overt morphological or regenerative defects (Supplementary Figures S1, S4). Although AChE inhibition of 70-80% has been shown to be associated with lethality in birds, fish, and mammals (Russom et al., 2014), a similar absence of systemic toxicity or lethality despite significant inhibition of AChE has been previously demonstrated. Exposure of zebrafish larvae for 5 days to varying concentrations of chlorpyrifos, diazinon, or parathion decreased AChE activity by more than 50-80% without inducing significant lethality (Yen et al., 2011). Moreover, in *C. elegans*, double mutants with nonfunctional *ace-1* and *ace-2*, which together account for

approximately 95% of AChE activity, are not lethal (Selkirk et al., 2005). Thus, in these species, as well as in planarians, it seems that very low levels of cholinesterase activity are sufficient to maintain viability.

In this study, both inhibitor-treated and *Djche1/Djche2 (RNAi)* animals displayed delayed and less reactive responses to heat stress, suggesting that increased thermo-tolerance is specific to loss of DjChE activity and subsequent overstimulation of the cholinergic system. This agrees with previous studies in *C. elegans*, which showed that excess ACh, either through exogenous ACh exposure or inhibition of AChE by neostigmine, led to increased thermo-tolerance, which was mediated by activation of a muscarinic receptor (Furuhashi and Sakamoto, 2016; Kalinnikova et al., 2013).

Normal planarian locomotion is achieved through beating of cilia in a layer of mucus (Martin, 1978). Changes in mucus secretion or composition can change the adhesive properties of the worm, as observed during physiological events such as fission (Malinowski et al., 2017) or in response to noxious stimuli to trigger an escape gait (Cochet-Escartin et al., 2015). Therefore, generally, an increase in worm stickiness would be considered an adverse effect on worm physiology and behavior. In this study, we found that while worms that were acutely treated with diazinon or physostigmine had increased stickiness, *Djche1/Djche2 (RNAi)* animals did not. This suggests that this endpoint may be modulated in part or total by some other mechanism besides decreased ChE activity. We have previously shown that the detergent Triton-X 100 increases mucus secretion and planarian stickiness (Malinowski et al., 2017) raising the possibility that increased mucus secretion and subsequent increased stickiness may be a nonspecific defense response to external toxicants. However, subchronic exposure (11-12 days) of regenerating planarians to the same concentrations of these ChE inhibitors did not elicit increased stickiness,

compared to control animals (Figure 6.6). Thus, as this effect could be modulated, it is unlikely to be a general toxicant response. Additionally, inhibitor-treated regenerating planarians and RNAi animals did not show defects in gliding speed, although acute inhibitor-treated animals did. In our previous screen, we found that regenerating planarians were more sensitive than full worms to effects on gliding speed when treated with chlorpyrifos or dichlorvos (Hagstrom et al., 2015). Additionally, only dichlorvos, but not chlorpyrifos, caused a gliding speed defect in full animals (8 day exposure), suggesting that different effects beyond ChE inhibition may modulate how different OPs affect planarian locomotion. It is worth noting, however, that in the current study, we exchanged the chemical solutions daily to keep exposure conditions constant, while we did not exchange them in the previous screen. Together, these data suggest potential compensatory mechanisms may be activated in the regenerating animals to mitigate the long-term effects on stickiness and gliding speed.

Therefore, we propose that long-term overstimulation of the developing planarian cholinergic system may lead to adaptive mechanisms to gain tolerance to certain aspects of cholinergic toxicity, particularly increased stickiness and decreased gliding. In rats, down-regulation of the nicotinic and muscarinic ACh receptors has been proposed to be responsible for long-term tolerance to diazinon treatment (Ivanović et al., 2016). Moreover, down-regulation of muscarinic receptors has been proposed to at least partially explain the surprisingly mild phenotypes of AChE knockout mice (Li et al., 2003). Increased secretions, including increased sweating, lacrimation, and salivation, due to overstimulation of muscarinic receptors are a hallmark of cholinergic toxicity (Eleršek and Filipic, 2011; Pope et al., 2005; Taylor, 2017). We have previously shown that increased planarian stickiness is correlated with an increase in mucus secretion (Malinowski et al., 2017). Therefore, we speculate that, while being induced through

ChE inhibition, increased worm stickiness may not be correlated directly with decreased ChE activity as compensatory mechanisms may allow planarians to adapt to long-term cholinergic overstimulation by down-regulating muscarinic receptors. The role of planarian muscarinic receptors in this process, whether modulation is due to direct or indirect effects of ChE inhibitors, and whether adaptation is specific to regenerating planarians remains to be verified. Understanding of the potential role of non-ChE targets and effects in modulating ChE inhibitor toxicity is an important regulatory concern. Currently, levels of AChE inhibition are the gold standard biomarker to determine significant OP exposure (Kapka-Skrzypczak et al., 2011). However, growing evidence suggests that toxic outcomes may manifest from exposure to OP concentrations below those needed to inhibit AChE. This is of particular concern for chronic, low dose exposure and for prenatal exposure to the developing fetus (Pancetti et al., 2007). Here, we show that the wide repertoire of planarian morphological and behavioral endpoints, combined with accessible molecular biology techniques, enables us to dissect potential mechanisms underlying specific phenotypes of ChE inhibitor exposure. So far, however, we have only assayed a small subset of accessible behaviors based on endpoints that have previously been published to be affected by OP exposure in planarians or other systems. Thus, other effects of OP exposure may also exist that are not captured in this study. A comprehensive map quantifying the wide range of possible behaviors in planarians will be necessary for future studies aimed at elucidating the differential actions of OPs on neuronal function and behavior. As rates of OP inhibition of ChE are similar to mammals (Hagstrom et al., 2017) and the planarian brain contains many of the same important genes as the vertebrate brain, these mechanisms are likely to be conserved and could be further investigated in mammalian models. Together, these characteristics make planarians a well-suited model system to analyze OP toxicity.

ACKNOWLEDGEMENTS

Chapter 6, in full, is a reformatted reprint of the material as it appears in Hagstrom, Danielle; Zhang, Siqi; Ho, Alicia; Tsai, Eileen S.; Radić, Zoran; Jahromi, Aryo; Kaj, Kelson J.; He, Yingtian; Taylor, Palmer; and Collins, Eva-Maria S. "Planarian cholinesterase: molecular and functional characterization of an evolutionarily ancient enzyme to study organophosphorus pesticide toxicity", Archives of Toxicology, vol. 92, 2018. The final publication is available at: https://link.springer.com/article/10.1007%2Fs00204-017-2130-7. Permission to use this manuscript was granted to Danielle Hagstrom by Springer Nature. Danielle Hagstrom and Eva-Maria S. Collins designed the experiments and co-wrote the manuscript. Danielle Hagstrom, Siqi Zhang, Alicia Ho, Eileen S. Tsai, Aryo Jahromi, and Yingtian He performed the experiments and analyzed the associated data. Kelson Kaj assembled the *Dugesia japonica* transcriptome. Zoran Radić and Palmer Taylor performed analysis of the sequence and protein structure characteristics and contributed to writing and editing of the manuscript. Danielle Hagstrom was the primary investigator and author of this material.

REFERENCES

Arnold, K., Bordoli, L., Kopp, J. and Schwede, T. (2006). The SWISS-MODEL workspace: a web-based environment for protein structure homology modelling. *Bioinformatics* **22**, 195–201.

Arpagaus, M., Fedon, Y., Cousin, X., Chatonnet, A., Bergé, J.-B., Fournier, D. and Toutant, J.-P. (1994). cDNA sequence, gene structure, and in vitro expression of ace-1, the gene encoding acetylcholinesterase of class A in the nematode Caenorhabditis elegans. *J. Biol. Chem.* **269**, 9957–9965.

Asthana, S., Greig, N. H., Hegedus, L., Holloway, H. H., Raffaele, K. C., Schapiro, M. B. and Soncrant, T. T. (1995). Clinical pharmacokinetics of physostigmine in patients with Alzheimer's disease. *Clin. Pharmacol. Ther.* **58**, 299–309.

Atwood, D. and Paisley-Jones, C. (2017). *Pesticides Industry Sales and Usage 2008 - 2012 Market Estimates*. Washington, DC.

Benkert, P., Biasini, M. and Schwede, T. (2011). Toward the estimation of the absolute quality of individual protein structure models. *Bioinformatics* **27**, 343–350.

Bentley, G. N., Jones, A. K. and Agnew, A. (2003). Mapping and sequencing of acetylcholinesterase genes from the platyhelminth blood fluke Schistosoma. *Gene* **314**, 103–112.

Bentley, G. N., Jones, A. K. and Agnew, A. (2005). Expression and comparative functional characterisation of recombinant acetylcholinesterase from three species of Schistosoma. *Mol. Biochem. Parasitol.* **141**, 119–123.

Biagioni, S., Tata, A. M., De Jaco, A. and Augusti-Tocco, G. (2000). Acetylcholine synthesis and neuron differentiation. *Int. J. Dev. Biol.* **44**, 689–97.

Biasini, M., Bienert, S., Waterhouse, A., Arnold, K., Studer, G., Schmidt, T., Kiefer, F., Cassarino, T. G., Bertoni, M., Bordoli, L., et al. (2014). SWISS-MODEL: modelling protein tertiary and quaternary structure using evolutionary information. *Nucleic Acids Res.* **42**, W252–W258.

Bigbee, J. W., Sharma, K. V, Chan, E. L. and Bögler, O. (2000). Evidence for the direct role of acetylcholinesterase in neurite outgrowth in primary dorsal root ganglion neurons. *Brain Res.* **861**, 354–362.

Brown, D. D. R. and Pearson, B. J. (2015). One FISH, dFISH, three FISH: sensitive methods of whole-mount fluorescent in situ hybridization in freshwater planarians. In *In Situ Hybridization Methods* (ed. Hauptmann, G.), pp. 127–150. New York: Springer Science.

Camp, S., Zhang, L., Krejci, E., Dobbertin, A., Bernard, V., Girard, E., Duysen, E. G., Lockridge, O., De Jaco, A. and Taylor, P. (2010). Contributions of selective knockout studies to understanding cholinesterase disposition and function. *Chem. Biol. Interact.* **187**,

72–7.

Casida, J. E. and Quistad, G. B. (2004). Organophosphate toxicology: safety aspects of nonacetylcholinesterase secondary targets. *Chem. Res. Toxicol.* **17**, 983–998.

Cebrià, F. and Newmark, P. A. (2005). Planarian homologs of netrin and netrin receptor are required for proper regeneration of the central nervous system and the maintenance of nervous system architecture. *Development* **132**, 3691–703.

Cebrià, F., Nakazawa, M., Mineta, K., Ikeo, K., Gojobori, T. and Agata, K. (2002a). Dissecting planarian central nervous system regeneration by the expression of neural-specific genes. *Dev. Growth Differ.* **44**, 135–146.

Cebrià, F., Kudome, T., Nakazawa, M., Mineta, K., Ikeo, K., Gojobori, T. and Agata, K. (2002b). The expression of neural-specific genes reveals the structural and molecular complexity of the planarian central nervous system. *Mech. Dev.* **116**, 199–204.

Chu, H.-T., Hsiao, W. W. L., Chen, J.-C., Yeh, T.-J., Tsai, M.-H., Lin, H., Liu, Y.-W., Lee, S.-A., Chen, C.-C., Tsao, T. T. H., et al. (2013). EBARDenovo: highly accurate de novo assembly of RNA-Seq with efficient chimera-detection. *Bioinformatics* **29**, 1004–1010.

Clarke, P. B. S., Reuben, M. and El-Bizri, H. (1994). Blockade of nicotinic responses by physostigmine, tacrine and other cholinesterase inhibitors in rat striatum. *Br. J. Pharmacol.* **111**, 695–702.

Cochet-Escartin, O., Mickolajczk, K. J. and Collins, E.-M. S. (2015). Scrunching: a novel escape gait in planarians. *Phys. Biol.* **12**, 055001.

Combes, D., Fedon, Y., Toutant, J.-P. and Arpagaus, M. (2003). Multiple ace genes encoding acetylcholinesterases of Caenorhabditis elegans have distinct tissue expression. *Eur. J. Neurosci.* **18**, 497–512.

Cowles, M. W., Brown, D. D. R., Nisperos, S. V, Stanley, B. N., Pearson, B. J. and Zayas, R. M. (2013). Genome-wide analysis of the bHLH gene family in planarians identifies factors required for adult neurogenesis and neuronal regeneration. *Development* **140**, 4691–702.

Currie, K. W., Molinaro, A. M. and Pearson, B. J. (2016). Neuronal sources of hedgehog modulate neurogenesis in the adult planarian brain. *Elife* **5**,.

Dawson, R. M. (1994). Rate constants of carbamylation and decarbamylation of acetylcholinesterase for physostigmine and carbaryl in the presence of an oxime. *Neurochem. Int.* **24**, 173–182.

Eleršek, T. and Filipic, M. (2011). Organophosphorus pesticides - mechanisms of their toxicity. In *Pesticides - The Impacts of Pesticides Exposure* (ed. Stoytcheva, M.), pp. 243–260. Rijeka: Intech.

Ellman, G. L., Courtney, K. D., Andres, V. and Featherstone, R. M. (1961). A new and rapid

colorimetric determination of acetylcholinesterase activity. *Biochem. Pharmacol.* **7**, 88–95.

EUROSTAT (2016). *Agriculture, forestry and fishery statistics - 2016 edition*. (ed. Forti, R.) and Henrard, M.) Luxembourg, Belgium: European Union.

Furuhashi, T. and Sakamoto, K. (2016). Central nervous system promotes thermotolerance via FoxO/DAF-16 activation through octopamine and acetylcholine signaling in Caenorhabditis elegans. *Biochem. Biophys. Res. Commun.* **472**, 114–117.

Giacobini, E. (2000). Cholinesterase inhibitors: from the Calabar bean to Alzheimer therapy. In *Cholinesterases and Cholinesterase Inhibitors* (ed. Ezio Giacobini), pp. 181–219. London: Martin Dunitz Ltd.

Gnagey, A. L., Forte, M. and Rosenberry, T. L. (1987). Isolation and characterization of acetylcholinesterase from Drosophila. *J. Biol. Chem.* **262**, 13290–13298.

González-Alzaga, B., Lacasaña, M., Aguilar-Garduño, C., Rodríguez-Barranco, M., Ballester, F., Rebagliato, M. and Hernández, A. F. (2014). A systematic review of neurodevelopmental effects of prenatal and postnatal organophosphate pesticide exposure. *Toxicol. Lett.* **230**, 104–121.

Hagstrom, D., Cochet-Escartin, O., Zhang, S., Khuu, C. and Collins, E.-M. S. (2015). Freshwater planarians as an alternative animal model for neurotoxicology. *Toxicol. Sci.* **147**, 270–285.

Hagstrom, D., Cochet-Escartin, O. and Collins, E.-M. S. (2016). Planarian brain regeneration as a model system for developmental neurotoxicology. *Regeneration* **3**, 65–77.

Hagstrom, D., Hirokawa, H., Zhang, L., Radić, Z., Taylor, P. and Collins, E.-M. S. (2017). Planarian cholinesterase: in vitro characterization of an evolutionarily ancient enzyme to study organophosphorus pesticide toxicity and reactivation. *Arch. Toxicol.* **91**, 2837–2847.

Inoue, T., Yamashita, T. and Agata, K. (2014). Thermosensory signaling by TRPM is processed by brain serotonergic neurons to produce planarian thermotaxis. *J. Neurosci.* **34**, 15701–14.

Ivanović, S. R., Dimitrijević, B., Ćupić, V., Jezdimirović, M., Borozan, S., Savić, M. and Savić, D. (2016). Downregulation of nicotinic and muscarinic receptor function in rats after subchronic exposure to diazinon. *Toxicol. Reports* **3**, 523–530.

Kalinnikova, T. B., Shagidullin, R. R., Kolsanova, R. R., Osipova, E. B., Zakharov, S. V. and Gainutdinov, M. K. (2013). Acetylcholine deficiency in Caenorhabditis elegans induced by hyperthermia can be compensated by ACh-esterase inhibition or activation of GAR-3 mAChRs. *Environ. Nat. Resour. Res.* **3**, 98–113.

Kapka-Skrzypczak, L., Cyranka, M., Skrzypczak, M. and Kruszewski, M. (2011). Biomonitoring and biomarkers of organophosphate pesticides exposure - state of the art. *Ann. Agric. Environ. Med.* **18**, 294–303.

King, A. M. and Aaron, C. K. (2015). Organophosphate and carbamate poisoning. *Emerg. Med.*

Clin. North Am. **33**, 133–151.

King, R. S. and Newmark, P. A. (2013). In situ hybridization protocol for enhanced detection of gene expression in the planarian Schmidtea mediterranea. *BMC Dev. Biol.* **13**,.

Layer, P. G., Klaczinski, J., Salfelder, A., Sperling, L. E., Thangaraj, G., Tuschl, C. and Vogel-Höpker, A. (2013). Cholinesterases in development: AChE as a firewall to inhibit cell proliferation and support differentiation. *Chem. Biol. Interact.* **203**, 269–276.

Lenfant, N., Hotelier, T., Velluet, E., Bourne, Y., Marchot, P. and Chatonnet, A. (2013). ESTHER, the database of the α/β-hydrolase fold superfamily of proteins: tools to explore diversity of functions. *Nucleic Acids Res.* **41**, D423-9.

Li, Y., Camp, S., Rachinsky, T. L., Getman, D. and Taylor, P. (1991). Gene structure of mammalian acetylcholinesterase. Alternative exons dictate tissue-specific expression. *J. Biol. Chem.* **266**, 23083–90.

Li, B., Duysen, E. G., Volpicelli-Daley, L. A., Levey, A. I. and Lockridge, O. (2003). Regulation of muscarinic acetylcholine receptor function in acetylcholinesterase knockout mice. *Pharmacol. Biochem. Behav.* **74**, 977–986.

Liu, J. and Pope, C. N. (1998). Comparative presynaptic neurochemical canges in rat striatum following exposure to chlorpyrifos or parathion. *J. Toxicol. Environ. Heal. Part A* **53**, 531–544.

Malinowski, P. T., Cochet-Escartin, O., Kaj, K. J., Ronan, E., Groisman, A., Diamond, P. H. and Collins, E.-M. S. (2017). Mechanics dictate where and how freshwater planarians fission. *Proc. Natl. Acad. Sci. U. S. A.* **114**, 10888–10893.

Martin, G. G. (1978). A new function of rhabdites: Mucus production for ciliary gliding. *Zoomorphologie* **91**, 235–248.

Muñoz-Quezada, M. T., Lucero, B. A., Barr, D. B., Steenland, K., Levy, K., Ryan, P. B., Iglesias, V., Alvarado, S., Concha, C., Rojas, E., et al. (2013). Neurodevelopmental effects in children associated with exposure to organophosphate pesticides: a systematic review. *Neurotoxicology* **39**, 158–168.

Mutch, E. and Williams, F. M. (2006). Diazinon, chlorpyrifos and parathion are metabolised by multiple cytochromes P450 in human liver. *Toxicology* **224**, 22–32.

Nishimura, K., Kitamura, Y., Taniguchi, T. and Agata, K. (2010). Analysis of motor function modulated by cholinergic neurons in planarian Dugesia japonica. *Neuroscience* **168**, 18–30.

Pagán, O. R., Rowlands, A. L. and Urban, K. R. (2006). Toxicity and behavioral effects of dimethylsulfoxide in planaria. *Neurosci. Lett.* **407**, 274–278.

Pancetti, F., Olmos, C., Dagnino-Subiabre, A., Rozas, C. and Morales, B. (2007). Noncholinesterase effects induced by organophosphate pesticides and their relationship to

cognitive processes: implication for the action of acylpeptide hydrolase. *J. Toxicol. Environ. Heal. Part B Crit. Rev.* **10**, 623–630.

Paraoanu, L. E., Steinert, G., Klaczinski, J., Becker-Röck, M., Bytyqi, A. and Layer, P. G. (2006). On functions of cholinesterases during embryonic development. *J. Mol. Neurosci.* **30**, 201–4.

Paz, A., Xie, Q., Greenblatt, H. M., Fu, W., Tang, Y., Silman, I., Qiu, Z. and Sussman, J. L. (2009). The crystal structure of a complex of acetylcholinesterase with a bis-(−)- nor - meptazinol derivative reveals disruption of the catalytic triad. *J. Med. Chem.* **52**, 2543–2549.

Pezzementi, L. and Chatonnet, A. (2010). Evolution of cholinesterases in the animal kingdom. *Chem. Biol. Interact.* **187**, 27–33.

Pezzementi, L., Nachon, F. and Chatonnet, A. (2011). Evolution of acetylcholinesterase and butyrylcholinesterase in the vertebrates: An atypical butyrylcholinesterase from the medaka Oryzias latipes. *PLoS One* **6**, e17396.

Picciotto, M. R., Higley, M. J. and Mineur, Y. S. (2012). Acetylcholine as a neuromodulator: cholinergic signaling shapes nervous system function and behavior. *Neuron* **76**, 116–129.

Pope, C. N. (1999). Organophosphorus pesticides: do they all have the same mechanism of toxicity? *J. Toxicol. Environ. Heal. Part B Crit. Rev.* **2**, 161–181.

Pope, C., Karanth, S. and Liu, J. (2005). Pharmacology and toxicology of cholinesterase inhibitors: uses and misuses of a common mechanism of action. *Environ. Toxicol. Pharmacol.* **19**, 433–46.

Qin, Y. F., Fang, H. M., Tian, Q. N., Bao, Z. X., Lu, P., Zhao, J. M., Mai, J., Zhu, Z. Y., Shu, L. L., Zhao, L., et al. (2011). Transcriptome profiling and digital gene expression by deep-sequencing in normal/regenerative tissues of planarian Dugesia japonica. *Genomics* **97**, 364–371.

Ray, D. E. and Richards, P. G. (2001). The potential for toxic effects of chronic, low-dose exposure to organophosphates. *Toxicol. Lett.* **120**, 343–351.

Rink, J. C. (2013). Stem cell systems and regeneration in planaria. *Dev. Genes Evol.* **223**, 67–84.

Rink, J. C., Gurley, K. A., Elliott, S. A. and Sánchez Alvarado, A. (2009). Planarian Hh signaling regulates regeneration polarity and links Hh pathway evolution to cilia. *Science (80-.).* **326**,.

Rouhana, L., Weiss, J. a., Forsthoefel, D. J., Lee, H., King, R. S., Inoue, T., Shibata, N., Agata, K. and Newmark, P. a. (2013). RNA interference by feeding in vitro-synthesized double-stranded RNA to planarians: Methodology and dynamics. *Dev. Dyn.* **242**, 718–730.

Russom, C. L., LaLone, C. A., Villeneuve, D. L. and Ankley, G. T. (2014). Development of an

adverse outcome pathway for acetylcholinesterase inhibition leading to acute mortality. *Environ. Toxicol. Chem.* **33**, 2157–2169.

Sánchez-Santed, F., Colomina, M. T. and Herrero Hernández, E. (2016). Organophosphate pesticide exposure and neurodegeneration. *Cortex* **74**, 417–426.

Sanders, M., Mathews, B., Sutherland, D., Soong, W., Giles, H. and Pezzementi, L. (1996). Biochemical and molecular characterization of acetylcholinesterase from the hagfish Myxine glutinosa. *Comp. Biochem. Physiol. , Part B Biochem. Mol. Biol.* **115**, 97–109.

Selkirk, M. E., Lazari, O., Hussein, A. S. and Matthews, J. B. (2005). Nematode acetylcholinesterases are encoded by multiple genes and perform non-overlapping functions. *Chem. Biol. Interact.* **157**–**158**, 263–268.

Shelton, J. F., Geraghty, E. M., Tancredi, D. J., Delwiche, L. D., Schmidt, R. J., Ritz, B., Hansen, R. L. and Hertz-Picciotto, I. (2014). Neurodevelopmental disorders and prenatal residential proximity to agricultural pesticides: the CHARGE study. *Environ. Health Perspect.* **122**, 1103–9.

Slotkin, T. A. and Seidler, F. J. (2007). Comparative developmental neurotoxicity of organophosphates in vivo: transcriptional responses of pathways for brain cell development, cell signaling, cytotoxicity and neurotransmitter systems. *Brain Res. Bull.* **72**, 232–274.

Soreq, H. and Seidman, S. (2001). Acetylcholinesterase--new roles for an old actor. *Nat. Rev. Neurosci.* **2**, 294–302.

Sperling, L. E., Klaczinski, J., Schütz, C., Rudolph, L. and Layer, P. G. (2012). Mouse acetylcholinesterase enhances neurite outgrowth of rat R28 cells through interaction with laminin-1. *PLoS One* **7**, e36683.

Takano, T., Pulvers, J. N., Inoue, T., Tarui, H., Sakamoto, H., Agata, K. and Umesono, Y. (2007). Regeneration-dependent conditional gene knockdown (Readyknock) in planarian: Demonstration of requirement for Djsnap-25 expression in the brain for negative phototactic behavior. *Dev. Growth Differ.* **49**, 383–394.

Taylor, P. (2017). Anticholinesterase agents. In *Goodman and Gilman's The Pharmacological Basis of Therapeutics* (ed. Laurence L Brunton), pp. 239–254. McGraw Hill.

Taylor, P. and Radić, Z. (1994). The cholinesterases: from genes to proteins. *Annu. Rev. Pharmacol. Toxicol.* **34**, 281–320.

Terry, A. V. J. (2012). Functional consequences of repeated organophosphate exposure: potential non-cholinergic mechanisms. *Pharmacol. Ther.* **134**, 355–65.

Timofeeva, O. A., Roegge, C. S., Seidler, F. J., Slotkin, T. A. and Levin, E. D. (2008a). Persistent cognitive alterations in rats after early postnatal exposure to low doses of the organophosphate pesticide, diazinon. *Neurotoxicol. Teratol.* **30**, 38–45.

Timofeeva, O. A., Sanders, D., Seemann, K., Yang, L., Hermanson, D., Regenbogen, S., Agoos, S., Kallepalli, A., Rastogi, A., Braddy, D., et al. (2008b). Persistent behavioral alterations in rats neonatally exposed to low doses of the organophosphate pesticide, parathion. *Brain Res. Bull.* **77**, 404–411.

Umesono, Y., Tasaki, J., Nishimura, K., Inoue, T. and Agata, K. (2011). Regeneration in an evolutionarily primitive brain--the planarian Dugesia japonica model. *Eur. J. Neurosci.* **34**, 863–9.

Waterhouse, A. M., Procter, J. B., Martin, D. M. A., Clamp, M. and Barton, G. J. (2009). Jalview Version 2--a multiple sequence alignment editor and analysis workbench. *Bioinformatics* **25**, 1189–1191.

Yang, D., Howard, A., Bruun, D., Ajua-Alemanj, M., Pickart, C. and Lein, P. J. (2008). Chlorpyrifos and chlorpyrifos-oxon inhibit axonal growth by interfering with the morphogenic activity of acetylcholinesterase. *Toxicol. Appl. Pharmacol.* **228**, 32–41.

Yen, J., Donerly, S., Linney, E. A., Levin, E. D. and Linney, E. A. (2011). Differential acetylcholinesterase inhibition of chlorpyrifos, diazinon and parathion in larval zebrafish. *Neurotoxicol. Teratol.* **33**, 735–741.

Zheng, D.-M., Xie, H.-Q., Wang, A.-T. and Wu, C.-C. (2011). The nerve system identificiation by histochemical localization of acetylcholinesterase in planarian Dugesia japonica. *Chinese J. Zool.* **45**, 68–75.

Chapter 7: Comparative analysis of the mechanisms of organophosphorus pesticide developmental neurotoxicity in freshwater planarians

ABSTRACT

Organophosphorus pesticides (OPs), are among the most prominent pesticides used in agriculture and kill insects by inhibiting acetylcholinesterase (AChE), leading to over-excitation of the cholinergic system. Growing evidence suggest that exposure to environmental concentrations of OPs during development may cause life-long neurological damage and behavioral disorders. However, it is debated whether these effects are due to AChE inhibition. Several alternative molecular targets have been suggested to be affected by OP exposure, including cytoskeletal proteins, regulators of endocannabinoid signaling, and oxidative stress, although the significance of these targets on functional adverse outcomes is unknown. Moreover, it is unclear whether different OPs, which can cause different adverse outcomes, act through the same mechanism(s). We therefore tested whether the distinct toxicological profiles induced by different OPs are due to differential effects on these alternative pathways by screening for effects on various morphological and behavioral readouts in asexual freshwater planarians. Using a custom robotic screening platform, a comparative screen was performed of 6 OPs (chlorpyrifos, chlorpyrifos oxon, dichlorvos, diazinon, malathion and parathion) and of compounds known to activate pathways suggested in the literature to be OP targets (cholinergic overstimulation, cytoskeletal depolymerization, endocannabinoid system activation, and oxidative stress). By comparing each toxicant's toxicological profile, we link specific mechanisms with their functional toxicological outcomes and determine the role these play in differential OP toxicity. Thus, we provide mechanistic insight into how different OPs can distinctly damage the developing brain and identify relevant molecular targets and the functional consequences of their disruption.

INTRODUCTION

Organophosphorus pesticides (OPs) are among the most agriculturally important and common pesticides used today (Atwood and Paisley-Jones, 2017; EUROSTAT, 2016). Because of their environmental abundance, it is alarming that growing evidence correlates chronic prenatal and infant exposure to subacute levels of OPs with life-long neurological damage and behavioral disorders (Burke et al., 2017; González-Alzaga et al., 2014; Muñoz-Quezada et al., 2013; Rauh et al., 2011; Shelton et al., 2014). Acute OP toxicity is due to inhibition of acetylcholinesterase (AChE) (Russom et al., 2014; Taylor, 2018), which is responsible for hydrolyzing the neurotransmitter acetylcholine (ACh). However, it is debated whether this is the predominant mechanism by which OPs cause developmental neurotoxicity (DNT), especially as some animal studies have observed OP-induced DNT in the absence of significant AChE inhibition (Mamczarz et al., 2016; Yang et al., 2008; Zarei et al., 2015) or found that the extent of AChE inhibition did not correlate with the presence of DNT, such as when comparing gender-selective effects of chlorpyrifos (CPF) exposure in rats (Dam et al., 2000). However, a direct link between disruption of non-AChE targets and neurodevelopmental defects and the extent that these and/or cholinergic mechanisms contribute to DNT has been difficult to ascertain. A multitude of potential alternative targets have been suggested to be affected by OP exposure, including the ACh receptors (AChRs), other esterases, and non-esterase, non-cholinergic targets such as cytoskeletal proteins (Burke et al., 2017; Carr et al., 2014; Flaskos, 2014; Pope, 1999; Pope et al., 2005; Slotkin et al., 2017). The impact of these effects is unclear, however, because few connections between molecular/cellular endpoints and brain function (behavioral) deficits have been made.

The majority of mechanistic OP research has been focused on the most abundant OP CPF.

Thus, it has been largely assumed that all OPs, due to their common action on AChE, act in the same way. However, comparative studies in rats have shown that different OPs damage the developing brain to varying extents, resulting in different adverse outcomes (Moser, 1995; Pope, 1999; Richendrfer and Creton, 2015; Slotkin et al., 2006), reinforcing the need to thoroughly evaluate individual OPs to better understand any potential compound-specific toxicity. Thus far, however, studies have been limited in scope to either 1-3 compounds at a time (Richendrfer and Creton, 2015; Slotkin et al., 2006) or only acute effects (Moser, 1995).

To fill this data gap, we utilized our automated high-throughput whole animal screening platform (Zhang et al., 2018) to perform a comparative screen of 6 OPs (CPF, chlorpyrifos oxon (CPFO), dichlorvos, diazinon, malathion, and parathion) in an asexual freshwater planarian, *Dugesia japonica.* These OPs were chosen because of their environmental abundance, differences in chemical structures, and known potency in planarians from our previous work quantifying the *in vitro* inhibition rates of the respective oxons (Hagstrom et al., 2017). CPF and its active oxon metabolite, CPFO, were both tested as it has been suggested that some of toxicity may occur from the parent form directly without bioactivation into CPFO (Crumpton et al., 2000). Planarians are an unique and apt system for developmental neurotoxicology, as development can be induced by amputation, wherein the tail piece will regenerate a new brain within 12 days (Hagstrom et al., 2016). As full and amputated regenerating planarians are of similar size, adult and regenerating animals can be tested in parallel with the same assays, providing the unique opportunity to directly identify effects specific to development. Planarian neuro-regeneration shares fundamental processes with vertebrate neurodevelopment. Moreover, the planarian central nervous system, while morphologically simple, has considerable cellular and functional complexity (Cebrià, 2007; Ross et al., 2017). Planarians and mammals share key

neurotransmitters (Ribeiro et al., 2005), including ACh, which has been shown to regulate motor activity in *D. japonica* (Nishimura et al., 2010). Moreover, our previous work identified 2 putative genes responsible for cholinesterase function in *D. japonica* which were sensitive to OP inhibition and whose knockdown recapitulated some phenotypes of subacute OP exposure (Hagstrom et al., 2017; Hagstrom et al., 2018). Lastly, planarians have a variety of different quantifiable behaviors which can be assayed to assess neuronal functions. Importantly, many of these behaviors have been shown to be coordinated by distinct neuronal subpopulations (Birkholz and Beane, 2017; Inoue et al., 2014; Nishimura et al., 2010) allowing us to link functional adverse outcomes with distinct cellular effects.

To delineate the molecular mechanisms underlying OP toxicity, we compared the toxicological profiles of 6 OPs to chemicals with known modes of action. These included cholinergic activators, such as carbamate AChE inhibitors (aldicarb and physostigmine) and nicotinic and muscarinic AChR agonists (nicotine/anatoxin-a and muscarine/bethanechol, respectively). We also tested several alternative targets suggested in the literature to be affected by OPs. First, as cytoskeletal proteins such as actin and tubulin have been suggested to be direct targets of OPs (Flaskos, 2012; Flaskos, 2014; Jiang et al., 2010; Zarei et al., 2015), we tested the cytoskeletal depolymerization drugs, cytochalasin D and colchicine. Second, fatty acid amide hydrolase (FAAH) has been shown to be inhibited by CPF leading to accumulation of the endocannabinoid anandamide and subsequent activation of the CB-1 receptor (Carr et al., 2014; Casida and Quistad, 2004; Liu et al., 2013). Thus, we characterized the toxicological effects of anandamide and the CB-1 receptor agonist WIN 55 212-2, which has been shown previously to affect planarian behavior (Buttarelli et al., 2002). Lastly, to test the effects of oxidative stress, a common mechanism of toxicity also suggested to play a role in OP DNT (Crumpton et al., 2000;

Singh et al., 2018), we evaluated the effects of rotenone and L-buthionine sulfoxime. Using this comparative approach, we find DNT induced by different OPs falls into one of three major groupings: 1) toxicity mainly due to cholinergic overstimulation (DDVP, malathion), 2) toxicity mainly due to endocannabinoid stimulation (CPF, CPFO, and parathion), and 3) other, non-classifiable (diazinon). Moreover, the endpoints affected by the OPs differed between adult and regenerating planarians, reinforcing the unique utility of the planarian system to identify development-specific toxicity. Together, these results provide new insight into the mechanisms of compound-specific OP DNT and provide new evidence for the important role non-cholinergic targets, specifically the endocannabinoid system, can play in specific toxic outcomes.

MATERIALS AND METHODS

Test animals

Freshwater planarians of the species *Dugesia japonica*, originally obtained from Shanghai University, China and cultivated in our lab for > 5 years, were used for all experiments. Planarians were stored in 1x Instant Ocean (IO, Blacksburg, VA) in Tupperware containers and kept at 20°C in a Panasonic refrigerated incubator in the dark. The animals were fed organic freeze-dried chicken liver (either Mama Dog's or Brave Beagle, both from Amazon, Seattle , WA) once a week and their aquatic environment cleaned twice a week (Dunkel et al., 2011). For all experiments, only fully regenerated worms which had not been fed within one week and which were found gliding normally in the container were used. Worms were manually selected to fall within a certain range of sizes, with larger planarians used for amputation/regeneration experiments, such that the final sizes of adult and regenerating tails were similar. To induce development/regeneration, intact planarians were amputated on day 1 by cutting posterior to the auricles and anterior to the pharynx with an ethanol-sterilized razor blade. Exposure began within 3 hours of amputation. Of note, for animals which underwent fission during the course of the screen, only the head piece was considered in all analyses, as this would represent the first regenerated brain (Zhang et al., 2018).

Chemical preparation

Table 7.1 lists the chemicals used in this study. Two negative control chemicals, D-glucitol and L-ascorbic acid, which we have previously shown do not affect planarian behavior or morphology (Zhang et al., 2018), were also screened. Stock solutions were prepared in 100% dimethyl sulfoxide (DMSO, Sigma-Aldrich, Saint Louis, MO), with the exception of anatoxin-a, muscarine, and L-buthionine sulfoxime (BSO), which were prepared in water due to low

solubility in DMSO. All stock solutions were stored at -20ºC. For each chemical, 5 concentrations were tested. The highest concentrations were chosen, based on preliminary tests, to be at the threshold to cause lethality or overt systemic toxicity or the highest soluble concentration. The remaining concentrations are serial half-log dilutions (Table 7.1).

The set of 20 compounds was separated into 2 "Chemical Sets" of 10 chemicals, such that one chemical from each "class" (see Table 7.1) was tested in each Chemical Set. Chemicals in the same Chemical Set were tested on the same day, i.e. the same experiment. For the majority of the chemicals, 0.5% DMSO was used as solvent control, which we have previously shown has no effects on planarian morphology or behavior (Hagstrom et al., 2015). For chemicals prepared in water (anatoxin-a, muscarine, BSO), IO water was used as a control. Chemical stock plates were prepared in 96-well plates (Genesee Scientific, San Diego, CA) by adding 200X stock solutions in DMSO or water from the highest tested concentration to one well of the plate. Half-log serial dilutions were then made in DMSO or water with a multi-pipettor. The control well contained DMSO or IO water only. Stock plates were sealed and stored at -20 ºC.

Table 7.1. Chemicals tested in this screen.

Chemical Name	CAS	Class/mode of action	Concentrations tested (µM)	Supplier	Purity (%)	Chemical Set
Chlorpyrifos (CPF)	2921-88-2	OP	31.6, 10, 3.16, 1, 0.316	Sigma-Aldrich	100	1
Chlorpyrifos oxon (CPFO)	5598-15-2	OP	3.16 ,1, 0.316 , 0.1, 0.0316	Chem Service	98.8	1
Diazinon	333-41-5	OP	31.6, 10, 3.16, 1, 0.316	Sigma-Aldrich	98	1
Dichlorvos (DDVP)	62-73-7	OP	3.16, 1, 0.316, 0.1, 0.0316	Sigma-Aldrich	98	2
Malathion	121-75-5	OP	31.6, 10, 3.16, 1, 0.316	MP Biomedicals	96	2
Parathion	56-38-2	OP	31.6, 10, 3.16, 1, 0.316	Sigma-Aldrich	100	2
Aldicarb	116-06-3	Carbamate AChE inhibitor	316, 100, 31.6, 10, 3.16	Sigma-Aldrich	98	2
Physostigmine	57-47-6	Carbamate AChE inhibitor	10, 3.16, 1, 0.316, 0.1	Sigma-Aldrich	99	1
Anatoxin-A	64285-06-9	Nicotinic AChR agonist	100, 31.6, 10, 3.16, 1	Abcam	98	1
Nicotine	54-11-5	Nicotinic AChR agonist	1000, 316, 100, 31.6, 10	Sigma-Aldrich	98	2
Bethanechol	590-63-6	Muscarinic AChR agonist	316u, 100, 31.6, 10, 3.16	TCI America	98	2
Muscarine	2936-25-6	Muscarinic AChR agonist	100, 31.6, 10, 3.16, 1	Sigma-Aldrich	98	1
Colchicine	64-86-8	disrupts microtubule polymerization	316, 100, 31.6, 10, 3.16	Acros Organics	97	2
Cytochalasin D	22144-77-0	disrupts actin polymerization	31.6, 10, 3.16, 1, 0.316	MP Biomedicals	99	1
Anandamide	94421-68-8	Endocannabinoid	100, 31.6, 10, 3.16, 1	Sigma-Aldrich	97	1
WIN 55 212-2	131543-23-2	CB-1 receptor agonist	10, 3.16, 1, 0.316, 0.1	Sigma-Aldrich	98	2
L-buthionine sulfoxime	83730-53-4	induces oxidative stress	10000, 3160, 1000, 316, 100	Sigma-Aldrich	97	2
Rotenone	83-79-4	induces oxidative stress	0.316, 0.1, 0.0316, 0.010,0.00316	Sigma-Aldrich	100	1
L-ascorbic acid	50-81-7	Negative control	100, 31.6, 10, 3.16, 1	Alfa Aesar	99	1
D-glucitol	50-70-4	Negative control	100, 31.6, 10, 3.16, 1	Sigma-Aldrich	99	2

Screening plate setup

Each 48-well screening plate (Genesee Scientific) assayed 8 planarians in the solvent control (0.5% DMSO or IO water), and 8 planarians each per concentration of chemical (5 test concentrations per plate). Experiments were performed in triplicate (independent experiments performed on different days). The orientation of the concentrations in the plate was shifted down 2 rows in each replicate to control for edge effects (Zhang et al., 2018). For each chemical and experiment, one plate containing full (intact) planarians and one plate containing regenerating tails (2 plates total) were assayed.

On the day of plate set-up, the appropriate 200X chemical stock plate was thawed at room temperature for approximately 30 minutes. The 200X stocks were then diluted 20X in IO water to create 10X stock plates. These plates were mixed by rotation on an orbital shaker for approximately 10 minutes before use.

Screening plates were prepared as described in (Zhang et al., 2018) with one full planarian or amputated tail piece in each well of a 48-well plate containing 200µl of the nominal concentration of test solution and sealed with ThermalSeal RTS seals (Excel Scientific, Victorville, CA). The plates were stored, without their lids, in stacks in the dark at room temperature when not being screened. Since we previously found that fissioning worms produced challenges in our automated data analysis pipeline (Zhang et al., 2018) and because planarian fission is suppressed when disturbed (Malinowski et al., 2017), the plates were gently agitated by hand once every day when not being screened to discourage fission. Prepared plates were only moved to the screening platform when screened at day 7 and day 12.

Screening platform

We have further expanded the custom-built planarian screening platform described in (Zhang et al., 2018). Briefly, the platform consists of a commercial robotic microplate handler (Hudson Robotics, Springfield Township, NJ), two custom-built imaging systems and multiple assay stations. The imaging systems, assay stations and plate handler were controlled automatically by the computer. In addition to the assays performed in (Zhang et al., 2018), we have expanded the platform in the following ways (described in detail below): 1) expansion of the phototaxis assay to test both blue and green light stimuli, 2) modification of the scrunching assay to capture differences in the timing of reaction, and 3) addition of an automated "stickiness" assay. Moreover, analysis of the morphology/regeneration assay was expanded to also detect body shape changes.

In the expanded phototaxis assay, we replaced the previously used blue LED lights (Zhang et al., 2018) with RGB lights (DAYBETTER, Shenzhen, China) to test reactions to both green and blue light stimuli, building upon a previous study that showed that planarians detect blue, but not green, light with pigment in the skin in addition to their photoreceptors in the eyes (Birkholz and Beane, 2017; Paskin et al., 2014). Therefore, using the separate green and blue light stimuli allows us to discern between effects specific to the photoreceptors (green light) versus effects on extraocular perception through the skin. The expanded assay was performed in the following steps. First, to lower the variability of the animals' background activity, the plate was placed onto the phototaxis station 4 minutes prior to the assay, allowing the planarians in the plate to acclimate. After 4 minutes, the plate was imaged for 5 minutes: 1-min red light acclimation (1^{st} dark cycle), 1-min green light stimulation (light cycle), 2-min red light acclimation (2^{nd} dark cycle), 1-min blue light stimulation (light cycle). Of note, the second dark

cycle was 2 minutes to allow the planarians to acclimate and settle before the blue light stimulation, but only the activity in the last minute in the 2nd dark cycle was analyzed. The average speed in each 1-min dark and light cycle was quantified as in (Zhang et al., 2018). However, the phototactic response was quantified by calculating the difference of the average speed in each light cycle to that in the preceding dark cycle:

$$\Delta_{green\ light} = average\ speed_{green\ light\ cycle} - average\ speed_{1st\ dark\ cycle}$$

$$\Delta_{blue\ light} = average\ speed_{blue\ light\ cycle} - average\ speed_{2nd\ dark\ cycle}$$

Dead planarians were discarded from the analysis.

A new assay, termed "stickiness assay" since it quantifies the worm's tendency to stick to the substrate (Hagstrom et al., 2018; Malinowski et al., 2017), was added to the screening platform. We used a microplate orbital shaker (Big Bear Automation, Santa Clara, CA) to create controlled water flow to unstick the planarians from the bottom of the plate well. Different rotation speeds for full planarians and regenerating tails at day 7 and 12 were chosen based on preliminary testing to achieve a reproducible majority fraction of wild-type planarians to unstick. This intermediate unsticking capacity was chosen to be able to detect both an increase or decrease in planarian "stickiness". Day 7 for regenerating tails was observed as the relatively stickiest time-point, potentially due to locally increased secretion of mucus since the worms are less motile during regeneration. At day 7, the full planarian plates were shaken for 3 seconds at 552 revolutions per minute (rpm) and the tail plates for 3 seconds at 1017 rpm. Based on preliminary testing, full planarians kept in the screening plates for 12 days require greater water flow to be unstuck. Therefore at day 12, both full and tail plates, which are now more like adult animals (Hagstrom et al., 2015), were shaken for 3 seconds at 665 rpm. The plate was imaged from above by a USB3 camera (FLIR Systems Inc., Wilsonville, OR) mounted on a ring stand

and imaged at 8 frames per second (fps). Each worm was manually scored as either “unstuck” (defined as being displaced by the water flow and floating in the well) or “stuck” (defined as worms which did not float during the whole plate shaking session). The fraction of unstuck planarians was calculated as:

$$Fraction\ \ of\ unstuck\ planarians = \frac{the\ number\ of\ unstuck\ planarians}{the\ number\ of\ alive\ planarians}$$

In the morphology assay, different body shapes were classified for each alive planarian, including normal body shape, general sickness (lesions), contraction and ruffling, curled up or C-shape, corkscrew-like, head regression, pharynx extrusion, and tail anchored with head flailing around (Figure 7.1). Of note, one animal could be classified as having multiple body shapes, for example, C-shape and pharynx extrusion.

All assays were performed in the following order, whereby the notation in brackets indicates on which day(s) the assay was performed: phototaxis (d7/d12), unstimulated locomotion (d7/d12), lethality/regeneration (d7/d12), stickiness assay (d7/d12), thermotaxis (d12), and scrunching (d12). Data analysis was performed blinded by one investigator with no chemical information provided.

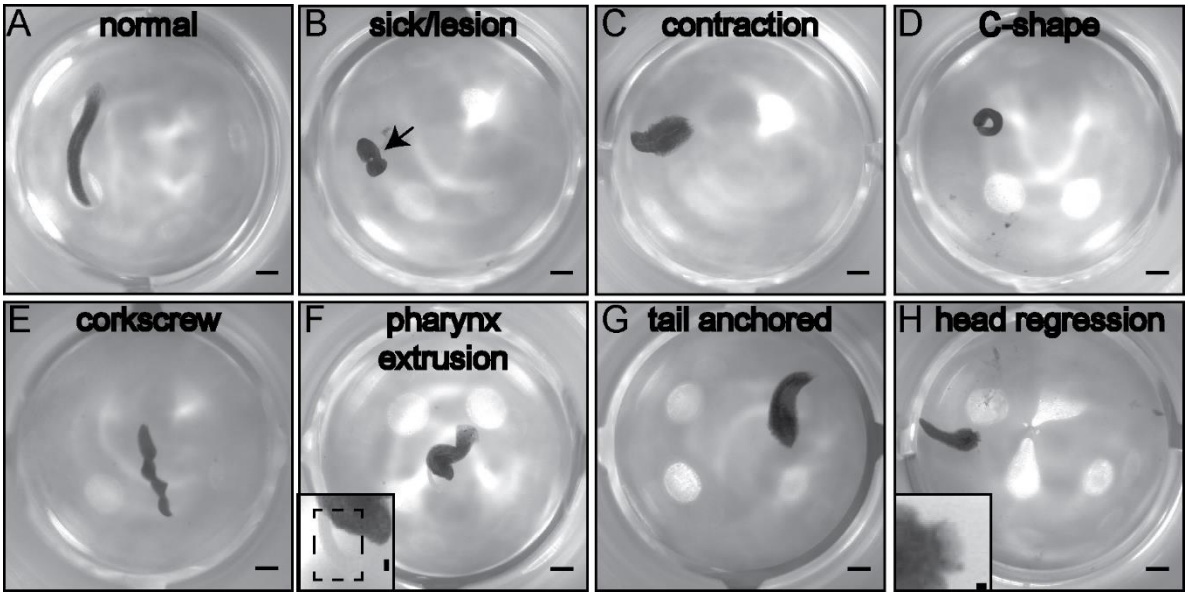

Figure 7.1. Body shape classifications in the morphology assay. High-resolution imaging was used to classify the body shape of the exposed planarians. Classifications of body shape included: (A) normal, (B) general sickness, with or without lesions (shown with an arrow), (C) contraction, ruffling of periphery, (D) curled or C-shape, (E) corkscrew-like hyperkinesia, (F) pharynx extrusion, inset shows close-up of the pharynx (shown in a dashed box) which is extended outside of the body, (G) tail anchoring while the head is freely moving, and (H) head regression, inset shows a close-up of the head which has disintegrated. Main scale bars are 1mm. Inset scale bars are 0.1mm.

Statistical testing

Statistical testing was performed on the compiled data from the triplicate runs. For all endpoints comparisons were made between the test population and the internal set of controls for that chemical. For lethality, eye regeneration, body shape morphology, stickiness, phototaxis and scrunching endpoints, a one-tailed Fisher's exact test was used. For thermotaxis and unstimulated behavioral endpoints, Tukey's interquartile test was first used to remove any outliers, with at most 5% of the data removed. A non-parametric one-tailed Mann Whitney U-test was used to determine significant effects in thermotaxis. For unstimulated behavior endpoints (speed and fraction of time resting), Lilliefors test was first used to test the normality of the samples. Thus, we performed either a parametric two-tailed t-test or a nonparametric two-tailed Mann-Whitney U-test depending on whether the sample distributions were normal or not,

respectively. A sample was determined to be defective in unstimulated behavior if there was a significant difference in either speed or fraction of time resting compared with the controls. For all endpoints, significance was determined by a p-value less than 0.05. Biological relevancy cutoffs were used to remove effects within the assay-specific variability of all controls, as in (Zhang et al., 2018). Moreover, inconsistencies between the triplicate runs, wherein a single plate was responsible for designating a “hit”, were flagged and excluded as hits. The lowest observed effect level (LOEL) was determined as the lowest tested concentration which showed a significant effect (statistically and biologically). If dose response for a particular endpoint was found to be non-monotonic, the lowest significant concentration is reported and flagged (asterisks in Figures 7.2 and 7.3). All statistical analyses were performed in MATLAB.

RESULTS AND DISCUSSION

Exposure to the 6 OPs elicits different types of DNT

Using our multi-dimensional planarian screening platform, we characterized the toxicological effects of 6 OPs (CPF, CPFO, DDVP, diazinon, malathion, and parathion) on various morphological and behavioral endpoints. For our comparative analysis, we will focus on the results obtained in regenerating planarians (Figure 7.2), as this would be the most relevant for understanding DNT elicited by these compounds.

In agreement with other studies (Moser, 1995; Pope, 1999; Richendrfer and Creton, 2015; Slotkin et al., 2006), and our previous work with CPF and DDVP (Hagstrom et al., 2015), we found that exposure to the different OPs elicited a wide and variable range of phenotypes. The most widespread effects were seen with CPF and CPFO which caused effects in lethality, body shape, eye regeneration, increased stickiness, unstimulated behavior and blue light phototaxis. The only differences observed were that CPF, but not CPFO, caused defects in day 12 unstimulated behavior and blue light phototaxis, despite both compounds causing such defects at day 7. However, these day 12 differential effects are only seen at a lethal concentration of CPF, and thus may represent further manifestations of the systemic toxicity observed at this concentration. CPFO tended to have lightly more potency in regards to endpoints affected at sublethal concentrations (i.e. concentrations not deemed active in the lethality assay), as all affected morphological and behavioral phenotypes, except for body shape at day 12, occurred below the threshold for lethality. On the other hand, only day 7 body shape, increased stickiness (day 7/12), and unstimulated behavior (day 7) were affected at sublethal concentrations of CPF. For both CPF and CPFO, the most sensitive endpoint (i.e. endpoint affected at the lowest LOEL) is day 7 body shape (Table 7.2). Although some studies have suggested that CPF may cause

toxicity independently of its bioactivation into CPFO (Crumpton et al., 2000), our data suggests that exposure to either the parent or oxon form results in very similar adverse outcomes in regenerating planarians.

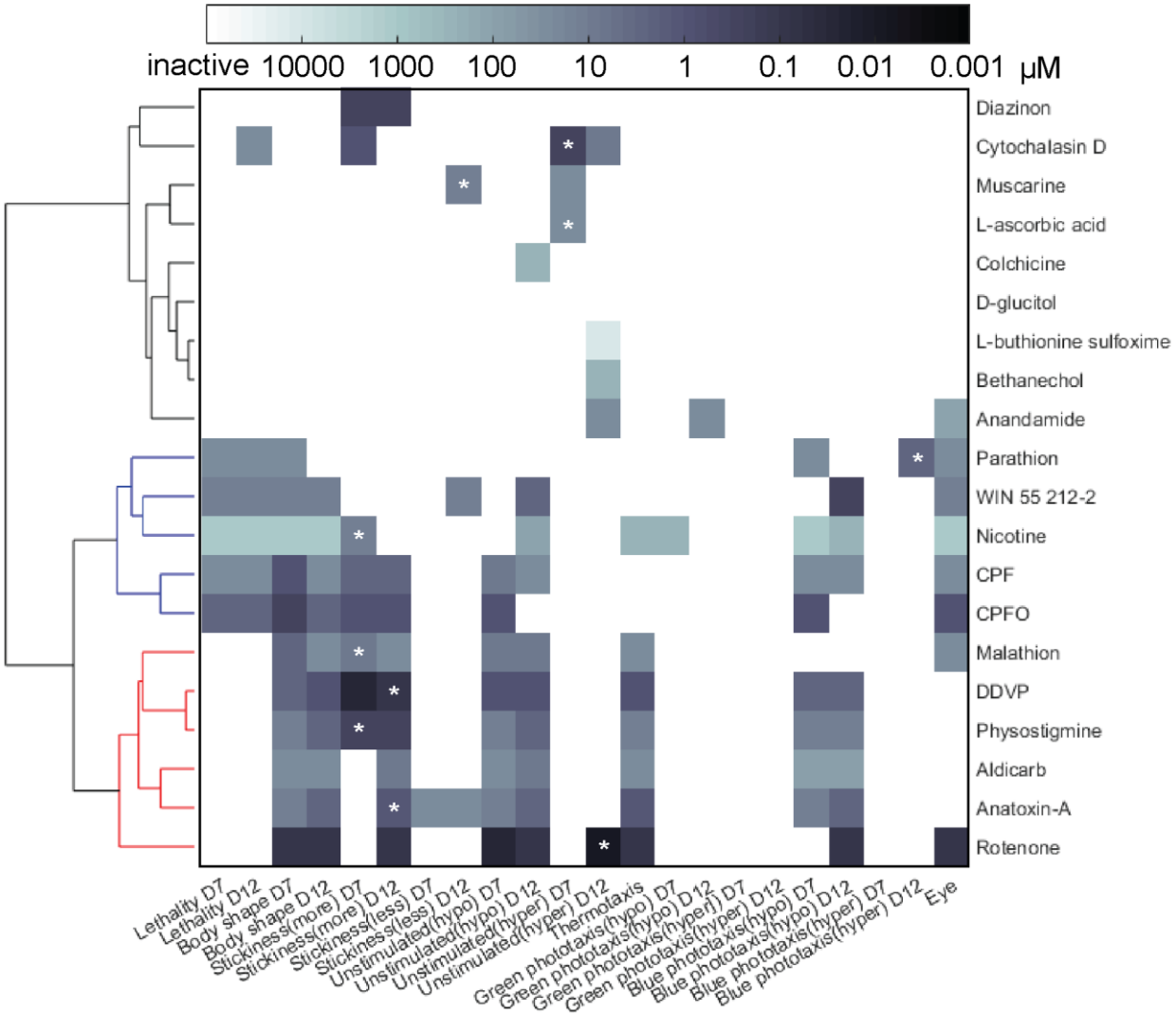

Figure 7.2. Regenerating planarian toxicological profiles. Heat map of endpoints affected in regenerating planarians for each chemical with LOEL color-coded. The chemicals' hits were clustered using Ward's method by calculating Euclidean distance between LOELs. LOELs defined by non-monotonic dose responses are marked with *. Clusters were manually color-coded for ease of comparison.

Table 7.2. Most sensitive endpoints affected by each chemical in regenerating planarians. List of endpoints affected at the overall lowest observed effect level (LOEL) for each compound. If a response is non-monotonic, the parameters are marked with (*) and the next highest concentration with a dose-dependent response is also listed.

	Overall LOEL (uM)	**Most sensitive endpoint**
Chlorpyrifos (CPF)	1	body shape (day 7)
Chlorpyrifos oxon (CPFO)	0.32	body shape (day 7)
Diazinon	0.32	↑ stickiness (day 7/12)
Dichlorvos (DDVP)	0.032	↑ stickiness (day 7)
Malathion	3.2	body shape (day 7)
Parathion	3.2*; 32	↑blue light phototaxis (day 7); lethality (day 7/12), body shape (day 7), ↓blue light phototaxis (day 7), eye regeneration
Aldicarb	10	↑ stickiness (day 12), ↓unstimulated behavior (day 12)
Physostigmine	0.32	↑ stickiness (day 7*/12)
Anatoxin-A	1	↑ stickiness day 12*, thermotaxis
Nicotine	10*; 316	↑ stickiness (day 7)*; thermotaxis, ↓ green phototaxis (day 7), ↓ blue phototaxis (day 12)
Bethanechol	316	↑ unstimulated behavior (day 12)
Muscarine	10*; 32	↓ stickiness (day 12)*; ↑ unstimulated (day 7)
Colchicine	316	↓unstimulated behavior (day 12)
Cytochalasin D	0.32*; 1	↑ unstimulated behavior (day 7)*; ↑ stickiness (day 7)
Anandamide	32	↓unstimulated behavior (day 12), ↓ green light phototaxis (day 12)
WIN 55 212-2	0.32	↓ blue light phototaxis (day 12)
L-buthionine sulfoxime	10000	↑unstimulated behavior (day 12)
Rotenone	0.01*; 0.032	↑ unstimulated behavior (day 12)*; ↓ unstimulated behavior (day 7)
L-ascorbic acid	32*	↑ unstimulated behavior (day 7)*
D-glucitol	inactive	N/A

Many, but not all, of the endpoints affected by CPF/CPFO were also affected by malathion and DDVP. Both malathion and DDVP exposure caused effects at sublethal concentrations on body shape (day 7/12), increased stickiness (day 7/12), unstimulated behavior (day 7/12), and thermotaxis. All of these endpoints, with the exception of thermotaxis, were also

affected by CPF/CPFO exposure. However, several of these effects were only induced at lethal concentrations of CPF or CPFO, but were not concomitant with lethality in DDVP and malathion, suggesting that DDVP and malathion may be more potent at eliciting sublethal non-systemic toxicity. In addition to these shared phenotypes, malathion also caused defects in eye regeneration. Similarly to CPF and CPFO, the most sensitive endpoint to malathion exposure was day 7 body shape (Table 7.2). Unlike malathion, but similar to CPF, DDVP also caused defects in blue light phototaxis (day 7/12); however, the most sensitive endpoint was increased stickiness at day 7 with effects as low are 0.03 µM (the lowest tested concentration).

Conversely, parathion and diazinon affected fewer endpoints than the other 4 tested OPs. Parathion toxicity was mostly observed at a lethal concentration (32 µM). Of note, morphological and behavioral effects at this concentration, including body shape, blue light phototaxis, and eye regeneration, were only quantified at day 7 because all planarians were dead by day 12. The only effect observed at a sublethal concentration of parathion (3.16 µM) was hyperactivity in the day 12 blue light phototaxis assay. This effect was not dose-dependent, but because it was shared among different replicates and in both regenerating and adult planarians, it is unlikely to be an artifact. Together, this toxicological profile suggests that parathion toxicity is a result of systemic toxicity and not any specific DNT. This is in agreement with previous studies showing that in zebrafish and neonatal rats, parathion induces lethality before producing the significant levels of AChE inhibition or neurodevelopmental effects seen with CPF (Slotkin et al., 2006; Yen et al., 2011). Unlike all the other OPs tested, diazinon only caused a specific effect on increased planarian stickiness at both day 7 and 12 at as low as 3.2 µM, and in the absence of lethality. The absence of systemic toxicity for diazinon at the tested concentration range was surprising to us, since the oxon form of diazinon (diazinon oxon) was found to be the

most potent of all OPs tested here at inhibiting DjChE activity *in vitro* (Hagstrom et al., 2017). Thus, we would predict that diazinon has the greatest potential to produce cholinergic shock leading to lethality. However, the lack of systemic toxicity or lethality at up to 31.6 µM, which was sufficient to cause lethality for CPF and parathion, suggests alternative mechanisms may be involved as well. It should be noted that CPF, parathion, and diazinon are all diethyl organothiophosphates with similar structures and pharmacokinetic properties, thus differences in uptake and metabolism are likely negligible. However, direct measurements of AChE activity at these concentrations should be performed to confirm this hypothesis.

Thus, in summary, although the precise endpoints affected by the OPs did vary considerably and no one endpoint was affected by all OPs, some endpoints were shared by the majority of the OPs. 5/6 OPs caused defects in body shape (day 7) and increased stickiness (day 7 and 12). These two endpoints also comprise the most sensitive endpoints in all the OPs tested and thus are sensitive predictors of OP toxicity in regenerating planarians. Planarian body shape has been previously shown to be a sensitive and characteristic readout for pharmacological manipulation of neurotransmitter systems. For example, cholinergic stimulation has been shown to induce “fixed postures” akin to our contraction classification, whereas dopaminergic stimulation produces planarian hyperkinesia (Buttarelli et al., 2008). In agreement with this, the most common body shape classifications observed in OP-exposed worms were contraction and C-shapes, thus suggesting cholinergic stimulation. On the other hand, increased secretions (including bronchial, lacrimal, salivary, sweat, and intestinal secretions) are a major hallmark of acute cholinergic toxicity due to stimulation of muscarinic AChRs (Pope et al., 2005; Taylor, 2018). We have previously shown that increased planarian stickiness is associated with increased

mucus secretion (Malinowski et al., 2017). Thus, the shared effects of the OPs on planarian stickiness may also be a result of the OPs shared action on AChE inhibition.

Comparison of OP toxicity with known effectors of mechanistic pathways

The phenotypes shared among the OPs suggest that some toxicity is likely due to cholinergic stimulation. To dissect the underlying mechanisms of OP DNT, comprising both shared and compound-specific effects, we compared the toxicological profiles of the 6 tested OPs with that of chemicals known to target pathways suggested to be affected by OPs, including cholinergic overstimulation, endocannabinoid system stimulation, oxidative stress and cytoskeletal depolymerization. The clinical manifestations of cholinergic shock are typically a mix of effects on downstream nicotinic and muscarinic AChRs (Taylor, 2018). Thus, to dissect whether some planarian toxicology profiles are affected by one or both pathways, we characterized the phenotypes of animals treated with agonists for either the nicotinic or muscarinic AChRs as well as carbamate AChE inhibitors, which would theoretically cause downstream effects in both. Ward's method of clustering was used to determine whether the toxicological profiles produced by these mechanistic control chemicals would group with any of the tested OPs. Focusing on the results in regenerating planarians, we found the toxicological profiles of the 20 chemicals (6 OPs, 12 mechanistic controls, and 2 negative controls) clustered into 3 main groups in regenerating planarians, denoted in red, blue, and black in Figure 7.2.

The red cluster consists of malathion, DDVP, physostigmine, aldicarb, anatoxin-A, and rotenone. Containing 3 cholinergic stimulators (2 carbamate AChE inhibitors and 1 nicotinic AChR agonist), this grouping may represent common effects due to cholinergic stimulation. All chemicals in this cluster caused effects in body shape (day 7/12), increased stickiness (day 12), unstimulated behavior (day 7/12), and thermotaxis. The majority of the chemicals (with the

exception of malathion and rotenone for day 7, and only malathion for day 12) also caused defects in blue light phototaxis. Although rotenone, a pesticide which disrupts mitochondrial function and thus induces oxidative stress, was also part of this cluster, it was not as closely linked as the other 5 chemicals. Just as in the OPs overall, all cholinergic stimulators in this cluster (physostigmine, aldicarb, and anatoxin-a) shared increased stickiness as one of their most sensitive endpoints (Table 7.2), further substantiating this endpoint as a readout of cholinergic overstimulation.

Another nicotinic AChR agonist, nicotine, also affected many of the same endpoints found in the red cluster, including body shape morphology (day 7/12), unstimulated behavior (days 12), thermotaxis, and blue light phototaxis (day 7/12). However, unlike the other cholinergic stimulators, nicotine only caused increased stickiness at day 7, but not day 12. In addition, defects were also observed in green light phototaxis at day 7 and eye regeneration. Moreover, some of these effects were observed at a lethal concentration (1 mM). Thus, the toxicological profile of nicotine differed enough to create a separate cluster (blue in Figure 7.2) from the other cholinergic stimulators. This cluster, also contained parathion, CPF, CPFO, and the CB-1 receptor agonist, WIN 55 212-2, and was mainly characterized by additional defects in lethality and eye regeneration, while losing some of the effects on day 7 stickiness, unstimulated behavior, and thermotaxis observed in the red cholinergic cluster. It may be surprising that nicotine did not group more closely with the carbamate inhibitors or the other nicotinic agonist anatoxin-A. However, interestingly, studies have suggested there may be extensive cross-talk between nicotine and the endocannabinoid system (Gamaleddin et al., 2015), which may explain the similar effects seen with WIN 55 212-2 and nicotine.

Lastly, the remaining chemicals (diazinon, cytochalasin D, muscarine, L-ascorbic acid, colchicine, D-glucitol, BSO, bethanechol, and anandamide) formed one large cluster mainly affecting few readouts across the various endpoints. Each of these chemicals only caused effects in 1-4 endpoints with little similarities among the chemicals. The only common endpoint shared among these chemicals is hyperactivity in the unstimulated behavior assay. Cytochalasin D, muscarine, and L-ascorbic acid caused hyperactivity at day 7 while BSO, bethanechol, and anandamide caused hyperactivity at day 12. It should be noted that this cluster contained two of our negative controls, D-glucitol and L-ascorbic acid. As expected, D-glucitol was inactive in all tested endpoints. L-ascorbic acid, however, was observed to have a dose-independent effect on hyperactivity in the unstimulated behavior assay at day 7. Thus, these shared sporadic effects to induce hyperactivity in the unstimulated assay are difficult to interpret, as their toxicological significance is unclear. Interestingly, diazinon, the only OP in this cluster, only caused increased stickiness at both day 7 and 12 and did not show significant similarities to any of the other mechanistic controls. In the future, additional mechanistic control chemicals, and more concentrations of these, should be evaluated to clarify the significance of the observed phenotypes and delineate the mechanisms within this "other" cluster.

Developmentally selective OP toxicity characterized by comparison of toxicity in regenerating versus adult planarians

A unique strength of the planarian system is the ability to directly compare the toxicity seen in developing/regenerating planarians (Figure 7.2) with that in adult (intact) planarians (Figure 7.3) to identify effects which may be specific or more sensitive to development. When considering any endpoint, CPF, diazinon, and malathion were found to be developmentally selective with the overall LOEL being lower in regenerating than in adult planarians (Table 7.3).

When delving into the individual endpoints, this selectivity arises from increased sensitivity of regenerating planarians to body shape shapes (day 7/12) and/or increased stickiness (day 7/12) induced by these OPs. As mentioned above, these endpoints were also the most sensitive endpoints for OP toxicity overall and thus appear to be sensitive indicators of OP DNT in planarians. In addition, although not determined to be selective on the chemical level, some endpoints affected by the OPs also showed developmental selectivity. For example, CPFO showed selectivity for day 7 body shape and increased stickiness, and DDVP showed selectivity for increased stickiness and unstimulated behavior, both at day 7. Parathion did not show any developmental selectivity and in fact even showed greater sensitivity in full rather than regenerating planarians resulting in overt systemic toxicity and lethality. In our previous work, we found that adult planarians generally tend to be more sensitive to lethality, and thus systemic toxicity (Hagstrom et al., 2015; Zhang et al., 2018), which we speculate may be the reason for the increased sensitivity of adult planarians to parathion.

These differences in toxic effects in adult and regenerating planarians were also apparent in the general toxicological profiles of the OPs. Unlike in regenerating planarians, effects of this chemical library in adult planarians were grouped into 3 broad categories: 1) cholinergic stimulation, 2) other, and 3) inactive (Figure 7.3). As in the regenerating tails, DDVP clustered with the cholinergic stimulators. However, all other OPs fell into the "other" cluster consisting of a mix of mechanistic controls, including the endocannabinoid stimulators, cytoskeletal disruptors, rotenone, and nicotine. Together, these data suggest that different mechanisms may be responsible for general versus developmental neurotoxicity induced by different OPs.

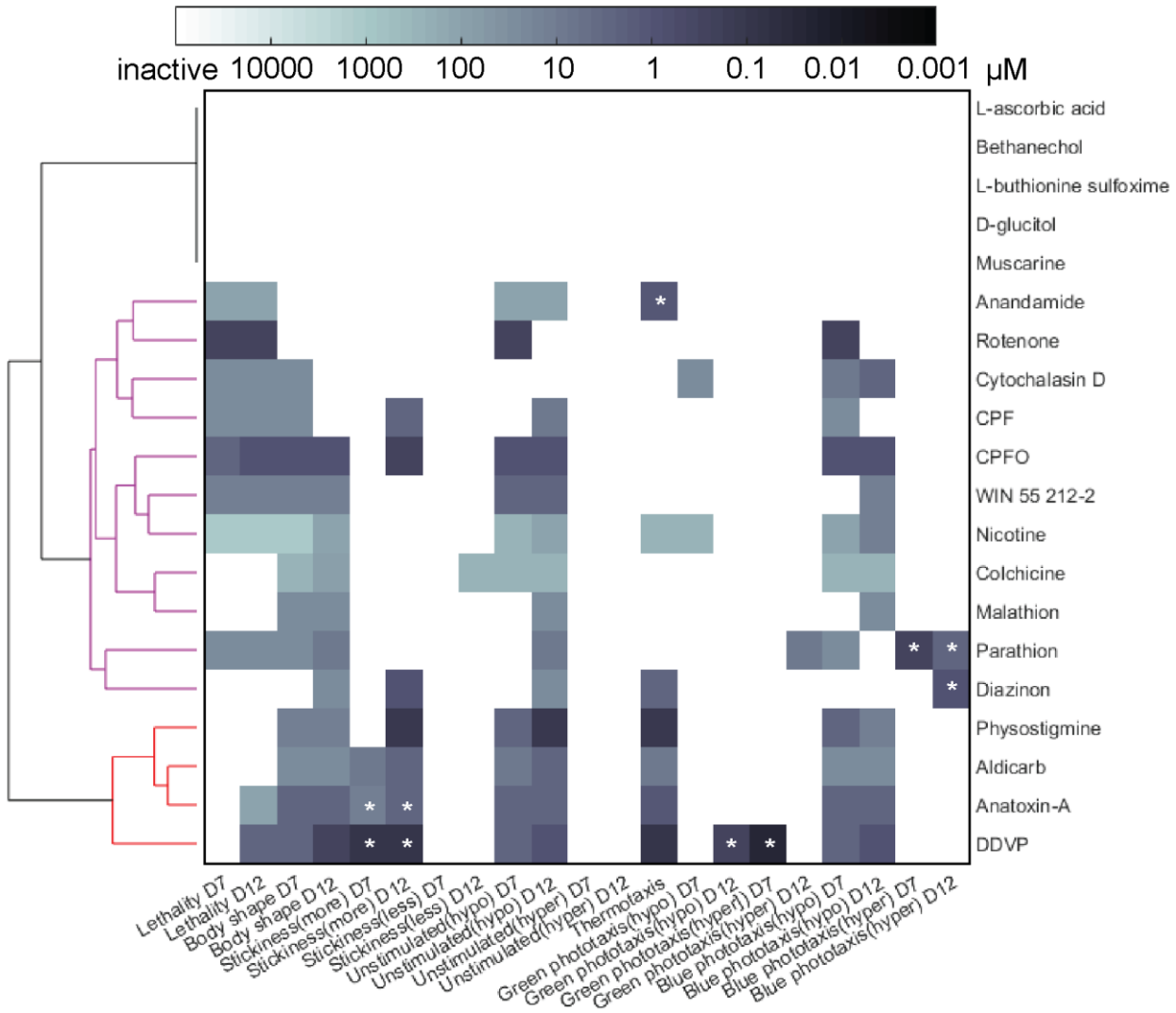

Figure 7.3. Full planarian toxicological profiles. Heat map of endpoints affected by each chemical in full planarians with LOEL color-coded. The chemicals' hits were clustered using Ward's method by calculating Euclidean distance between LOELs. LOELs defined by non-monotonic concentration responses are marked with *. Clusters were manually color-coded to aid comparison.

Table 7.3. Developmental selectivity scores, quantified as the log($LOEL_{full}/LOEL_{regen}$), for endpoints shared in both worm-types. Positive scores (>0), shaded in grey, suggest the chemical was more potent in regenerating versus adult planarians for that endpoint. (-) indicates no activity was observed in that endpoint in regenerating planarians. If activity was observed in regenerating but not full planarians, the selectivity was estimated to be > than if the $LOEL_{full}$ was the highest tested concentration.

Chemical	Lethality D7	Lethality D12	Body shape D7	Body shape D12	↑ Stickiness D7	↑ Stickiness D12	↓ Stickiness D7	↓ Stickiness D12	↓ Unstimulated D7	↓ Unstimulated D12	↑ Unstimulated D7	↑ Unstimulated D12	Thermotaxis	↓ Green phototaxis D7	↓ Green phototaxisD12	↑ Green phototaxis D7	↑ Green phototaxis D12	↓ Blue phototaxis D7	↓ Blue phototaxis D12	↑ Blue phototaxis D7	↑ Blue phototaxisD12	overall
Chlorpyrifos	0	0	1.5	>0	>1	0	-	-	>0.5	-0.5	-	-	-	-	-	-	-	0	>0	-	-	0.5
Chlorpyrifos oxon	0	-0.5	0.5	-0.5	>0.5	-0.5	-	-	0	-	-	-	-	-	-	-	-	0	-	-	-	0
Diazinon	-	-	-	-	>2	0.5	-	-	-	-	-	-	-	-	-	-	-	-	-	-	-	0.5
Dichlorvos	-	-	0	-0.5	0.5	0	-	-	0.5	0	-	-	-1.0	-	-	-	-	0	-0.5	-	-	0
Malathion	-	-	1.0	0	>0.5	>0	-	-	>0.5	0.5	-	-	>0	-	-	-	-	-	-	-	-	1.0
Parathion	0	0	0	-	-	-	-	-	-	-	-	-	-	-	-	-	-	0	-	-	0	-1.0
Aldicarb	-	-	0	0	-	-0.5	-	-	-0.5	-0.5	-	-	-0.5	-	-	-	-	-0.5	-0.5	-	-	-0.5
Physostigmine	-	-	0	0.5	>1.5	-0.5	-	-	-0.5	-1.5	-	-	-2.0	-	-	-	-	-0.5	0	-	-	-0.5
Anatoxin-A	-	-	-0.5	0	-	0.5	>0.5	>0.5	-0.5	0	-	-	0	-	-	-	-	-0.5	0	-	-	0
Nicotine	0	0	0	-1.0	>2	-	-	-	-	0	-	-	0	0	-	-	-	-1.0	-1.5	-	-	0
Bethanechol	-	-	-	-	-	-	-	-	-	-	-	>0	-	-	-	-	-	-	-	-	-	>0
Muscarine	-	-	-	-	-	-	-	>1	-	-	>0.5	-	-	-	-	-	-	-	-	-	-	>1
Colchicine	-	-	-	-	-	-	-	-	-	0	-	-	-	-	-	-	-	-	-	-	-	-0.5
Cytochalasin D	-	0	-	-	>1.5	-	-	-	-	-	>2	>0.5	-	-	-	-	-	-	-	-	-	1.0
Anandamide	-	-	-	-	-	-	-	-	-	-	-	>0.5	-	-	>0.5	-	-	-	-	-	-	-1.5
WIN 55 212-2	0	0	0	0	-	-	-	>0	-	0	-	-	-	-	-	-	-	-	1.5	-	-	1.0
L-buthionine sulfoxime	-	-	-	-	-	-	-	-	-	-	-	>0	-	-	-	-	-	-	-	-	-	>0
Rotenone	-	-	>0.5	>0.5	-	>0.5	-	-	1.0	>0.5	-	>1.5	>0.5	-	-	-	-	-	>0	-	-	1.5
L-ascorbic acid	-	-	-	-	-	-	-	-	-	-	>0.5	-	-	-	-	-	-	-	-	-	-	>0.5
D-glucitol	-	-	-	-	-	-	-	-	-	-	-	-	-	-	-	-	-	-	-	-	-	-

Summary

Our analysis showed that 5/6 OPs shared key phenotypic signatures, namely body shape changes and increased stickiness; however, the differential effects on other endpoints suggest compound-specific toxicities. DNT toxicological profiles were characterized by 1 of 3 mechanistic classes: 1) cholinergic overstimulation, exemplified by malathion and DDVP, 2) endocannabinoid and nicotinic AChR overstimulation, exemplified by CPF, CPFO and parathion, and 3) an unclassifiable "other" category containing diazinon. Despite being in a category by itself, diazinon's effects on increased stickiness, which was a common shared phenotype of almost all OPs and cholinergic stimulators, may suggest involvement of cholinergic toxicity. In fact, the most sensitive readouts to OP toxicity, body shape changes and increased stickiness, were also sensitive shared readouts of cholinergic toxicity induced by physostigmine, aldicarb, anatoxin-a, and (to a lesser extent) nicotine, strongly suggesting these effects are cholinergic-dependent. To confirm this, the levels of AChE activity should be quantified in planarians exposed for 12 days to the LOEL of each OP to directly correlate these sensitive effects with AChE inhibition. When comparing effects on adult and regenerating planarians, body shape changes and increased stickiness were also the most developmentally selective readouts of OP toxicity suggesting specific DNT. Interestingly, although in mammals increased secretions due to cholinergic shock are a result of stimulation of muscarinic AChRs (Taylor, 2018), stimulation of muscarinic receptors by muscarine exposure in planarians resulted in decreased stickiness, suggesting less mucus secretion. Moreover, the shared effects of the nicotinic agonists on increased stickiness suggest mucus secretion may be regulated to a greater extent by nicotinic AChRs in planarians, but this finding requires further investigation. Furthermore, although the current analysis places the OPs into 1 of 3 mechanistic clusters, the

toxicological profiles of the different OPs likely results from concurrent effects on multiple targets. For example, CPF and CPFO, although clustering with the endocannabinoid/nicotine group, also have many similarities and shared readouts of the cholinergic cluster. Thus, toxicity induced by CPF/CPFO could be due to shared effects on both systems. Future analysis will focus on delineating these differences by creating a behavior map, linking endpoints and phenotypic signatures with mechanisms of action. These mechanistic connections could be further substantiated by screening additional mechanistic controls, as well as antagonists to the targets of interest, to better understand the functional significance of different perturbations of the target pathways. Moreover, co-exposure of OPs with well-characterized antagonists, such as the nicotinic AChR antagonist atropine, would allow us to confirm our proposed target-endpoint connections. These future steps would be performed with both regenerating and adult planarians; thus, allowing us to also clarify the observed differences between the toxicities of the two worm types. Lastly, previous studies suggest that due to the targeting of specific developmental events, such as synaptogenesis, certain developmental periods are more sensitive to OP exposure and that the timing of OP exposure affects which adverse outcomes are observed (Dam et al., 1999; Garcia et al., 2003; Qiao et al., 2002). Thus, future experiments comparing different exposure periods over the course of planarian regeneration could further dissect whether a critical vulnerable period exists for any of the planarian endpoints affected by OP exposure to connect effects on specific developmental milestones with their functional significance.

Together, these results demonstrate a strong link between effects on non-cholinergic targets and significant organismal adverse outcomes. Realization of the significance of compound-specific non-cholinergic OP toxicity is key to better understanding and protecting against environmental OP exposure, which are often administered in mixtures. Thus, this work

substantiates the need to evaluate the toxicity of different OPs alone and in mixtures to better understand any non-additive effects that may arise from effects and interactions on non-cholinergic targets.

ACKNOWLEDGEMENTS

A modified version of Chapter 7 will be submitted for publication as a Research Article (Hagstrom, Danielle; Zhang, Siqi; and Collins, Eva-Maria S. Comparative analysis of the mechanisms of organophosphorus pesticide developmental neurotoxicity in a freshwater planarian). Danielle Hagstrom, Siqi Zhang, and Eva-Maria S. Collins designed the experiments, interpreted the data and co-wrote the manuscript. Danielle Hagstrom set up all chemicals and experiments and analyzed the data. Siqi Zhang updated the screening platform, performed the screening of the chemicals, and analyzed the data. Danielle Hagstrom and Siqi Zhang were the primary investigators and authors of this material.

REFERENCES

Atwood, D. and Paisley-Jones, C. (2017). *Pesticides Industry Sales and Usage 2008 - 2012 Market Estimates*. Washington, DC.

Birkholz, T. R. and Beane, W. S. (2017). The planarian TRPA1 homolog mediates extraocular behavioral responses to near-ultraviolet light. *J. Exp. Biol.* **220**, 2616–2625.

Burke, R. D., Todd, S. W., Lumsden, E., Mullins, R. J., Mamczarz, J., Fawcett, W. P., Gullapalli, R. P., Randall, W. R., Pereira, E. F. R. and Albuquerque, E. X. (2017). Developmental neurotoxicity of the organophosphorus insecticide chlorpyrifos: from clinical findings to preclinical models and potential mechanisms. *J. Neurochem.* **142**, 162–177.

Buttarelli, F. R., Pontieri, F. E., Margotta, V. and Palladini, G. (2002). Cannabinoid-induced stimulation of motor activity in planaria through an opioid receptor-mediated mechanism. *Prog. Neuro-Psychopharmacology Biol. Psychiatry* **26**, 65–68.

Buttarelli, F. R., Pellicano, C. and Pontieri, F. E. (2008). Neuropharmacology and behavior in planarians: Translations to mammals. *Comp. Biochem. Physiol. - C Toxicol. Pharmacol.* **147**, 399–408.

Carr, R. L., Graves, C. A., Magnum, L. C., Nail, C. A. and Ross, M. K. (2014). Low level chlorpyrifos exposure increases anandamide accumulation in juvenile rat brain in the absence of brain cholinesterase inhibition. *Neurotoxicology* **43**, 82–89.

Casida, J. E. and Quistad, G. B. (2004). Organophosphate toxicology: safety aspects of nonacetylcholinesterase secondary targets. *Chem. Res. Toxicol.* **17**, 983–998.

Cebrià, F. (2007). Regenerating the central nervous system: how easy for planarians! *Dev. Genes Evol.* **217**, 733–48.

Crumpton, T. L., Seidler, F. J. and Slotkin, T. A. (2000). Is oxidative stress involved in the developmental neurotoxicity of chlorpyrifos? *Dev. Brain Res.* **121**, 189–195.

Dam, K., Garcia, S. J., Seidler, F. J. and Slotkin, T. A. (1999). Neonatal chlorpyrifos exposure alters synaptic development and neuronal activity in cholinergic and catecholaminergic pathways. *Brain Res. Dev. Brain Res.* **116**, 9–20.

Dam, K., Seidler, F. J. and Slotkin, T. A. (2000). Chlorpyrifos exposure during a critical neonatal period elicits gender-selective deficits in the development of coordination skills and locomotor activity. *Brain Res. Dev. Brain Res.* **121**, 179–87.

Dunkel, J., Talbot, J. and Schötz, E.-M. (2011). Memory and obesity affect the population dynamics of asexual freshwater planarians. *Phys. Biol.* **8**, 026003.

EUROSTAT (2016). *Agriculture, forestry and fishery statistics - 2016 edition*. (ed. Forti, R.) and Henrard, M.) Luxembourg, Belgium: European Union.

Flaskos, J. (2012). The developmental neurotoxicity of organophosphorus insecticides: a direct role for the oxon metabolites. *Toxicol. Lett.* **209**, 86–93.

Flaskos, J. (2014). The neuronal cytoskeleton as a potential target in the developmental neurotoxicity of organophosphorothionate insecticides. *Basic Clin. Pharmacol. Toxicol.* **115**, 201–8.

Gamaleddin, I. H., Trigo, J. M., Gueye, A. B., Zvonok, A., Makriyannis, A., Goldberg, S. R. and Le Foll, B. (2015). Role of the endogenous cannabinoid system in nicotine addiction: novel insights. *Front. psychiatry* **6**, 41.

Garcia, S. J., Seidler, F. J. and Slotkin, T. A. (2003). Developmental neurotoxicity elicited by prenatal or postnatal chlorpyrifos exposure: Effects on neurospecific proteins indicate changing vulnerabilities. *Environ. Health Perspect.* **111**, 297–303.

González-Alzaga, B., Lacasaña, M., Aguilar-Garduño, C., Rodríguez-Barranco, M., Ballester, F., Rebagliato, M. and Hernández, A. F. F. (2014). A systematic review of neurodevelopmental effects of prenatal and postnatal organophosphate pesticide exposure. *Toxicol. Lett.* **230**, 104–121.

Hagstrom, D., Cochet-Escartin, O., Zhang, S., Khuu, C. and Collins, E.-M. S. (2015). Freshwater planarians as an alternative animal model for neurotoxicology. *Toxicol. Sci.* **147**, 270–285.

Hagstrom, D., Cochet-Escartin, O. and Collins, E.-M. S. (2016). Planarian brain regeneration as a model system for developmental neurotoxicology. *Regeneration* **3**, 65–77.

Hagstrom, D., Hirokawa, H., Zhang, L., Radić, Z., Taylor, P. and Collins, E.-M. S. (2017). Planarian cholinesterase: in vitro characterization of an evolutionarily ancient enzyme to study organophosphorus pesticide toxicity and reactivation. *Arch. Toxicol.* **91**, 2837–2847.

Hagstrom, D., Zhang, S., Ho, A., Tsai, E. S., Radić, Z., Jahromi, A., Kaj, K. J., He, Y., Taylor, P. and Collins, E. M. S. (2018). Planarian cholinesterase: molecular and functional characterization of an evolutionarily ancient enzyme to study organophosphorus pesticide toxicity. *Arch. Toxicol.* **92**, 1161–1176.

Inoue, T., Yamashita, T. and Agata, K. (2014). Thermosensory signaling by TRPM is processed by brain serotonergic neurons to produce planarian thermotaxis. *J. Neurosci.* **34**, 15701–14.

Jiang, W., Duysen, E. G., Hansen, H., Shlyakhtenko, L., Schopfer, L. M. and Lockridge, O. (2010). Mice treated with chlorpyrifos or chlorpyrifos oxon have organophosphorylated tubulin in the brain and disrupted microtubule structures, suggesting a role for tubulin in neurotoxicity associated with exposure to organophosphorus agents. *Toxicol. Sci.* **115**, 183–193.

Liu, J., Parsons, L. and Pope, C. (2013). Comparative effects of parathion and chlorpyrifos on extracellular endocannabinoid levels in rat hippocampus: Influence on cholinergic toxicity. *Toxicol. Appl. Pharmacol.* **272**, 608–615.

Malinowski, P. T., Cochet-Escartin, O., Kaj, K. J., Ronan, E., Groisman, A., Diamond, P. H. and Collins, E.-M. S. (2017). Mechanics dictate where and how freshwater planarians fission. *Proc. Natl. Acad. Sci. U. S. A.* **114**, 10888–10893.

Mamczarz, J., Pescrille, J. D., Gavrushenko, L., Burke, R. D., Fawcett, W. P., DeTolla, L. J., Chen, H., Pereira, E. F. R., Albuquerque, E. X. and Albuquerque, E. X. (2016). Spatial learning impairment in prepubertal guinea pigs prenatally exposed to the organophosphorus pesticide chlorpyrifos: Toxicological implications. *Neurotoxicology* **56**, 17–28.

Moser, V. C. (1995). Comparisons of the acute effects of cholinesterase inhibitors using a neurobehavioral screening battery in rats. *Neurotoxicol. Teratol.* **17**, 617–625.

Muñoz-Quezada, M. T., Lucero, B. A., Barr, D. B., Steenland, K., Levy, K., Ryan, P. B., Iglesias, V., Alvarado, S., Concha, C., Rojas, E., et al. (2013). Neurodevelopmental effects in children associated with exposure to organophosphate pesticides: a systematic review. *Neurotoxicology* **39**, 158–168.

Nishimura, K., Kitamura, Y., Taniguchi, T. and Agata, K. (2010). Analysis of motor function modulated by cholinergic neurons in planarian Dugesia japonica. *Neuroscience* **168**, 18–30.

Paskin, T. R., Jellies, J., Bacher, J. and Beane, W. S. (2014). Planarian phototactic assay reveals differential behavioral responses based on wavelength. *PLoS One* **9**, e114708.

Pope, C. N. (1999). Organophosphorus pesticides: do they all have the same mechanism of toxicity? *J. Toxicol. Environ. Health. B. Crit. Rev.* **2**, 161–81.

Pope, C., Karanth, S. and Liu, J. (2005). Pharmacology and toxicology of cholinesterase inhibitors: uses and misuses of a common mechanism of action. *Environ. Toxicol. Pharmacol.* **19**, 433–446.

Qiao, D., Seidler, F. J., Padilla, S. and Slotkin, T. A. (2002). Developmental neurotoxicity of chlorpyrifos: what is the vulnerable period? *Environ. Health Perspect.* **110**, 1097–103.

Rauh, V., Arunajadai, S., Horton, M., Perera, F., Hoepner, L., Barr, D. B. and Whyatt, R. (2011). Seven-year neurodevelopmental scores and prenatal exposure to chlorpyrifos, a common agricultural pesticide. *Environ. Health Perspect.* **119**, 1196–1201.

Ribeiro, P., El-Shehabi, F. and Patocka, N. (2005). Classical transmitters and their receptors in flatworms. *Parasitology* **131**, S19-40.

Richendrfer, H. and Creton, R. (2015). Chlorpyrifos and malathion have opposite effects on behaviors and brain size that are not correlated to changes in AChE activity. *Neurotoxicology* **49**, 50–58.

Ross, K. G., Currie, K. W., Pearson, B. J. and Zayas, R. M. (2017). Nervous system development and regeneration in freshwater planarians. *Wiley Interdiscip. Rev. Dev. Biol.* **6**, 1–26.

Russom, C. L., LaLone, C. A., Villeneuve, D. L. and Ankley, G. T. (2014). Development of an

adverse outcome pathway for acetylcholinesterase inhibition leading to acute mortality. *Environ. Toxicol. Chem.* **33**, 2157–2169.

Shelton, J. F., Geraghty, E. M., Tancredi, D. J., Delwiche, L. D., Schmidt, R. J., Ritz, B., Hansen, R. L. and Hertz-Picciotto, I. (2014). Neurodevelopmental disorders and prenatal residential proximity to agricultural pesticides: the CHARGE study. *Environ. Health Perspect.* **122**, 1103–9.

Singh, N., Lawana, V., Luo, J., Phong, P., Abdalla, A., Palanisamy, B., Rokad, D., Sarkar, S., Jin, H., Anantharam, V., et al. (2018). Organophosphate pesticide chlorpyrifos impairs STAT1 signaling to induce dopaminergic neurotoxicity: Implications for mitochondria mediated oxidative stress signaling events. *Neurobiol. Dis.* **117**, 82–113.

Slotkin, T. A., Levin, E. D. and Seidler, F. J. (2006). Comparative developmental neurotoxicity of organophosphate insecticides: Effects on brain development are separable from systemic toxicity. *Environ. Health Perspect.* **114**, 746–751.

Slotkin, T. A., Skavicus, S. and Seidler, F. J. (2017). Diazinon and parathion diverge in their effects on development of noradrenergic systems. *Brain Res. Bull.* **130**, 268–273.

Taylor, P. (2018). Anticholinesterase agents. In *Goodman and Gilman's The Pharmacological Basis of Therapeutics* (ed. Laurence L Brunton), pp. 163–176. San Francisco: McGraw Hill Education.

Yang, D., Howard, A., Bruun, D., Ajua-Alemanj, M., Pickart, C. and Lein, P. J. (2008). Chlorpyrifos and chlorpyrifos-oxon inhibit axonal growth by interfering with the morphogenic activity of acetylcholinesterase. *Toxicol. Appl. Pharmacol.* **228**, 32–41.

Yen, J., Donerly, S., Linney, E. A., Levin, E. D. and Linney, E. A. (2011). Differential acetylcholinesterase inhibition of chlorpyrifos, diazinon and parathion in larval zebrafish. *Neurotoxicol. Teratol.* **33**, 735–741.

Zarei, M. H., Soodi, M., Qasemian-Lemraski, M., Jafarzadeh, E. and Taha, M. F. (2015). Study of the chlorpyrifos neurotoxicity using neural differentiation of adipose tissue-derived stem cells. *Environ. Toxicol.*

Zhang, S., Hagstrom, D., Hayes, P., Graham, A. and Collins, E.-M. S. (2018). Multi-behavioral endpoint testing of an 87-chemical compound library in freshwater planarians. *Toxicol. Sci.*

Chapter 8: Conclusion and future outlook

CONCLUSION

In this dissertation, I have shown that the asexual freshwater planarian, *D. japonica*, is a promising alternative animal model for developmental neurotoxicology. In addition to the strengths shared by most alternative animal models, such as short developmental time and low-cost to breed and screen, planarians possess several unique characteristics that are unmatched in other currently used systems. These include the ability to dissect defects on specific neuronal subpopulations and functions through their large repertoire of quantifiable behaviors and the ability to directly compare effects between adult and regenerating/developing animals. Together, these unique strengths have allowed us to connect molecular and cellular mechanisms of toxicity with their functional effects on organismal behavior, as exemplified in our proof-of-concept screen in Chapter 2, NTP 87-compound library screen in Chapters 3 and 4, and most strongly in the comparative screen of organophosphorus pesticides (OPs) in Chapter 7.

Moreover, by comparing results gained in our system from those in other alternative models, such as zebrafish, and traditional mammalian models, discussed in Chapter 4, we have demonstrated that planarians are a valuable complement to the modern toxicology pipeline. While developing zebrafish have a multitude of morphological endpoints, planarians possess multiple different types of quantifiable behavioral endpoints which are amenable to automated high-throughput screening to delineate specific versus general neurotoxicity, as well as developmental versus general neurotoxicity. As with any model, it is important to understand the strengths and weaknesses of the system so that it can be used effectively going forward. For example, planarians are an inadequate system to study polycyclic aromatic hydrocarbons, because they lack the relevant targets and thus absence of toxicity must be interpreted accordingly. Planarians are, however, a sensitive and powerful model to evaluate the effects of

pesticides. In the NTP 87-compound library screen presented in Chapters 3 and 4, we found that developmental neurotoxicity observed in the planarian system was highly concordant with effects observed in mammalian models. For example, we found that Chlorpyrifos (CPF), the most widely used OP and one of most highly used pesticides in the world, caused developmentally-selective effects on planarian neuronal function. This is in agreement with growing concerns over the potential irreversible damage to infant and children brains that has been correlated with chronic environmental exposure to CPF. However, CPF is only one of many OPs, and it is debated whether all OPs damage the developing brain in the same way. To this point, we found in our proof of concept screen presented in Chapter 2, that different OPs had differential toxicities and increased potency on regenerating animals. Together, our initial findings suggested that planarians would be an apt model to delve into the mechanisms underlying compound-specific developmental neurotoxicity caused by OPs.

As acetylcholinesterase (AChE), the shared target of all OPs, had not been previously characterized in planarians, we identified the putative genes responsible for cholinesterase activity in *D. japonica*, termed DjChE. Studies of the enzymatic (Chapter 5) and molecular and functional characteristics (Chapter 6) revealed DjChE activity was sensitive to inhibition by OPs and that knockdown of DjChE activity could recapitulate some, but not all, phenotypes of subacute OP toxicity, suggesting some alternative mechanisms of toxicity are likely also involved. Delving further into the mechanisms of toxicity of 6 OPs, our preliminary results suggest that other mechanisms, such as activation of the endocannabinoid system, can also play a major role in the neurotoxicity of some OPs. Moreover, we find that the extent that certain mechanisms are involved also differs between adult and regenerating planarians, suggesting some developmental-specific effects. Together, our results provide exciting insights into

compound-specific mechanisms of OP developmental neurotoxicity and lay the groundwork for in depth mechanistic studies in planarians and mammalian models, which are necessary to effectively protect children from harmful OP exposure.

FUTURE OUTLOOK

First, we must perform a more detailed mechanistic comparative analysis of the OP toxicity presented in Chapter 7. Preliminary analysis using Ward's method of clustering, suggests the developmental neurotoxicity observed with the 6 OPs tested mainly clusters into 3 mechanistic groups: 1) cholinergic stimulation, 2) endocannabinoid stimulation and 3) other. However, to provide a more nuanced and unbiased analysis, principle component analysis (PCA) will be performed to delineate how the different OPs and various control chemicals affecting different pathways segregate. By reducing the multi-variate data, consisting of 21 different endpoints, into its principal components, we will not only simplify the analysis but can uncover which endpoints (or set of endpoints) are the most important and predictive for mechanistic classifications. In the context of OPs, this will allow us to dissect the relative importance of different mechanisms in the differential manifestations of OP developmental neurotoxicity and may provide novel insight into the importance that non-cholinergic mechanisms can play. Identification of key alternative targets with functional significance, thus, opens the door for strategic, targeted mechanistic studies in mammalian models to validate whether results in planarians are relevant to human health. Of note, increasing the efficiency of the toxicology pipeline through first-tier screening in non-mammalian models, such as described for planarians, is an important goal for the U.S. Environmental Protection Agency (EPA), as evidenced by the recent release of a Strategic Plan, as part of the Toxic Substances Control Act, to promote the "development and implementation of alternative test methods to reduce, refine, or replace

vertebrate animal testing" (https://www.federalregister.gov/documents/2018/03/12/2018-04938/tsca-alternative-testing-methods-draft-strategic-plan-notice-of-availability-and-notice-of-public). In the larger context of the planarian system moving forward, connecting relevant pathways often targeted by toxicants with specific phenotypic readouts will allow us to create a behavior map linking targets with their phenotypic signatures and provide a rubric to compare to compounds of unknown toxicity. Thus, the planarian screening platform could become a powerful tool by which to rapidly and effectively evaluate bioactivity of so far untested compounds and contextualize in regards to mechanism. This would open up a large realm of possibilities, providing utility not only for toxicology but also for drug discovery, particularly for neuroactive compounds.

To get to this goal, although much of the ground work has been completed to establish freshwater planarians as an alternative animal model for high-throughput phenotypic screening, further work is needed to properly validate the system and understand important pharmacokinetic (PK) properties underlying all toxicity. System validation requires understanding the robustness of the system and its relative sensitivity to other models. Ultimately, to be useful as a model, planarians should be predictive of toxicity in mammals, and particularly in humans. To understand whether this is true, screening of many well-characterized toxicants with known toxicities in other systems should be performed. For example, the EPA has established a list of approximately 100 compounds with substantial evidence of developmental neurotoxicity in mammalian studies. These compounds, some of which were also contained in the NTP 87-compound library, could be screened in the planarian system and directly compared to the data-rich animal studies. One difficulty herein is that many of these environmentally important toxicants, such as CPF, may have widespread toxic effects due to effects on multiple, possibly

unknown, molecular targets. Thus, in addition, screening of additional "control" chemicals with known targeted effects should also be performed to bolster the planarian phenotypic map. These could include more chemicals affecting the targets we have already screened, including the endocannabinoid system, cytoskeleton, and oxidative stress, as well as additional chemicals which affect other important toxicological targets (such as mitochondria or glia) or neurodevelopmental pathways (such as differentiation, axonal transport, axon guidance, inflammation, etc.). In addition, true negative compounds which have not shown toxicity in other systems should also be tested to understand the sensitivity and false positive rate of the planarian system. As our mechanistic knowledge increases, more sophisticated data analysis techniques, such as machine learning, may be needed to differentiate phenotypic signatures. Excitingly, this also means that the power of the planarian screening platform should increase over time as the more data gets incorporated into the behavioral map database the better predictions of unknown toxicity should become.

Whether a compound is deemed toxic is ultimately dependent on the dose necessary to cause adverse effects. Although first-pass hazard screening can be done without detailed dose comparisons, to be able to accurately and quantitatively compare toxic doses in planarians with those in other models, and connect to relevant human exposures, will require an understanding of the PK characteristics of the system, including how compounds are absorbed, distributed throughout the body, metabolized, and eliminated. In this way, comparisons can be made between the actual (or estimated) concentrations at the relevant site of actions between systems, and not just the nominal exposure dose. Initially, the precise PK parameters do not need to be characterized per se, as useful comparisons can be made by directly measuring the internal concentrations found within the planarians after toxicologically relevant exposures. This will

provide valuable information to determine whether results in different systems are generally comparable. However, since this would likely require expensive and low-throughput mass-spectroscopy, this could only be performed on a limited number of compounds and doses, but could be used for smaller targeted studies or to test characteristic chemical traits (e.g. high versus low hydrophobicity, large versus small molecular weight, etc.). In the long term, it would benefit the system to understand all the variables which determine these internal concentrations, including, but not limited to, absorption rate for different types of chemicals and routes of uptake, presence of various metabolic enzymes (cytochrome P450, carboxylesterase, p-glycoprotein, etc.), and elimination rates. However, sophisticated PK modeling algorithms exist which could potentially allow us to estimate many of these parameters based on what has already been experimentally determined in other animal models. PK modeling would then allow us to predict internal concentrations and estimate toxicodynamics for any chemical as long as the chemistry is known, increasing the predictive power of the system since findings could be put into their dose context. This would allow for direct comparisons with other alternative systems, such as zebrafish, gold-standard rodent systems, and even human exposure.

We ultimately envision planarians as a component of initial first-tier screening batteries, along with cell culture systems and zebrafish. Comparative screens in these models will provide strong weight-of-evidence to identify and prioritize hazardous compounds for further in depth testing. Beyond hazard identification, the proposed additions will strengthen the planarian system to contextualize toxicity by connecting phenotypic effects with mechanism. Thus, initial screening in planarians will provide the necessary foundation for strategic testing in second-tier mammalian studies, helping to reduce, refine, or replace vertebrate animal testing in the toxicology pipeline.

Appendix: Studying planarian regeneration aboard the International Space Station within the Student Space Flight Experimental Program

Reprinted from: Vista SSEP Mission 11 Team; Hagstrom, Danielle; Bartee, Christine; and Collins, Eva-Maria S. “Studying planarian regeneration aboard the International Space Station within the Student Space Flight Experiment Program”, Frontiers in Astronomy and Space Sciences, vol. 5, 2018.

ABSTRACT

The growing possibilities of space travel are quickly moving from science fiction to reality. However, to realize the dream of long-term space travel, we must understand how these conditions affect biological and physiological processes. Planarians are master regenerators, famous for their ability to regenerate from very small parts of the original animal. Understanding how this self-repair works may inspire regenerative therapies in humans. Two studies conducted aboard the International Space Station (ISS) showed that planarian regeneration is possible in microgravity. One study reported no regenerative defects, whereas the other study reported behavioral and microbiome alterations post-space travel and found that 1 of 15 planarians regenerated a Janus head, suggesting that microgravity exposure may not be without consequences. Given the limited number of studies and specimens, further microgravity experiments are necessary to evaluate the effects of microgravity on planarian regeneration. Such studies, however, are generally difficult and expensive to conduct. We were fortunate to be sponsored by the Student Spaceflight Experiment Program (SSEP) to investigate how microgravity affects regeneration of the planarian species Dugesia japonica on the ISS. While we were unable to successfully study planarian regeneration within the experimental constraints of our SSEP Mission, we systematically analyzed the cause for the failed experiment, leading us to propose a modified protocol. This work thus opens the door for future experiments on the effects of microgravity on planarian regeneration on SSEP Missions as well as for more advanced experiments by professional researchers.

INTRODUCTION

Space travel and inhabitation capture the human imagination. They also pose biological and engineering challenges that are not encountered on Earth. The National Center for Earth and Space Science Education (NCESSE) runs the Student Spaceflight Experiment Program (SSEP) for students from different communities, including Grades 5-12, community colleges, and universities "to inspire the next generation of scientists and engineers" (http://ssep.ncesse.org). A key aspect of the program is to have students work like "real scientists", and be involved in all parts of the scientific process, including conceptualization and design of a scientific experiment, participating in a two-step proposal competition, and performing the actual experiment while learning to work within financial and experimental constraints. Students design an experiment that can be from a number of fields, including geosciences, biology, physics, and physiology, which can be completely contained within a "MixStix mini-laboratory" consisting of a proprietary Teflon fluids mixing enclosure (FME) tube (Nanoracks). This enclosure can hold up to three separate sample materials, separated by clamps that can be opened to allow mixing of the components (http://nanoracks.com/products/mixstix/). The SSEP experiments had to be designed such that they could be conducted with a single interaction (unclamping) between the astronauts and the tube on a specific date (limited to 5 possible options) and allow for an initial dormancy period (approximately 2 weeks) while the experiments were transported to the ISS.

Since its inception in 2010, the SSEP program has conducted ten Space Missions. Biological specimens used in these missions have included various species of insects, worms, echinoderms and fish. The life cycles of many of these species allow for experiments to be conducted by placing eggs or larvae, often in a dormant state, in the FME tubes. Development can then be initiated in space, such as by the switch from cold to ambient storage, to determine

the effects of microgravity on these processes. The outcomes of these studies, however, remain largely unknown, because student teams primarily report at the Annual SSEP Conference *prior to* the flight experiment and thus post-flight results are often not publically available. According to the SSEP website, 76 biological experiments have been presented at the Annual SSEP conference between 2012-2017. However, of these, only about a quarter reported results and about half of those were inconclusive due to limited time, tube space or sample size.

To the best of our knowledge, the results of only one biological SSEP experiment have been published (Warren et al., 2013). In this study, the authors used an earlier version of the FME mini-lab system with *Caenorhabditis elegans* to study the effect of the transcription factor DAF-16 on previously reported genomic expression changes induced by spaceflight in *C. elegans.* While the study was unsuccessful, partially due to incorrect activation of the experiment in space, it established that nematode viability could be maintained in the FME system for a maximum of three weeks (Warren et al., 2013).

Our experiment, as part of the 2017 SSEP Mission 11, aimed to test the effect of microgravity on the regeneration of freshwater planarians of the species *Dugesia japonica*. To fulfill the SSEP requirements, the experiment was designed such that planarians were amputated on Earth and the resulting tail pieces were kept dormant at 4 °C during transportation to the ISS, where they were moved to ambient temperature to initiate regeneration in microgravity. Regeneration was terminated by the astronauts after 2-4 weeks by releasing a fixing agent, formaldehyde, from the second compartment. Upon sample retrieval, the microgravity sample was compared with Earth laboratory controls.

Studying invertebrate regeneration is a popular experiment in schools because students can readily engage with this fascinating phenomenon. Planarians are particularly interesting,

because they can regenerate a complete animal, including eyes and a fairly complicated brain, from small fragments of the original body within 7-12 days (Cebrià, 2007; Morgan, 1989). While this process is quite robust, regeneration can be influenced by molecular (Reddien et al., 2005), chemical (Best and Morita, 1982; Hagstrom et al., 2015; Hagstrom et al., 2016) and physical factors (Brondsted and Brondsted, 1961; Marsh and Beams, 1952; Novikov et al., 2008).

To the best of our knowledge, only three studies have investigated the role of gravity in planarian regeneration. While one study found that extended exposure to simulated microgravity is generally detrimental to planarian health (Adell et al., 2014), others have shown that planarians are able to regenerate fully under these conditions (Gorgiladze, 2008; Morokuma et al., 2017). Notably, while Adell et al. conducted their experiments on Earth using a random positioning machine to mimic space conditions, Gorgiladze and Morokuma et al. performed their experiments on board the ISS. It is also worth noting that lethality in the simulated microgravity experiments only occurred under specific rotation conditions (i.e. 60º/s but not 10º/s) and after long-term exposure (13 days) (Adell et al., 2014), which may not be representative of actual space conditions. Furthermore, the planarian species differed in each of the three studies, complicating direct comparisons of the results, especially since species-specific sensitivities to spatial confinement have been reported (Carter et al., 2015). Adell et al. used *Schmidtea mediterranea*, Gorgiladze used *Dugesia tigrina*, and Morokuma et al. used *Dugesia japonica*, the same planarian species used in this study. While neither study on board the ISS found planarians incapable of regeneration, differences in the findings nevertheless exist. Gorgiladze reported no regeneration defects monitoring 60 planarians. In contrast, Morokuma et al. found 1 of 15 planarians regenerated into a two-headed animal, which is a rare event that the authors never observed in the approximate 15,000 planarians they cultured in the laboratory over the past 5

years. Similarly, we have never observed such a phenotype in our toxicology screens (Hagstrom et al., 2015), which also comprise thousands of *D. japonica* planarians. Furthermore, Morokuma et al showed long-term behavioral and microbiotic changes that were attributed to space travel (Morokuma et al., 2017). Taken together, the discrepancies in the existing studies call for further experiments to determine the effects of microgravity on planarian regeneration and physiology. However, these experiments are expensive and difficult to realize. The SSEP, thus, provides a unique opportunity to address these kinds of intriguing questions by facilitating and engaging aspiring young scientists in the scientific process.

In this paper, we report our experiences conducting a planarian regeneration experiment within SSEP. Because of the lack of published SSEP experiments, we could not build upon prior work to optimize our experimental protocol. Correspondence with the SSEP Director at the 2017 Annual SSEP Conference revealed that all previous planarian regeneration experiments had failed. Because our experiment was similarly unsuccessful, our goal is to explain why it failed and how it could be improved to allow for future successful studies within the experimental constraints imposed by the SSEP program.

MATERIALS AND METHODS

Animals

Asexual planarians of the species *Dugesia japonica* were used for the experiments. Planarians were maintained in bulk in Instant Ocean (IO)-water, fed organic chicken or beef liver once a week and cleaned twice a week, as previously described (Hagstrom et al., 2017). Animals were starved for at least 5 days before being used for an experiment. Animals used for experiments were 6.9 ±1.1 mm (mean ± standard deviation) in length. To induce regeneration, intact animals were amputated between the auricles and pharynx with an ethanol-sterilized razor blade as in Hagstrom et al. (2015). The heads were returned to the animal stocks and the tails were allowed to heal for 1 hour before loading into the tubes.

Fluids Mixing Enclosure (FME) Type 2

The Type 2 Fluids Mixture Enclosure (FME) Mark II Mini Laboratory was used for SSEP Mission 11 to the ISS. The silicone tube is 170 mm long with an outer diameter of 13 mm and an inner diameter of 9.5 mm. The Type 2 FME tube can be subdivided into two or three separate compartments through the use of clamps. The total volume of sample the Type 2 FME can hold is 9.2 ml. For the planarian experiments, each FME tube was split into two compartments: an 8 ml compartment containing the animals and a 1 ml compartment containing 37% formaldehyde (Fisher Scientific, Waltham, MA). NCESSE shipped 5 Fluids Mixing Enclosure Mini-lab Kits to each participating community. Three were reserved for the selected flight (1 tube) and ground (2 tubes) truth experiments.

Pre-experiment: Regeneration Test at 4 ºC

To support the experimental proposal, we conducted an initial test to determine the degree of regeneration at 4 ºC of *D. japonica* planarians. This test was performed using 5 ml

plastic culture tubes (Falcon, Corning, NY), since FME tubes were not available prior to proposal approval. 10 *D. japonica* tails were placed in a parafilm-sealed tube in 4 ºC refrigeration in the dark. A second set of 10 *D. japonica* tails were prepared the same way and placed at room temperature (RT) in the dark. The tubes were filled approximately to the top, but without an exact measurement of the volume added, thus leaving varying amounts (up to 20%) of air. After two weeks, both samples were compared using a Leica S6 trinocular stereo microscope (Wetzlar, Germany) equipped with a Basler A601f camera (Basler, Germany). This comparison revealed that all planarians were able to survive two-week enclosure at either temperature and that minimal regeneration occurred during incubation at 4 ºC (Figure A.1A-B).

Pre-experiment: Viability Test in FME Tubes

During the experimental design phase, one FME tube was prepared with 5 tails and one FME tube was prepared with 10 tails to determine how many worm pieces could survive in a single FME tube. A critical difference from the actual flight experiment was that formaldehyde was not placed in the second volume of the FME tube, since only the effect of lack of oxygen on worm viability was tested. Both FME tubes were kept at 4 ºC for 3 weeks and then moved to ambient temperature. After two more weeks at ambient temperature, the tube containing 5 worms was emptied and the worms evaluated (Figure A.1C-E). In this tube, 4 worms were found alive with 3 out of the 4 regenerating normal. The 4th worm had a closed wound but no blastema (Figure A.1C). The worms in the second FME tube were fixed by adding 1 ml formaldehyde. The planarians were analyzed the following day after incubation overnight at 4 ºC. All 10 worms were still present. 6 of them had regenerated 2 eyes and 4 had no eyes. Thus, while lack of oxygen appeared to affect their ability to regenerate properly, planarians were able to survive 5 weeks in the FME tube without formaldehyde in the second chamber.

Pre-launch Preparation

The FME tubes were rinsed thoroughly with IO-water in the laboratory. On July 24, 2017, thirty *D. japonica* were decapitated between the auricles and the pharynx with an ethanol-sterilized razor blade in IO-water. The animals were allowed to close the wound for 1 hour. Pre-chilled (4 ºC) Crystal Geyser (CG) spring water was aerated by pouring back and forth between two glass beakers at least 5 times. 10 *D. japonica* tails were added to each of the three FME tubes with 8 ml of pre-chilled CG water. CG-water was used instead of IO-water because it was commercially available.

1 ml of 37% formaldehyde was added to the second chamber of each FME tube so the planarians could be fixed, and thus end the experiment, after sufficient time for regeneration in microgravity. The two ground truth FME tubes were sealed and stored horizontally at 4 ºC for 25 days. The flight experiment FME tube was placed in a Cold Shipping Package at 2-8 ºC for transport to Nanoracks in Houston. The FME was refrigerated at approximately 2-4 ºC until handover to NASA. This allowed the experiment to be kept in a dormant state until arrival on the ISS.

Flight Experiment on the ISS

SpaceX CRS-12 launched from Space Launch Complex 39 at Cape Canaveral Air Force Station, Florida on August 14, 2017. The mini-labs were captured by the ISS on August 16, 2017 with subsequent unloading to ambient temperature (21 - 24 ºC) on August 17, 2017. The two ground truth experiments in the laboratory were transferred to ambient temperature in the dark on the same day.

After three weeks in microgravity, an ISS crew member performed the U-14d interaction on September 4, 2017 by opening the clamp that separated the planarians and formaldehyde, and

shaking vigorously for 5 seconds to release the formaldehyde, thus terminating and preserving the experiment in microgravity. The two ground truth experiments in the laboratory were treated using similar actions on the same day.

Post-flight Analysis

On the day of harvesting, the liquid was poured into Petri dishes for analysis. All planarians in both ground truth and flight experiments had disintegrated. Images of the disintegrated pieces were taken with a Leica KL300 LED dissecting microscope and Point Grey Flea3 color camera (FLIR Systems Inc., Wilsonville, OR).

Post-flight: FME Viability Test

To assay which factors may have contributed to worm death during the experiment, additional post-flight experiments were performed. New FME tubes were set up as described in Table 1. Specifically, we assayed the effects of the presence of formaldehyde, presence of air, and tube type. Of note, due to the high cost of FME tubes, when possible and appropriate, certain conditions were tested repeatedly in the same FME tube, with extensive washing before loading new worms. When repeating conditions which contained formaldehyde, the original formaldehyde compartment was left intact. For the tube type experiments, we used 5 ml culture tubes (VWR International, Radnor, PA) containing 6 tails and 5 ml of CG spring water and 9 ml glass borosilicate tubes (Corning, Corning, NY) containing 10 tails and 9 ml spring water to keep the worm:volume ratio relatively constant. Experiments were stored at 4 °C for 2-3 weeks and then, when possible, moved to RT for an additional 2-3 weeks (5 weeks total). Planarian viability was checked by eye every 3-4 days.

RESULTS

The goal of this study was to analyze the effect of microgravity on planarian head regeneration. Ideally, planarians would be amputated on board the ISS and then their regeneration documented. This, however, was not possible within the constraints of the SSEP, which only allowed a single interaction of the astronauts with the experiment. Therefore, we designed an experimental protocol where the worms would be amputated on Earth before loading into 8 ml pre-chilled spring water on one side of the FME tube and adding 1 ml of 37% formaldehyde on the other side, separated by a clamp (Figure A.3A, B and Methods). Because the Mission 11 SSEP timeline consisted of an initial 2.5 week period at 4 ºC for transport of the flight FME tubes to Nanoracks and the ISS, the amputated planarians needed to be dormant or in stasis until arrival on the ISS. While it was expected that regeneration would be delayed at colder temperatures (Brondsted and Brondsted, 1961), it was uncertain whether we could sufficiently delay it for such a long time. Furthermore, the regenerating planarians needed to be able to survive without oxygen for 2.5 weeks at 4 ºC, followed by an additional 2-4 weeks at RT on board the ISS before fixation with formaldehyde would occur to stop the experiment. Given these experimental constraints, we conducted several pre-flight experiments to assay (a) the planarians' ability to survive and regenerate in an enclosed tube for such a long time, and (b) the extent of regeneration occurring during storage at 4ºC.

Pre-flight Experiments

To test whether planarian regeneration could be put in a dormant state, we conducted a comparative study of regeneration at 4 ºC and RT, as described in Materials and Methods. First, we evaluated how long the regenerating worms were able to survive without oxygen. Under these conditions, all planarians survived in enclosed tubes for 2 weeks at either 4 °C or RT.

While some studies have shown limited survival in enclosed conditions, with worms disintegrating within 5 days at a density of 0.2 worms/ml at 10 ºC or 20 ºC without any oxygen (Morokuma et al., 2017), our preliminary experiments using 2 worms/ml at 4 ºC and RT have shown that 2 week enclosure was possible. Moreover, a comparison of 10 *D. japonica* tails stored at 4 ºC versus at RT for 2 weeks, under otherwise identical conditions, showed that regeneration was sufficiently delayed, so the 2-weeks transport time to the ISS would not lead to significant regeneration. Planarians stored at 4 ºC showed only a small blastemal tissue and no eyes whereas worms stored at RT had fully regenerated (Figure A.1A and B). Further, we confirmed that at least 10 regenerating tail pieces could survive enclosed in the FME tubes when stored for three weeks at 4 °C, followed by two weeks at RT (Figure A.1C-E and Materials and Methods). However, some of the enclosed animals did show regeneration defects (Figure A.1C).

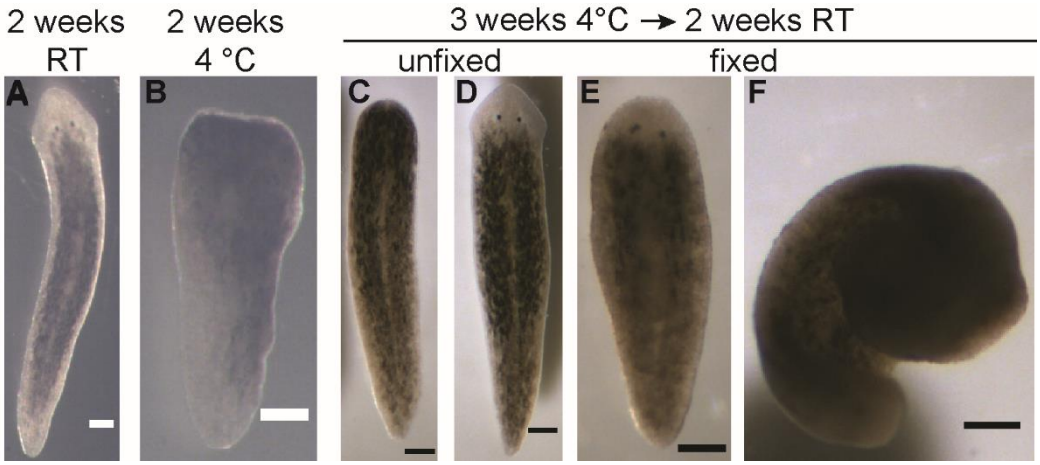

Figure A.1. Pre-flight experiments on planarian viability and regeneration. (A) Representative image of a regenerated planarian, from an original tail piece, stored in a sealed 5 ml culture tube for 2 weeks at RT. (B) Representative image of a planarian tail piece which had not regenerated after being stored in a sealed 5 ml culture tube for 2 weeks at 4 °C. (C-D) Either 5 or 10 planarian tail pieces were stored in the FME tubes for 3 weeks at 4 °C, followed by an additional 2 weeks at RT. (C) Representative image of a planarian which failed to regenerate during this time as no blastema has formed. (D) Representative image of a successfully regenerated planarian. (E, F) Representative images of planarians that were fixed following storage in the FME tubes. While some planarians were fixed extended (E), others curled up (F). Scale bars: 0.25 mm.

Finally, we confirmed that the one-step fixation of the regenerated tails using formaldehyde would work for our purposes, since standard planarian fixation protocols contain a mucus-removal step before the administration of formaldehyde or other fixatives (Pearson et al., 2009; Umesono et al., 1997). While some of the planarians remained straight (Figure A.1E), others curled up during fixation (Figure A.1F), making imaging difficult. However, in those cases we were still able to manually determine whether the tails had fully regenerated and quantify the number of eyes. We therefore deemed the protocol adequate given the experimental constraints imposed by the mission, which prohibited a multiple step fixation procedure.

Flight and Ground Control Experiments

On July 24, 2017, two ground control and one flight experiment were prepared in the FME tubes as described in Materials and Methods (Figure A.2). The flight experiment was sent to Nanoracks, LLC and the ISS according to the timeline in Figure A.2E. The ground truth controls were kept on the ground at 4 ºC in the dark and the necessary actions (movement to RT and unclamping of the tube) were performed on the same days as in the flight experiment. Of note, the original launch was scheduled for August 10, but was delayed until August 14. This caused the planarians to be stored 5 additional days at 4 ºC, which was not planned for in the original experiment.

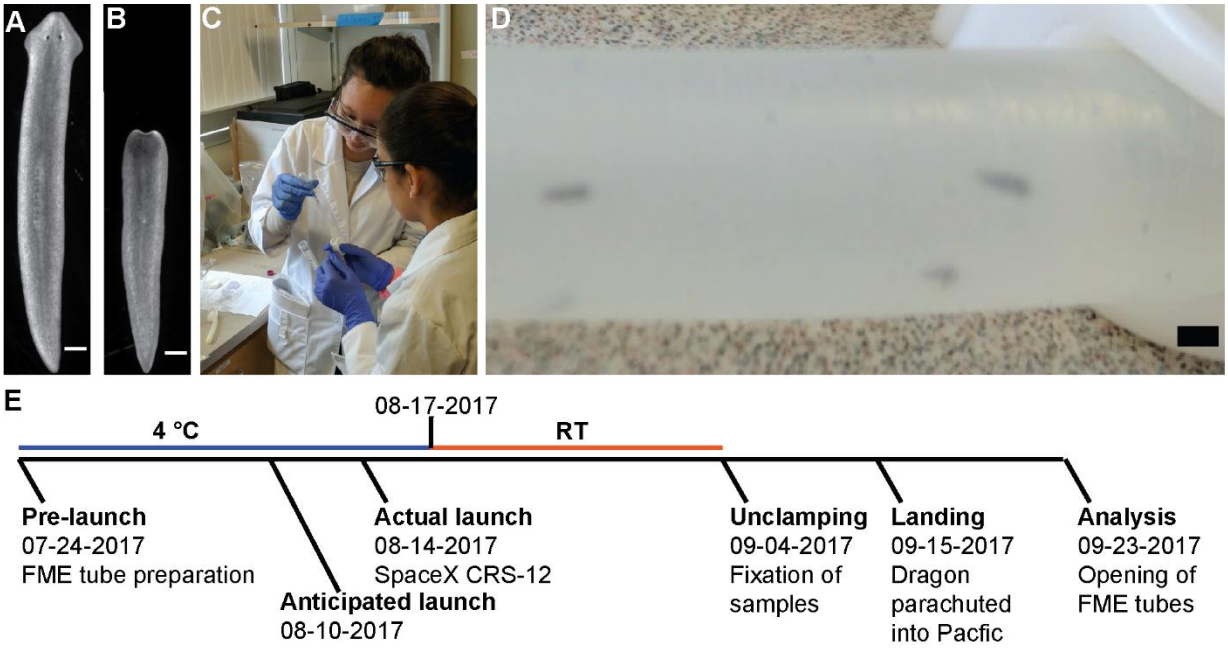

Figure A.2. Setup and timeline of experiment. (A-B) Representative pictures of planarians A) before loading or B) after being cut. Scale bar: 0.5 mm. (C) Two of the girls load planarians into the FME tubes. Written informed consent from the students' parents was obtained for use of this image. (D) Worms inside the FME tube. Scale bar: 2 cm (E) Schematic of experimental time line. A detailed description of the flight schedule can be found on the SSEP website.

On September 23, 2017, the FME tubes were opened and analyzed. The liquid from each FME mini-lab was poured into small Petri dishes for harvesting and analysis. In all experiments, the planarians were dead and had completely disintegrated into small pieces (Figure A.3). Interestingly, the planarian fragments in the ground truth experiments were larger compared to the flight experiment (compare Figure A.3C and D with A.3E). Of note, we observed some disintegration in the ground truth experiments during the initial movement to RT suggesting death may have occurred before the flight experiments were exposed to microgravity. It is therefore possible that the difference in worm fragment size of Earth and flight experiments is a consequence of the multi-g forces experienced during space launch and return.

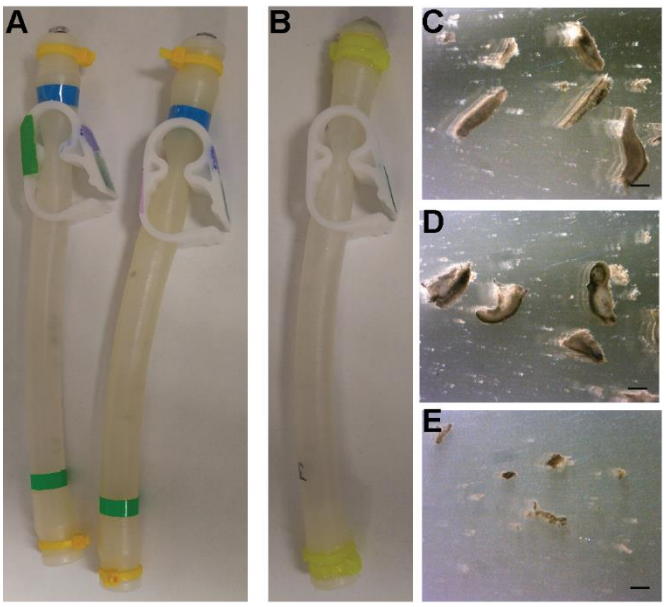

Figure A.3. Results from Ground and Flight experiments. (A) Ground control FME tubes before opening. (B) Flight FME tube returned from space before opening. (C-E) Representative images of disintegrated planarians from (C-D) ground controls or (E) the flight experiment. Scale bars: 0.1 mm.

The failure of the experiment, including the ground-truth control, was surprising given that our pre-flight ground control experiments indicated that the worms were able to survive 5 weeks in the FME mini-lab. However, these preliminary experiments had been conducted without formaldehyde in the second chamber, raising the possibility that the fumes from the formaldehyde affected the planarians' ability to survive in the FME tubes in the real experiment. Although the clamp separated the liquid and no leakage was observed, as confirmed by post-flight tests using food coloring (Figure A.4G), it may not have separated the fumes.

Post-flight Experiments

As the planarians in both the ground control and flight experiments had disintegrated over the course of the experiment, post-flight experiments were performed to determine how long planarians could survive under these conditions and whether different factors (presence of formaldehyde, presence of air or tube type) could affect viability. Thus, using new FME tubes, different conditions were set up in the same manner as the real experiment with the alterations

listed in Table A.1. Conditions 2 and 5 contained 1 ml 37% formaldehyde in the second chamber while in the remaining tubes the second chamber was left empty. To determine whether lack of oxygen caused the worms to die, condition 5 was set up with only 6 ml of CG spring water (and 2 ml of air) in the 8 ml chamber. Moreover, to test whether both the lack of oxygen and presence of formaldehyde caused the observed worm lethality, Condition 6 was set up in an FME tube without the clamp to give only one chamber containing 10 amputated tails, 8 ml of CG spring water and approximately 1.2 ml of air. Lastly, to determine if components of the FME tube were detrimental to planarian health, control experiments were performed with 5 ml culture tubes or with 9 ml glass borosilicate tubes using the same worm:volume ratio as in our FME experiments. For air tests, controls were prepared in culture tubes with 3.75 ml CG water and 1.25 ml air or in glass tubes with 8 ml spring water and 1 ml air. All tubes were stored horizontally. The viability of the worms was checked by eye every 3-4 days.

Table A.1. Post-flight test conditions in FME tubes. Results can be found in Figures A.4A and A.4D-F.

Condition	**Presence of formaldehyde**	**Volume of CG (ml)**	**Volume of air (ml)**	**Number of replicates**
1	No	8	0	1
2	Yes	8	0	2
3	No	8	0	1
4	No	8	0	2
5	Yes	6	2 ml	3
6	No	8	1.8 ml (no clamp)	1

Our post-flight experiments (Figure A.4) show that the presence of air ("+ air" in Figure A.4) in the various enclosures generally increased planarian long-term viability. While little differences were observed between the - air and + air conditions in the first week at 4 °C, at longer times worms without air in all tube types died more rapidly (Figure A.4A-C). Notably, tube type/material appears to affect the results as we observed the largest variability in the data in the FME tubes (Figure A.4A), followed by the culture tubes (Figure A.4B), and then the glass tubes (Figure A.4C, see Figure A.4D for direct comparison). The positive effect of air in the tube on worm viability was least obvious in the FME tubes, as in some cases the animals in the - air conditions lived significantly longer than the animals in the + air conditions. However, in the culture (Figure A.4B) and glass tubes (Figure A.4C), planarians stored in tubes with air survived significantly longer than those without air. For example, in the glass tubes, all worms in tubes without air died within 20 days, while worms in glass tubes with air only showed about 40% death in the same time frame. Thus, while the general trend in the data suggests that presence of some air in the FME tubes promotes planarian viability, it is not a guarantee for planarian viability over the course of the experiment.

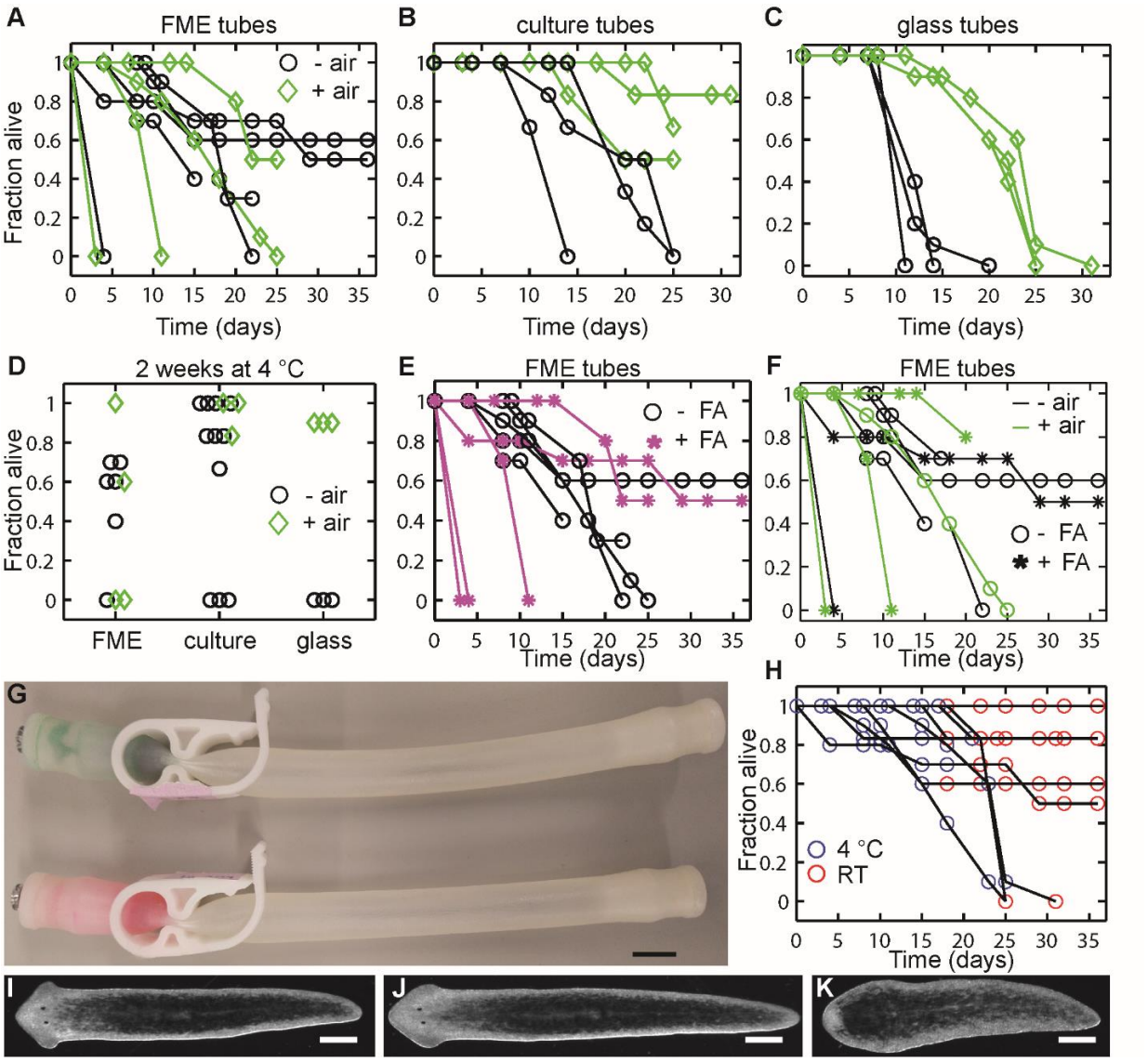

Figure A.4. Post-flights tests on planarian viability. (A-C) Planarian viability is increased in tubes which contain air (green diamonds) compared to tubes without air (black circles) in A) FME tubes, B) culture tubes, or C) glass tubes. (D) Considerable variability exists within the different set ups. Graph shows a comparison of all data collected in each tube type after 2 weeks (14-17 days) at 4 °C and compares tubes with and without air (green diamonds and black circles, respectively). (E) Addition of formaldehyde (FA) generally negatively affects planarian viability. (F) Comparison of all FME tube experiments (data from panels A and E) comparing with and without air (green or black color, respectively) and with and without FA (stars and circles, respectively). (G) No leakage of liquid was found between FME compartments. Food coloring and formaldehyde was added to the left compartment of the FME tube and IO water to the right compartment. Image was taken after the tubes were stored at 4 °C for 2 weeks (17 days). No leakage of the formaldehyde/food coloring mixture was observed. Scale bar: 1 cm. (H) Moving planarians from 4 °C (blue) to RT (red) generally does not affect viability. (I-K) Representative images of regenerated planarians which survived 5 week enclosure (2 weeks at 4 °C and 3 weeks at RT) in either a I) FME or J) culture tube. (K) Representative image of a planarian which failed to regenerate properly after 3 weeks at 4 °C and 2 weeks at RT. Image is from FME tube, condition 2. Scale bar: 0.5 mm.

Additionally, we found that the presence of formaldehyde generally negatively impacts planarian viability in the FME tubes (Figure A.4E and A.4F). In 3 of the 5 tests, addition of formaldehyde caused rapid death (within 11 days). This is not due to leakage of the formaldehyde liquid into the planarian chamber as potential leakage through the clamp was checked by tapping on the tube before the formaldehyde was added. Moreover, we found no leakage between the two chambers after 2 weeks of storage (Figure A.4G). However, it is still possible that formaldehyde vapors may have been able to leak into the second chamber. Again, as observed in the +/- air tests, the variability in the FME tube data makes it difficult to draw strong conclusions.

Finally, and importantly for future experimental design as elaborated on in the Discussion, we observed that planarian viability stayed relatively constant when the tubes were moved to RT (Figure A.4H). This suggests that the initial storage conditions at 4 °C to induce dormancy are the main determinant of whether the planarians are able to survive. Generally, if the animals were able to survive this 2-3 week period at 4 °C, they were able to persist and regenerate in the subsequent storage at RT (Figure A.4I-K). Similarly to our pre-flight tests, we also found that some worms had regeneration defects (no blastema, small blastema or abnormal eyes) following regeneration at RT. These defects were more prevalent in tubes which had been stored at 4 °C for 3 weeks rather than only 2 weeks and in the FME tubes when compared to the culture tubes (Figure A.4K and Table A.2).

Table A.2. Lethality and regeneration defects in planarians stored for 2 or 3 weeks at 4 °C in either FME or culture tubes. Counts of normal animals versus animals with a regeneration defect are based on the number of living worms.

Tube type	Total n	Time at 4 °C	Time at RT	% alive	% normal survivors	% regeneration defect or sick
FME	10	2 weeks	3 weeks	60	100	0
FME	10	3 weeks	2 weeks	50	0	100
Culture tube	12	2 weeks	3 weeks	92	91	9
Culture tube	12	3 weeks	1 week[1]	75	44	56

[1] Planarians were removed from the tube after 3 weeks at 4 °C. Extent of regeneration was observed after one week incubation in a petri dish.

DISCUSSION

The parameters set within the SSEP made it challenging to create a successful microgravity experiment using live biological samples. Despite the pre-launch tests that indicated that the experimental conditions were viable, all planarians (flight and ground truth) disintegrated over the 43 days of the experiment. Our post-flight ground-control experiments suggest that a combination of the extended storage at 4 °C due to the launch slip and the lack of oxygen were likely the largest factors contributing to this outcome.

Extended Storage at 4 °C

Our pre- and post-flight experiments have shown that planarian regeneration can be put into a dormant state at 4 °C. However, we found increased death and a significantly higher percentage of planarians with regeneration defects upon longer cold storage, suggesting extended cold storage negatively affected worm health (Table A.2). The launch slip, necessitating the experiment to be kept at 4 °C for 5 more days than planned, therefore may be the main reason for the negative experimental outcomes. From the time our flight experiment was prepared to the time it arrived on the ISS was 25 days. Generally, such a long transportation time is not ideal for biological experiments. It has been previously emphasized that late loading and early retrieval are optimal to maximize organismal health for life science experiments conducted in space (Hughes-Fulford, 2004; National Research Council of the National Academies, 2011; Warren et al., 2013). Travel time was considerably shorter in the non-SSEP planarian ISS experiments, with launch occurring within 12-14 or 31 hours for the Gorgiladze and Morokuma et al. (2017) studies, respectively. Thus, these significantly shorter transportation times may be responsible for why their planarians were viable and regenerated while ours disintegrated. In fact, in the case of studying the effect of microgravity on regeneration, the ideal experiment would be to

amputate the planarians on board the ISS and not on Earth (Morokuma et al., 2017). The study by Gorgiladze has thus come closest to these ideal conditions.

Lack of Oxygen and Air to Water Ratio

Interestingly, we observed a highly variable effect of lack of oxygen on our test planarians; while a few tubes showed hardly any effects, others showed significant or complete death under the exact same experimental conditions (Figure A.4A-C). It was more difficult to eliminate all air in the FME and culture tubes compared to the glass tubes, thus small air bubbles may have been present in some of the samples, contributing to the variability in the data. However, compared to the air volume in the + air conditions, these bubbles are negligible and thus cannot explain why some - air conditions outperformed the + air conditions in the FME-tubes.

Morokuma et al. (2017) concluded that the optimal condition for 30-day survival of intact planarians at 20 ºC was a 50-50 air-to-water ratio and that using 100% water and no air resulted in complete lethality of intact planarians within 5 days. On the other hand, experiments with *G. tigrina* were viable for the duration of the 10 day flight in tubes without additional oxygen (Gorgiladze, 2008). Of note, in our no-air setups using regenerating tail pieces stored at 4 ºC, initial deaths begin to appear between 5-8 days though complete lethality was not always observed, even up to 36 days. Our original experimental setup contained no air due to concerns that planarians may crawl out of the water and dry out, which has been observed in other instances (Hagstrom et al., 2015). However, this did not appear to be an issue in our post-flight tests when volume was left for air.

Taken together, the extended storage at 4 ℃ and the observed randomness in worm health under identical experimental conditions can explain why our pre-flight experiments

showed no worm death, whereas all worms in the actual experiment, including ground-controls, died. The previously reported experiments with *C. elegans* similarly found that chance largely dictated whether the nematodes survived long-term storage in the FME tubes (Warren et al., 2013).

Planarian Density

Related to the considerations above is the question of how many planarians should be used per tube. There is a trade-off between using more worms and thus getting more reliable data and compromising the individuals' health by increasing the population density. Morokuma et al. (2017) used a density of 1 worm/2.5 ml Poland Spring water and 2.5 ml air for their initial water-air ratio tests and experiments with intact planarians, but in their regeneration experiments, 15 amputated pieces (heads, trunks and tails) were placed in a single tube, resulting in a density of 1 worm piece/1.7 ml Poland Spring water/1.7 ml air. Gorgiladze reported using 1 trunk piece/2 ml fresh water. In contrast, we used nearly double that density by placing 1 tail in 0.8 ml CG water. Previous experiments (Carter et al., 2015) have shown that the carrying capacity of *D. japonica*, the species used in this study and by (Morokuma et al., 2017), is twice that of *D. tigrina*, used by (Gorgiladze, 2008), suggesting that we should be able to use higher densities without compromising worm viability. The reason for choosing this higher worm density was based on two considerations: 1) Our preliminary experiments revealed no difference in worm health when comparing 5 versus 10 worms in the same volume of water. 2) To account for the possibility that some planarians may die over the course of the experiment, 10 worms increased the likelihood of obtaining survivors upon space travel completion. Of note, while we were restricted to a single FME tube with 9.2 ml maximum volume in this SSEP study, the other two studies were able to use one 50 ml (Morokuma et al., 2017) and six 20 ml tubes (Gorgiladze, 2008), respectively.

Other Considerations that May Improve the Success Rate of Live Biological SSEP Experiments

The most important change which we expect to significantly improve the success rate of biological experiments, besides shorter transportation times, is a requirement to report the SSEP project results and make this information publicly available. This will allow future research to build upon the experience of prior experiments. We therefore suggest that the SSEP requires a short summary write-up of the results of all participating teams that can then be posted on its website.

There are a few other issues that would be worth exploring for future experiments. Biological samples for SSEP are currently transported in a specialized cold package, FedEx Temp-Assure, which keeps the shipment at a constant temperature of 2 - 8 °C. Such variance in temperature during transport for the flight experiment is suboptimal. Similarly, the temperature of the ground truth experiment likely also fluctuated, since the samples were stored in a common laboratory refrigerator or cold room (post-flight experiments), respectively. In both cases, opening of the door will lead to temporarily higher temperatures. Morokuma et al. (2017) used a temperature-controlled portable incubator for their experiment. While such an incubator is likely outside the budget for SSEP Missions, it would be worthwhile to conduct pre-flight experiments to evaluate the effect of temperature fluctuations on the samples.

Thirdly, the currently limited options for timing of crew interactions is not ideal to track planarian regeneration. Crew interactions were limited to only 5 options provided by the SSEP: day of arrival on the ISS, 2 days post-arrival, 2 weeks prior to undock, 5 days prior to undock and 2 days prior to undock. For the purposes of studying planarian regeneration, which takes about 7 days, only the 2 week prior to undock interaction was appropriate, although this can vary

from 2 to 4 weeks of microgravity exposure. Adding this broad time window to potential delays in launch or transportation thus can significantly alter the timeline of the experiment and cause experimental milestones to deviate from initial plans. A crew interaction of 7 days post-arrival would be ideal to increase the viability of the experiment and minimize the time the live worms are in the enclosed FME mini lab. Furthermore, longer regeneration times may also obscure any possible regeneration delays that may occur as a consequence of microgravity exposure.

Proposed New Working Protocol

Based on our post-flight experiments, we propose that the transport time at 4 °C should be minimized as much as possible. Since this is not always under the control of the individual research teams, we also suggest a few modifications to optimize the current protocol. We propose that addition of air in the FME set-up would provide a greater chance of success. This would mean using 6 ml CG in the 8 ml compartment. Due to the smaller volume of water, one could also adjust the amount of formaldehyde in the second compartment, thus saving resources. Due to the constraints of the SSEP experimental timelines, the addition of formaldehyde to the mini-lab is necessary to be able to stop the experiment mid-flight. This would, thus, decrease the time the worms are enclosed and halt regeneration after a sufficient period. While having a generally negative effect on planarian health, our post-flight tests indicate that some planarians can survive in the FME tube with formaldehyde in the second chamber (Figure A.4E, F). Although we observed some regeneration defects in the ground controls under these conditions, the prevalence of defects can still be compared between Space and Earth samples to decipher the effects of microgravity on planarian regeneration. Since the viability of the worms seems to be largely affected by chance, we suggest still using 10 *D. japonica* tails for each experiment to maximize the chance that enough will survive to provide conclusive data. Because of this

randomness, it would also be highly beneficial if teams could send two FME tubes to the ISS instead of the current one. Executing a single experiment is not customary or sufficient in most sciences. Therefore, allowing for two tubes would also incorporate the concept of experimental replicates, thus more closely mimicking professional science conditions.

In summary, our data suggests that using these proposed changes (addition of air, 2 tubes instead of 1) and a shorter experimental timeline (ideally ≤2 weeks at 4 °C and 1 week at RT under microgravity conditions) would greatly improve the chance of obtaining meaningful data. Importantly, the proposed changes increase the chances of successful regeneration in the controls, which is a necessity for accurate interpretations as a high defect rate in ground control experiments would obscure the interpretation of defects observed in the space samples.

Value of Project for Middle School Student Scientists

The value of the SSEP is clearly (1) the potential gathering of new knowledge about the effects of microgravity on various processes, and (2) the impact this program has on student development and future trajectories. Although our study on the effect of microgravity on planarian regeneration was inconclusive, the SSEP did offer us an invaluable journey to experience the work of "real scientists". We learned to critically design an experiment within financial, logistical, and technical constraints to explore an outstanding scientific question, "How does microgravity affect planarian regeneration?", and were provided with the unique opportunity to have our experiment performed on board the ISS.

Our hands-on experience through this STEM education initiative opened our eyes to what science has to offer and has changed our views by allowing us to dig deeper, giving hands on experience and insight into what 'real' science looks like, and discover not only how, but why many things work together and in harmony. Furthermore, SSEP greatly impacted our career

plans, teaching us the importance and value of the team experience, which allowed us to work collaboratively with not only students but professionals, and improved our writing and presentation skills. We also learned to appreciate when students have the same mindset, and strive for different perspectives and views.

ACKNOWLEDGEMENTS

The appendix, in full, is a reformatted reprint of the material as it appears in Vista SSEP Mission 11 Team; Hagstrom, Danielle; Bartee, Christine; and Collins, Eva-Maria S. "Studying planarian regeneration aboard the International Space Station within the Student Space Flight Experiment Program", Frontiers in Astronomy and Space Sciences, vol. 5, 2018. The authors retain copyright of this manuscript, which is an open access article permitting the use herein. Vista SSEP Mission 11 Team, a team of 5 middle school students, designed the original space experiment. Vista SSEP Mission 11 Team, Danielle Hagstrom, and Eva-Maria S. Collins conducted experiments. All authors co-wrote the paper.

SUPPLEMENT

Remarks on the Journey of the Mission 11 Team from the professional researchers' perspective

Following the spirit of the SSEP program to give students a "real scientists' experience" and as part of this special issue aimed at highlighting the contribution of "Women in Science", this article was jointly written by the 5 female students (aged 11-13), their female teacher, and us, their professional female mentors, with the aim to accomplish two things: (1) to report why planarian regeneration experiments conducted within the constraints of these educational programs are prone to fail. (2) To document the young students' journey of persistence and discovery, and the importance of mentorship on the path to becoming a scientist. Notably, by co-writing this article, the students were also introduced to the process of scientific writing. Below we provide some context on the background of this collaboration and our experiences as mentors to these students.

For the 2017 SSEP Mission 11, student teams from participating communities were given 9 weeks to design and propose experiments which, if selected, would fly in low Earth orbit aboard the ISS to test the effects of microgravity. Each community's flight experiment was selected through a formal two-step proposal review process (see SSEP website for details). Our team of 5 female students was selected for SSEP Mission 11 in the Vista, CA community. One of these students had previously led a team of two that applied for SSEP Mission 8 but their proposal, although being the top proposal from the school, was denied at the school administration level. Importantly, the original team leader persevered, recruited four more girls, and tried again, leading to the work reported here.

By engaging in a community-wide competition via submission of a 2000+ word research proposal, the students learned the value and necessity of strong writing and communication skills

in science. The program further encouraged student teams to reach out to local and international researchers for advice and mentorship, thus connecting K-12 science education to the professional scientific community. Finally, the students were provided the opportunity to travel to the Kennedy Space Center to watch the SpaceX CRS-12 launch with their experiment on board, and to present to a scientific community at the annual SSEP National Conference at the Smithsonian's National Air and Space Museum in Washington, D.C.

The connection between the authors of this study was first established in 2015, when the two "founder students" sought advice for their original proposal for SSEP Mission 8. The students' perseverance and enthusiasm, as well as the passionate dedication of their teacher, has fueled this collaboration since and ultimately culminated in this article.

Through this joint article, we wanted to teach them that a lot can be learned from scientific failures and that publishing such knowledge can be beneficial to future research and the scientific community – in addition to introducing them with a "hands-on" experience to writing a scientific paper.

To us, as professional female scientists, the opportunity to mentor these young female students was particularly important. So far, these students report that they "have never felt any restrictions on going into science because of [their] gender". Research experiences and mentorship opportunities, such as those provided by the SSEP, aim to foster this sense of inclusion in the sciences so that these students hopefully will never experience exclusion. The drive, curiosity, and perseverance of these young student scientists is a testimony to what our next generation of scientists, both male and female, can accomplish, especially with the help of passionate mentors, and an inspiration to every professional scientist.

REFERENCES

Adell, T., Saló, E., Van Loon, J. J. W. A. and Auletta, G. (2014). Planarians sense simulated microgravity and hypergravity. *Biomed Res. Int.* 2014.

Best, J. B. and Morita, M. (1982). Planarians as a model system for in vitro teratogenesis studies. *Teratog. Carcinog. Mutagen.* **2**, 277–91.

Brondsted, A. and Brondsted, H. V. (1961). Influence of temperature on rate of regeneration in the time-graded regeneration field in planarians. *Development* **9**, 159–166.

Carter, J. A., Lind, C. H., Truong, M. P. and Collins, E.-M. S. (2015). To each his own. *J. Stat. Phys.* **161**, 250–272.

Cebrià, F. (2007). Regenerating the central nervous system: how easy for planarians! *Dev. Genes Evol.* **217**, 733–48.

Gorgiladze, G. I. (2008). Regenerative capacity of the planarian Girardia tigrina and the snail Helix lucorum exposed to microgravity during an orbital flight on board the International Space Station. *Dokl. Biol. Sci.* **421**, 244–247.

Hagstrom, D., Cochet-Escartin, O., Zhang, S., Khuu, C. and Collins, E.-M. S. (2015). Freshwater planarians as an alternative animal model for neurotoxicology. *Toxicol. Sci.* **147**, 270–285.

Hagstrom, D., Cochet-Escartin, O. and Collins, E.-M. S. (2016). Planarian brain regeneration as a model system for developmental neurotoxicology. *Regeneration* **3**, 65–77.

Hagstrom, D., Zhang, S., Ho, A., Tsai, E. S., Radić, Z., Jahromi, A., Kaj, K. J., He, Y., Taylor, P. and Collins, E.-M. S. (2017). Planarian cholinesterase: molecular and functional characterization of an evolutionarily ancient enzyme to study organophosphorus pesticide toxicity. *Arch. Toxicol.* **92**, 1–16.

Hughes-Fulford, M. (2004). Lessons learned about spaceflight and cell biology experiments. *J. Gravit. Physiol.* **11**, 105–9.

Marsh, G. and Beams, H. W. (1952). Electrical control of morphogenesis in regenerating dugesia tigrina. I. Relation of axial polarity to field strength. *J. Cell. Comp. Physiol.* **39**, 191–213.

Morgan, T. H. (1989). Experimental studies of the regeneration of Planaria maculata. *Arch. für Entwickelungsmechanik der Org.* **7**, 364–397.

Morokuma, J., Durant, F., Williams, K. B., Finkelstein, J. M., Blackiston, D. J., Clements, T., Reed, D. W., Roberts, M., Jain, M., Kimel, K., et al. (2017). Planarian regeneration in space: Persistent anatomical, behavioral, and bacteriological changes induced by space travel. *Regeneration* **4**, 85–102.

National Research Council of the National Academies (2011). *Recapturing a future for space exploration: Life and physical sciences research for a new era*. Washington, D.C.: National Academies Press.

Novikov, V. V., Sheiman, I. M. and Fesenko, E. E. (2008). Effect of weak static and low-frequency alternating magnetic fields on the fission and regeneration of the planarian dugesia (Girardia) tigrina. *Bioelectromagnetics* **29**, 387–393.

Pearson, B. J., Eisenhoffer, G. T., Gurley, K. A., Rink, J. C., Miller, D. E. and Sánchez Alvarado, A. (2009). Formaldehyde-based whole-mount in situ hybridization method for planarians. *Dev. Dyn.* **238**, 443–450.

Reddien, P. W., Bermange, A. L., Murfitt, K. J., Jennings, J. R. and Sánchez Alvarado, A. (2005). Identification of genes needed for regeneration, stem cell function, and tissue homeostasis by systematic gene perturbation in planaria. *Dev. Cell* **8**, 635–49.

Umesono, Y., Watanabe, K. and Agata, K. (1997). A planarian orthopedia homolog is specifically expressed in the branch region of both the mature and regenerating brain. *Dev. Growth Differ.* **39**, 723–7.

Warren, P., Golden, A., Hanover, J., Love, D., Shephard, F. and Szewczyk, N. J. (2013). Evaluation of the fluids mixing enclosure system for life science experiments during a commercial Caenorhabditis elegans spaceflight experiment. *Adv. Sp. Res.* **51**, 2241–2250.